Probing the behaviour of poly(ethylene oxide)-poly(propylene oxide)-poly(ethylene oxide) surfactants in the formation of hydrophilic polyurethane foam

by

JAMIE HURCOM

Thesis submitted for
DOCTOR OF PHILOSOPHY

SCHOOL OF CHEMISTRY
CARDIFF UNIVERSITY
2015

Dedicated to my Grandparents

who are always so proud but after much chatting still don’t understand my PhD!

Abstract

Polyurethane (PU) foams are widely used in the medical industry in the treatment of chronic wounds but the role of surfactants in the reaction process, which strongly influences foam structure and properties, is not well understood. In this research, a homologous series of non-ionic poly(ethylene oxide)-poly(propylene oxide)-poly(ethylene oxide) (Pluronic) block copolymer surfactants were studied, in order to elucidate the influence of surfactant structure on PU foam performance.

The behaviour of aqueous surfactant stabilised foams was investigated using a combination of surface science techniques (foaming ability / stability, surface tension) and small-angle neutron scattering (SANS). SANS has been successfully implemented to probe the adsorbed Pluronic surfactant layer of dynamic foams in-situ in the neutron beam. We propose the air-water interface comprises a paracrystalline stack consisting of a minimum of 5 adsorbed surfactant layers, with thickness ranging from 80-200Å interspersed with somewhat thicker (200Å) films of water. Total adsorbed layer thickness correlates directly with aqueous foam stability.

Correlations of aqueous behaviour to the cell structure and performance of PU foams manufactured on an industrial line were made in an attempt to determine the features of surfactant necessary to produce 'ideal' PU foam wound dressings. Analysis of foam cell size and fluid absorption properties demonstrated that greatest absorption was observed for small, fine cell size. This was typically produced by the smallest molecular weight, most hydrophobic surfactants of the series implying that the surface activity of the surfactant (i.e. its ability to reduce the surface tension of the system) is more important than its foaming behaviour. This study should provide a more rational approach when designing surfactant formulations for polyurethane foam systems.

Acknowledgements

Thanks must be given to the following:
To my supervisors Professor Peter Griffiths and Dr Alison Paul for their invaluable guidance, discussion and support throughout my PhD.

To my industrial supervisor Nick Woodman at Polymer Health Technology (PHT) for giving me the opportunity to gain industrial experience from my research and to all of the team at PHT who made me feel so welcome on my work placements.

Knowledge Economy Skills Scholarships (KESS), the European Social Fund, Cardiff University and Polymer Health Technology are gratefully acknowledged for funding this research.

Thanks to Dr Richard Heenan at ISIS for his advice and discussion when analysing SANS data.

To Alun Davies for constructing the SANS column and for the long hours he helped on the experiments.

To Gareth Jones and Oliver Hayes for carrying out the equilibrium and dynamic surface tension work.

Thanks to all members past and present of the Soft Matter Research Group at Cardiff University who made the long days in the lab more bearable.

And finally, love to the most important people; Mum, Dad, Sophie and Sam whose endless support and encouragement have allowed me to get to where I am today, and to Sean who has been my rock throughout the past three years and who has given me the motivation to complete this PhD.

Contents

Chapter 4. Probing the structure of PEO-PPO-PEO surfactant stabilised foams in-situ using small-angle neutron scattering

Chapter 5. The effect of temperature on aqueous PEO-PPO-PEO surfactant stabilised foams

Abbreviations and symbols

BF – bilayer film

CBF – common black film

CMC – critical micelle concentration

CMT – critical micelle temperature

CTAB – cetyl trimethyl ammonium bromide

DLVO Theory – Derjaguin, Landau, Vervey and Overbeek Theory

DST – dynamic surface tension

EO – ethylene oxide

HIPE – high internal phase emulsion

HLB – hydrophobic-lipophilic balance

NBF – Newton black film

NHS – National Health Service

PEO-PPO-PEO – poly(ethylene oxide)-poly(propylene oxide)-poly(ethylene oxide)

PO – propylene oxide

PU – polyurethane

Rg – radius of gyration

SANS – small-angle neutron scattering

SDS – sodium dodecyl sulfate

TFPB – thin film pressure balance

USANS – ultra-small-angle neutron scattering

Γ – surface coverage

γ – surface tension

γ_m – meso-equilibrium surface tension

γ_t – dynamic surface tension

$\delta\gamma/\delta t$ – change in surface tension with time

$\bar{\varepsilon}$ – surface dilational modulus

ε – surface elasticity

ε_{crit} – liquid fraction at which film rupture occurs

ε_o – high frequency elasticity

η – surface viscosity

Π – disjoining pressure

τ_1 – timescale release of monomer from micelle into bulk

τ_2 – total micelle breakdown time

$t_{1/2}$ – foam half life

b – scattering length

D – density

d – Bragg length scale

I(Q) – scattering intensity

k_i – incident wavevector

k_s – scattered wavevector

n_p – number density of scattering bodies

ρ – scattering length density

$\Delta\rho^2$ – contrast term

P(Q) – form factor

Q – scattering vector

S(Q) – structure factor

Θ – scattering angle

M – number of layers

L – layer thickness

D – separation between layers

Rσ – Lorentz factor defining interface orientation

T – interface diffuseness

1. Introduction

1.1. Polyurethane foams as wound-care materials

The manufacture of advanced medical materials for use in the treatment of chronic wounds is a rapidly expanding area. Effective care and management of wounds such as ulcers and bedsores, costs the National Health Service (NHS) in Britain an estimated £2-3 billion a year.[1] In the year to December 2013, the NHS prescription costs in England for wound dressings alone totalled approximately £180 million.[2] Flexible, hydrophilic polyurethane foam dressings have a dominant market share accounting for approximately 20% of the total NHS expenditure on wound management, with in excess of 700,000 items prescribed per annum.[2] This is primarily due to the ability of these foams to satisfy many of the criteria of an 'ideal' wound dressing,[3] (Figure 1.1) such as providing a protective, waterproof barrier to infection whilst maintaining the wound in an optimum degree of hydration.[3-5] With an ageing population, the prevalence of such conditions and the subsequent cost of treatment is likely to rise dramatically. Therefore understanding how the foam forming process affects the end user properties of such foams is essential for designing next generation foams with optimum properties.

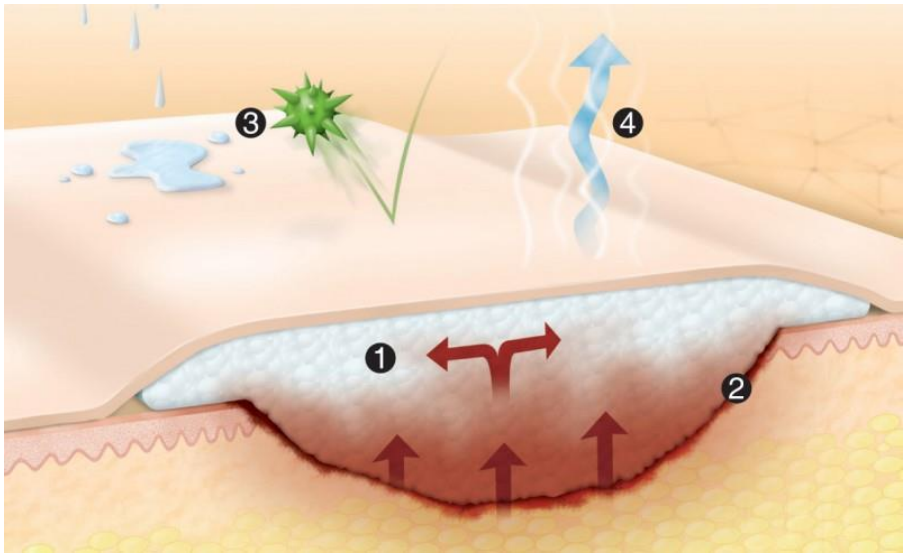

Figure 1.1; Ideal properties of a polyurethane foam wound dressing. 1:absorb excess wound fluid, 2: conform to the skin, 3: act as a barrier to infection and water, 4:maintain the wound in a suitably hydrated environment.[6]

1.2. Chemistry of polyurethane foam formation

The chemistry of polyurethane (PU) foams is well documented.[7-10] Polyol and di-isocyanate monomers are reacted together to form a polyurethane linkage, as shown in Figure 1.2. For a more in-depth understanding of hydrophilic polyurethane foams readers are referred to *Flexible Polyurethane Foams; Chemistry and Technology* by G.Woods.[7]

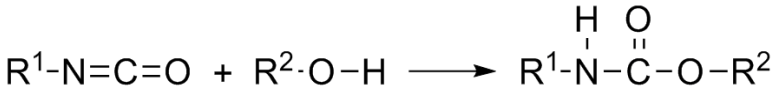

Figure 1.2; Polymerisation reaction of di-isocyanate and polyol to form polyurethane.

In the presence of water, the di-isocyanate reacts with water to produce carbon dioxide, known as the *blow* reaction. Through high speed mixing, this carbon dioxide is incorporated into the system thus producing foam. A simultaneous reaction, the *gelation* reaction, occurs between the polyol and isocyanate to form the polyurethane network. Control of the timing and rates of both reactions are essential to forming polyurethane foam with desired cell size and porosity.

In addition, surfactants are an important component in polyurethane foam manufacture. By adsorbing at the air-liquid interface, it is believed that surfactants have a number of key roles in the foam forming process, including;[7, 8]

- emulsifying incompatible starting materials;
- promoting bubble nucleation during mixing;
- stabilising the cell structure by lowering the surface tension at the air-water interface thus preventing coalescence of nucleating bubbles;
- controlling, to an extent, the timing and degree of cell opening;
- reducing defoaming effects that may arise throughout the reaction.

Many surfactants traditionally used in the manufacture of polyurethane foams are silicone based copolymers in which polyether pendant groups are attached to a siloxane backbone. Many variations have been developed and patented.[11-14] Alternatively, non-ionic

surfactants such as nonylphenol ethoxylates ($C_{15}H_{23}O(CH_2CH_2O)_nH$) and alkylene oxide block copolymers ($HO(CH_2CH_2O)_x$-$(CH_2CH(CH_3)O)_y$-$(CH_2CH_2O)_xH$) can also be used.[7]

No generic formula or mechanism to predict the structure and properties of polyurethane foams has been reported in the literature.[7] This is primarily due to differences in machinery and equipment, raw materials and processing conditions so that making direct comparisons across different systems is a challenge. As a result, PU foams with suitable properties for a desired application tend to be found using a 'trial and error' approach. In addition, the complexities of the reaction itself such as reaction rates and temperature gradients (the reaction is exothermic) complicate the study of these systems.

1.3. Introduction to foams

Foams are dispersions of gas in an aqueous, non-aqueous or solid phase. It is well known that pure liquids do not foam; gas bubbles rupture almost immediately on contact when introduced beneath the surface of pure water due to its high surface tension. Foam production must occur in the presence of surfactant with both small molecule and polymeric surfactants able to generate stable foam. More recently colloidal silica nanoparticles have also been shown to adsorb at air-water interfaces providing stabilisation.[15, 16] Foam can be formed in a number of ways including; through mechanical means (whipping or shaking), blowing air into a surfactant solution or during a chemical reaction in which gas is formed in-situ (as is the case in PU systems).

For any type of foam, two distinct structures can be observed. In newly prepared foam systems, *kugelschaum* or *wet* foam is produced.[17] Bubbles appear spherical and are separated by thick, viscous films. Upon aging, the spherical bubbles distort into multi sided polyhedral gas cells that are separated by thin, lamellae walls. *Polyderschaum* or *dry* foam is produced when the films thin to approximately 1000nm and interference colours are observed.[17] The bubbles meet at Plateau borders and are connected at junction points called nodes to form an interconnecting network. The larger degree of curvature in the plateau borders (along with thicker film) than the lamellae walls, has significant consequences for foam drainage (Figure 1.3). This is because the pressure inside the borders is lower than that of the cell walls so that liquid drains from the walls into the strut. The network of plateau borders provides a route through which the liquid flows out due to gravity. The adsorbed surfactant modifies this drainage rate.

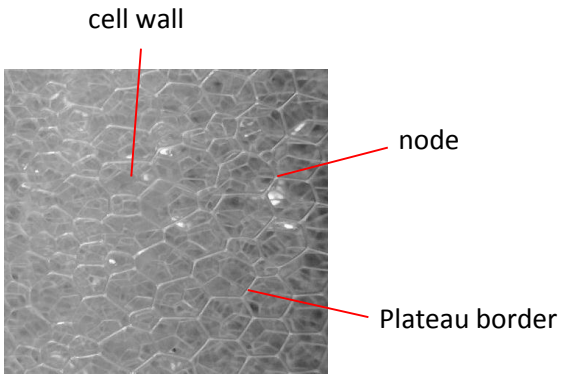

Figure 1.3; The structure of a polyhedral drained foam.

Foam destruction occurs via a number of processes (Figure 1.4) [18]:

- drainage due to gravity or surface tension gradients, the rate of which is affected by the density and viscosity of the liquid phase, the bubble size distribution and the stability of the foam;
- Ostwald ripening or coarsening driven by diffusion of gas across thin films from smaller to larger bubbles. This thermodynamically spontaneous process involves the growth of larger bubbles at the expense of smaller ones and arises due to the greater Laplace pressure difference present in the smaller bubbles than the larger ones;

$$\Delta P = \frac{2\gamma}{r}$$

  This results in a chemical potential difference between bubbles of different size and so molecules migrate across the aqueous phase from small to large droplets, decreasing the free energy of the system.
- and bubble coalescence leading to the thinning and eventual rupture of thin films.

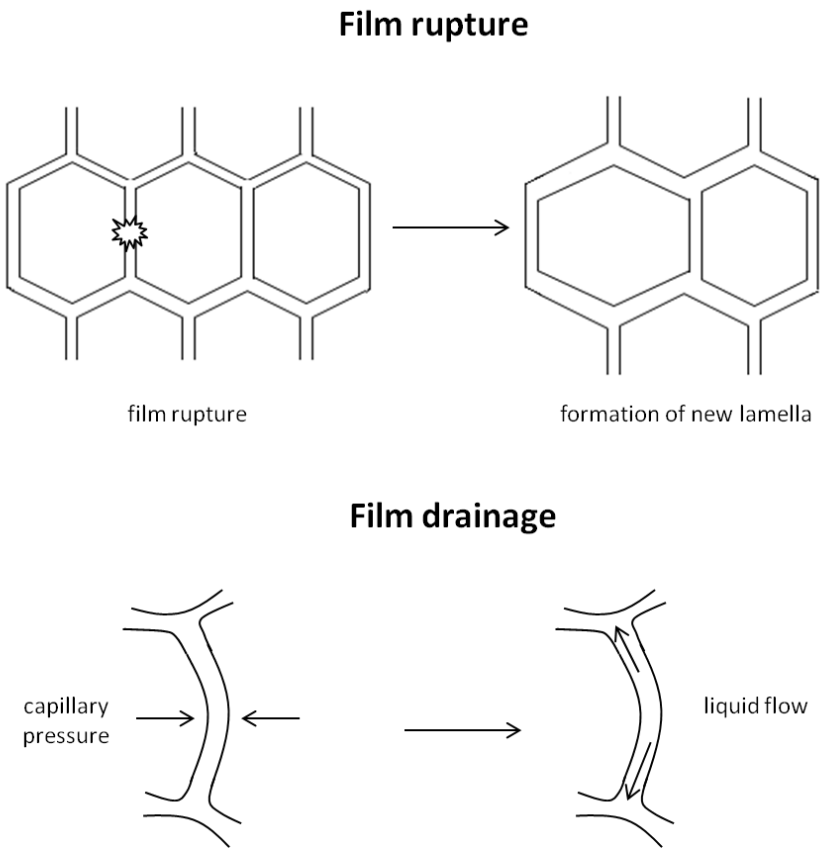

Figure 1.4; Film breakdown mechanisms in foams. Adapted from Kim et al.[19]

By adsorbing at the air-water interface, surfactants lower the surface tension providing a surface elasticity mechanism, the Gibbs-Marangoni effect, that opposes localised film thinning[17] (Figure 1.5). The theory combines the Gibbs effect (describing the change in surface tension with surfactant concentration) and the Marangoni effect (describing the change in surface tension with time). When localised thinning occurs in response to a stress, the area of the thinned region increases, this consequently increases the surface tension. A gradient is established resulting in a flow of liquid from the thicker surrounding regions to the thinned region preventing further thinning. The ability of the surfactant to resist these depletion processes is highly dependent on the nature of the adsorbed layer.

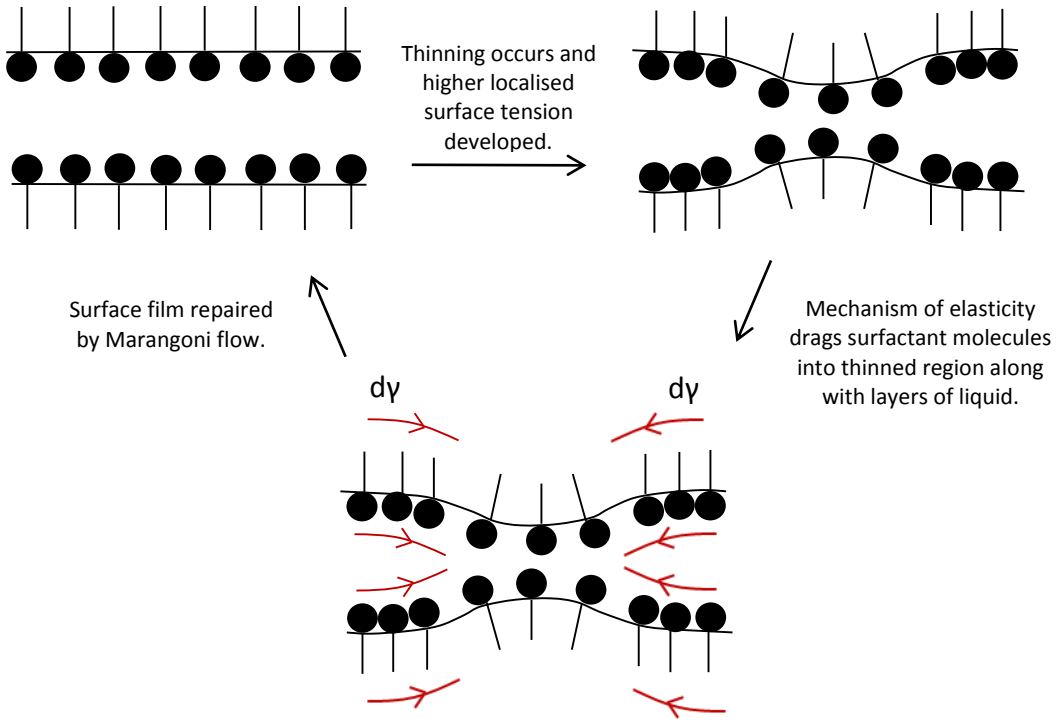

Figure 1.5; The Gibbs-Marangoni mechanism of foam stabilisation.

Before, moving on to discussing the literature surrounding foams, it is worth recalling definitions describing foaming behaviour.[20] Foam stability refers to how stable foam is after it has been produced, describing changes in the foam with time (in this case, foam height). In this study foamability describes the ability of a surfactant to generate foam in terms of the maximum foam volume that can be obtained under standard foam generation conditions (i.e. solution volume, temperature, shaking). It does not give any information about bubble size, liquid fraction, foam density however these parameters will affect foam stability.

1.4. Role of surfactant in PU foam formation

Surfactants are an essential component in the manufacture of polymeric foams such as polyurethane, however little is known about their role in the system and the influence they have on the structure and performance of the final cured foam. There is limited literature available concerning model polyurethane systems however polyurethane manufacture on a bulk scale is notoriously difficult to study and there have been no predictive mechanisms that can be transferred from one manufacturing process to another.

This is primarily due to differences in raw materials, mixing conditions, temperature gradients and machinery.[7]

It is commonly stated in the literature that the primary role of surfactant in polyurethane foam formation is to stabilise the expanding cell walls until the bubble is "locked in" by the polymer network.[21-24] In addition there is some controversy in the literature surrounding the role surfactants have in the precipitation of urea; a by-product formed during the reaction of isocyanate and water.[21, 25-27] Eventually, a 'hard segment' of several isocyanates covalently bonded through the urea forms which precipitate out into insoluble 'hard domains.' It has been postulated that the precipitation of urea hard domains relates to catastrophic cell opening and foam collapse. It is suggested that the addition of surfactant disperses the precipitate providing foam stabilisation.

Many studies have attempted to correlate cell wall stabilisation to foam properties. The early work of Owen *et al.*[28-30] established that in order to stabilise a flexible polyurethane foam, surfactants must have an appreciable but low surface viscosity postulated to be approximately 0.13 mPa.s (for comparison water has a viscosity of 1 mPa.s at 20°C), significantly lower the equilibrium surface tension of the system whilst also displaying a high rate of surface tension decrease across a range of about 20-40 mNm^{-1}. This work was later extended by Snow *et al.*[31] who found that polyurethane foam films stabilised with silicone surfactants grafted with polyethylene oxide-co-propylene oxide pendant groups were highly mobile i.e. they thinned quickly exhibiting 'rapid and complex liquid motion both on the face and edges.' Silicone surfactants were found to display low surface viscosity (in the region of zero to 0.2 mPa.s) which increased with surfactant concentration.[30] An optimum surface viscosity is required; too low and the foam will collapse, whilst too high and the cells will be over stabilised leading to closed cells and excessive shrinkage.

Model polyurethane films have been shown to exhibit Marangoni flow (movement of liquid due to surface tension gradients) suggesting the rate at which this occurs is linked to drainage rate.[29] Static surface tension measurements showed that silicone surfactants decrease the surface tension from approximately 34 to 21 mNm^{-1} in model polyol solution, however the best stabilisers were those which reduced the surface tension less than 23 mNm^{-1} allowing sufficient surface elasticity mechanisms to operate.[29] This was confirmed in a study in which the chain length of the polyether pendant groups in the

silicone surfactants was varied.[31] For small polyether chain length (EO [CH_2CH_2O]=6) the drainage rate increased with increasing surfactant concentration demonstrating that a reduction in surface tension gradients has a negative effect on foam drainage. The best stabilising surfactant (EO=18) displayed a balance of surface tension gradient and viscosity effects with drainage rate increasing up to a maximum (due to gradient effects) and then decreasing at a critical concentration (due to viscosity effects). Finally, for longer polyether chain lengths (EO=30) viscosity effects dominated with a reduction in drainage rate occurring even at low surfactant concentrations.

Similar silicone surfactants in a model polyurethane foam system have also been investigated with the properties of the polyurethane foam such as cell size and porosity correlated to surfactant structure.[24] As the percentage polyether in the surfactant decreased (silicone content increased), i.e. the silicone / polyether ratio varied from 0.1-1, surface tension decreased rapidly indicating greater surface activity. As a result, more bubbles were formed per unit volume (due to the surfactant reducing the bubble generation energy) exhibiting smaller cell diameters. Similar results have been observed upon increasing surfactant concentration although reduction in cell size only occurred at a critical surfactant concentration.[32] In addition, a maximum in silicone content was reached at which the foam experienced collapse thus highlighting the intimate relationship between surfactant composition and foam porosity.[24]

In a separate study[26] silicone surfactants with longer siloxane chain length produced films with lower air flow through the cell windows stated to be due to a higher surface viscosity which leads to slower drainage rate, thicker films and fewer open windows supporting the findings of Owen *et al.*[30] Zhang *et al.*[24] also showed that the longer silicone backbone length resulted in higher film elasticity along with a lower open cell window percentage. Moreover, open cell percentage has been shown to decrease with increasing surfactant concentration highlighting that over stabilisation of the polyurethane system impacts negatively on the properties of the foam such as water absorption.[32] These studies serve to show the importance of surfactant nature on cell window stabilisation and cell window opening.

1.5. Role of surfactant in aqueous foaming systems

1.5.1. The interfacial properties of thin films

Looking more broadly at surfactant stabilised foams, little theory exists in the literature describing predictive mechanisms for the behaviour of unstable, wet foams, presumably due to the difficulties involved in studying such a dynamic system (Figure 1.6).[17, 18, 33] Many previous studies of foams and foam stability have focussed on single thin films, in some cases assuming equilibrium adsorption conditions have been attained. Whilst an understanding of thin films, the building blocks of three-dimensional foams, is important, this method overlooks the key fact that foams are dynamic systems and may not have reached equilibrium. In addition, foams are not just a collection of many independent thin films, but are an interconnecting network therefore disturbance in one section of foam will inevitably impact on the remaining foam structure. Thus, the magnitude and nature of forces in both non-equilibrium foams and equilibrium thin films are likely to be very different and correlating the properties of thin films to foam has proved to be difficult. However, whilst caution should be taken when extrapolating results from thin film studies to foams they should not be dismissed as they can provide useful insights into the behaviour of foam systems. A discussion of some of the key surface properties of thin films stabilised with non-ionic surfactants and the surrounding literature is presented below.

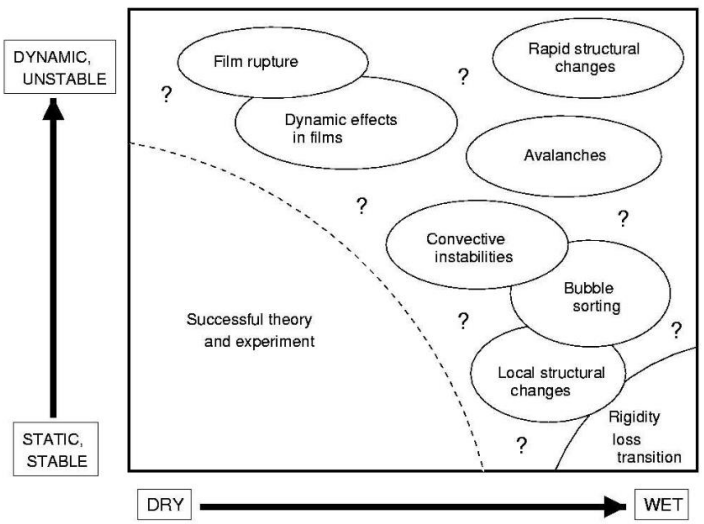

Figure 1.6; Phase diagram showing current understanding of stable / unstable and dry / wet foams.[34]

Much work of Exerowa and co-workers has involved studying the origin of the surface forces which stabilise non-ionic thin films; typically films less than 100nm in thickness.[18, 35-37] Both DLVO (Derjaguin, Landau, Vervey and Overbeek Theory) and non-DLVO contributions to stability have been determined; electrostatic and steric forces both stabilise non-ionic surfactant stabilised films.[38] DLVO theory explains the interaction of aqueous dispersions (i.e. interfaces, colloidal particles) which are electrostatically stabilised and combines van der Waals attractive forces and electrostatic repulsion. The energy potential as a function of distance between two surfaces is described in Figure 1.7. At close separation a deep energy minimum is present and the two interfaces will collide.[39]

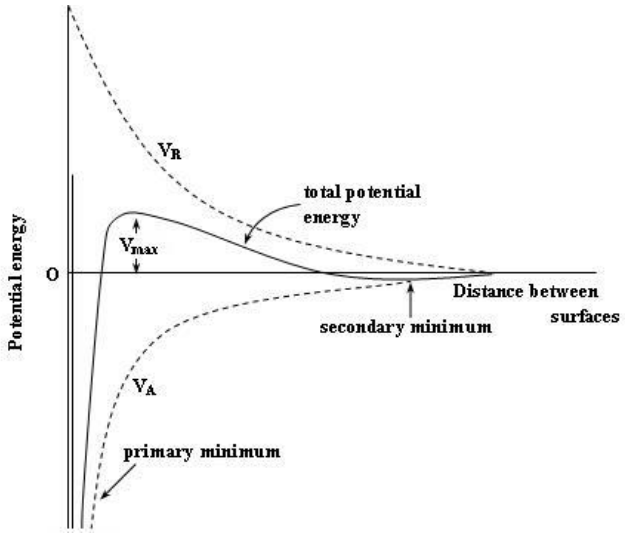

Figure 1.7; The principles of DLVO theory describing the energy potential as a function of distance between two surfaces as determined by repulsive V_R and attractive forces V_A.[40]

Non-DLVO forces describe steric interactions between surfaces which are stabilised by adsorbed polymer layers. The adsorbed polymer layers protrude into solution and preventing the surfaces from meeting due to the thermodynamic penalty involved when trying to reduce the polymer chains into a smaller volume.

Given that non-ionic surfactants are not charged species the present of DLVO forces ma may be somewhat surprising, however it has previously be shown that the air-water interface bears a slight negative charge.[41] Postulations surrounding the origin of these charges have been investigated. It is currently thought that the charges arise from the preferential adsorption of OH^- ions to the interface, however an exact mechanism for this

process is not known. For a full review of the topic see Stubenrauch *et al.*[42] Surface charge density as a function of non-ionic surfactant concentration has been studied and this demonstrated that competitive adsorption between the surfactant and OH^- ions does not take place.[43] The surface charge remained constant at low surfactant concentrations and then decreased sharply within the region of the CMC, contrary to typical surfactant adsorption.

1.5.1.1. Disjoining pressure

There are a range of studies in the literature which utilise the thin-film pressure balance technique (TFPB) to study disjoining pressure as a function of thin film thickness. The disjoining pressure describes the interaction forces between closely spaced films and is the sum of long range repulsion electrostatic (Π_{elec}), short range attractive van der Waals (Π_{vdW}) and short range repulsive steric (Π_{steric}) pressures.[38]

For thin films a transition from electrostatic to steric stabilising mechanisms has been observed for a number of polymer systems.[36, 44, 45] Schlarmann *et al.*[46] studied a range of non-ionic surfactants (β-dodecyl maltoside (β-$C_{12}G_2$), hexaethylene glycol monododecyl ether ($C_{12}E_6$), tetraethylene glycol monododecyl ether ($C_{10}E_4$)) (Figure 1.8) and determined that for all three surfactants this transition occurred upon increasing the surfactant concentration.

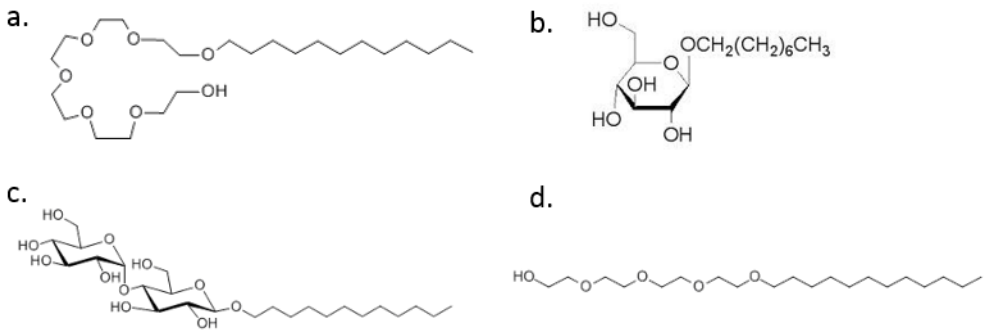

Figure 1.8; Structures of surfactants featured in this section. a) hexaethylene glycol monododecyl ether ($C_{12}E_6$), b) β-glucopyranoside (β-C_8G_1), c) β-dodecyl maltoside (β-$C_{12}G_2$), d) tetraethylene glycol monododecyl ether ($C_{10}E_4$).

This furthered the findings of a previous study focussing specifically on β-$C_{12}G_2$.[43] At low concentrations (<CMC), only *common black films* (CBF) are observed. These are stabilised by electrostatic repulsion induced by the presence of surface charge density.

The stability of these films depended on the length of the alkyl chain with a minimum length required, depending on surfactant type, to form a stable film. At concentrations above the CMC, the surface charge density is virtually zero, and a transition to *Newton black films* (NBF) was observed. Stability here is governed by the size of the head group. Perhaps, the most significant observation was that for $C_{10}E_4$ films, an increase in stability of CBF films was accompanied by a decrease in surface charge density. This induces a destabilising effect, thus demonstrating that surface charges alone cannot account for film stability.

Disjoining pressure in β-C_8G_1 (β-glucopyranoside) films was found to depend highly on surfactant and electrolyte concentration and results indicated that indeed an electrostatic double layer does exist which dominates long range interactions.[47] At the same surface charge density, two different surfactants (β-$C_{12}G_2$ and $C_{10}E_4$) displayed very different film stabilities also indicating that equal surface forces do not necessarily mean equal film stabilities. Stability must also be regulated by other factors such as surface elasticity and viscosity.

A study of Pluronic, $PEO_xPPO_yPEO_x$ ($H(OCH_2CH_2)_x(OCHCH_3CH_2)_y(OCH_2CH_2)OH$ stabilised films[38] (F108 and P85) indicated that below a critical electrolyte concentration $C_{ER,CR}$, films were stabilised via electrostatic repulsion and film thickness was independent of Pluronic concentration. However, above $C_{ER,CR}$ thicker films were formed by F108, the higher molecular weight surfactant with longer PEO chains, of which surface forces were steric in origin.[35] Similar behaviour is observed in Pluronic stabilised oil-in-water emulsions.[48] It was observed that stable films were only formed at surfactant concentrations close to full surface coverage and film thickness increased further until a plateau was reached in the region of the CMC. Of note, is that similar behaviour is typically observed in dynamic foam systems.[33] Interestingly, in a comparison of di-block and tri-block copolymers with similar molecular weights ($E_{41}B_8$, $E_{21}B_8E_{21}$ $E=CH_2CH_2O$, $B=CH(CH_2CH_3)CH_2O$) disjoining pressure isotherms indicated that the di-block copolymer produced more stable films.[44] Typically concentrations required to stabilise the tri-block films were 2-3 orders of magnitude higher than the di-block. Two reasons were postulated to explain this. Firstly, the di-block may pack better at the interface producing a smaller area per molecule. Secondly, the shorter EO chain lengths in the tri-block are just not capable of providing sufficient steric stabilisation.

Equilibrium film thickness of $C_{12}(EO)_5$ ($EO=CH_2CH_2O$) surfactant has been shown to decrease with increasing surfactant concentration and increasing electrolyte concentration suggesting that electrostatic disjoining pressure is responsible for stability.[49] In addition, these films were highly pH sensitive with a gradual decrease in film thickness in the basic pH range attributed to the suppression of the electrical double layer repulsion whilst a much sharper decrease in the acidic region implies reduction of the surface charge. Pluronic P85 thin films have also been shown to be pH dependent with thinner films that have shorter lifetimes produced at lower pH (closer to the isoelectric point).[50]

It is worth recalling that steric interactions occur at length scales that are typically twice the adsorbed layer thickness, therefore only in extremely thin bubble walls will this transition in disjoining pressures bear significant relevance. Short-range effects are likely to be negligible in foams separated by thick, viscous lamella walls.[20]

1.5.1.2. Surface elasticity and viscosity

As described in Section 1.3, for a surface to have some degree of stability it must be able to resist stresses induced from external disturbances. The mechanism by which this is achieved is known as the Gibbs-Marangoni effect. Previous studies of thin films described above determined that the surface forces normal to the film cannot solely describe film stability. Instead, it is necessary to look further at processes occurring tangential to the surface. Such mechanisms involve the surface dilational modulus, $\bar{\varepsilon}$ which describes the elasticity of the interface, and change in surface tension in response to a change in surface area i.e. when thinning occurs.

In studies of surface dilational moduli, both low frequency and high frequency elastic moduli ε are typically determined. These describe the rate at which the interface is expanded. At low frequencies, the system has sufficient time to reach equilibrium and ε tends towards zero, whereas at high frequencies the monolayer does not have time to respond and behaves as though it is insoluble. For dynamic foams, typically the high frequency modulus is expected to control fast foam breakdown process such as coalescence of bubbles whilst the low frequency modulus controls slower processes such as Ostwald ripening.[51]

In studies of $C_{10}E_4$ and β-$C_{12}G_2$ non-ionic surfactants (at concentrations below the CMC), it was determined that the higher the surfactant concentration, the smaller the low

frequency elasticity.[52, 53] Elasticity here is determined by molecular exchange as this process is faster than that of the disturbance. Conversely, the opposite was observed at high frequencies; the frequency of disturbance is higher than the frequency of molecular exchange so that the elasticity is determined by the surface excess concentration. Film stability was measured via disjoining pressure determination and DLVO theory. For $C_{10}E_4$ films, stability increased with increasing high frequency elasticity, ε_o. However, a decrease in surface charge density which destabilises the film was also seen, thus confirming that surface forces alone cannot account for stability. For β-$C_{12}G_2$, ε_o increased continuously with concentration however no increase in stability with increasing surfactant concentration was observed. Comparing both surfactants indicated that typically ε values were larger the more stable the film and that stability does not depend on surface coverage at the interface; β-$C_{12}G_2$ yielded more stable films yet had lower surface coverage values. Whilst it was concluded that more stable films appeared to correlate to higher surface elasticities, the authors acknowledge that there are still many unanswered questions, for example, is a minimum in elasticity required to produce stable films?

In similar experiments, high and low frequency elasticities of β-$C_{12}G_2$ and $C_{12}E_6$ were determined and an attempt to correlate the findings to dynamic foam structures was made.[51] Thin film results correlated to the findings of Stubenrauch *et al.*[53] β-$C_{12}G_2$ produced significantly more stable foam than $C_{12}E_6$, as quantified by the parameter $t_{1/2}$, the half-life of the foam. Interestingly, both surfactants displayed similar high frequency elasticities but β-$C_{12}G_2$ displayed a higher low frequency elasticity suggesting that it is Ostwald ripening which dominates foam stability in this case.

In the same study, two Pluronic block copolymers were also investigated (F68 and F127). In comparison to the shorter chain surfactants (β-$C_{12}G_2$ and $C_{12}E_6$), much lower high frequency Gibbs elasticity were observed for the Pluronic surfactants, however interestingly, $t_{1/2}$ was greater than that of $C_{12}E_6$ which had a much lower low frequency elasticity. Intermediate foam stability was observed attributed to slower Ostwald ripening but faster film rupture. Pluronic foams began to gradually deplete after only a short period of time unlike the short chain surfactants which remained stable and then broke down almost immediately. The results described are once again, qualitative and the authors themselves state that it is "not obvious to compare different surfactant families without a

detailed knowledge of the foam evolution." Whilst steps were taken to minimise issues when measuring elasticity such as the possibility of surface / bulk exchanges, the paper highlights the difficulties encountered when comparing dynamic foams to thin films.

The surface rheology of a series of Pluronic surfactants has been studied, with the surface dilational modulus $\bar{\varepsilon}$, the surface elasticity ε and the surface viscosity η measured as a function of time.[54] As the value of ε was so large in comparison to η, $\bar{\varepsilon}$ was considered to be equal to ε. $\bar{\varepsilon}$ was independent of concentration, only depending on the surface pressure value thus indicating that any changes in $\bar{\varepsilon}$ are only due to the rearrangement of molecules at the interface and not molecular exchange. From surface pressure versus $\bar{\varepsilon}$ plots, conformational changes at the interface could be determined. Attempts have been made[55] to compare surface elasticity with previous foam stability studies performed on the same surfactants[56]. The authors cautiously state there may be a link between the lower stability of P85 and its lower ε value however this is not conclusive within the error of the data. In addition, the maximum ε values obtained (19mNm^{-1} for F88 and 11mNm^{-1} for P85) also appear to correlate to stability with F88 producing the more stable foam. Much more investigation is involved before quantitative conclusions can be drawn.

Using oscillating bubble methods, Fruhner *et al.*[57] studied a range of ionic and non-ionic surfactant stabilised films and determined that the dilational surface viscosity does correlate to thin film stability. Conversely, no direct relationship between surface dilational elasticity values and film stability could be determined. At very low concentrations far below the CMC, film lifetimes were non-existent and dilational surface viscosity κ equalled zero. Focussing specifically on the non-ionic surfactant Triton X-100 ($C_{14}H_{22}O(C_2H_4O)_n$), film lifetime increased from <5sec to >3000s over a relatively small concentration increase of 2.4x10^{-4}M. Across this range surface dilational viscosity was also measureable suggesting that higher values of dilational viscosity of the adsorbed layers produce more stable thin films.

These findings agree with a much earlier study which employed an adapted viscometer to study surface viscosity.[58] Surface viscosity was compared to three-dimensional foam stability. It was qualitatively concluded that those systems which yielded higher surface viscosities, i.e. more coherent surface films gave the most stable foams. However, it was not possible to give a detailed correlation. Stubenrauch *et al.*[53] concluded that both surface

elasticity and surface viscosity pass through a maximum as surfactant concentration is increased (Figure 1.9). As concentration is increased at low concentrations, the surface coverage Γ is increased leading to higher elasticity and viscosity. However, at higher concentrations surface tension gradients are not removed immediately due to increased molecular exchange between bulk and surface so that the elasticity tends to zero. Indeed, the authors state that further data is required to give complete correlations between surface forces, theoretical models and film stability.

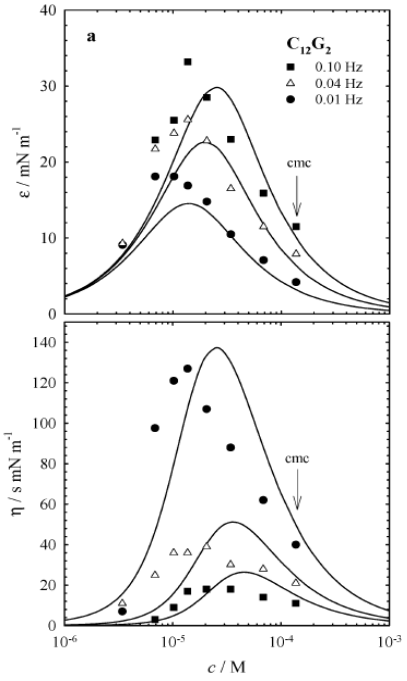

Figure 1.9; Dilational surface elasticities ε and viscosities η as a function of concentration for β-$C_{12}G_2$.[53]

1.5.1.3. Thinning and drainage

The drainage of films and foams stabilised with block co-polymers have been studied using a variety of methods. For a full review of the subject see Manev and Nguyen.[59] Typically electrolyte is added to the systems to produce a specific type of film (CBF or bilayer film BF). A schematic diagram to show the main processes in the draining of a thin film is presented in Figure 1.10. A study of Pluronic stabilised foams indicated that for foams stabilised with F108, drainage under gravity was slow and there was little dependence on the type of foam film involved.[60] However, when a pressure drop of 5000Pa was applied, the BF foam drained much faster than the CBF foam. This was attributed to lower water content in the plateau borders of the BF foam. Similar findings

i.e. faster drainage and lower final water content have been observed for P85 foams.[61] In foam lifetime versus applied pressure curves, a plateau was reached for CBF foams corresponding to the presence of steric surface forces. This increased with increasing length of the EO chain thus foams of F108 were more stable than P85.[60]

Simulescu *et al.*[62] studied the thinning and critical thickness of non-ionic surfactant mixtures and determined that below the CMC critical thickness decreased with increasing surfactant concentration which corresponded to a slower drainage rate whilst the opposite was observed on approach to the CMC. Similar findings were observed in studies of poly(propylene glycol) $H(OCCH_3CH_2)OH$ stabilised thin films.[63] In addition, the interaction forces, describing the interaction between two gas phases, monotonically decreased with increased surfactant concentration.

The drainage of non-ionic and ionic surfactants and their mixtures has been studied and compared to theoretical models for film drainage.[64] Thin films of β-$C_{12}G_2$ showed regular thinning consistent with classical models. Emulsions stabilised with the non-ionic surfactants Tween 20 and Span 20 displayed varying film lifetimes in which Tween 20 lifetimes were much longer and more stable.[65] Measured adsorption isotherms indicated that Tween 20 exhibited much higher adsorption at lower concentrations and the interfacial tension continued to decrease even above the CMC. This demonstrates the importance of surface activity in film lifetime.

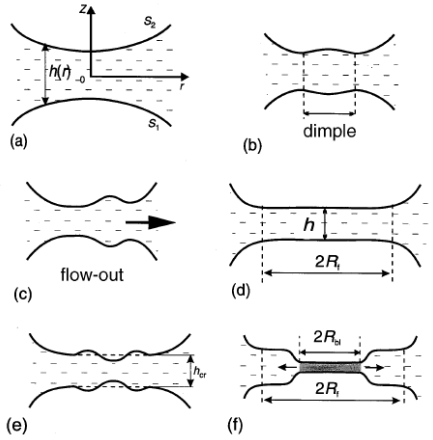

Figure 1.10; The stages of thinning of a thin liquid film; a) approach of films, b) below the thickness of film formation a dimple in the film is formed, c)dimple flow out, d) thinning of plane parallel film, e) at a critical thickness h_{cr}, a transition to a thin black film may occur, f) expansion of the black film.[65]

The gravitational drainage of Pluronic P123 films indicated that at concentrations above the CMC there was no difference in film lifetime or drainage rate however the surface elasticity (calculated from the film lifetime) decreased with increasing concentration above the CMC.[66] Elasticities compared well to previous literature. Arabadzhieva *et al.*[67] studied the effects of premicellar aggregates on film drainage for $C_{12}E_4$ stabilised films. Within an intermediate concentration regime, consistent with "kinks" in the surface tension data for these systems, a series of minima and maxima were observed in surface dilational elasticity data attributed to the formation of premicelles. These premicellar regions were found to stabilise the draining thin films by providing a reservoir of additional surfactant that can adsorb to the interface (Figure 1.11).

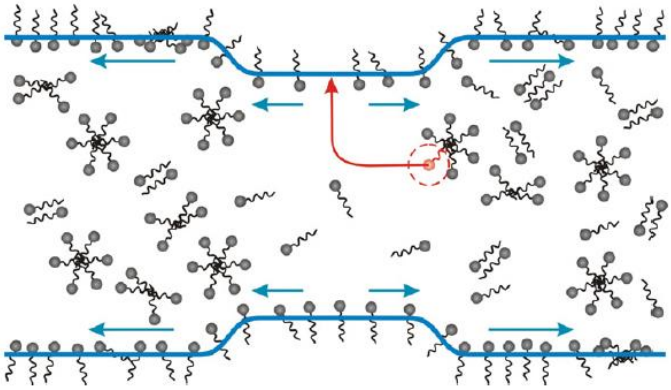

Figure 1.11; The impact of premicellar structures on the drainage kinetics of foam film.[67]

It was in the early part of the 20th century that it was determined by Johonnott[68] and Perrin[69] that organised molecular structures can form within thin films at surfactant concentrations above the CMC. This leads to a process known as *stratification* in which thin films drain in a step-wise manner. Wasan and co-workers[70-73] have extensively researched stratification in thin films and determined its occurrence in films stabilised with ionic and non-ionic surfactants. The colloidal structures pack in a layer by layer fashion into the restricted volume of the film. The step-wise decrease in film thickness is due to the formation of dark spots (areas of lower thickness) and the driving force of this stepwise thinning has been attributed to chemical potential gradients of micelles at the film periphery. Much of the work has focussed on thin films so the applicability of stratification in thick foam films is unclear. For a review of the subject see Wasan and Nikolov.[74]

1.5.2. Thin film properties and the foaming of non-ionic surfactants

A plethora of studies are present in the literature relating foaming to the surface properties found in thin films; for example surface elasticity or viscosity and how these properties influence the breakdown mechanisms of the foam such as drainage time, film rupture and bubble coalescence. There are numerous papers regarding ionic surfactants, in particular the anionic surfactant sodium dodecyl-sulfate (SDS)[75-83] and the cationic surfactant cetyltrimethyl ammonium bromide (CTAB).[84-89]

In analysis of foaming behaviour many authors have attempted to correlate foaming behaviour to the interfacial properties of the foams. Thin liquid film pressure balance techniques and foam pressure drop techniques have been used to determine the role of foam films in the stability of foams stabilised with Pluronics P85 and F108.[60] A plateau observed in the film thickness versus applied pressure curves was assigned to the sterically stabilised disjoining pressure component. The effect of steric surface forces increases with increasing length of the poly(ethylene oxide) PEO chain therefore F108 produced the most stable films which also translated into more stable foams.[90] Thus parallels between single thin film properties and foam are demonstrated. Using both foam pressure drop techniques and the FoamScan apparatus, the foaming of Pluronic P85 and F88 block copolymers has been studied.[56] Equal foamability was observed and the changes in foam volume (V_{foam}) and foam liquid content (V_{liquid}) were seen with time. Up to 580s after foam formation, there was minimal change in V_{foam}, however V_{liquid} changed significantly indicating that drainage dominates foam depletion. Above 800s, V_{foam} decreased significantly whereas only a slight decrease in V_{liquid} was seen. Foam drainage is thus no longer responsible for foam decay, rather film rupture affects foam lifetime in this regime. The authors state that under the conditions specified, a thin bilayer film (BF) foam is expected which are stabilised by steric interactions. The larger the surfactant, the thicker the BF, the more stable the foam and this was confirmed by much more stable foams of F88.

Stubenrauch *et al*.[91] used Foam Conductivity Apparatus to study the stabilities of $C_{12}E_6$ and β-$C_{12}G_2$ surfactants and established that foam stability must be driven by the coalescence of bubbles (foams had similar liquid fractions, bubble sizes and therefore drainage rates and the timescale of the experiment eliminated Ostwald ripening effects).

In a separate study by the group, foaming of dodecyl(dimethyl) phosphine oxide (C_{12}DMPO), C_{12}TAB and their mixtures were investigated.[92] Whilst these surfactants differ in the fact that the former is non-ionic and the latter is ionic, they exhibit a similar structure; both have a hydrophobic C_{12} chain and comparable molecular weights (246 and 308gmol^{-1} respectively). Similar drainage behaviour was observed attributed to the similarity of surfactant structure and bulk viscosities. The liquid fraction ε_{crit} at which film rupture occurred was found to be independent of foam height and bubble size however the timescales over which ε_{crit} occurred increased with decreasing bubble size.

A link between surface elasticity and stability has been determined with a larger value of high frequency elasticity ε_o correlating to more stable foam.[91] This agreed with the findings of Georgieva *et al*.[51] who postulated that low frequency elasticity controls Ostwald ripening whilst high frequency elasticity controls bubble coalescence. The Gibbs elasticity of poly(propylene glycol) (M_w=400gmol^{-1}) and various surfactants increased linearly with foam stability however variations in gradients for the different surfactants indicated that elasticity alone cannot solely account for foam stability and that disjoining pressure also contributes an important role.[93]

The foaming behaviour of commercial polyoxyethylene glycol esters with varying ethylene oxide units (EO=2 and 17) also showed apparent correlations to surface properties.[94] Similar dilatational viscosities were observed and this correlated to similar foamability however greater foam stability and smaller bubble sizes corresponded to the more hydrophilic surfactant (EO=17). This surfactant exhibited higher surface dilatational elasticity. The bubble coalescence time of PPG (M_w=425gmol^{-1}) surfactants has been shown to increase with concentration until at a specific concentration a reduction in coalescence time is observed.[95] No correlation to surface tension was seen however longer coalescence times at higher concentrations were attributed to faster adsorption kinetics. Bubble coalescence of Tween stabilised systems have been shown to correlate well with foam height tests.[96] Bubble coalescence time increased with increasing surfactant concentration, attributed to the steric stabilisation provided by the hydrophilic polyoxyethylene groups. Qualitative comparisons were made to surface viscosity which increased with surfactant concentration and related to the surface excess concentration. In addition, Marangoni effects were predicted to be most prominent when the maximum rate of surface tension $(\delta\gamma/\delta t)_{max}$ decrease is large. $(\delta\gamma/\delta t)_{max}$ decreases with increasing

hydrophobic portion of surfactant and increases with increasing hydrophilic segment. Marangoni effects were therefore greatest for foams of Tween 20, the most hydrophilic surfactant studied, and it was this surfactant that stabilised the system most effectively.

Buzzacchi *et al*.[97] determined a link between foam formation and dynamic surface tension values recorded at 100ms. Drainage behaviour was also determined to be strongly dependent on surfactant diffusion from bulk to interface. Tan *et al.*[98] studied the foamability of a series of poly(propylene glycol) surfactants and determined that maxima in foamability were always observed with concentration. This was attributed to Marangoni effects and diffusion kinetics of the surfactant to the interface. Tamura *et al.*[99] also investigated dynamic surface tension and foaming behaviour for a series of $C_{12}EO_n$ surfactants. Initial foam height increased linearly up to n=11 and then plateaued at greater EO units. Conversely, residual foam height decreased with increasing EO units. Over longer timescales (>1s) the meso-equilibrium surface tension γ_m increased with increasing EO units and this was attributed to the cross section occupied by the molecules at the interface. The dynamic surface tension γ_t however decreased with increasing EO units – essentially those surfactants with larger CMC increase the adsorption at the air water interface more effectively than those with lower CMC. $(d\gamma_t/d_t)_{max}$ correlated well to initial foam height whilst residual foam height correlated to $L_{lamellae}$ (the degree of lamellae elongation) which describes the stability of the lamellae under stress. It can therefore be concluded that different requirements are needed for good foamability and good foam stability and Marangoni effects are important. Faster adsorption kinetics and a surface of low rigidity are required to form foam however, for drainage to be slowed a more rigid surface is necessary. A balance of these two properties is therefore essential for producing optimum foam.

1.5.3. Foaming of non-ionic surfactants

The foaming of non-ionic surfactants has been largely neglected due to the fact that they are considered to be comparatively poor foamers.[100] As non-ionic surfactants are studied in this work, the following literature will be based on the foaming on non-ionic surfactants.

1.5.3.1. Concentration effects

Foaming behaviour as a function of surfactant concentration will firstly be discussed. Surfactant concentration is one of the few controllable variables in the manufacture of polyurethane foams. Foams formed from a range of Tween surfactants in water have been studied using the Ross-Miles method.[96] This method involves dropping aliquots of solution from a specific height into the bulk surfactant solution generating foam in order to measure initial foam height. At high surfactant concentrations, greater initial foam heights were obtained indicating that foam formation increased with increasing surfactant concentration.

Analogous findings were observed for Pluronic foams[90] as well as in a study of $C_{12}E_6$ and β-$C_{12}G_2$ and their 1:1 mixtures.[91] Both foamability and stability increased with increasing surfactant concentration. For the 1:1 mixture, foaming was dominated by the less foaming surfactant $C_{12}E_6$ indicating that a mixture of surfactants doesn't necessarily lead to intermediate foaming behaviour. Similar trends were observed in the foaming of Triton X100 surfactant.[100] A monotonic increase in foam height was observed with the decrease in foam height versus concentration slope occurring after 0.15% concentration. This plateau corresponded to eight times the CMC. However in a study of polyoxyethylene dodecyl ether foams, a maximum in initial foam volume was observed at a specific concentration, whilst foam stability continued to increase with increasing concentration.[101] Here, a wide concentration regime (0.1-35wt%) was studied therefore at the highest concentrations, viscosity effects will also become significant. Whilst higher viscosity promotes foam stability to an extent by decreasing the drainage rate, too high and the diffusion rate of surfactant to the interface will be compromised.[17]

Interestingly, for a series of Brij non-ionic surfactants, the initial foam height (describing the foamability) of Brij 35 (the surfactant with largest number of hydrophilic epoxy groups present of all studied) showed no increase above 0.015mol/m^3 however the residual foam height (defining foam stability) did increase quite significantly thus showing that higher surfactant concentrations can improve foam stability but do not necessarily improve foaming ability.[102] A maximum in foam stability with concentration has also been observed for a variety of "frothers" including PPG (Mw=400gmol^{-1}). Of the surfactants studied, those with larger hydrophilic-lipophilic balance (HLB) values and larger molecular weight produced more stable foam.[93] The importance of concentration

on surfactant phase behaviour and subsequently foaming has been demonstrated in a study of aqueous solutions of PPG surfactants of various molecular weight.[103] Two distinct regions in concentration versus foam retention time plots were seen (Figure 1.12); an initial increase with concentration culminating in a plateau, denoted C1 and a decrease in foam retention time upon further increasing the concentration, denoted C2. Comparison to adsorption isotherms indicated that C1 corresponded to monolayer surface coverage at the interface whilst the decrease in foaming at C2 was attributed to the solubility limit of PPG in water. Clearly, surfactant concentration, which defines the phase behaviour of the surfactant in solution, has important consequences for foaming.

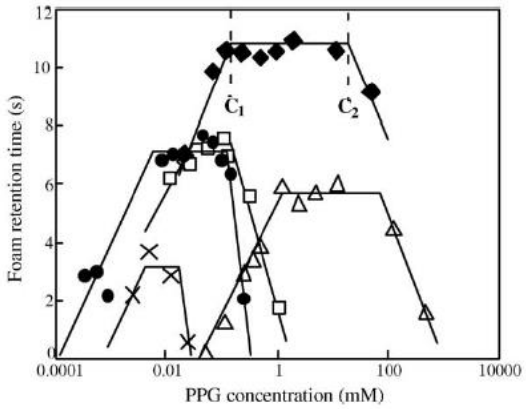

Figure 1.12; Foam retention time as a function of concentration for foams stabilised with varying molecular weight poly(propylene glycols).[103]

This is further illustrated in a dynamic foam study of Pluronic surfactants.[104] Foamability as a function of concentration was highly dependent on surfactant solubility. An increase in foam height for the least soluble surfactant, PE10100 which has the highest molecular weight and lowest cloud point was observed however for the most soluble surfactant PE6100 the reverse was true. At concentrations below 0.01% where no phase separation occurs, foamability increased with cloud point (Figure 1.13).

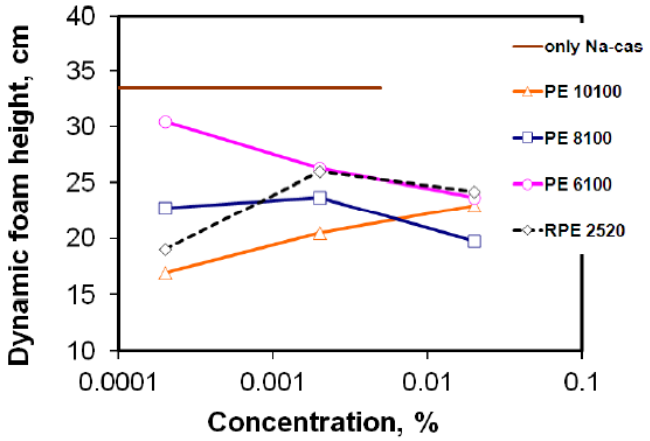

Figure 1.13; Dynamic foam height as a function of concentration for a range of Pluronic surfactants.[104]

1.5.3.2. Surfactant structural effects

Typically non-ionic surfactants are available as homologous series where changes in the molecular weight or ratio of the hydrophobic and hydrophilic blocks induce very different surface active properties, inevitably impacting on foaming. Of the Tween family of surfactants, Tween 20, the most hydrophilic surfactant of those studied, produced the greatest initial foam height.[96] This was attributed to its faster adsorption rate and smaller area per molecule at the interface. Similar results were observed in a study of Brij surfactants.[102] Comparing across a series, faster adsorption rates are typically observed for those surfactants across a series with the largest CMC,[99] therefore Brij 35, with the largest CMC produced the greatest initial foam height. Polyoxyethylene alkyl ethers (C_nE8) displayed analogous behaviour.[105] Initial foamability increased with decreasing length of the hydrocarbon chain, postulated to be due to increased monomer concentration. In addition, faster rates of dynamic surface tension ($\delta\gamma/\delta t$) were observed for the smallest hydrocarbon chain lengths indicating faster adsorption to the interface. Conversely, the stability of $C_{12}EO_n$ surfactants (where n=3-9) was greatest for the most hydrophobic surfactant studied $C_{12}EO_3$.[101] Enhanced stability was evident when lamellar liquid crystals were present indicating the important of the surfactant phase on foaming behaviour. For PPG surfactants, foaming was found to be a balance between surface activity and kinetics. The highest molecular weight PPG ($4000 gmol^{-1}$) displayed the lowest surface tension values i.e. it is more surface active, however the diffusion rate to the interface was much slower therefore foam was more unstable. Conversely, the lowest

molecular weight PPG (192gmol^{-1}) was also a poor foamer due to fast diffusion but low surface activity.

Specifically focussing on tri-block Pluronic surfactants in comparison to other non-ionic smaller molecular weight surfactants such as $C_{12}G_2$ and $C_{12}E_6$, Pluronic surfactants have been shown to display intermediate foam stability.[51] At bulk concentrations just below the CMC, the foam half-life for F68 ($PEO_{29}PPO_{76}PEO_{29}$) and F127 ($PEO_{100}PPO_{65}PEO_{100}$) has been determined to be 95 and 195 minutes respectively when foams were formed using a turbulent mixing procedure.[51] Here, it was the larger, more hydrophobic surfactant F127 which produced the more stable foam. In a separate study[56], P85 ($PEO_{26}PPO_{39}PEO_{26}$) and F88 ($PEO_{103}PPO_{40}PEO_{103}$), which have comparable PPO block sizes but differing PEO block sizes, displayed similar foamability at equimolar concentrations below the CMC. However F88 with its longer PEO blocks produced more stable foam suggesting that it is the PEO blocks which provide stabilisation presumably through long range steric interactions. Similar findings were observed in a study of the antifoaming properties of Pluronics on bovine serum albumin in which L62 ($PEO_6PPO_{33}PEO_6$) the lower molecular weight surfactant produced less stable foam than F68.[106] This was correlated to the length of the PEO chain, with the larger chain length of F68 again providing stabilisation.

1.5.3.3. Surfactant phase behaviour

PEO-PPO-PEO surfactants are highly temperature sensitive, with phase behaviour differing widely over seemingly small temperature ranges. This is typically the case for other non-ionic surfactants. Foam behaviour of Triton X100 surfactant has been investigated as a function of temperature (maximum temperature studied 37°C, was significantly below the cloud point of 65°C).[100] Initial foam heights increased modestly with a temperature change of approximately 30°C, whilst a reduction in foam stability was observed. At higher temperatures the polyoxyethylene (POE) moiety present, became less hydrated so that the radius of gyration (R_g) decreased, viscosity decreased and the drainage rate was faster, accounting for reduced foam stability. In contrast, poorer hydration means that the POE moiety displayed reduced solubility at higher temperature, becoming more surface active therefore producing a greater initial volume. Foaming typically increases significantly at the onset of micellisation and maximum foaming is seen at the CMC due to the increased surface activity of the surfactants.[107, 108] In addition,

a reduction in foam stability is normally observed above the cloud point of the surfactant and it has been proposed that this is as a result of the surfactant rich phase acting as an antifoam.[109] Thus the phase of the surfactant is important for foaming behaviour and this needs to be considered when describing the foaming of PEO-PPO-PEO surfactants.

1.6. Small-angle neutron scattering studies of foams

Neutron techniques have proven to be a useful tool to probe the adsorption of molecules at interfaces. It has long been known that it is the nature of the adsorbed surfactant layer which contributes to foaming behaviour. Pankhurst as early as 1941 stated that "it is not the low surface tension per se [of surfactants] that ensures stability, but the nature of the adsorbed layer giving rise to the lowering of surface tension."[110]

Small-angle neutron scattering has been used previously to probe the structure of stabilisers at foam interfaces. The most sophisticated studies were presented by Axelos and Boue and co-workers[111, 112] where they studied a series of foams formed from an aqueous solution of the anionic surfactant sodium dodecyl-sulfate (SDS) (Figure 1.14). A 22cm high, 30mm diameter Plexiglas cylinder foam column was constructed with quartz windows to accommodate the neutron beam. Both free draining dry foams and steady state wet foams were studied. Under steady-state foaming conditions, foams yielded a characteristic scattering pattern comprising a pronounced Q^{-4} dependence, with a number of superimposed peaks or "bumps". The Q^{-4} dependence at low Q was consistent with a well-defined structure (such as that from an air-liquid interface) from which the average bubble size could be determined.

For both wet and dry foams a peak was observed at Q ~ 0.15Å which corresponded to the same position as that of the bulk solution scattering. At 25g/L bulk surfactant concentration is well above the reported CMC of 2.3g/L. This suggested that there was a considerable contribution to the foam scattering from SDS micelles present in solution. In wet foams this peak is not unexpected; arising from solution situated within the bubble lamellae walls. Whilst the Plateau borders are much thinner in dry foams, the authors suggested that they still contain enough liquid to produce sufficient scattering. Upon suppressing the contrast between surfactant and solvent (d-SDS in D_2O) the peak

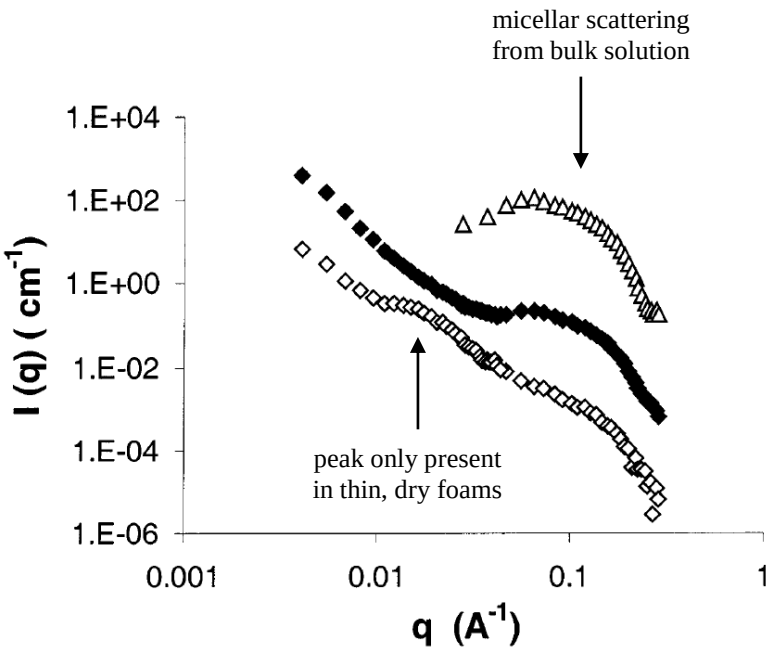

Figure 1.14; Small angle neutron scattering from foams stabilised with SDS [25g/L>>>CMC]; steady state wet foams during bubbling (closed diamonds), foam during drainage (closed diamonds) and bulk SDS solution (triangles).

disappeared, interpreted as originating from surfactant dispersed in solution. For only well drained, dry foam, an additional peak was present in the scattering data at an intermediate Q value of 0.027Å, regardless of SDS concentration. The authors determined that this cannot be due to surfactant structures present within the bulk solution as the dimensions are inconsistent with this. The peak was still present upon suppressing the contrast between surfactant and solvent. Thus the authors attributed this peak to parallel air-liquid interfaces which describe the lamellae thickness of the bubbles. Depending on concentration, an average film thickness of 160-180Å was obtained. Intuitively, this seems rather small and implies that the film must be extremely thin with little liquid present within the walls.

In addition, anisotropic measurements revealed spikes in the 2D scattering data, the origin of which were probed further in neutron reflection experiments involving bamboo foam structures.[113, 114] These are stacks of parallel surfactant films within a tube, linked together by a wetting film along the wall of the tube. Although Plateau borders of individual films are not connected, processes such as coalescence, drainage and film rupture can still occur therefore providing a better representation of the foam than a single thin film. Distinct

oscillations were observed over a wide Q range in the scattering plot consistent with Q^{-4} decay. Fringes were observed in the scattering curve and are suggested to be as a result of film curvature due to pressure differences at the surface of the films. The study shows the feasibility of using such methods to study foam systems.

More recently, foams stabilised with polyglycerol ester PGE 55 has been explored using small-angle neutron scattering.[115] Here a much greater bulk surfactant concentration was used (10wt%) with solution scattering previously confirming the presence of ordered multi-lamellar structures in solution. No difference was observed between bulk solution scattering and foam scattering implying that stability is dominated by multi-lamellar interfacial films. Unlike the SDS foams studied in which much lower concentrations were studied, it may be the case that the large interfacial structures observed here dominate scattering so that additional features in the foam data are masked.

1.7. Project aims

To summarise, the current literature indicates that surfactant stabilised foams are highly complex and their behaviour is governed by the nature of the surfactant itself, for example, structure and relative hydrophobicity/ hydrophilicity. Thus it is difficult to translate observations from one surfactant system to another and a detailed understanding of the foaming of the homologous surfactant series of interest in this work is required. The few small-angle neutron scattering studies of foams available suggest it is a feasible technique to study the adsorbed surfactant layer in non-ionic surfactant stabilised foams. With regards to polyurethane foam, previous work shows that the structure and performance of polyurethane foam is indeed highly dependent on the surface activity of the surfactant and the surface properties induced.

By adopting a model system of surfactant stabilised air-in-water foams and studying the fundamental chemistry of these systems, the aim of this research is to elucidate how differences in surfactant properties such as structure and hydrophobicity / hydrophilicity influence foam behaviour and the nature of the adsorbed surfactant layer. Through appropriately selected experiments on a PU foam production line, the aim is to translate the fundamental surfactant behaviour to PU foam behaviour and structure, designing appropriate methodology in which PU foam with optimum properties is formed. Although the effects of the monomer component are neglected in this instance, as water is the main

solvent in the polyurethane system it should nonetheless provide a suitable starting point to characterise the polyurethane systems.

Key challenges and aims of the project include;

- Characterising the foaming behaviour for a series of non-ionic polymeric surfactants in a model aqueous solution based on surfactant structure, surfactant concentration and solution temperature.
- Relating the foaming behaviour to surfactant phase behaviour. This will involve determining critical micellisation parameters using equilibrium and dynamic surface tension methods.
- Designing and validating suitable apparatus that allows foams to be studied using small-angle neutron scattering (SANS), giving insight into the nature of the adsorbed surfactant layer at the air-water interface.
- Designing experiments to be performed on a PU manufacturing line that will allow the determination of key parameters which produce PU foam with optimum properties.

1.8. References

1. National Prescribing Centre, *MeReC Bulletin*, 2010, **21**, vol.1, 1-7.

2. NHS Business Services Authority, *Wound Management National Charts*. [Online] Accessed 15.9.2014, Available at; http://www.nhsbsa.nhs.uk/PrescriptionServices/Documents/PPDPrescribingAnalysisCharts/Wound_Management_National_Feb_2014.pdf.

3. S. Thomas, *Surgical dressings and wound management*, Medetec, Cardiff, UK, 2010.

4. G. D. Winter, *Nature*, 1962, **193**, 293-294.

5. K. F. Cutting, *Journal of Wound Care; Sorbion Supplement*, 2010, **19**, 4-9.

6. *Sentry Medical*, [Online] Accessed 26.6.2013, Available at; http://www.sentrymedical.com.au/products/advanced-wound-care-dressings/suprasorb-p-sterile-pu-foam-non-adhesive-self-adhesive-moderately-exuding-superficial-wounds/.

7. G. Woods, *Flexible polyurethane foams; chemistry and technology*, Applied Science Publishers Ltd, Essex, UK, 1982.

8. M. J. Forrest, *Chemical characterisation of polyurethanes*, Rapra Technology Ltd, Shrewsbury, UK, 2001.

9. R. Herrington, R. Broos and P. Knaub, *Polymeric foams and foam technology*, 2nd edn., Carl Hanser Verlag, Munich, Germany, 2004.

10. T. Thomson, *Design and applications of hydrophilic polyurethanes*, CRC Press, Florida, USA, 2000.

11. D. L. Bailey, F.M. O'Connor, 1958, *Siloxane-oxyalkylene block copolymers*, USA Pat. 2834748.

12. R. E. Moeller, 1978, *Polysiloxane surfactants useful for foaming polyurethane foams*, USA Pat. 4081410.

13. R. A. Budnik, C. H. Blevins, G. J. Murphy, W. Grabowski, R. L. Cobb, 1992, *Surfactants for manufacture of urethane foams*, USA Pat. 5145879.

14. Z. Gu, L. Feng, W. Zhang, P. Austin, 2009, *Polyurethane foams containing silicone surfactants*, USA Pat. 8044109.

15. A. Stocco, E. Rio, B. P. Binks and D. Langevin, *Soft Matter*, 2011, **7**, 1260-1267.

16. B. P. Binks and T. S. Horozov, *Angewandte Chemie-International Edition*, 2005, **44**, 3722-3725.

17. R. J. Pugh, *Advances in Colloid and Interface Science*, 1996, **64**, 67-142.

18. D. Exerowa, P. M. Kruglyakov, *Foam and Foam Films; Theory, Experiment, Application*, Elsevier, Amsterdam, NL, 1998.

19. Y. H. Kim, K. Koczo and D. T. Wasan, *Journal of Colloid and Interface Science*, 1997, **187**, 29-44.

20. K. Malysa and K. Lunkenheimer, *Current Opinion in Colloid & Interface Science*, 2008, **13**, 150-162.

21. G. Rossmy, H. Kollmeier, W. Lidy, H. Schator and M. Wiemann, *Journal of Cellular Plastics*, 1977, **13**, 26-35.

22. Y. Zhang, C.W. Macosko, H.T. Davis, *Polymeric Foams: Science and Technology*, 1997, **669**, 130-142.

23. R.E. Stevens, G.P Dado, M.J. Kimock, M.L. Listemann, *Journal of Cellualr Plastics*, 1999, **35**, 69-91.

24. X. D. Zhang, C. W. Macosko, H. T. Davis, A. D. Nikolov and D. T. Wasan, *Journal of Colloid and Interface Science*, 1999, **215**, 270-279.

25. A. Aneja and G. L. Wilkes, *Journal of Applied Polymer Science*, 2002, **85**, 2956-2967.

26. K. Yasunaga, R. A. Neff, X. D. Zhang and C. W. Macosko, *Journal of Cellular Plastics*, 1996, **32**, 427-448.

27. X. D. Zhang, H. T. Davis and C. W. Macosko, *Journal of Cellular Plastics*, 1999, **35**, 458-476.

28. T. C. Kendrick, B. M. Kingston, N. C. Lloyd and M. J. Owen, *Journal of Colloid and Interface Science*, 1967, **24**, 135-140.

29. M. J. Owen, T. C. Kendrick, B. M. Kingston and N. C. Lloyd, *Journal of Colloid and Interface Science*, 1967, **24**, 141-150.

30. M. J. Owen and T. C. Kendrick, *Journal of Colloid and Interface Science*, 1968, **27**, 46-52.

31. S. A. Snow, U. C. Pernisz and R. J. Braun, *Silicon Chemistry*, 2005, **3**, 1-10.

32. C. S. Sipaut, N. Ahmad, R. Adnan, I. A. Rahman and M. N. M. Ibrahim, *Cellular Polymers*, 2010, **29**, 1-22.

33. M. Rosen, *Surfactants and interfacial phenomena*, 2nd edn., Wiley, New York, USA, 1989.

34. D. Weaire, S. Cox, K. Brake, Liquid Foams. In; M. Scheffler and P. Colombo, eds. *Cellular Ceramics*, Wiley, Weinheim, 2005.

35. D. Exerowa, R. Sedev, R. Ivanova and T. Kolarov, *Colloids and Surfaces A: Physicochemical and Engineering Aspects*, 1997, **123**, 277-282.

36. D. Exerowa, N. V. Churaev, T. Kolarov, N. E. Esipova, N. Panchev and Z. M. Zorin, *Advances in Colloid and Interface Science*, 2003, **104**, 1-24.

37. D. Exerowa, N. V. Churaev, T. Kolarov, N. E. Esipova and S. V. Itskov, *Colloid Journal*, 2006, **68**, 155-161.

38. R. Sedev and D. Exerowa, *Advances in Colloid and Interface Science*, 1999, **83**, 111-136.

39. T. Cosgrove ed, *Colloid Science: Principles, methods and applications*, Wiley, West Sussex, 2010.

40. University of Washington, *Electrostatic Stabilisation*, [Online] Accessed 20.5.2015. Available at; http://depts.washington.edu/solgel/pages/courses/MSE_502/Electrostatic_Stabilization.html

41. D. Exerowa, *Kolloid-Zeitschrift and Zeitschrift Fur Polymere*, 1969, **232**, 703-710.

42. C. Stubenrauch and R. von Klitzing, *Journal of Physics-Condensed Matter*, 2003, **15**, R1197-R1232.

43. C. Stubenrauch, J. Schlarmann and R. Strey, *Physical Chemistry Chemical Physics*, 2002, **4**, 4504-4513.

44. B. Rippner, K. Boschkova, P. M. Claesson and T. Arnebrant, *Langmuir*, 2002, **18**, 5213-5221.

45. D. Exerowa, T. Kolarov, I. Pigov, B. Levecke and T. Tadros, *Langmuir*, 2006, **22**, 5013-5017.

46. J. Schlarmann and C. Stubenrauch, *Tenside Surfactants Detergents*, 2003, **40**, 190-195.

47. C. Marquez-Beltran and D. Langevin, *Journal of Colloid and Interface Science*, 2007, **312**, 47-51.

48. G. Gotchev, T. Kolarov, K. Khristov and D. Exerowa, *Advances in Colloid and Interface Science*, 2011, **168**, 79-84.

49. E. D. Manev and R. J. Pugh, *Langmuir*, 1991, **7**, 2253-2260.

50. M. Krasowska, E. Hristova, K. Khristov, K. Malysa and D. Exerowa, *Colloid and Polymer Science*, 2006, **284**, 475-481.

51. D. Georgieva, A. Cagna and D. Langevin, *Soft Matter*, 2009, **5**, 2063-2071.

52. E. Santini, F. Ravera, M. Ferrari, C. Stubenrauch, A. Makievski and J. Kraegel, *Colloids and Surfaces a-Physicochemical and Engineering Aspects*, 2007, **298**, 12-21.

53. C. Stubenrauch and R. Miller, *Journal of Physical Chemistry B*, 2004, **108**, 6412-6421.

54. B. R. Blomqvist, T. Warnheim and P. M. Claesson, *Langmuir*, 2005, **21**, 6373-6384.

55. C. Stubenrauch, B. Rippner Blomqvist, Foam Films, Foams and Surface Rheology of Non-ionic Surfactants. In; T. F. Tadros, ed. *Colloid Stability; The role of surface forces - Part 1*, Wiley, Germany, 2007.

56. B. R. Blomqvist, S. Folke and P. M. Claesson, *Journal of Dispersion Science and Technology*, 2006, **27**, 469-479.

57. H. Fruhner, K. D. Wantke and K. Lunkenheimer, *Colloids and Surfaces A: Physicochemical and Engineering Aspects*, 2000, **162**, 193-202.

58. A. G. Brown, W. C. Thuman and J. W. McBain, *Journal of Colloid Science*, 1953, **8**, 491-507.

59. E. D. Manev and A. V. Nguyen, *International Journal of Mineral Processing*, 2005, **77**, 1-45.

60. K. Khristov, B. Jachimska, M. Kazimierz and D. Exerowa, *Colloids and Surfaces A:-Physicochemical and Engineering Aspects*, 2001, **186**, 93-101.

61. C. Stubenrauch, A. V. Makievski, K. Khristov, D. Exerowa and R. Miller, *Tenside Surfactants Detergents*, 2003, **40**, 196-201.

62. V. Simulescu, J. Angarska and E. Manev, *Colloids and Surfaces A: Physicochemical and Engineering Aspects*, 2008, **319**, 21-28.

63. L. G. Wang, *International Journal of Mineral Processing*, 2012, **102**, 58-68.

64. D. S. Ivanova, Z. K. Angarska, S. I. Karakashev and E. D. Manev, *Colloids and Surfaces A: Physicochemical and Engineering Aspects*, 2011, **382**, 93-101.

65. K. P. Velikov, O. D. Velev, K. G. Marinova and G. N. Constantinides, *Journal of the Chemical Society-Faraday Transactions*, 1997, **93**, 2069-2075.

66. S. Sett, S. Sinha-Ray and A. L. Yarin, *Langmuir*, 2013, **29**, 4934-4947.

67. D. Arabadzhieva, E. Mileva, P. Tchoukov, R. Miller, F. Ravera and L. Liggieri, *Colloids and Surfaces A: Physicochemical and Engineering Aspects*, 2011, **392**, 233-241.

68. E. S. Johonnott, *Philosophical Magazine*, 1906, **11**, 746-753.

69. J. Perrin, *Annals of Physics*, 1918, **10**, 1918.

70. A. D. Nikolov and D. T. Wasan, *Journal of Colloid and Interface Science*, 1989, **133**, 1-12.

71. A. D. Nikolov, D. T. Wasan, N. D. Denkov, P. A. Kralchevsky and I. B. Ivanov, *Surfactants and Macromolecules : Self-Assembly at Interfaces and in Bulk*, 1990, **82**, 87-98.

72. P. A. Kralchevsky, A. D. Nikolov, D. T. Wasan and I. B. Ivanov, *Langmuir*, 1990, **6**, 1180-1189.

73. D. T. Wasan, A. D. Nikolov, P. A. Kralchevsky and I. B. Ivanov, *Colloids and Surfaces*, 1992, **67**, 139-145.

74. D. Wasan and A. Nikolov, *Current Opinion in Colloid & Interface Science*, 2008, **13**, 128-133.

75. B. K. Jha, A. Patist and D. O. Shah, *Langmuir*, 1999, **15**, 3042-3044.

76. D. O. Shah, N. F. Djabbarah and D. T. Wasan, *Colloid and Polymer Science*, 1978, **256**, 1002-1008.

77. S. Pandey, R. P. Bagwe and D. O. Shah, *Journal of Colloid and Interface Science*, 2003, **267**, 160-166.

78. A. Patist, T. Axelberd and D. O. Shah, *Journal of Colloid and Interface Science*, 1998, **208**, 259-265.

79. A. Patist, P. D. T. Huibers, B. Deneka and D. O. Shah, *Langmuir*, 1998, **14**, 4471-4474.

80. N. Schelero, G. Hedicke, P. Linse and R. V. Klitzing, *Journal of Physical Chemistry B*, 2010, **114**, 15523-15529.

81. V. Bergeron and C. J. Radke, *Langmuir*, 1992, **8**, 3020-3026.

82. Q. Xu, M. Nakajima, S. Ichikawa, N. Nakamura, P. Roy, H. Okadome and T. Shiina, *Journal of Colloid and Interface Science*, 2009, **332**, 208-214.

83. L. G. Wang and R. H. Yoon, *Minerals Engineering*, 2006, **19**, 539-547.

84. V. Bergeron, D. Langevin and A. Asnacios, *Langmuir*, 1996, **12**, 1550-1556.

85. E. Carey and C. Stubenrauch, *Journal of Colloid and Interface Science*, 2009, **333**, 619-627.

86. D. Varade, D. Carriere, L. R. Arriaga, A. L. Fameau, E. Rio, D. Langevin and W. Drenckhan, *Soft Matter*, 2011, **7**, 6557-6570.

87. N. Kristen, A. Vullings, A. Laschewsky, R. Miller and R. von Klitzing, *Langmuir*, 2010, **26**, 9321-9327.

88. A. Bhattacharyya, F. Monroy, D. Langevin and J. F. Argillier, *Langmuir*, 2000, **16**, 8727-8732.

89. N. Kristen and R. von Klitzing, *Soft Matter*, 2010, **6**, 849-861.

90. R. Sedev, B. Jachimska, K. Khristov, K. Malysa and D. Exerowa, *Journal of Dispersion Science and Technology*, 1999, **20**, 1759-1776.

91. C. Stubenrauch, L. K. Shrestha, D. Varade, I. Johansson, G. Olanya, K. Aramaki and P. Claesson, *Soft Matter*, 2009, **5**, 3070-3080.

92. E. Carey and C. Stubenrauch, *Colloids and Surfaces A: Physicochem. Eng. Aspects*, 2013, **419**, 7-14.

93. L. Wang and R.-H. Yoon, *International Journal of Mineral Processing*, 2008, **85**, 101-110.

94. L. A. Trujillo-Cayado, P. Ramírez, L. M. Pérez-Mosqueda, M. C. Alfaro and J. Muñoz, *Colloids and Surfaces A: Physicochemical and Engineering Aspects*.

95. G. Bournival, S. Ata, S. I. Karakashev and G. J. Jameson, *Journal of Colloid and Interface Science*, 2014, **414**, 50-58.

96. S. Samanta and P. Ghosh, *Chemical Engineering Research & Design*, 2011, **89**, 2344-2355.

97. M. Buzzacchi, P. Schmiedel and W. von Rybinski, *Colloids and Surfaces A: Physicochemical and Engineering Aspects*, 2006, **273**, 47-54.

98. S. N. Tan, D. Fornasiero, R. Sedev and J. Ralston, *Journal of Colloid and Interface Science*, 2005, **286**, 719-729.

99. T. Tamura, Y. Kaneko and M. Ohyama, *Journal of Colloid and Interface Science*, 1995, **173**.

100. H. Schott, *Journal of the American Oil Chemists Society*, 1988, **65**, 816-819.

101. Z.-L. Chen, Y.-L. Yan and X.-B. Huang, *Colloids and Surfaces A: Physicochemical and Engineering Aspects*, 2008, **331**, 239-244.

102. S. Samanta and P. Ghosh, *Industrial & Engineering Chemistry Research*, 2011, **50**, 4484-4493.

103. S. N. Tan, D. Fornasiero, R. Sedev and J. Ralston, *Colloids and Surfaces A: Physicochemical and Engineering Aspects*, 2005, **263**, 233-238.

104. K. G. Marinova, L. M. Dimitrova, R. Y. Marinov, N. D. Denkov and A. Kingma, *Bulg. J. Phys*, 2012, **39**, 53-64.

105. T. Tamura, Y. Takeuchi and Y. Kaneko, *Journal of Colloid and Interface Science*, 1998, **206**, 112-121.

106. Z. Nemeth, G. Racz and K. Koczo, *Colloids and Surfaces A: Physicochemical and Engineering Aspects*, 1997, **127**, 151-162.

107. M. J. Rosen and J. Solash, *Journal of the American Oil Chemists Society*, 1969, **46**, 399-402.

108. C. Morrison, L. L. Schramm and E. N. Stasiuk, *Journal of Petroleum Science and Engineering*, 1996, **15**, 91-100.

109. A. BonfillonColin and D. Langevin, *Langmuir*, 1997, **13**, 599-601.

110. K. G. A. Pankhurst, *Transactions of the Faraday Society*, 1941, **37**, 0496-0505.

111. M. A. V. Axelos and F. Boue, *Langmuir*, 2003, **19**, 6598-6604.

112. M. H. Ropers, B. Novales, F. Boue and M. A. V. Axelos, *Langmuir*, 2008, **24**, 12849-12857.

113. E. Terriac, J. Emile, M. A. Axelos, I. Grillo, F. Meneau and F. Boue, *Colloids and Surfaces A; Physicochemical and Engineering Aspects*, 2007, **309**, 112-116.

114. J. Etrillard, M. A. V. Axelos, I. Cantat, F. Artzner, A. Renault, T. Weiss, R. Delannay and F. Boue, *Langmuir*, 2005, **21**, 2229-2234.

115. C. Curschellas, J. Kohlbrecher, T. Geue, P. Fischer, B. Schmitt, M. Rouvet, E. J. Windhab and H. J. Limbach, *Langmuir*, 2013, **29**, 38-49.

2. Materials and Methods

2.1. Materials

2.1.1. Pluronics

A series of structurally analogous poly(ethylene oxide)-poly(propylene oxide)-poly(ethylene oxide) tri-block polymeric surfactants known commercially as Pluronics (BASF) or Poloxamers (ICI) were used as received, as listed in Figure 2.1.

The polydispersity of the polymeric surfactants was not measured however typical values of polydispersity index as quoted in the literature are approximately 1.1-1.2 for Pluronic molecular weight of approximately 5000gmol^{-1}.[1] Therefore, it is expected that there is a small degree of polydispersity within these polymers.

Name	PPO block		PEO block			Total Mw	HLB
	g/mol	segments	g/mol	segments	%	g/mol	
L62	1750	30	500	12	20	2500	1-7
PE6400	1750	30	1160	26	40	2900	12-18
P84	2250	43	1680	38	40	4200	12-18
P103	3250	60	1485	34	30	4950	7-12
P123	4000	70	1725	40	30	5750	7-12
P104	3250	60	2360	54	40	5900	12-18
P105	3250	58	3250	37	50	6500	12-18
PE6800	1750	30	6720	150	80	8400	>24
F108	3250	60	11680	260	80	14600	>24

Figure 2.1; Molecular weight and approximate composition characteristics of the Pluronic copolymers used in this work. The stated PEO composition is for both blocks. The hydrophilic-lipophilic balance (HLB) for each copolymer is also quoted[2].

PEO-PPO-PEO block copolymers are used widely in industry in applications such as detergency, emulsification and foaming. They are comprised of a central poly(propylene oxide) block which is hydrophobic and surrounded by two blocks of hydrophilic poly(ethylene oxide) (Figure 2.2). The advantage of these copolymers is that their composition (PPO/PEO ratio) and molecular weight (PEO and PPO block lengths) can be varied to produce a range of polymers with very different surface active properties.[2] Hence, optimum properties can be selected for a desired application.

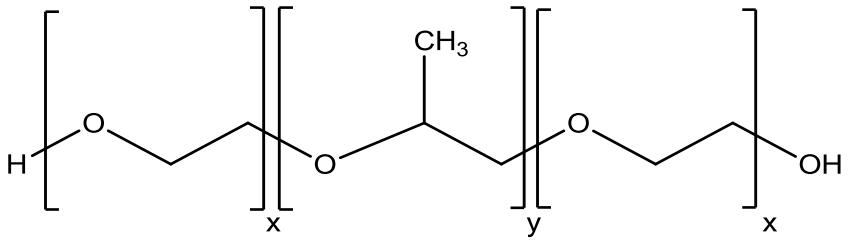

Figure 2.2; The structure of PEO-PPO-PEO block copolymers.

For the purposes of understanding foam behaviour, it is necessary to have an understanding of the nature of Pluronic adsorption and the phase behaviour adopted in solution. Therefore, a brief literature review of the solution behaviour of Pluronics in water will be outlined below.

In air-in-water foam stabilised with PEO-PPO-PEO copolymers, the hydrophobic PPO block (the anchor), with its low affinity for water, is preferentially adsorbed and locates at the interface in the air phase. The hydrophilic PEO blocks (the buoy) with its much higher affinity for water, is situated within the aqueous phase protruding into solution. (Figure 2.3) The dissolution of any surfactant in a solvent causes the free energy of the system to increase due to the presence of the hydrophobic group which produces un-favourable distortion of the solvent structure. Consequently, less work is required to bring the surfactant molecule to the interface than a solvent molecule and so surfactant spontaneously accumulates at the interface reducing the surface tension of the system.[3]

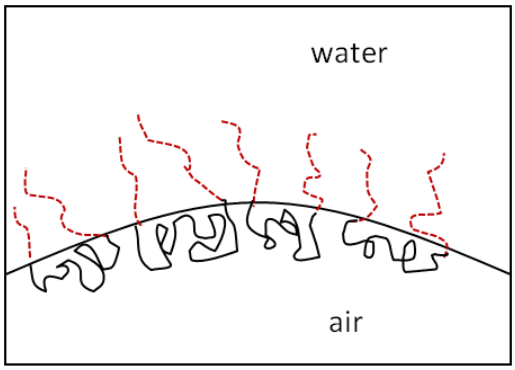

Figure 2.3; Schematic diagram to show the adsorption of PEO-PPO-PEO copolymers at an air-water interface. PPO blocks (solid line), PEO blocks (dotted line).

2.1.1.1. Pluronic structure at the air-water interface

The structure of the PEO-PPO-PEO adsorbed layer at an air-water interface has been extensively studied and it is generally accepted that the central poly(propylene oxide) block will adsorb at the interface located out of the aqueous phase, whilst the hydrophilic blocks remain in solution.[4-6] An inverted 'U' orientation at the interface has been proposed.[7] Even at bulk concentrations below the CMC, dense adsorbed layers are formed,[8] with no change in surface coverage observed at concentrations in the region of 10^{-3}-10^{-6} %[2]. Ellipsometric measurements have confirmed that the thickness of the adsorbed layer increases linearly with PEO chain length. This was probed further using neutron reflectivity which allowed quantitative analysis of the film thickness.[9] Film thickness was shown again to increase linearly with PEO chain length with typical values ranging from approximately 50 to 100Å and a polymer brush formed at the interface. It is worth noting that the PEO-PPO-PEO polymers used in this study were reasonably hydrophilic with a percentage ethylene oxide of 80%.

2.1.1.2. Pluronic phase behaviour

PEO-PPO-PEO copolymers display varied phase behaviour. At low temperatures both PEO and PPO chains are hydrophilic so that unimers; individual polymer chains, are present in solution (typically about 1nm in size)[2] which follow a Gaussian (normal) distribution with radius of gyration (R_g) approximately 20Å.[10-12] Above a certain concentration, the critical micelle concentration (CMC) or temperature, the critical micelle temperature (CMT), aggregation (micellisation) of surfactant molecules takes place. This is due to the increasing hydrophobicity of the PPO block and to a lesser extent

the PEO block. The nature and structure of the aggregate formed is affected by temperature, block sizes, solvent and molecular weight.[10, 12-19].

Various techniques such as static and dynamic light scattering, fluorescence, small-angle neutron scattering and surface tension have been implemented to study such structures[10, 20-23]. In dilute solutions (less than 10% concentration), spherical micelles consisting of a dense PPO core and hydrated PEO corona are formed.[12, 15] An increase in aggregation number and decrease in micelle size has been typically observed upon increasing temperature[16, 18, 24, 25]. However in some instances the micelle hydrodynamic radius has remained constant upon increasing temperature whilst the aggregation number has increased and this has been attributed to the dehydration of the PEO headgroups.[25-29] Furthermore, there has been some debate surrounding the mechanism of association with both multiple association and stepwise association of unimers reported.[13, 16] Aggregation number is however apparently independent of polymer concentration.[19, 30, 31]

Unlike small molecule surfactants in which the CMC or CMT is observed at a well-defined concentration or temperature, PEO-PPO-PEO copolymers tend to form micelles over a wide temperature range. Three temperature regions; unimer, transition and micelle have been observed for Pluronic F68 using static and dynamic light scattering.[26] For the low molecular weight Pluronic, P85 (Mw 4500 $gmol^{-1}$, 50% PEO) light scattering techniques were used to determine the properties of the aqueous system.[36] It was found that at concentrations of approximately 5% polymer and 25°C temperature, micelles and monomers co-exist within solution.

In order to assess foaming as a function of behaviour it is necessary to know the critical micelle concentrations for these polymeric surfactants. Wide discrepancies in the few CMC values available for various PEO-PPO-PEO copolymers have been reported in the literature. This has been attributed to lack of temperature control, wide concentration regimes studied and differences in polydispersity originating from differing supply source.[32] Perhaps the most comprehensive study of Pluronic CMC's and CMT's is that of Alexandridis *et al.* who used dye solubilisation techniques.[33] This involved studying the UV-visible spectra of copolymer solutions containing the insoluble dye DPH (1,6-diphenyl-1,3,5-hexatriene). Above the CMC, the additive is solubilised into micelles, thus increasing its concentration in solution and this is characterised by a sharp increase in absorption intensity. The first inflexion in the temperature versus absorption intensity plot

was assigned to the formation of a hydrophobic domain i.e. the formation of micelles. Larger PPO blocks present within the polymer decreases the CMC, with micellisation driven by the hydrophobicity of the surfactant.

Many previous studies have employed surface tension techniques to determine the CMC and a comparison to results obtained by Alexandridis typically show wide variations.[34, 35] Two breaks in the surface tension versus concentration curves for Pluronics have been noted.[17, 27, 36] Misinterpretation of these inflexions has likely resulted in the apparent disparities in CMC's across various data. Prasad *et al.*[36], proposed the two inflexions corresponded to the formation of two different aggregates; a monomolecular "micelle" at low concentrations and a conventional polymolecular micelle at higher concentrations. Alternatively, it has been suggested that wide molecular weight distributions could also account for such behaviour.[17] Alexandridis *et al.*[23], confirmed that the values determined from the second break point in surface tension data correlated well to the CMC's obtained via dye solubilisation experiments. Thus the second break point was assigned to the formation of "polymolecular micelles with well-defined hydrophobic interior." Here, it was proposed that a configurational rearrangement of polymer molecules at the interface occurs allowing the surface tension to decrease further beyond the first break point as the layer thickness increases.

The above review has highlighted the need to understand the fundamental phase behaviour of the commercial samples used in this work. This is essential in order to make accurate comparisons to the foaming behaviour of PEO-PPO-PEO copolymers.

2.1.2. Sodium dodecyl sulfate (SDS)

The anionic surfactant sodium dodecyl sulfate (SDS) (Sigma Aldrich) was used as received. Both hydrogenated and deuterated samples were used in contrast small-angle neutron scattering (SANS) experiments to determine the origin of the scattering data.

2.1.3. Cetyltrimethylammonium bromide (CTAB)

The cationic surfactant cetyltrimethylammonium bromide (CTAB) (Sigma Aldrich) was used as received. Both hydrogenated and deuterated samples were used in contrast small-angle neutron scattering (SANS) experiments to determine the origin of the scattering data.

2.2. Methods

2.2.1. Solution preparation

For foaming tests, all solutions were prepared by % weight volume. A known mass of polymeric surfactant was added to a standard volumetric flask and the solution made up to the desired volume with deionised water (Millepore RiOs 5 water purification system).

2.2.2. Foam stability

Foam stability tests were performed in a graduated glass column (45cm height and 20mm internal diameter) fitted with a porous fritted disk (nominal porosity of 2µm) situated at the base of the column and insulated with a water jacket to ensure temperature control (Figure 2.4). Air flow was controlled via a pressure controller and flow meter (0-0.5L/min).

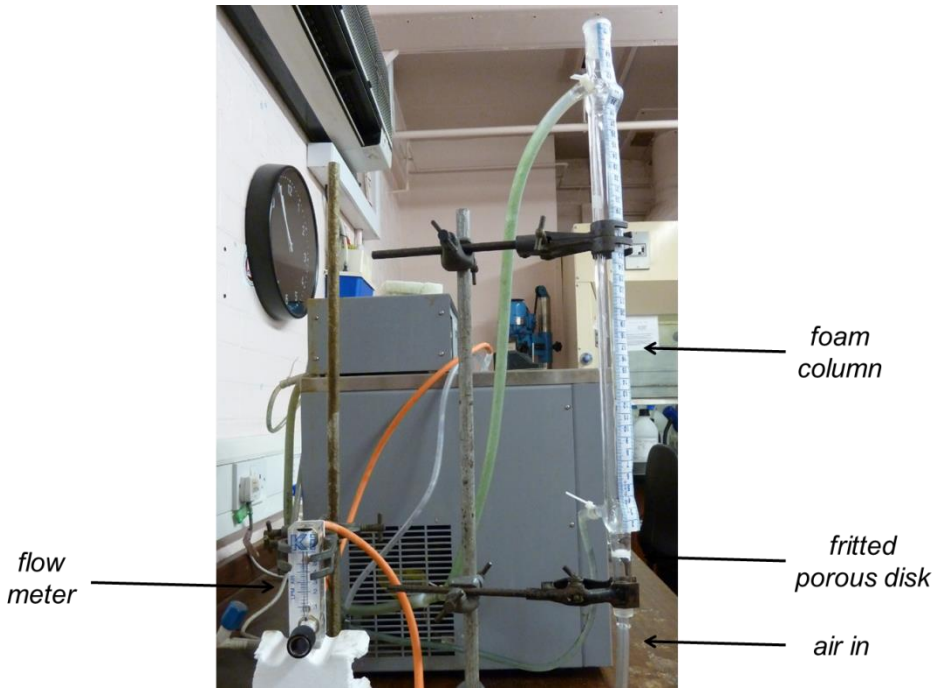

Figure 2.4; Foam column apparatus to study the foaming behaviour of aqueous foams.

Fixed temperature experiments were performed at 20 ± 0.5 °C with both the column and surfactant solution equilibrated to the desired temperature prior to beginning the measurements. For temperature effect studies, solutions were equilibrated to the desired experiment in the same manner. A 2.5 cm^3 aliquot of surfactant solution was inserted into the top of the column above the fritted disk. Nitrogen gas was passed through the disk into the surfactant solution at a constant flow rate of 0.08±0.01 L/min and 0.8 bar

pressure. A standard height of foam (15cm) was created for a fixed surfactant concentration (flow rate 0.08 L/min, 0.8 bar) after which the gas flow was turned off and the static foam allowed to drain under gravity. The half-life of the foam ($t_{1/2}$), the time taken for the foam to decay to half of its original height, was recorded. This involved measuring the foam height at specific time intervals following foam generation. All measurements were recorded in triplicate at a minimum. New aliquots of solution were used for each foam test and the column thoroughly rinsed with deionised water between each test, to ensure reproducibility of results.

2.2.3. Foamability

Foamability tests were performed in a closed cylinder (65 cm^3 total volume, graduated to 50 cm^3) containing 15 cm^3 surfactant solution. All fixed temperature measurements were performed at 20 ± 0.5°C by equilibrating the surfactant solution in a water bath prior to the measurements. For temperature effect studies, the same method of equilibration to the desired temperature was implemented. Foam was generated by ten vigorous hand-shakes of the cylinder. The maximum foam volume at t = 0 seconds characterised the surfactant foamability. All tests were performed a minimum of three times.

2.2.4. Tensiometry

Glassware was cleaned and repeatedly rinsed with deionised water prior to measurements being recorded. Equilibrium surface tension measurements were performed using the Krüss K10 tensiometer via both du Nouy ring and Wilhelmy plate methods. Both ring and plate were rinsed with ethanol and deionised water and flamed between each measurement. A minimum of three repeat measurements were made at each temperature until values concurred within 0.1mN/m. Reproducibility was checked periodically with fresh solutions. Measurements were thermostated to ± 0.1°C using a Fisher Isotemp circulating water bath. Dynamic surface tension measurements were obtained using the Sita Science Line t60 Maximum Bubble Pressure tensiometer. Bubble lifetimes were varied from 0.05-20 seconds.

Gareth Jones and Oliver Hayes are acknowledged for measuring equilibrium and dynamic surface tension respectively.

2.2.5. Image analysis

Images of static foams in the foam column were obtained using a Veho VMS-004 USB microscope at 20x zoom. Images were recorded from the side profile, through the column wall and were taken within 5 seconds of foam formation and sometime after foam formation to demonstrate how foam structure varies with foam age. The time at which the aged foam images were captured varied depending on the half-life of the foam.

Images of polyurethane foam cell structure were also obtained with the Veho VMS-004 USB microscope at 20x zoom and analysed using the open access scientific software Image J. A minimum of three images were recorded, at random, for each foam. The cell diameter, defining the cell size, was measured by hand on Image J for at least 50 bubbles in each image and the average bubble size and standard deviation determined. To calculate the bubble count, an 8x8mm boundary was drawn on each image and the number of bubbles within this region counted. Those bubbles on the perimeter which had approximately greater than half their area within the boundary were counted as half whilst those with approximately less than half their area within the boundary were excluded from the count.

2.2.6. Small-angle neutron scattering

Small-angle neutron scattering (SANS) was used primarily to probe the structure of the adsorbed polymer layer in Pluronic stabilised foams. SANS is a diffraction technique involving the scattering of incident radiation, neutrons, by sample matter to give information about the size, shape and orientation of the sample.

A brief overview of the technique is described below; for a more detailed description readers are referred to *Polymers and Neutron Scattering* by Higgins and Benoit.[37]

In a SANS experiment, each atom of the sample acts as a point scatterer to the incident neutron beam and the scattering power of individual atoms is described by their scattering length, *b*. For convenience, the *scattering length density* ρ is used to quantify the scattering power of a molecule of *i* atoms;

$$\rho = \sum i b_i \frac{D N_A}{M_w}$$

where b_i is the scattering length of the *ith* atom in a molecule with bulk density *D* and molecular weight *Mw*.

Figure 2.5 shows a typical instrument setup in a SANS experiment. An incident beam of neutron radiation with wavelength λ is directed at the sample. Some of the neutrons will be absorbed, some transmitted and a small proportion scattered by the sample with angle θ. These scattered neutrons are recorded by a detector positioned at a distance L_{sd} from the sample.

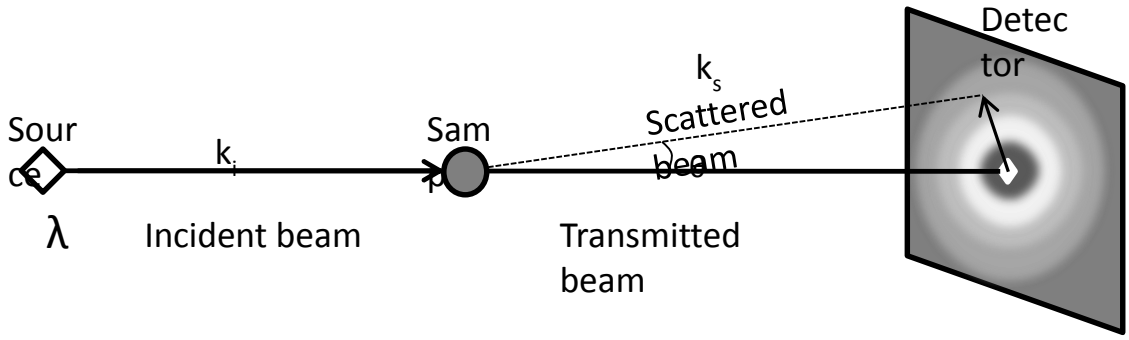

Figure 2.5; Schematic diagram showing the principle of a SANS experiment. Neutrons of wavelength λ are scattered by the sample and the scattered neutrons detected.

The scattering vector Q relates to the incident k_i and scattered k_s wavevectors by;

$$Q = |Q| = |k_s - k_i| = \frac{4\pi n}{\lambda}\sin\left(\frac{\theta}{2}\right)$$

where n is the neutron refractive index and can be considered as ~ 1. Thus the magnitude of Q is directly related to λ and θ. Q has units of reciprocal length which are typically quoted in nm^{-1} or $Å^{-1}$. Substituting into Braggs Law;

$$\lambda = 2dsin\left(\frac{\theta}{2}\right)$$

yields the relationship;

$$d = \frac{2\pi}{Q}$$

allowing simple determination of length scales within the sample based on the Q value.

A SANS experiment involves measuring the scattering intensity I(Q) as a function of wavevector Q;

$$I(Q) = n_p \Delta\rho^2 V_p^2 P(Q) S(Q) + B_{inc}$$

where n_p is the number density of scattering bodies within a given volume V_p. $\Delta\rho^2$ is the contrast term i.e. the difference in scattering length density between the sample part of interest and its surrounding medium, which allows selective regions of the sample to be highlighted. P(Q) is the form factor, a function which describes the size and shape of the scattering bodies and S(Q) is the structure factor which describes interactions between different scattering bodies.

Hydrogen and its isotope deuterium (^{2}H) have very different scattering lengths and it is this which has largely made small-angle neutron scattering such an important tool for colloidal scientists. By selectively deuterating parts of the system, for example solvent or sample, it is possible to highlight regions of the system thereby simplifying the scattering data and subsequent analysis. This process is known as contrast matching and this has been utilised throughout this research to aid in the interpretation of scattering from air-in-water foam.

The contrast term, $\Delta\rho^2$ is the difference in scattering length density between the sample and the medium in which it is dispersed.

Unfortunately, it was not possible to obtain deuterated Pluronic samples as they are not available to purchase and time did not permit these samples to be synthesised. Instead, foams prepared from the ionic small molecule surfactants, sodium dodcyl sulfate (SDS) and cetyl trimethylammonium bromide (CTAB) were investigated. The scattering length densities and contrast terms for the various components of the SDS foam are presented in Figure 2.6. A large value for $\Delta\rho^2$ signifies high contrast between molecule and solvent, for example h-SDS in D_2O whilst a small value indicates the neutron only "sees" a homogeneous medium, for example d-SDS in D_2O.

	ρ (10^{10} cm^{-2})
D_2O	6.35
H_2O	-0.56
H_2O(90%)/D_2O	0.41
h-SDS	0.36
d-SDS	6.73
Air	~0

	$\Delta\rho^2$ ($10^{20}$$cm^{-4}$)
h-SDS / D_2O	35.74
d-SDS / D_2O	0.148
SDS / (H_2O(90%)/D_2O)	0.0016
D_2O / air	40.26
SDS / air	0.135
(H_2O(90%)/D_2O) / air	0.166
d-SDS / air	45.29

Figure 2.6; Scattering length densities (ρ) and contrast term ($\Delta\rho^2$) for various foam components. Scattering length densities are calculated for the pure molecule.[38]

Pictorial representations of the contrast in various h-SDS and d-SDS foams are presented in Figure 2.7.

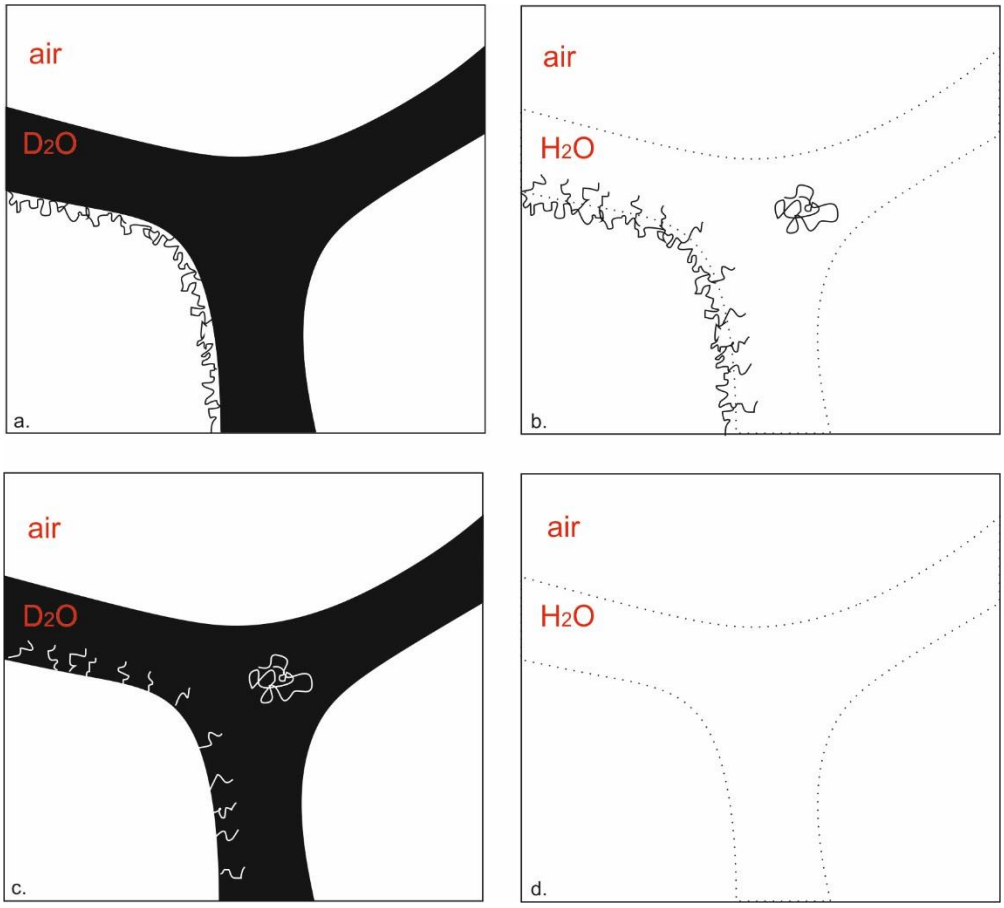

Figure 2.7; Cartoons to show the contrast in various SDS stabilised air-in-water foams. a) d-SDS in D_2O, b) d-SDS in H_2O, c) h-SDS in D_2O, d) h-SDS in H_2O.

2.2.6.1. SANS sample preparation

All Pluronic solutions were prepared by % weight volume in deuterated water (99.9%, Sigma Aldrich).

For the contrast experiments samples involving SDS and CTAB both hydrogenated and deuterated surfactants were studied in deionised water, deuterated water (99.9%, Sigma Aldrich), a 1:1 H_2O/D_2O mixture and null reflecting water (90% H_2O, 10% D_2O).

2.2.6.2. Foam generation

The foam sample was contained in a purpose built Perspex column of height 25cm and diameter (5cm) into which a 2cm wide groove has been removed, and covered with aluminium foil to act as the neutron transparent windows for beam access (Figure 2.8). Approximately 50cm^3 of surfactant solution was added to the sample holder at the base of the column. The foam is generated by bubbling gas through the frit at A. The neutron beam impinges on the aluminium foil between B and C behind which the Perspex has been partially removed. For stable foams, the reservoir D collects the foam sample and returns it to the base via the plastic tube at E. The heating jackets at F and G have been removed in this picture.

Steady state wet foams were studied in which continuous air flow produces constantly regenerated foam. As such, the bubbles appear spherical and are separated by thick lamella walls. Experiments were conducted at room temperature. Experimental measuring times were approximately 5 minutes.

Figure 2.8; SANS sample environment for studying foams.

To ensure reproducibility of the data, foams were also prepared and studied in a foam column of smaller diameter (2cm) into which a 1cm wide groove was removed to accommodate the neutron beam.

2.2.6.3. Instrument configuration

Small-angle neutron scattering experiments were performed on either;

(i) the time-of flight LOQ or SANS2d diffractometers at the ISIS pulsed Spallation Neutron Source, Rutherford Appleton Laboratory, Didcot, UK. Typically, a range defined by $Q = (4\pi/\lambda)\sin(\theta/2)$ between 0.005 and ≥ 0.3 $Å^{-1}$ is obtained by using neutron wavelengths (λ) spanning 2.2 to 10 Å (LOQ) or 1.75 to 16.5Å (SANS2d) with a fixed sample-detector distance of ~ 4m, or

(ii) (ii) the steady-state reactor source, D11 diffractometer at the ILL, Grenoble where a Q range between 0.005 and 0.5 $Å^{-1}$ was obtained by choosing three instrument settings at a constant neutron wavelength (λ) of 8 Å and sample-detector distances of 1.2, 8 and 39 m.

All scattering data were (a) normalized for the sample transmission, (b) background corrected using the empty foam cell, and (c) corrected for the linearity and efficiency of the detector response using the instrument specific software package and the scattering from a polystyrene standard taped to the front of the foam cell.

2.2.6.4. Solution scattering

Small-angle neutron scattering from aqueous surfactant solutions were performed on both the SANS2d diffractometer at ISIS and the D11 diffractometer at the ILL. Instrument configurations were as described in section 2.2.6.3. Samples were contained in 2mm path length, analytical grade quartz cuvettes (Hellma) and mounted into an enclosed, computer controlled sample holder. Sample volumes were approximately 0.4cm^3. Temperature control was achieved using a circulating water bath that pumps liquid through the base of the sample holder. Experimental measuring times were approximately 20 minutes.

2.2.6.5. FISH modelling

SANS data was fitted with the data fitting program FISH, written by R.K. Heenan and is based on a standard, iterative, least squares method. Foam scattering was fitted to the model comprising a paracrystalline stack of surfactant layers, developed by Kotlarchyk *et al.*[39] to which a Q^{-4} term was added. The model comprises form factors for scattering

from a thin interface which are orientated in a one dimensional paracrystalline stack. The form factor P(Q) and structure factor S(Q) are separate to allow information about the interfacial structure to be determined. The model parameters of most importance define the layer thickness (L), layer separation (D) and number of layers (M).

2.2.7. Polyurethane foam manufacture

Polyurethane (PU) foams were manufactured on an industrial coating line. A schematic representation of the process is presented in Figure 2.9.

2.2.7.1. Processing

- Mixing

The polyol and isocyanate (in the form of a commercially sensitive pre-polymer blend) was pre-heated to a uniform temperature whilst the aqueous surfactant phase was cooled. The prepolymer and surfactant were combined by mixing in a low pressure mixer, initiating the reaction. The aqueous phase consisted of 2wt% surfactant. This concentration was selected as in most polyurethane applications the concentration of surfactant typically spans a range from 0-2%.[40] Thus this concentration was deemed appropriate to model the polyurethane reaction whilst clearly allowing any effects of surfactant foaming behaviour and phase behaviouhydrophobicr to be observed.

- Coating

From the mix, the polymer and water mixture was poured directly into the coating head. The PU liquid was spread evenly between two casting papers via a roller system. The casting papers carried the polymer mix over the cure tables which consisted of controlled temperature zones heated between 30 and 60°C. On the cure table, the liquid reacted to form foam and was then cured. The coating and curing process took approximately 90 seconds.

- Drying

Upon exit from the cure table the product was transferred to the drying oven and dried through a series of independently controlled temperature regions.

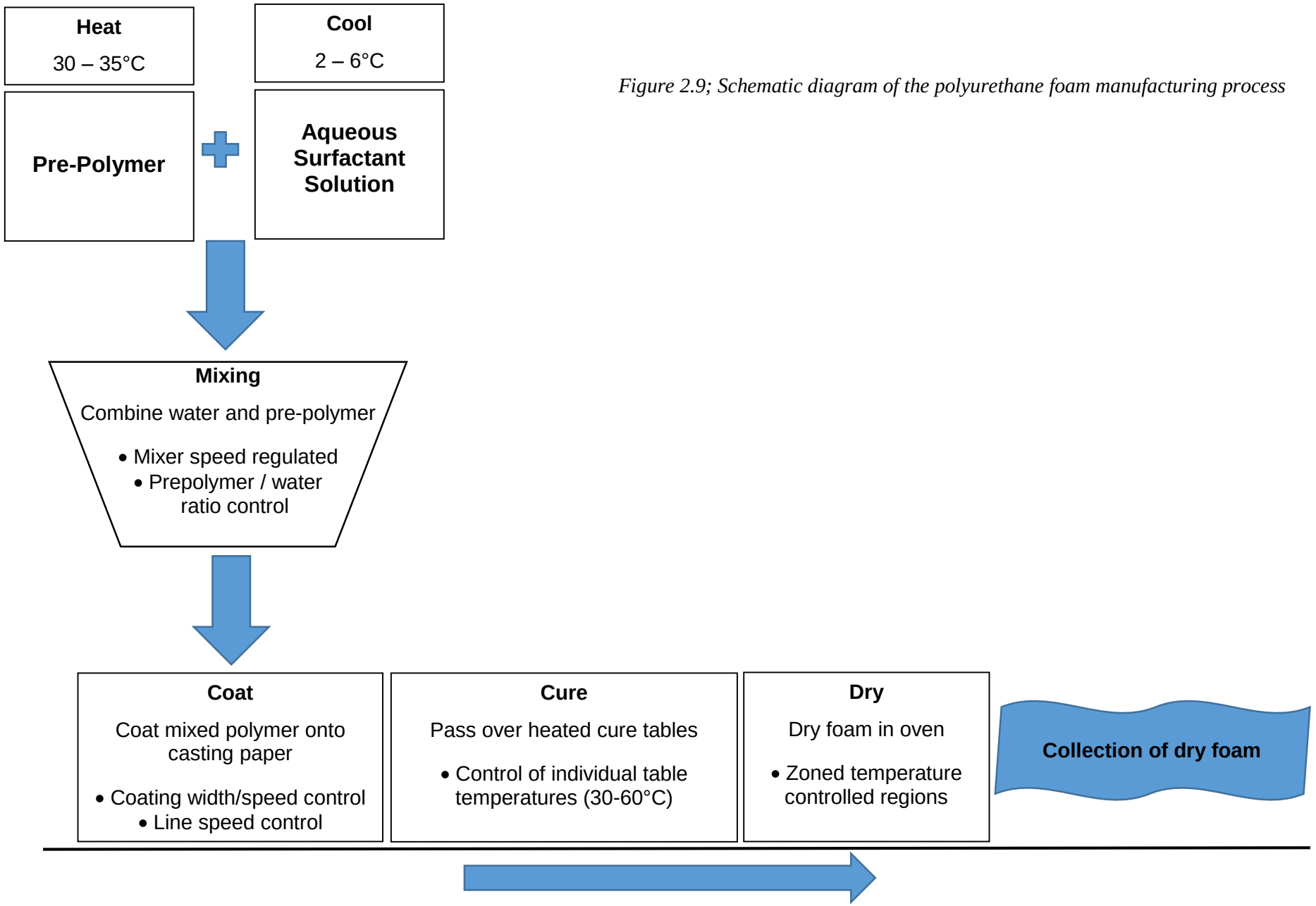

Figure 2.9; Schematic diagram of the polyurethane foam manufacturing process

2.2.7.2. Fluid handling tests

Fluid handling tests were performed post production immediately and typically 24-48 hours after manufacture. Fluid handling tests were performed with a salt solution that conforms to the British Standard EN 13726-1:2002 "Test Methods for Primary Wound Dressings"[41]. The solution comprises sodium chloride (142 mmol) and calcium chloride (2.5 mmol) prepared in deionized water. Such solution has an ionic composition comparable to human serum or wound exudate.

Thickness — A piece of foam was cut taking care not to compress or crush the sample. The thickness was measured using a Kafer handheld dial thickness gauge and recorded in mm.

Density — A 10x10cm sample of foam was cut and weighed in grams. Density is calculated as followed;

$$Density\left(\frac{kg}{m3}\right) = \frac{Thickness\ (mm)}{Weight\ (g)} x100$$

Absorption — A 5x5cm sample of foam was weighed and immersed in the salt solution for one minute. The sample was removed, drained for 10 seconds and re-weighed. Absorption is calculated as followed;

$$Absorption\ (g/g) = \frac{wet\ weight - dry\ weight}{dry\ weight}$$

Wicking — $2cm^3$ of salt solution was poured from a syringe onto the full width of the foam. The time taken for the liquid to be fully absorbed by the foam was recorded in seconds.

2.3. References

1. B. Foster, T. Cosgrove and B. Hammouda, *Langmuir*, 2009, **25**, 6760-6766.

2. P. Alexandridis and T. A. Hatton, *Colloids and Surfaces A: Physicochemical and Engineering Aspects*, 1995, **96**, 1-46.

3. M. Rosen, *Surfactants and interfacial phenomena*, 2nd edn., Wiley, New York, USA, 1989.

4. J. B. Vieira, Z. X. Li, R. K. Thomas and J. Penfold, *Journal of Physical Chemistry B*, 2002, **106**, 10641-10648.

5. B. R. Blomqvist, T. Warnheim and P. M. Claesson, *Langmuir : the ACS journal of surfaces and colloids*, 2005, **21**, 6373-6384.

6. E. Kiss, T. Keszthelyi, G. Kormany and O. Hakkel, *Macromolecules*, 2006, **39**, 9375-9384.

7. A. F. Gallaugher and H. Hibbert, *Journal of the American Chemical Society*, 1937, **59**, 2514-2521.

8. R. Sedev and D. Exerowa, *Advances in Colloid and Interface Science*, 1999, **83**, 111-136.

9. R. Sedev, R. Steitz and G. H. Findenegg, *Physica B-Condensed Matter*, 2002, **315**, 267-272.

10. K. Mortensen, *Journal of Physics-Condensed Matter*, 1996, **8**, A103-A124.

11. E. Hecht, K. Mortensen and H. Hoffmann, *Macromolecules*, 1995, **28**, 5465-5476.

12. K. Mortensen and J. S. Pedersen, *Macromolecules*, 1993, **26**, 805-812.

13. N. K. Reddy, P. J. Fordham, D. Attwood and C. Booth, *Journal of the Chemical Society-Faraday Transactions*, 1990, **86**, 1569-1572.

14. M. Almgren, W. Brown and S. Hvidt, *Colloid and Polymer Science*, 1995, **273**, 2-15.

15. W. Brown, K. Schillen, M. Almgren, S. Hvidt and P. Bahadur, *Journal of Physical Chemistry*, 1991, **95**, 1850-1858.

16. A. A. Alsaden, T. L. Whateley and A. T. Florence, *Journal of Colloid and Interface Science*, 1982, **90**, 303-309.

17. G. Wanka, H. Hoffmann and W. Ulbricht, *Macromolecules*, 1994, **27**, 4145-4159.

18. K. Pandya, P. Bahadur, T. N. Nagar and A. Bahadur, *Colloids and Surfaces A: Physicochemical and Engineering Aspects*, 1993, **70**, 219-227.

19. G. Fleischer, *Journal of Physical Chemistry*, 1993, **97**, 517-521.

20. S. L. Nolan, R. J. Phillips, P. M. Cotts and S. R. Dungan, *Journal of Colloid and Interface Science*, 1997, **191**, 291-302.

21. J. Jansson, K. Schillen, G. Olofsson, R. C. da Silva and W. Loh, *Journal of Physical Chemistry B*, 2004, **108**, 82-92.

22. X. Zhou, X. Wu, H. Wang, C. Liu and Z. Zhu, *Physical Review E*, 2011, **83**, 041801.

23. P. Alexandridis, V. Athanassiou, S. Fukuda and T. A. Hatton, *Langmuir*, 1994, **10**, 2604-2612.

24. M. Almgren, P. Bahadur, M. Jansson, P. Y. Li, W. Brown and A. Bahadur, *Journal of Colloid and Interface Science*, 1992, **151**, 157-165.

25. J. G. Alvarez-Ramirez, V. V. A. Fernandez, E. R. Macias, Y. Rharbi, P. Taboada, R. Gamez-Corrales, J. E. Puig and J. F. A. Soltero, *Journal of Colloid and Interface Science*, 2009, **333**, 655-662.

26. Z. K. Zhou and B. Chu, *Journal of Colloid and Interface Science*, 1988, **126**, 171-180.

27. P. Bahadur and K. Pandya, *Langmuir*, 1992, **8**, 2666-2670.

28. P. Alexandridis, T. Nivaggioli and T. A. Hatton, *Langmuir*, 1995, **11**, 2847-2847.

29. T. Nivaggioli, P. Alexandridis, T. A. Hatton, A. Yekta and M. A. Winnik, *Langmuir*, 1995, **11**, 730-737.

30. K. Mortensen, W. Brown and B. Norden, *Physical Review Letters*, 1992, **68**, 2340-2343.

31. G. Fleischer, P. Bloss and W. D. Hergeth, *Colloid and Polymer Science*, 1993, **271**, 217-222.

32. P. Linse and M. Malmsten, *Macromolecules*, 1992, **25**, 5434-5439.

33. P. Alexandridis, J. F. Holzwarth and T. A. Hatton, *Macromolecules*, 1994, **27**, 2414-2425.

34. I. R. Schmolka and A. J. Raymond, *Journal of the American Oil Chemists Society*, 1965, **42**, 1088-1091.

35. W. Saski and S. G. Shah, *Journal of Pharmaceutical Sciences*, 1965, **54**, 71-75.

36. K. N. Prasad, T. T. Luong, A. T. Florence, J. Paris, C. Vaution, M. Seiller and F. Puisieux, *Journal of Colloid and Interface Science*, 1979, **69**, 225-232.

37. J. Higgins and C. Benoit, *Polymers and Neutron Scattering*, Clarendon Press, Oxford, UK, 1997.

38. M. A. V. Axelos and F. Boue, *Langmuir*, 2003, **19**, 6598-6604.

39. M. Kotlarchyk and S. M. Ritzau, *Journal of Applied Crystallography*, 1991, **24**, 753-758.

40. M. J. Owen, T. C. Kendrick, B. M. Kingston and N. C. Lloyd, *Journal of Colloid and Interface Science*, 1967, **24**, 141-150.

41. British Standards Institution, *Test methods for primary wound dressings - Part 1: Aspects of absorbancy.* BSI, London, 2002, BS EN 13726-1:2002.

3. The influence of surfactant structure on the foaming of PEO-PPO-PEO surfactants

3.1. Abstract

The aqueous foaming behaviour of a homologous series of poly(ethylene oxide)-poly(propylene oxide)-poly(ethylene oxide) (EO_x-PO_y-EO_x) polymeric surfactants (2500-14500gmol^{-1}) has been investigated and classified according to polymer molecular weight, hydrophobicity and hydrophilicity and concentration. Both the ability of the surfactant to foam and its resulting foam stability have been defined according to maximum foam volume and foam half-life ($t_{1/2}$) using laboratory based foam column techniques. Below the critical micelle concentration (CMC), good foaming was characterised by large overall molecular weight of surfactant which induced greater bulk solution viscosity. Improved foaming was observed for surfactants with larger PEO chains and to a lesser extent larger PPO chains postulated to be due to the formation of a thicker adsorbed layer at the air-water interface. Foaming was correlated to the surface activity of the surfactants, by namely studying equilibrium and dynamic surface tension. Whilst there was no quantifiable change in bubble size for the surfactants studied, the drainage behaviour of the foam were very much different, suggesting that interfacial properties such as elasticity and viscosity are highly important in defining the bulk foaming properties.

3.2. Introduction

To characterise polyurethane foaming systems as used in industry presents a significant experimental challenge primarily due to the simultaneous progress of both the blow and gelation reactions, making it impossible to isolate the surfactant behaviour at the interface. In addition, the raw materials involved are highly toxic so undertaking foaming and interfacial measurements daily proves highly impractical. We have therefore adopted a model system of air-in-water foams to determine the fundamental foaming properties of PEO-PPO-PEO stabilised systems, and how this relates to surfactant structure, concentration and phase behaviour. Water is the main solvent in the polyurethane foaming

process therefore this model system will provide a suitable starting point for understanding and characterising foaming behaviour.

Whilst it may be expected that the ability of the surfactant to form and stabilise foam are intrinsically linked i.e. a surfactant that is more able to foam is more likely to stabilise foam, any differences between these parameters may be important to understanding the polyurethane system. For example, if the formation of PU foam is governed by kinetics i.e. how quickly the surfactant can reach the interface then the ability to form foam will be of key importance. However, if in the PU reaction bubbles form early on, then the issue may be one of stability, with the surfactant stabilising the interface until it is 'locked in' by the formation of the polymer network.

Here, solutions of PEO-PPO-PEO surfactants are characterised using foaming studies, surface tension measurements and analysis of the bubble size. The ability of the surfactants to both form foam "foamability" and stabilise foam "foam stability" are investigated. Experiments were carried out with systematic variation in surfactant structure and concentration and the effect of these properties on foaming are discussed.

3.3. Foamability

Surfactant foamability has been investigated to determine differences induced by surfactant molecular weight and hydrophilicity / hydrophobicity. Whilst it is recognised that the foam volume produced is highly dependent on the conditions under which the foam is generated, such as solution volume, bubble generation method *etc*, it must be highlighted that the purpose of this experiment was not to attempt to compare explicit values of foam volume to foam lifetime, nor was it an attempt to replicate the polyurethane foam forming conditions. Instead, the aim was to identify the fundamental trends in surfactant foaming ability.

3.3.1. Effect of overall molecular weight

Surfactant foamability for a variety of Pluronic surfactants at 5%(w/v) concentration and 20°C is presented in Figure 3.1. Under these conditions the surfactants, represented in the figures by the block grey bars, are above their critical micelle concentration (CMC) and

critical micelle temperature (CMT) so that micelles are present in solution. For those surfactants below the CMC, foamability typically increases with increasing molecular weight in the order L62<PE6400<PE6800<F108 suggesting that larger molecular weight surfactants are more effective foamers. However, interestingly the magnitude of difference in values of foamability is actually small compared to the substantial changes in molecular weight observed. This indicates that foamability does not increase linearly with molecular weight and that significantly increasing the overall molecular weight doesn't guarantee significantly enhanced foaming.

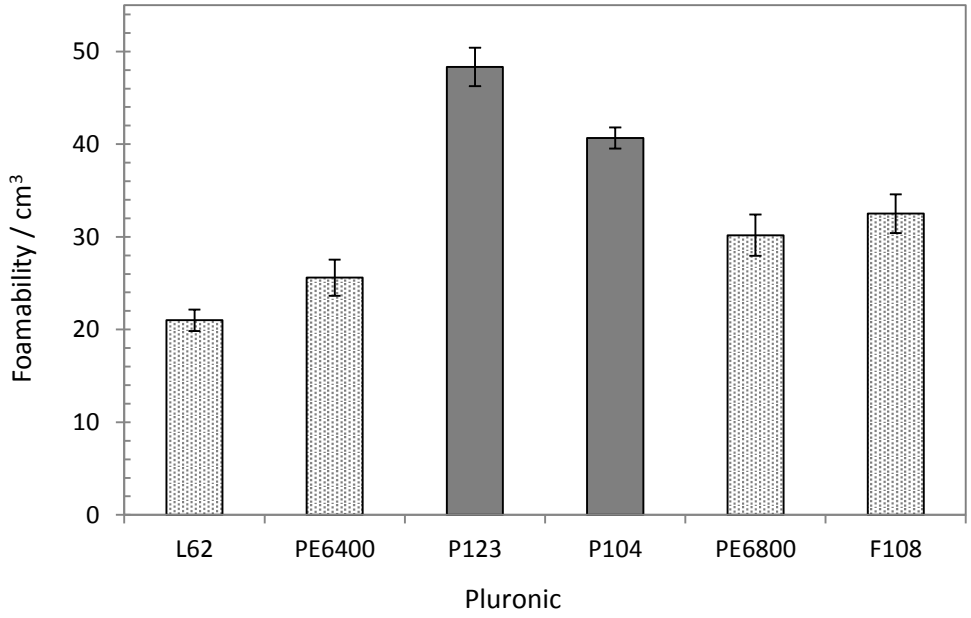

Figure 3.1; Foamability of air-in-water foams as a function of Pluronic type; [Pluronic] = 5% (w/v), 20°C. Pluronic molecular weight increases from left to right. Those Pluronics highlighted by the block grey bars are above their CMC's.

The effects of surfactant phase behaviour can also be probed by studying additional surfactants which under the specified conditions are above their CMC (Figure 3.1). Foamability for P123 and P104 is higher than would be predicted based on the trend of molecular weight alone suggesting that the presence of micelles improves foaming. It is known that at the CMC, maximum foaming is observed due to greater surface activity of the surfactant. The effects of phase behaviour on foaming will be explored further in Chapter 5.

The ability of the surfactant to lower the surface tension of the interface, and how quickly it does this is important when defining foamability. Typically bubble formation occurs across very short timescales thus whilst equilibrium surface tension can be useful to an extent, it is unlikely that the foam system will be at equilibrium and so dynamic surface tension is a more appropriate parameter. In addition, as the foam is a dynamic system, surface tension gradients will be present throughout due to the occurrence of foam depletion and stabilising mechanisms thus it is difficult to define a localised surface tension value. The dynamic surface tension (DST) for the series of surfactants presented in Figure 3.1 has been measured at 20°C and a bubble lifetime range of 0.05 to 20 seconds (Figure 3.2).

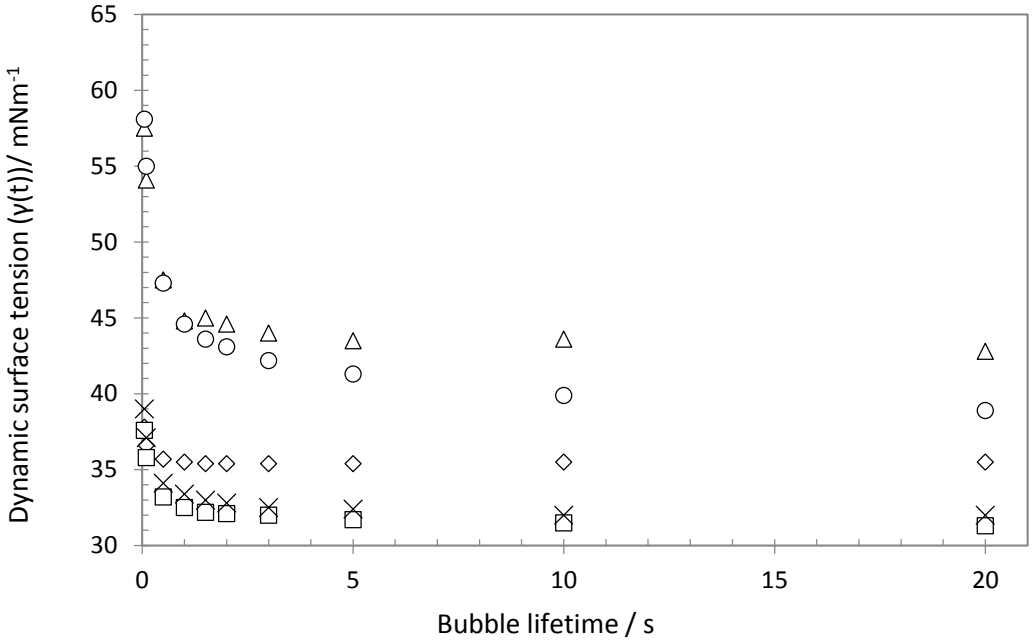

Figure 3.2; Dynamic surface tension of PEO-PPO-PEO aqueous solutions. [Pluronic]=2%(w/v), 20°C. L62 (diamonds), P123 (squares), P104 (crosses), PE6800 (triangles), F108 (circles). Data obtained by O.Hayes.

For L62, P123 and P104 at a bubble lifetime of approximately 10 seconds, the equilibrium surface tension has been reached for all the surfactants defined by the plateau in surface tension beyond this region. At the longest bubble lifetime recorded, the equilibrium surface tension for PE6800 and F108 is yet to be reached. Focussing on the shortest bubble lifetime, 0.05s, dynamic surface tension decreases in the order F108≈PE6800>>P104>L62≈P123.

L62 lowers the surface tension most quickly from that of pure solvent however produces the smallest foam height indicating that foamability is not solely dependent on the surface tension reduction the surfactant induces and must be affected by additional factors such as a the structure of the adsorbed surfactant layer. It is inevitable that some degree of foam stability is incorporated into foamability measurements as both are inextricably linked. The smaller molecular weight of L62 and its greater hydrophobicity than that of the other surfactants implies that diffusion to the interface will be fastest.[1]

As will be discussed further in Section 3.4.2, both PE6800 and F108 have the same block composition and hydrophobic-lipophilic balance values (>24) however F108 is almost double the size of PE6800. These surfactants are the largest and most hydrophilic of those presented in Figure 3.1 suggesting that they are less surface active and will take longer to diffuse to and rearrange themselves at the interface (compared to the other surfactants studied). Two mechanisms have been proposed in the literature to describe surfactant adsorption; the diffusion controlled mechanism and mixed kinetic diffusion mechanism.[2] The differences are summarised in Figure 3.3. The fact that both PE6800 and F108 exhibit similar dynamic surface tension values at each bubble lifetime suggests that for this concentration and temperature at least the process of adsorption to the interface is not diffusion controlled only. The larger molecular weight of F108 implies slower diffusion and thus a slower decay in DST.

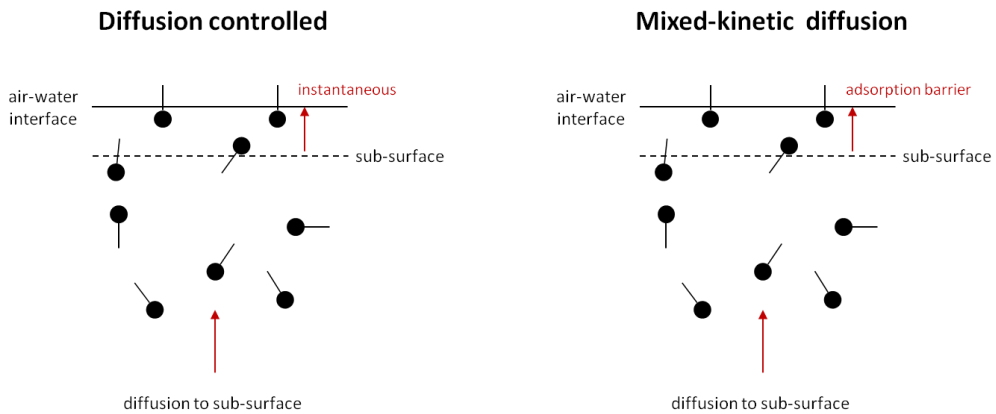

Figure 3.3; Cartoon describing the diffusion controlled (left) and mixed kinetic diffusion (right) mechanisms of surfactant adsorption at the air-water interface.

For the surfactants above the CMC (P123 and P104), a slightly lower dynamic surface tension is observed for P123 which produces the greater foam volume suggesting that there may be some relationship between dynamic surface tension and foamability. However, the difference in surface tension is small so this cannot be stated definitively. The effect of micelles on dynamic surface tension is important as the break down time of the micelles to supply monomer to the interface needs to be considered. A slower decay in DST will be observed if the time taken for the micelle to break down is longer than the time taken to reach the equilibrium surface tension value.[3] From a study of $C_{12}E_n$ (n=5 and 6) non-ionic surfactants it was postulated that the dissociation of micelles is only prevalent when the concentration of monomer present at the subsurface is low.[3] Given the large surfactant concentration used here (relative to the CMC), it is unlikely that the presence of micelles will significantly influence the DST as there is a bulk monomer concentration of surfactant in solution, approximately equal to the CMC, that is available to diffuse to the interface. In fact, in a study of A-B copolymers, Johner and Joanny[4] suggested that the shorter relaxation time associated with the release of monomer from the micelle into the bulk (τ_1) is more important that the longer timescale which correlates to total micelle breakdown (τ_2). For PEO-PPO-PEO surfactants τ_1 varies from 10 microseconds to 10ms, faster than the timescale of the DST measurements recorded here.[5] Thus in essence it is not possible to probe the region in which the breakdown of micelles is important with the maximum bubble pressure technique available to us.

3.3.2. Effect of surfactant structure

3.3.2.1. Increasing PEO molecular weight (PPO=1750gmol^{-1})

The effect on foamability of increasing PEO content (at constant PPO content) is shown in Figure 3.1 by considering the L62, PE6400, PE6800 series. Foamability increases with increasing PEO content as observed by L62<PE6400<PE6800 suggesting that the presence of larger PEO groups (and subsequently overall molecular weight) improve foaming. It is worth noting here that these surfactants are all below their CMT and are therefore all in their molecular phase. Surprisingly, it is the most hydrophilic surfactant PE6800 which produces the greatest foam volume which is a somewhat counterintuitive observation; one would maybe expect the most hydrophobic surfactant (L62) to exhibit the strongest driving force for adsorption at the interface and the greatest foam volume.

However it is here that other factors which contribute to foaming need to be considered. Dynamic and equilibrium surface tension measurements have shown that L62 lowers the surface tension more effectively than PE6800 suggesting greater surface activity. However the change in surface tension with time $\delta\gamma/\delta t$ i.e. the surface tension gradient (based on the data collected) observed over 0.05-1s is much larger for PE6800 than L62 ($13.6 mNm^{-1}s^{-1}$ and $2.4 mNm^{-1}s^{-1}$ respectively). Tamura *et al*.[6] studied the foaming and DST of $C_{12}E_n$ surfactants and demonstrated a relationship between $\delta\gamma/\delta t$ and initial foam height. The author's state that those surfactants which have a large $\delta\gamma/\delta t$, have the potential to produce a large total surface area of bubbles. Essentially more interface can be created for the same amount of work done. Thus the larger surface tension gradient of PE6800 could account for its greater foamability. Studying the surface gradient over a shorter bubble lifetime would confirm such trends. In addition, the correlation to foam stability needs to be considered. L62 produces very unstable foam (see Section 1.4.1) therefore during the foam formation process foam generation and foam depletion will occur simultaneously and the magnitude of this will undoubtedly impact on the maximum foam volume observed. Thus, the foamability value quoted may actually be an under-representation and the more stable the foam, as is the case for PE6800, the closer to a true foamability value is reached. Furthermore, the larger surface tension gradient of PE6800 implies greater Marangoni effects.[6] Sufficient surface tension gradients are required for the surface to resist and restore any thinning that may occur.

Similar findings were observed in a foamability study of Pluronics P85 ($EO_{27}PO_{39}EO_{27}$ Mw $4600 gmol^{-1}$) and F108.[7] Here it was F108 which produced the greatest foam volume at 1μM concentration. After comparing results to a previous study which found that thin film thickness for F108 was larger than P85, the authors concluded that thin film properties did appear to correlate to the properties of the wet foams studied. It was identified that the longer PEO chains of F108 are likely to form a thicker brush layer which will contribute to film thickness producing a greater foam volume. This correlated to the findings of Nemeth *et al*.[8] who studied the antifoaming properties of L62 and F68 (PE6800) and determined that foam stability and foam volume is much greater for the copolymer which has the largest PEO block i.e. PE6800.

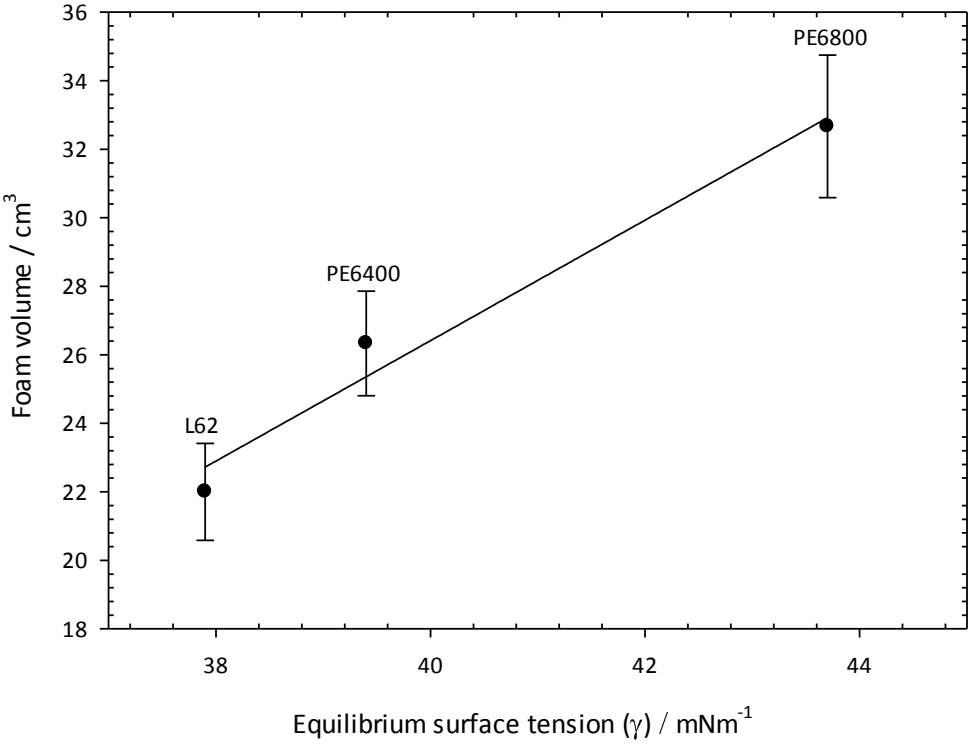

Figure 3.4; Foamability as a function of surface tension for a series of Pluronic surfactants in which the PEO block increases in the order L62<PE6400<PE6800. [Pluronic] = 2%(w/v), 20°C.

As shown in Figure 3.4, foamability scales linearly with equilibrium surface tension; with surface tension also increasing with increasing PEO content (and molecular weight). However, the fact that foam is a dynamic system makes it difficult to compare foamability with an equilibrium surfactant state at the interface. Here, PE6800, the most hydrophilic surfactant of the series, shows the smallest reduction in surface tension from that of pure water with equilibrium surface tension ranked in the order PE6800>PE6400>L62. In a study of the dynamic surface tension of a range of Poloxamers in water, Buckton *et al.*[9] determined that the difference in dynamic and equilibrium surface tension values (at 25°C and a bubble lifetime of 10s) was larger the larger the surfactant i.e. as the total molecular weight of the surfactant increases the lower the reduction in surface tension. The diffusion of larger molecules to the interface is typically slower than that of smaller molecules suggesting that PE6800 with its largest molecular weight will take longer to arrive at the interface. Given that the concentration of surfactant in comparison to the large amount of newly forming interface is small, and assuming there is no activation barrier to adsorption,

this trend demonstrates how foamability is not only governed by the kinetics of adsorption but also the nature of the adsorbed layer itself. At constant PPO block size it has been shown that the area per molecule increases with increasing PEO chain length,[10] so that PE6800 provides fewer surfactant molecules to the interface accounting for the reduced surface activity observed (Figure 3.5). However this also implies that fewer surfactant molecules are required to provide a stable interface and that it is the nature of this interface which produces more stable foam than that of L62 or PE6400.

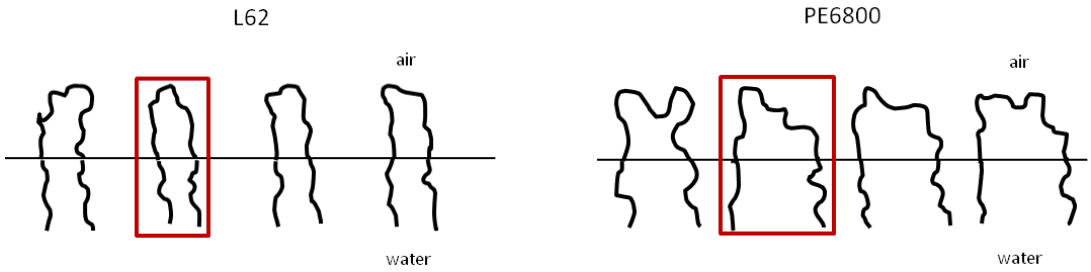

Figure 3.5; Cartoon to show the difference in area per molecule of surfactant at the air-water interface for L62 (left) and PE6800 (right). Not to scale.

3.3.2.2. Increasing PPO molecular weight (PPO=3250gmol^{-1})

The effects of increasing PEO block can also be seen by considering the P103, P104, P105, F108 series which again has increasing PEO content at constant PPO molecular weight, however now the PPO block is larger at 3250gmol^{-1} (Figure 3.6). Foamability does not increase with increasing PEO block as was the trend for the L62, PE6400, PE6800 series. Instead, the trend in foamability follows P103~F108<P105<P104. As Figure 3.6 demonstrates, foamability does not increase linearly with equilibrium surface tension for this series.

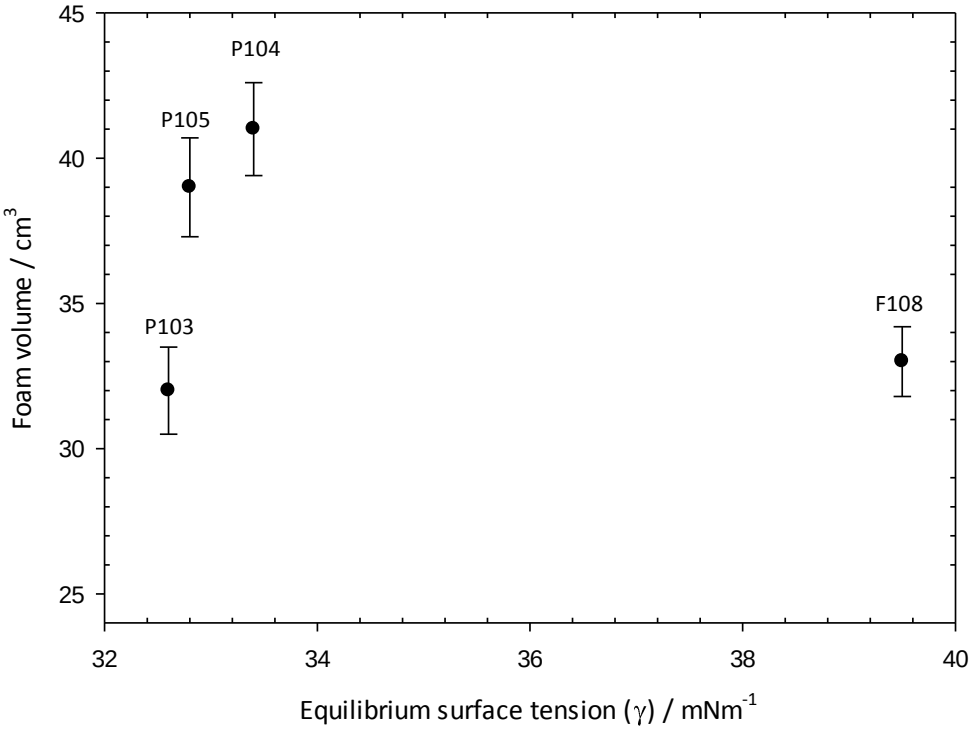

Figure 3.6; Foamability as a function of surface tension for a series of Pluronic surfactants in which the PEO block increases in the order P103<P104<P105<F108. [Pluronic] = 2%(w/v), 20°C.

It is known that the phase behaviour of a surfactant can drastically influence foaming behaviour.[11-13] Therefore to interpret the apparent trends in foamability, the equilibrium surface tension curves for these surfactants have been considered (see Appendix 1). Unlike the previous series (L62, PE6400, PE6800) which were all below their CMT's at the concentration studied, analysis of the break in surface tension with temperature indicates that under the conditions specified in Figure 3.6, (20°C, 2%(w/v)) this series of surfactants are within different phases. P104 is just above the critical micelle temperature (CMT=18°C), P103 is just at the CMT (CMT=21°C), whilst F108 is just below the CMT (CMT=21.8°C). This implies, in principle, that better defined micelles; aggregated species of newly forming micelles; and molecules are likely to be present in the bulk solution for P104, P103 and F108 respectively. However, it is known that above the CMT for polymeric surfactants typically a unimer-micellar transition region occurs over a temperature range of approximately 10-15°C[14] therefore at this temperature there is likely

to be aggregation occurring across all the systems although to a lesser extent for the F108 surfactant.

Thus the fact that P104 displays the greatest foamability in the presence of micelles implies that the presence of micelles in the bulk solution does indeed produce better foaming. It is known that maximum foam height is generally reached at the CMC as this is where the greatest reduction in surface tension and maximum surfactant adsorption is observed.[15] Interestingly, F108 which has high molecular weight (14000gmol^{-1}) but is in its molecular phase (however probably with some aggregation occuring) displays similar foamability to P103 which has more micelles present but a lower Mw (4950gmol^{-1}). This serves to show how foamability is a delicate balance between surfactant structure and phase behaviour.

In order to make a more appropriate comparison of foamability it is therefore necessary to ensure the surfactants in this series are all within the same phase. This can be achieved by measuring foamability at 40°C in which all surfactants are above their critical micelle temperatures (Figure 3.7). It can now be seen that a trend which is approaching that of that of the L62, PE6400, PE6800 series is followed, however a true linear increase is not observed. This is again due to differences in phase behaviour. Beyond the CMT, a reduction in foamability is observed (see Chapter 5) and so the apparent distance from the CMT is also important. In addition, it is again the most hydrophilic surfactant F108 which displays the greatest foam volume and this has the highest equilibrium surface tension value.

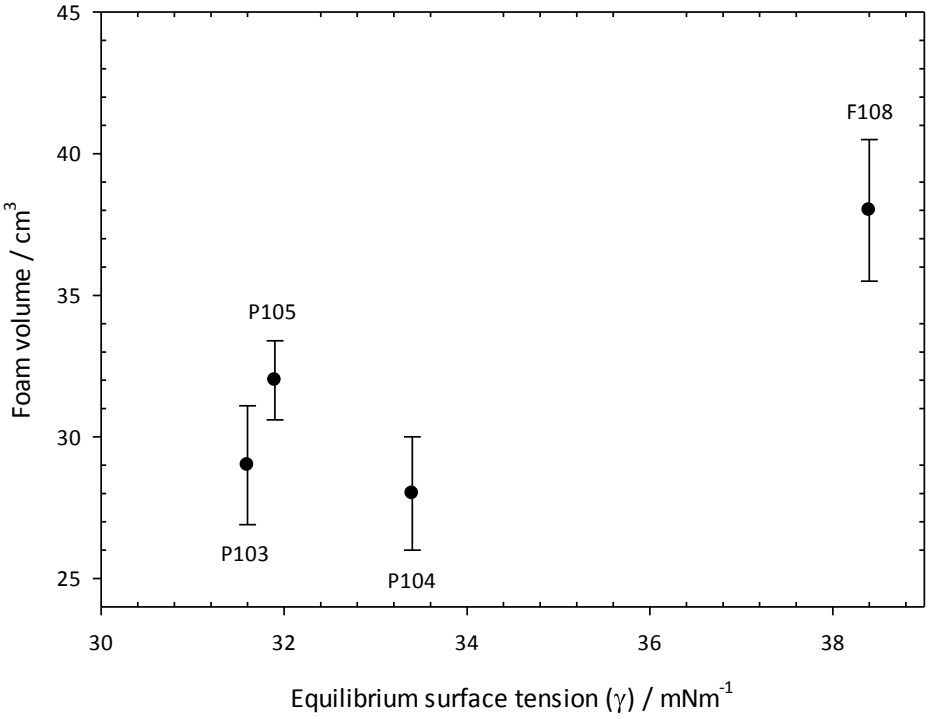

Figure 3.7; Foamability as a function of surface tension for a series of Pluronic surfactants in which the PEO block increases in the order P103<P104<F108. [Pluronic] = 2%(w/v), 40°C..

3.3.2.3. Increasing PPO molecular weight

Figure 3.8 shows an increase in foamability is observed upon increasing PPO block (at constant PEO block), with foamability following the order P84<P103<P123. P123 is the most hydrophobic of this series and therefore is expected to exhibit a stronger driving force for adsorption to the interface thus accounting for its greater initial foam height. There is no obvious trend in equilibrium surface tension with foamability for this series of surfactants (Figure 3.9). However, it is noted that there is little difference in the absolute values of surface tension at 20°C. Given that there is some variation in the number of PEO segments P103 = 34, P84 = 38, P123 = 40 (there is no available series which has identical PEO segments) this suggests that the equilibrium surface tension is independent of PPO segments.

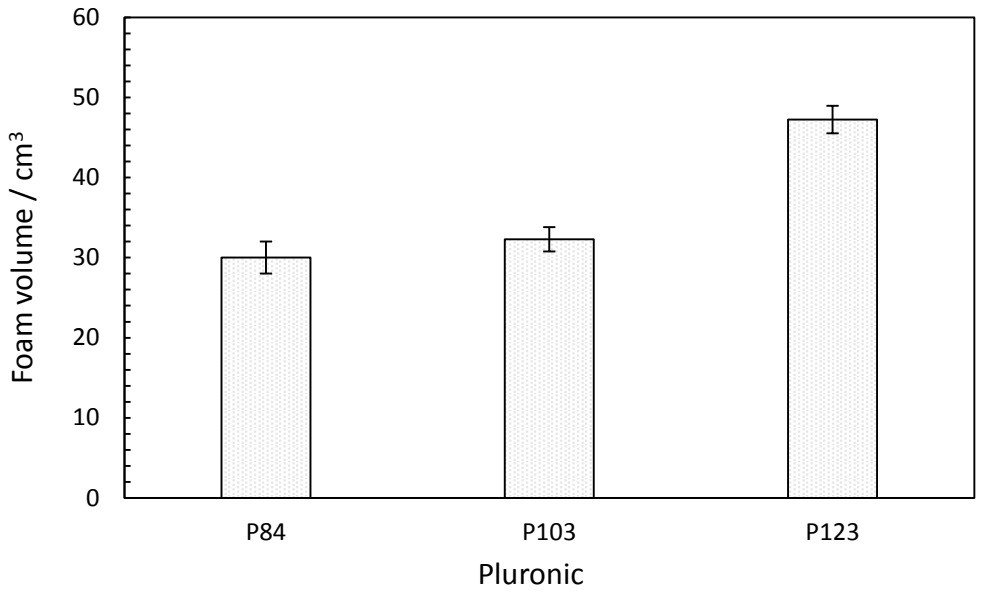

Figure 3.8; Foamability for air-in-water foams for a series of Pluronic surfactants in which the PPO block increases in the order P84<P103<P123. [Pluronic] = 2%(w/v), 20°C.

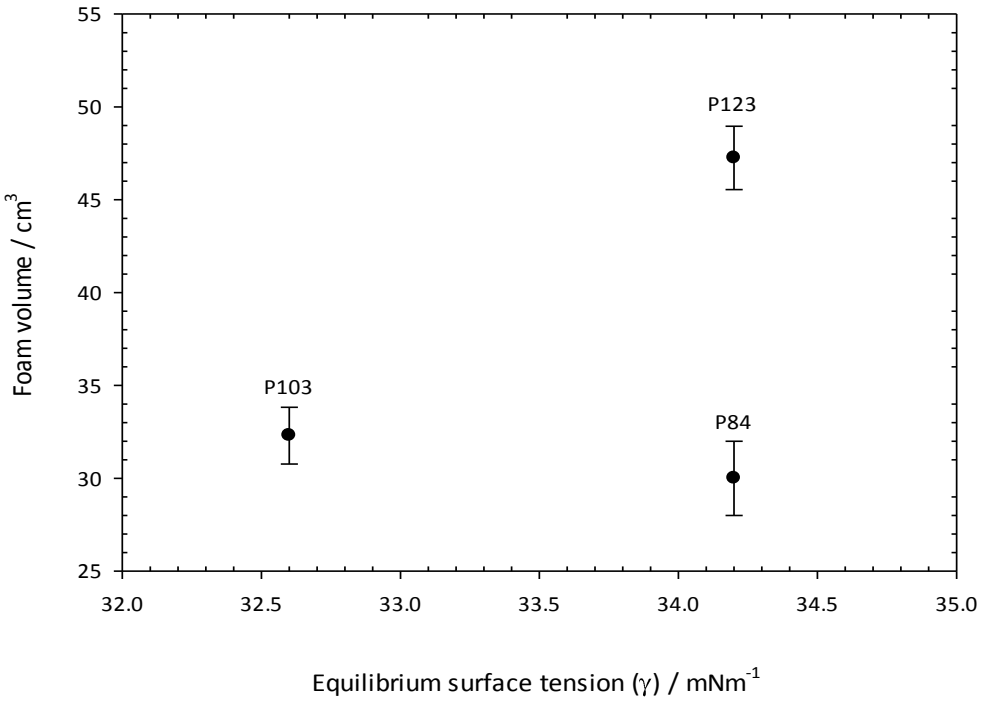

Figure 3.9; Foamability as a function of surface tension for a series of Pluronic surfactants in which the PPO block increases in the order P84<P103<P123. [Pluronic] = 2%(w/v), 20°C.

3.4. Foam stability

3.4.1. Effect of overall molecular weight

Figure 3.10 shows foam stability, as described by the foam half-life ($t_{1/2}$), for a selection of Pluronic surfactants again at 5% (w/v) concentration and 20°C. The first observation to note is that, for this selection of surfactants at least, foam stability increases with increasing overall molecular weight in the order L62<PE6400<PE6800<F108 suggesting that larger molecular weight surfactants stabilise aqueous foams more effectively. Similar behaviour was observed in a study of aqueous Pluronic foams by Rippner-Blomqvist *et al.*[16] who found that the smallest molecular weight surfactant that generated sufficient foam for study, P85 (4600gmol^{-1}) produced the most unstable foam with the majority of bulk liquid drained within the shortest timescale (approximately 400s). It is known that increased solution viscosity promotes foam stability by reducing the drainage rate of liquid from the bubble walls into the plateau borders, thus delaying bubble coalescence and rupture.[17] Therefore, F108 with its larger molecular weight would be expected to display a greater solution viscosity at the bulk concentration of 5% (w/v) studied here and so this may account for the enhanced foam stability observed. In fact, viscosity measurements performed for the smallest molecular weight surfactant (L62) and the largest molecular weight surfactant (F108) indicated that at 5%(w/v) concentration, the kinematic viscosity of the bulk solutions varied from 1.39mm^2/s to 2.85mm^2/s respectively. Thus confirming solutions that contain those surfactants with larger molecular weight will exhibit greater viscosity and consequently produce a more stable foam.

It is difficult to de-convolute the effects of overall molecular weight and foam stability as inevitably any increase in overall molecular weight will involve increasing either or both of the PEO and PPO block molecular weights and this can induce other changes in the surface behaviour of the surfactant. However, in probing further the structure of these surfactants such as PEO and PPO block ratio and block size, it is possible to explore how relative hydrophobicity and hydrophilicity influence foam stability.

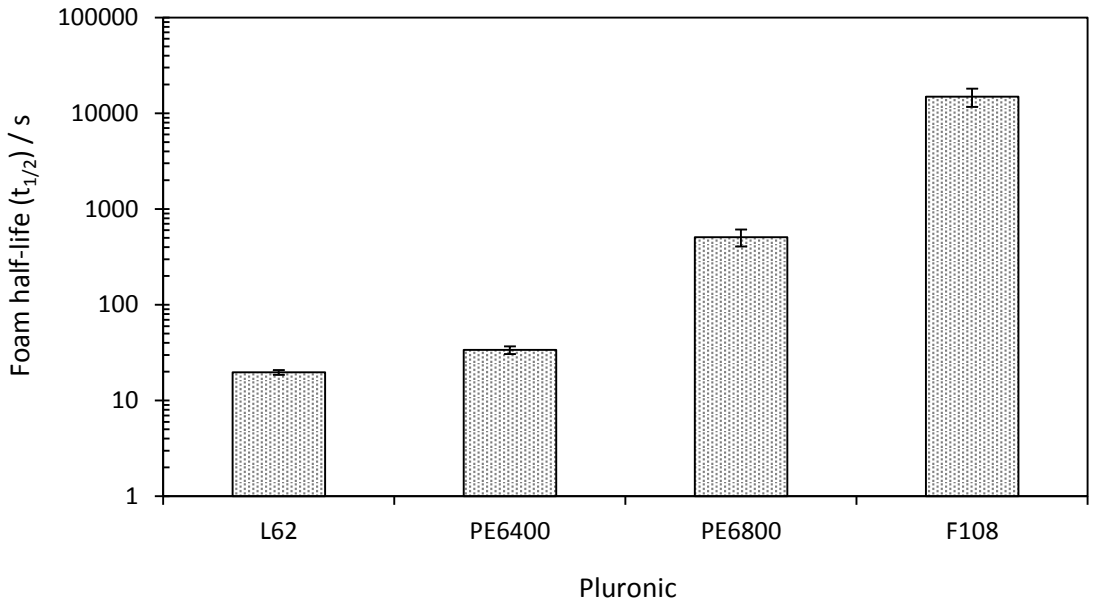

Figure 3.10; Stability of the air-in-water foams as a function of Pluronic type; [Pluronic] = 5% (w/v), 20°C, flow rate 0.08L/min, 0.8bar. The stability of the foam presented on a logarithmic scale is quantified in terms of the foam half-life, $t_{1/2}$ as described in the experimental section.

3.4.2. Effect of increasing PEO and PPO block sizes

It is first noted that F108 has PEO and PPO block sizes that are approximately double those in PE6800. This allows the overall molecular weight to be increased without altering the hydrophilic lipophilic balance (HLB) of the surfactant. An increase in foam stability is observed upon increasing the overall molecular weight suggesting that larger block sizes do indeed contribute to foam stability however it cannot be stated with certainty that this effect is due solely to the increased overall molecular weight. Interestingly, foam stability for F108 is almost 30 fold that of PE6800 indicating that foam stability does not correlate to molecular weight in a purely additive manner i.e. although the molecular weight of F108 is almost double that of PE6800, a doubling in foam stability is not observed. This suggests that molecular weight is not the only parameter which governs foam stability.

Neutron reflection studies at equilibrium have shown that for F108 the adsorbed layer thickness at 0.1wt% concentration, attributed to the swollen PEO chain, is nearly double the size of that for PE6800 (98Å and 57Å respectively) and this did not change appreciably upon increasing the concentration to ~2wt%.[18] Assuming a polymer brush

model, film thickness also scaled linearly with number of EO segments. This suggests that it is the larger PEO chain length of F108 which promotes stability by forming a thicker layer at the interface which in turn produces a thicker film. In addition, F108 has a larger PPO block size. The hydrophobic block, with its low affinity for water, adsorbs at the air-water interface thereby lowering the surface tension of the system ultimately providing a mechanism of elasticity that repairs the foam when excessive localised thinning occurs.[19]

The area per molecule under equilibrium conditions for a variety of Pluronic surfactants has previously been determined using surface tension data at 0.1% concentration and 25°C, providing insight into the adsorbed layer structure.[10] Two observations were noted; those surfactants with larger hydrophobic block were found to occupy less area at the air-water interface forming a more tightly packed layer, whilst the area per molecule increased with increasing PEO segments. Surfactants P65 (3600gmol^{-1}) and P105 (6500gmol^{-1}), which appear at comparable locations on the Pluronic grid to PE6800 and F108, displayed areas per molecule of 118 and 99Å^2 respectively. This implies that F108 will have the smaller area per molecule suggesting a more compact structure at the interface which may impart greater foam stabilisation. Moreover, larger hydrophobic blocks implies a greater driving force for adsorption. However, using light ellipticity Sedev *et al.*[20] state that the area per molecule of both PE6800 and F108 is the same (1.8 and 1.9 nm^2 respectively). This would imply that it is the size of the PEO block which contributes most greatly to foam stability.

In this work, an increase in foam half-life is observed with increase in hydrophilic portion, i.e. larger poly(ethylene oxide) (PEO) block. This can be observed for Pluronics L62, PE6400 and PE6800 in which the hydrophobic block is of constant mass but the percentage hydrophile in the molecule increases from 20 to 40 to 80% respectively. It is generally accepted that adsorption of tri-block copolymers of this nature at the air-water interface involves the hydrophobic poly(propylene oxide) block anchoring the polymer to the interface whilst the poly(ethylene oxide) blocks protrude into the aqueous phase due to their strong affinity for water.[21] Whilst repulsion of these blocks will occur over small distance scales imparting steric stabilisation (as is seen in colloidal particle

systems)[22] it is unlikely that short-range steric repulsion will occur here. We estimate PEO-PPO-PEO bubble lamellae in newly prepared systems in which the bubbles appear spherical are of millimetre size. Even in thin, dry foams in which distortion of cells to a polyhedral structure occurs, the cell walls are still visible to the naked eye. Typically, length scales for adsorbed layer thickness at the air-water interface are in the region of tens of angstroms whilst typical thin bubble lamellae are generally hundreds of nanometres wide.[19] As steric interactions are most significant when the separation between surfaces is twice the adsorbed layer thickness, only in very thin, dry foams would we expect to see repulsion between PEO groups.[23, 24]

For very thick foams in which bubbles appear spherical, as is the case for the unstable foams observed here, hydrostatics are believed to be the cause of breakdown, with these films being more sensitive to thermal and vibrational fluctuations.[19] As mentioned previously, larger PEO chains lengths have been attributed to thicker films therefore it would be expected that film thickness would follow in the order of PE6800>PE6400>L62 for this series. The longer chains of PE6800 will be immersed more deeply into the aqueous layer presumably providing an additional degree of stabilisation. This correlates to findings from SANS studies performed on three-dimensional Pluronic stabilised foams (see Chapter 4) in which PE6800 displayed the thickest adsorbed surfactant layer of this series.

3.4.3. Effect of surfactant phase behaviour

Foam stability has been further investigated by considering the phase behaviour of the surfactant at a specified concentration and temperature. Figure 3.11 shows foam stability as a function of surfactant in which both molecular phase (L62, PE6400, PE6800, F108) and micellar phase (P103, P123, P104) surfactants are presented. The first observation to note is that as per the foamability experiments, foam stability does not follow the trend of increasing with increasing molecular weight in the presence of micelles. Instead enhanced stability is observed for those surfactants in their micellar phase. This suggests that for those surfactants above their CMC the presence of micelles provides an additional stabilising effect. Moreover, this is supported by probing further the overall molecular weight; PE6800 has a larger molecular weight (8400gmol^{-1}) than P123 (5750gmol^{-1}) however a shorter foam half-life therefore the stability trends observed cannot be only

due to molecular weight effects. The effect of micelles on foam stability will be discussed in greater detail in Chapter 5.

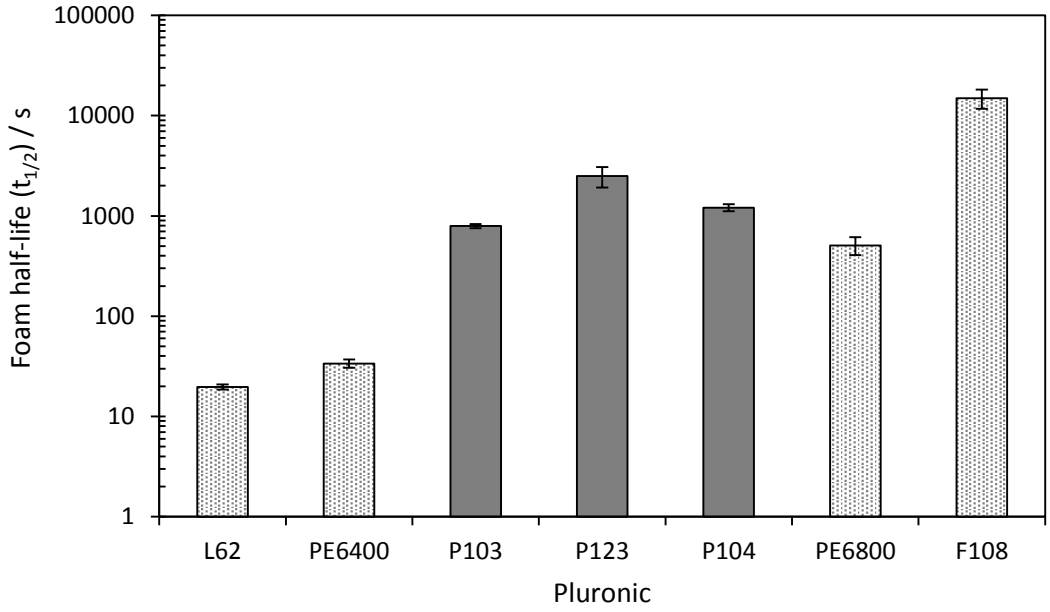

Figure 3.11; Stability of the air-in-water foams as a function of Pluronic type; [Pluronic] = 5% (w/v), 20°C, flow rate 0.08L/min, 0.8bar. The stability of the foam presented on a logarithmic scale is quantified in terms of the foam half-life, $t_{1/2}$ as described in the experimental section. Those Pluronics highlighted by the block grey bars are above their CMC's.

It is not possible to completely eliminate the effects of phase behaviour at a standard concentration and temperature. However, foam stability has also been studied at a polymer concentration of 0.05%(w/v) (Figure 3.12) to make direct comparisons to small-angle neutron scattering (SANS) data presented in Chapter 4. Here, the majority of surfactants are below their CMT (with the exception of P104 and P123), although the relative distance from the CMT varies for each surfactant. In addition, viscosity effects are eliminated here, the kinematic viscosity of L62 and F108 solutions at a higher concentration of 0.5%(w/v) showed little difference (0.87mm^2/s and 0.93mm^2/s). It will be seen in Chapter 5 that foaming is highly dependent on temperature therefore it is difficult to make direct comparisons due to the differing points on the phase diagram these surfactants are at (under the specified conditions).

Across all of the surfactants there is no correlation between foam stability and molecular weight suggesting that other factors such as phase behaviour and PEO/PPO block size

and ratio must also contribute to foam stability. However, it is worth noting that the surfactant series, PE6400, P84 and F108 have similar CMT's (42°C, 39.5°C and 38°C respectively) and so are all at the same approximate positions on the phase diagram allowing quantitative observations to be made. It can be seen that foam lifetime does increase with increasing molecular weight confirming that molecular weight does indeed influence foam stability, however a linear increase is not observed.

Comparisons of adsorbed layer structure for these surfactants determined by SANS and foam stability will be discussed in Chapter 4.

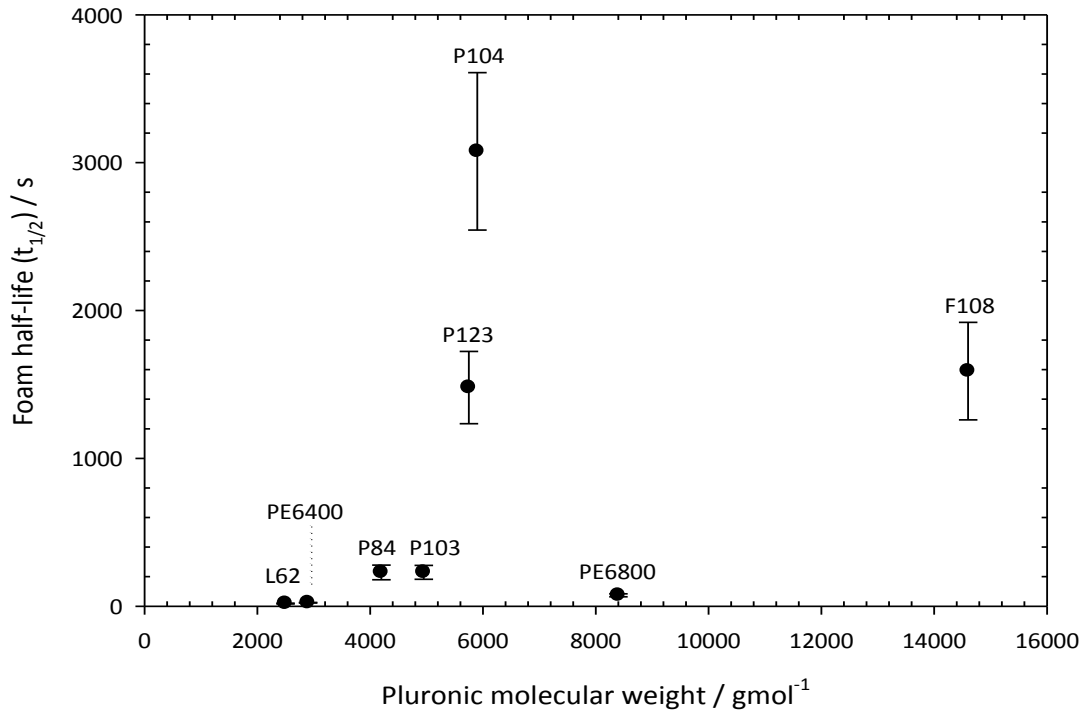

Figure 3.12; Stability of the air-in-water foams as a function of Pluronic molecular weight; [Pluronic] = 0.05% (w/v), 20°C, flow rate 0.08L/min, 0.8bar. The stability of the foam presented on a logarithmic scale is quantified in terms of the foam half-life, $t_{1/2}$ as described in the experimental section.

3.4.4. Concentration effects

A smaller number of polymeric surfactants were down-selected to assess the concentration dependence of the foam stability (Figure 3.13). The foam lifetime for the series L62, PE6400 and PE6800 is reminiscent of the high affinity adsorption isotherm

for surfactants of this type adsorbed onto polystyrene latex dispersions; foam stability increases rapidly at low concentrations, before ultimately attaining a plateau value at some characteristic concentration, suggesting that there is a relationship between the foam stability and surface coverage, and that excess polymeric surfactant in solution increases the foam stability, but less markedly. Based on the foam data obtained, it could be speculated that the plateau in foaming correlates to monolayer coverage. However, the work of Berg *et al*.[25] at the polystyrene latex surface showed that the concentration corresponding to the adsorbed plateau was well above that required to create a monolayer and an extended conformation at the interface was proposed. Study of the adsorbed layer structure using small-angle neutron scattering, in Chapter 4, will confirm the existence of a monolayer, bilayer or further structure at the interface.

Typically enhanced stability is observed with increasing concentration due to viscosity effects, in which greater viscosity retards thinning and drainage.[19] Viscosity measurements performed for Pluronic L62 indicated that viscosity does indeed increase upon increasing concentration (0.87mm^2/s at 0.5%(w/v) and 1.39mm^2/s at 5%(w/v). The drainage rate of films at concentrations near to the CMC is also reduced when high surface tension gradients are observed.[19] This is due to small bulk diffusion coefficients and large Gibbs elasticity. Thus maximum stability at the CMC is typically expected.* However, over the concentration range studied here, the bulk surfactant concentration for each system is below the CMC therefore it is unlikely that the plateau in foam stability is due to micellisation. Given the large bubble surface area it is unlikely that molecules will aggregate in solution.

At all concentrations, the stability of the foam for this series again followed the order PE6800>PE6400>L62. As described in Section 1.4.1.1 PEO block size increases in the order L62<PE6400<PE6800 so that larger PEO blocks provide increased foam stability.

For P123 the foam lifetime looks somewhat different, in that foam lifetime again increases rapidly at low concentrations but then reaches a maximum value at 0.5% (w/v).

* For polymeric surfactants the CMC is typically observed over a concentration range due to large polydispersity.

This maximum in concentration has been attributed to the onset and subsequent formation of well-defined micelles in bulk solution, corresponding reasonably well to the CMC of P123 quoted in the literature at 0.18%(w/v).[26] As previously mentioned, it is known that reduced drainage rates and maximum stabilities are observed when the surface tension gradients are at a maximum i.e. on approach to the CMC.[19, 27] The reduction in stability that is observed at higher concentrations is postulated to be due to the Gibbs-Marangoni effect. The Gibbs-Marangoni effect states that at high surfactant concentrations (above the CMC) surface tension gradients are dissipated too quickly due to the fast diffusion of surfactant to the interface which results in thin films which can easily rupture. Moreover, the elasticity of thin films stabilised with P123 has been shown to decrease above the CMC.[28]

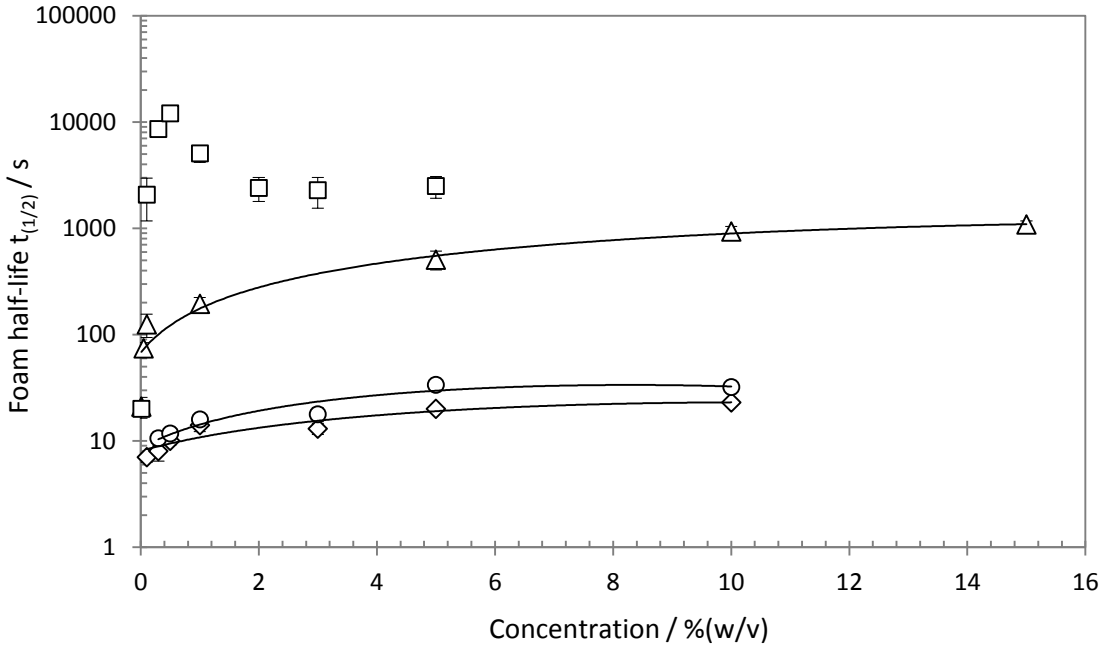

Figure 3.13; Stability of the air-in-water foams for four representative polymer surfactants (L62 diamonds; PE6400 circles; PE6800 triangles and P123 squares) with gas flow rate 0.08 L/min, 0.8 bar). The stability of the foam presented on a logarithmic scale is quantified in terms of the foam half-life, $t_{1/2}$, as described in the Experimental section.

3.5. Comparison of foamability and foam stability

In most cases foamability and foam stability exhibit the same trend and this is not unexpected (Figure 3.14); foamability and foam stability are closely interwoven with

greater foamability typically linked to more stable foams.[29] F108 is the only exception in which it displays a smaller foam volume than would be expected based on the trends in foam stability. As this is the largest, most hydrophilic surfactant studied, it would be expected that the diffusion rate to the interface would be slowest. Additionally, it will inevitably exhibit a greater bulk solution viscosity which would further reduce the diffusion rate thus accounting for its decreased foamability. The formation of foam bubbles is a dynamic process which depends on; the kinetics of adsorption, the ability of the surfactant to rapidly lower the surface tension of the system, the velocity of bubble formation and the nature of the adsorbed layer.[30] Without stability, bubbles will not form, therefore although foamability is measured independently; there is a degree of foam stability involved. In addition, it is worth noting that the differences in absolute values of foam lifetime are much greater than that of foam volume, implying that foam stability is more strongly dependent on structural changes within the surfactant than foamability.

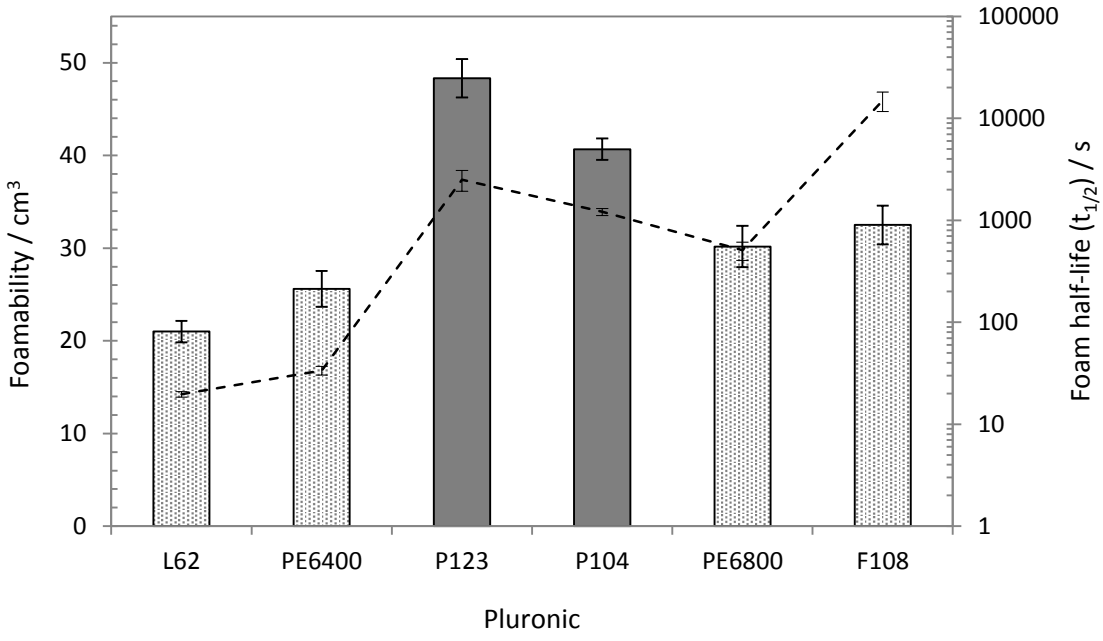

Figure 3.14; Comparison of foamability (bars) and foam stability (dotted line) (note the logarithmic scale) for a variety of Pluronic surfactants; [Pluronic] = 5%(w/v), 20°C. Those surfactants highlighted by the block grey bars are above their CMC's.

3.6. Foam breakdown

Plotting the foam stability data as a function of time versus foam height / foam height at zero seconds also gives insight into the depletion behaviour of the foams (Figure 3.15). It can be seen that the most stable foams, F108 and P123, remain stable for a much longer period of time and then gradually break down whilst the least stable foams, L62 and PE6400, break down almost immediately after formation. This supports the observations of Georgieva *et al*.[31] who observed that after fairly short timescales the height of PE6800 foam decreased (this was in comparison to the short chain non-ionic surfactants $C_{12}E_6$ and β-$C_{12}G_2$). The thinning of cell walls from spherical bubbles to polyhedral cells was visually observed in foams from F108 and P123. This was not the case for the other systems in which foam breakdown was so rapid suggesting that the mechanism for foam drainage and destruction is very different in the most stable foams. Previous literature studies suggest that there may be some correlation between foam stability and the elasticity of films stabilised with Pluronics.[32] A larger elasticity value correlated to greater foam stability, however, only two surfactants were studied and so a systematic analysis of a range of surfactant is needed in order to draw quantitative conclusions. Based on this reasoning, foams stabilised with F108 and P123 would be expected to display greater elasticity. A full understanding of how surface rheology properties such as elasticity and viscosity correlate to the mechanisms of film collapse (drainage, coalescence and Ostwald ripening) is needed to fully understand these systems however translating the theory of thin film behaviour to real foam systems is very difficult due to their inherent complexity.

Visual inspection of foam structure for the Pluronic surfactants indicated that the various surfactants behave rather differently (Figure 3.16) and that the structures of the bubbles formed varies markedly with Pluronic. Illustrative data only are presented. For all newly prepared foams, bubbles appeared spherical, separated by thick lamellae walls (Figure 3.16, 1-3a). However, as P123 (and F108 – data not shown) foams aged, the spherical structures distorted into multi-sided polyhedral cells with thinner cell walls (Figure 3.16, 3b). This was also observed for PE6800 although to a lesser extent (Figure 3.16, 2b), whereas foams of L62 (Figure 3.16, 1b) and PE6400 (not shown) broke down before drainage and distortion of cells occurred.

This implies that the adsorbed surfactant layer of P123 and F108 foams are better at stabilising the interface by withstanding film breakdown mechanisms and allowing drainage to proceed until persistent dry films are formed. Based on previous literature findings, typically greater viscosity and elasticity produce more stable foams.[1] In addition, we know from the detailed foam stability studies described in Section 1.4 that structural properties of the surfactant are highly important in defining stability. Without a detailed account of the surface properties of these systems such as disjoining pressure, elasticity, viscosity and drainage rates it is not possible to draw quantitative conclusions.

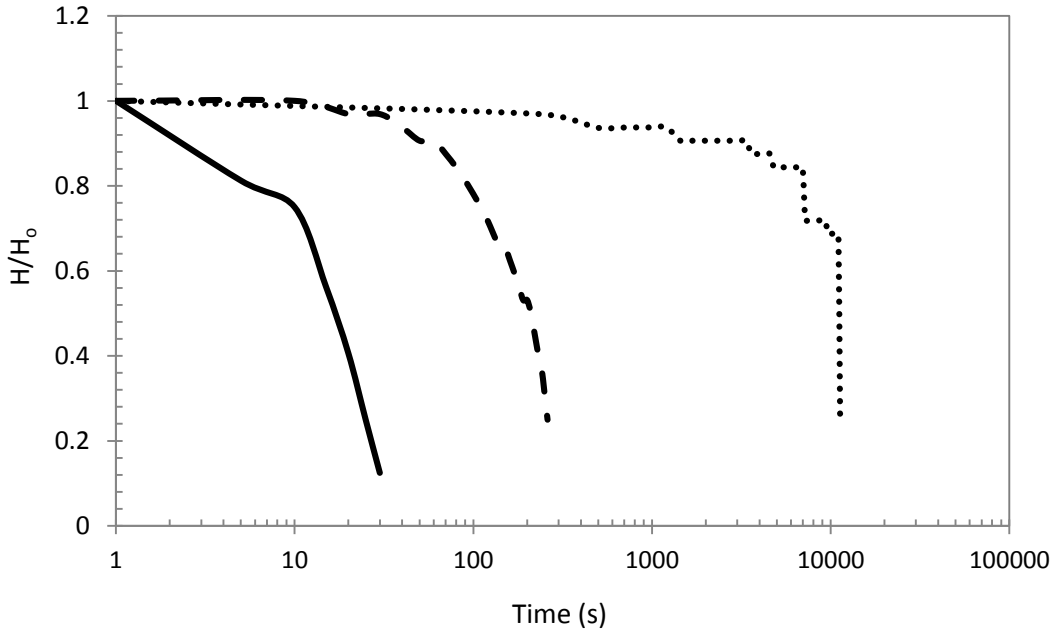

Figure 3.15; Normalised foam height versus time for air-in-water Pluronic stabilised foams. H/Ho defines the foam height / foam height at time = 0s; [Pluronic] = 5% (w/v), 20°C, flow rate 0.08L/min, 0.8bar. PE6400 (solid line), PE6800 (dashed line), P123 (dotted line).

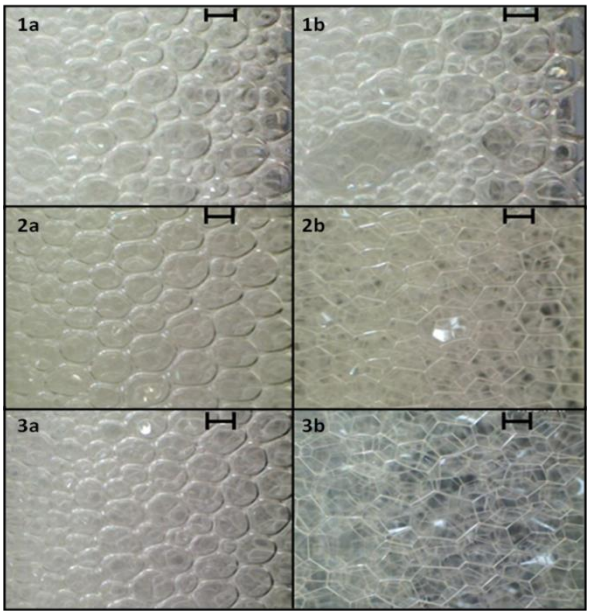

Figure 3.16; Differences in foam structure for newly prepared foam (left) and aged foam (right) for 5% (w/v) solutions of PE6400 (1a,b), PE6800 (2a,b) and P123 (3a,b) at 20°C. Scale bar is 1mm in all cases.

3.7. Bubble size determination

Average bubble size (quantified by the bubble perimeter) has been determined for foams produced within 10 seconds of formation at 20°C and 5%w/v surfactant (Figure 3.17). The frequency distribution curves for bubble size are presented in Figure 3.19 and the average bubble count per $10mm^2$ area of foam in Figure 3.18 . Within the error of the data there is little difference in the average bubble size across the surfactants studied or the average bubble count. These parameters for each surfactant were obtained by measuring bubble sizes and bubble counts from a minimum of three foams. Thus the polydispersity of bubble sizes within each system is large probably due to the dynamic nature of the foam and the fact that all generated foams will inevitably be different. Therefore, it is not possible to elucidate quantitative differences in bubble size and the results suggest that at constant air flow, the nature of the surfactant does not induce differences in the volume fraction of the bubbles produced.

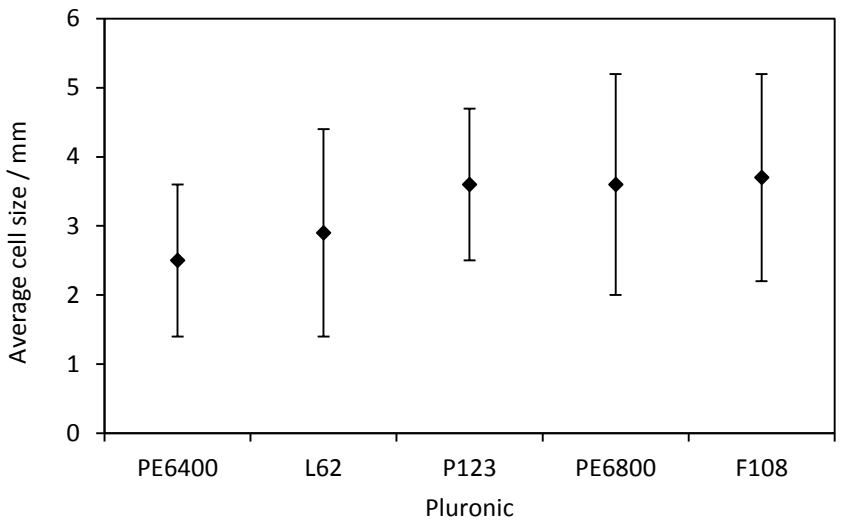

Figure 3.17; Average cell size for a range of Pluronic stabilised air-in-water foams; [Pluronic] = 5% (w/v), 20°C, flow rate = 0.08L/min, 0.8 bar.

There is little difference in bubble size frequency distribution for P123, PE6800 and F108 (Figure 3.19). However, PE6400 and L62 have the highest frequency of bubbles falling within the smallest bubble area categories i.e. less than 3mm. Smaller cell size has been attributed to a greater surface activity[33] suggesting that the surface activity of PE6400 and L62 is the greatest. In terms of driving force for adsorption it is L62 that is the most hydrophobic. However as this is a small surfactant which exhibits fairly low foaming ability and stability it is clear that foaming behaviour must also be complicated by additional factors such as surface coverage at the interface, adsorbed layer thickness *etc* which are influenced by the overall surfactant molecular weight and the molecular weight of the individual blocks.

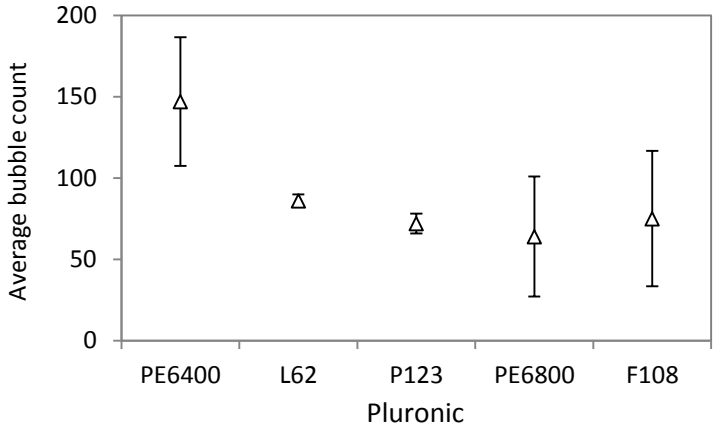

Figure 3.18; Bubble count within 10mm^2 of foam;[Pluronic] = 5%(w/v), 20°C.

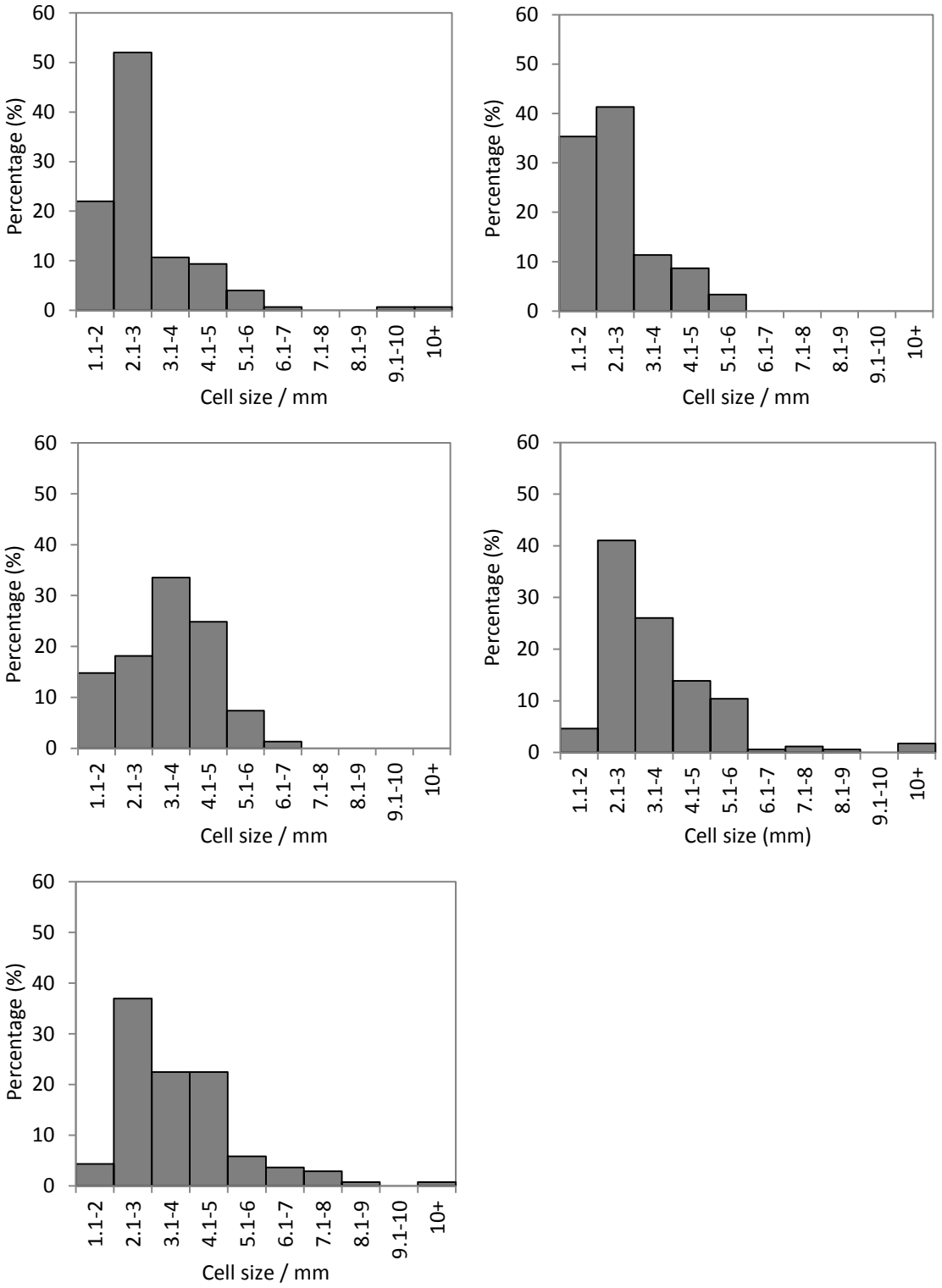

Figure 3.19; Bubble size distribution plots for Pluronic stabilised air-in-water foams; [Pluronic] = 5%(w/v), 20°C, flow rate = 0.08L/min, 0.8 bar.

3.8. Conclusion

The foaming behaviour of PEO-PPO-PEO block copolymer surfactants has been characterised and results indicate that both foaming ability and foam stability are closely related and are strongly dependent on the composition of the block copolymer. Foam stability was found to be more sensitive to structural variations within the polymers with greater magnitude differences in foam stability observed compared to foamability. Studying systematic changes in the polymer composition allowed the effects of relative PEO and PPO block size to be probed and some key conclusions are drawn;

- Below the CMC or CMT, foams of large volume and good stability are characterised by typically large overall molecular weight which exhibit greater bulk solution viscosity thus slowing the drainage rate of liquid in the cell walls. However overall molecular weight alone does not guarantee good foam.

- Increasing the length of the PEO chains (at constant PPO) contributes to foaming presumably due to the thicker adsorbed layer formed at the interface. Although these are the most hydrophilic surfactants and display the smallest reduction in surface tension, clearly foaming is a balance between the surface active properties of the stabiliser and the nature of the adsorbed layer itself. Whilst the same effect is observed upon increasing PPO blocks (at constant PEO) this is much less notable.

- The phase of the surfactant is crucial and must always be considered when comparing foaming from different Pluronics. On approach and in the region of the CMC / CMT, the presence of micelles in solution promotes foaming due to high surface tension gradients. However, concentration effects are also important and at bulk concentrations far beyond the CMC, the presence of micelles induces an antagonistic effect. This is an important consideration when determining surfactant concentrations for use in polyurethane systems.

- Those surfactants which form the most stable foams exhibit very different drainage and breakdown mechanisms which can be observed visually. The interfacial properties of the foam such as elasticity and viscosity are postulated to be very important here. Determining the structure of the adsorbed layer (Chapter 4) for these systems may give insight and understanding into the apparent behaviour observed.

3.9. References

1. T. Tadros, *Applied Surfactants: Principles and Applications*, Wiley, Weinheim, 2005.

2. J. Eastoe and J. S. Dalton, *Advances in Colloid and Interface Science*, 2000, **85**, 103-144.

3. J. Eastoe, J. S. Dalton, P. G. A. Rogueda, E. R. Crooks, A. R. Pitt and E. A. Simister, *Journal of Colloid and Interface Science*, 1997, **188**, 423-430.

4. A. Johner and J. F. Joanny, *Macromolecules*, 1990, **23**, 5299-5311.

5. I. Goldmints, J. F. Holzwarth, K. A. Smith and T. A. Hatton, *Langmuir*, 1997, **13**, 6130-6134.

6. T. Tamura, Y. Kaneko and M. Ohyama, *Journal of Colloid and Interface Science*, 1995, **173**, 493-499.

7. R. Sedev, B. Jachimska, K. Khristov, K. Malysa and D. Exerowa, *Journal of Dispersion Science and Technology*, 1999, **20**, 1759-1776.

8. Z. Nemeth, G. Racz and K. Koczo, *Colloids and Surfaces A: Physicochemical and Engineering Aspects*, 1997, **127**, 151-162.

9. G. Buckton and E. O. Machiste, *Journal of Pharmaceutical Sciences*, 1997, **86**, 163-166.

10. P. Alexandridis, V. Athanassiou, S. Fukuda and T. A. Hatton, *Langmuir*, 1994, **10**, 2604-2612.

11. A. D. Nikolov, D. T. Wasan, N. D. Denkov, P. A. Kralchevsky and I. B. Ivanov, *Surfactants and Macromolecules : Self-Assembly at Interfaces and in Bulk*, 1990, **82**, 87-98.

12. A. BonfillonColin and D. Langevin, *Langmuir*, 1997, **13**, 599-601.

13. K. Oetjen, C. Bilke-Krause, M. Madani and T. Willers, *Colloids and Surfaces A: Physicochemical and Engineering Aspects*, **460**, 280-285.

14. R. Zana, C. Marques and A. Johner, *Advances in Colloid and Interface Science*, 2006, **123**, 345-351.

15. M. Rosen, *Surfactants and interfacial phenomena*, 2nd edn., Wiley, New York, USA, 1989.

16. B. R. Blomqvist, S. Folke and P. M. Claesson, *Journal of Dispersion Science and Technology*, 2006, **27**, 469-479.

17. D. Exerowa, P. M. Kruglyakov, *Foam and Foam Films; Theory, Experiment, Application*, Elsevier, Amsterdam, NL, 1998.

18. R. Sedev, R. Steitz and G. H. Findenegg, *Physica B-Condensed Matter*, 2002, **315**, 267-272.

19. R. J. Pugh, *Advances in Colloid and Interface Science*, 1996, **64**, 67-142.

20. R. Sedev, D. Exerowa and G. H. Findenegg, *Colloid and Polymer Science*, 2000, **278**, 119-123.

21. P. Alexandridis and T. A. Hatton, *Colloids and Surfaces A - Physicochemical and Engineering Aspects*, 1995, **96**, 1-46.

22. J. van. Duijneveldt, *Colloid Science; principles, methods and applications*, Wiley, Sussex, UK, 2010.

23. T. F. Tadros, ed., *Colloid Stability; The role of surface forces - Part 1*, Wiley, Germany, 2007.

24. R. Sedev, T. Kolarov and D. Exerowa, *Colloid and Polymer Science*, 1995, **273**, 906-911.

25. J. A. Baker and J. C. Berg, *Langmuir*, 1988, **4**, 1055-1061.

26. P. Alexandridis, J. F. Holzwarth and T. A. Hatton, *Macromolecules*, 1994, **27**, 2414-2425.

27. C. Morrison, L. L. Schramm and E. N. Stasiuk, *Journal of Petroleum Science and Engineering*, 1996, **15**, 91-100.

28. S. Sett, S. Sinha-Ray and A. L. Yarin, *Langmuir*, 2013, **29**, 4934-4947.

29. K. Malysa and K. Lunkenheimer, *Current Opinion in Colloid & Interface Science*, 2008, **13**, 150-162.

30. P. Somasundaran, ed., *Encyclopedia of Surface and Colloid Science*, 2 edn., CRC Press, Florida, USA, 2006.

31. D. Georgieva, A. Cagna and D. Langevin, *Soft Matter*, 2009, **5**, 2063-2071.

32. X. D. Zhang, C. W. Macosko, H. T. Davis, A. D. Nikolov and D. T. Wasan, *Journal of Colloid and Interface Science*, 1999, **215**, 270-279.

4. Probing the structure of PEO-PPO-PEO surfactant stabilised foams in-situ using small-angle neutron scattering

4.1. Abstract

Small-angle neutron scattering was used to probe the interfacial structure of air-in-water foams stabilised with a series of tri-block copolymers of the poly(ethylene oxide)-poly(propylene oxide)-poly(ethylene oxide) ($PEO_xPPO_yPEO_x$) type from which the nature of the adsorbed polymeric surfactant layer could be characterised. The scattering data followed a pronounced Q^{-4} decay and showed a number of inflexions at various intermediate Q values. The data was well described by a model embodying paracrystalline stacks of adsorbed surfactant layers at the air-water interface. A minimum of approximately five paracrystalline surfactant layers of thickness ranging from 80-160Å, interspersed with somewhat thicker (200Å) films of water were found to best fit the data. Correlations to surfactant structure and foaming behaviour are made.

4.2. Introduction

Foams are complex, inherently difficult to study systems and therefore many previous investigations in the literature have focussed on qualitatively comparing the properties of single thin films to three-dimensional foams.[1-3] However, this is not always the most suitable approach given that foams are not just a collection of single thin films, but an interconnecting network of air bubbles.

The popularity of using small-angle neutron scattering (SANS) to probe colloidal systems has grown in recent years amongst the soft matter community primarily because it is such a useful tool to probe length scales on the nanometre scale. As described in Chapter 1, Section 1.7, there are only a few studies in the literature implementing SANS to study the structure of ionic surfactant stabilised foams. Here, an investigation of the structure of non-ionic Pluronic stabilised foams using SANS is presented. By studying the nature of the adsorbed surfactant layer, the aim is to correlate foam structure to the foaming behaviour of these surfactants (described in Chapter 3). If foaming ability and stability of such foams are directly correlated to the adsorbed layer structure, in particular its thickness, this will provide the first evidence of its kind to

demonstrate the adsorbed layer structure is a key parameter in defining foaming. Such understanding of the interfacial structure and foaming behaviour should allow a more rational approach when designing formulations for polyurethane foam manufacture.

4.3. Small-angle neutron scattering

4.3.1. Features of the data

Small-angle neutron scattering (SANS) has been used to characterise the distribution of surfactant in the foam system whether this be situated within the aqueous regions of the bubble cell walls or adsorbed at the air-water interface. As foams are such multi-component structures i.e. cell walls, Plateau borders, adsorbed surfactant, aqueous regions, it is firstly worth noting which features can contribute to the measured scattering intensity;

1) air-water interfaces in which structures normal to the interface are seen. For perfectly smooth, randomly orientated interfaces the decay in Q should follow a Q^{-4} dependence. Therefore we would expect an approximate Q^{-4} dependence given that in foams these interfaces are not perfectly flat,
2) any in-plane structure that is normal to the air-water interface,
3) composition fluctuations in planes parallel to the beam,
4) structures that would be present within the liquid junctions between bubbles resembling "bulk surfactant solution" i.e. micelles or lamellae structures at appropriate concentrations,
5) in aged, polyhedral foam, scattering arising from the Plateau borders, the long cylindrical-like regions forming the junctions between bubble cell walls.

Representative scattering recorded on LOQ is presented in Figure 4.1 and it is clearly evident that there are a number of features common to the scattering curves regardless of the surfactant used.

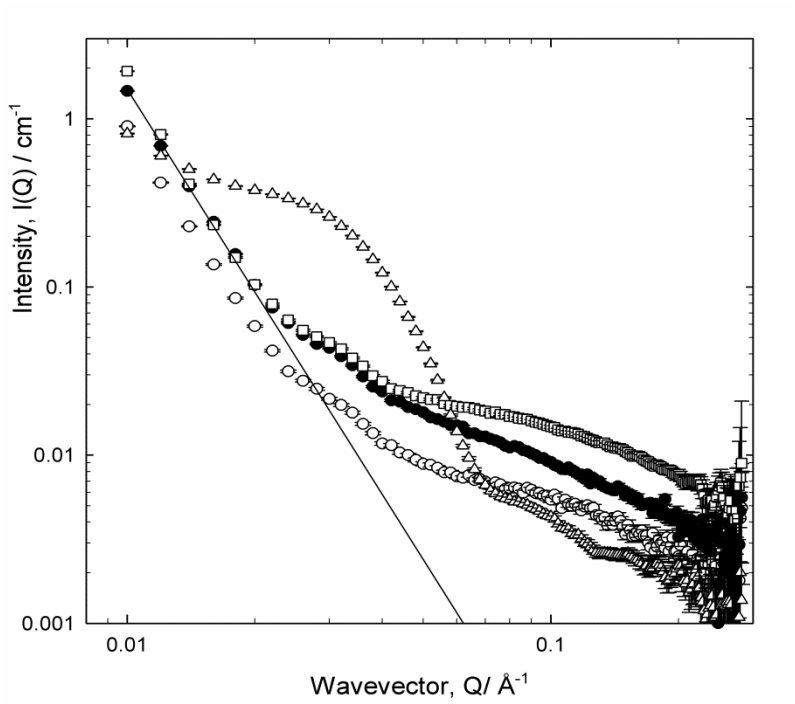

Figure 4.1; Small-angle neutron scattering from foams stabilised by four polymeric surfactants with [Pluronic] = 5% (w/v); PE6400 (open circles), PE6800 (closed circles), L62 (squares), P123 (triangles). Gas flow varied slightly through this series in order to generate foam of sufficient height. Also shown is the low Q limiting value of Q^{-4}.

At low Q the decay of intensity with wavevector Q follows a pronounced Q^{-4} dependence. A Q^{-4} dependence is characteristic of three-dimensional structures with a smooth surface,[4] essentially a smooth interface with large radius, in this case the surfactant stabilised air-water interface. As bubbles are much too large to be seen via SANS (they are of the order of millimetres in size) a small region of the air-water interface is being probed. The contrast term, $\Delta\rho^2$ for the air-D_2O interface is 40.3 x $10^{10}cm^{-2}$ therefore strong scattering is observed.

At high Q, the observed scattering is representative of the solution scattering of the polymeric surfactants and decays into an incoherent background which varies for each system reflecting the amount of material in the beam. The background is composed of both incoherent scattering from the residual hydrogen content in the solvent as well as the polymer. Most interestingly, there is a pronounced inflexion in the data over an intermediate Q range of approximately $Q \approx 0.025\text{-}0.04 Å^{-1}$ for three of the systems. For P123 foams (open triangles), the scattering is far more intense and this will be discussed in more detail below.

Focussing first on the high Q scattering, it has been possible to identify this as scattering from bulk surfactant solution situated within the Plateau borders and nodes of the bubbles. Figure 4.2 (left) shows the solution scattering of 5%(w/v) PE6800 in water, recorded in a conventional SANS cell, overlaid on the foam scattering with arbitrary scaling to match the relative intensities at high Q and therefore the amount of sample in the beam. This approach was suitable for three of the systems L62, PE6400 and PE6800, but less so for the P123 foam. Fitting the high Q data to a Debye model for random polymer chains in solution, yields radii of gyration of 18, 17 and 24Å for L62, PE6400 and PE6800 respectively. This is consistent with the dimensions obtained from an analysis of the sample cell scattering of the polymeric species in solution (16, 14 and 20Å) and correlates well to typical values reported in the literature.[5] Therefore, at the bulk surfactant concentration studied here, 5%(w/v), there is a significant contribution to the overall scattering from surfactant situated within the cell walls forming the aqueous regions of the foam.

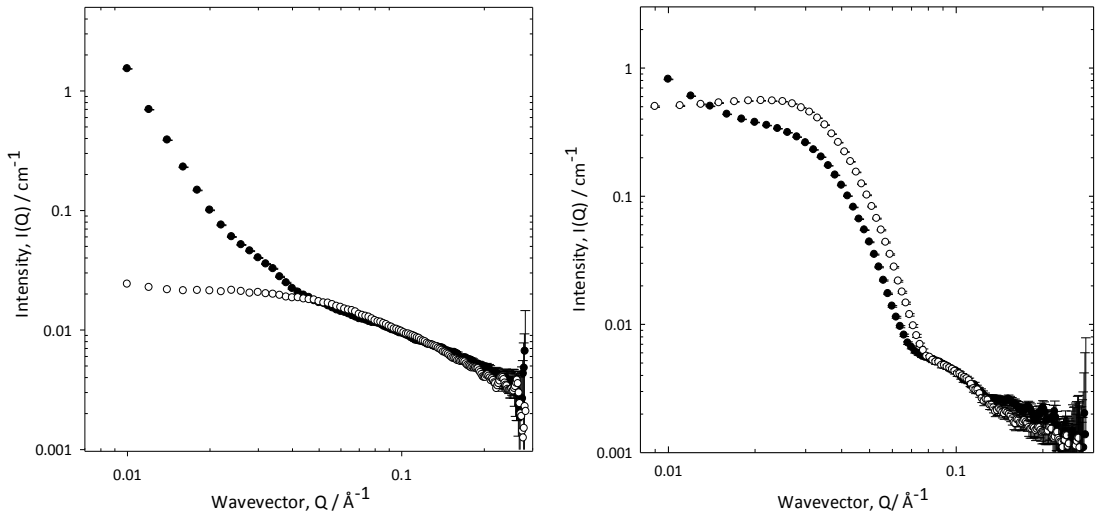

Figure 4.2; Small-angle neutron scattering from the air-in-water stabilised foam (filled circles) and a simple aqueous solution (open circles) for polymeric surfactants PE6800 (left) and P123 (right). [Pluronic] = 5% (w/v). Intensity arbitrarily scaled for comparison.

For the P123 foam, the situation is a little more complex, however the same conclusion can be drawn (Figure 4.2 (right)). At 5%(w/v) P123 is above its critical micelle concentration (CMC) so in this case the form factor for micellar scattering dominates scattering at high and intermediate Q. This essentially masks the additional features associated with the foam structure that are observed in the systems in which only

surfactant molecules are present. Interestingly, it is not possible to simultaneously overlay the (intensity of the) peaks associated with the inter-micellar structure factor ($0.03Å^{-1}$) and those associated with the core-shell morphology of the micelle ($0.1Å^{-1}$), suggesting that the structure of the micelle may be perturbed in the foam system.

Attempts were made to determine the effective concentration of micelles situated within the foam from the scaling based on the volume fraction of micelles in the bulk solution. From this an estimation of the surfactant present at the interface could be made. However the results of such calculations were physically unreasonable, attributed to the fact that we do not know if the size of the micelle changes from bulk solution to foam.

4.3.2. Effect of surfactant concentration

The inflexions at intermediate Q are perhaps the most significant features in the data and identifying their origin is non-trivial. The effects of bulk surfactant concentration on foam scattering for two representive surfactants are presented in Figure 4.3 and Figure 4.4. Here the data was recorded on D11 over an extended Q range (compared to LOQ). The Q^{-4} decay at low Q is now even more evident due to the lower Q range accessible on this instrument.

As the concentration is diluted, the high Q scattering reduces to an incoherent, flat background due to the low concentrations of surfactant within the beam. The inflexion at $Q \approx 0.025\text{-}0.04Å^{-1}$ is more pronounced and additionally a second inflexion at $Q \approx 0.01\text{-}0.015Å^{-1}$ is evident. Unfortunately, for the data recorded on D11, this peak overlapped the edge of the detector used in this particular experimental geometry however later experiments confirmed it to be real. Thus to highlight the features in the scattering that arise from the foam structure it is necessary to remove any additional contributions to the scattering from excess surfactant in solution.

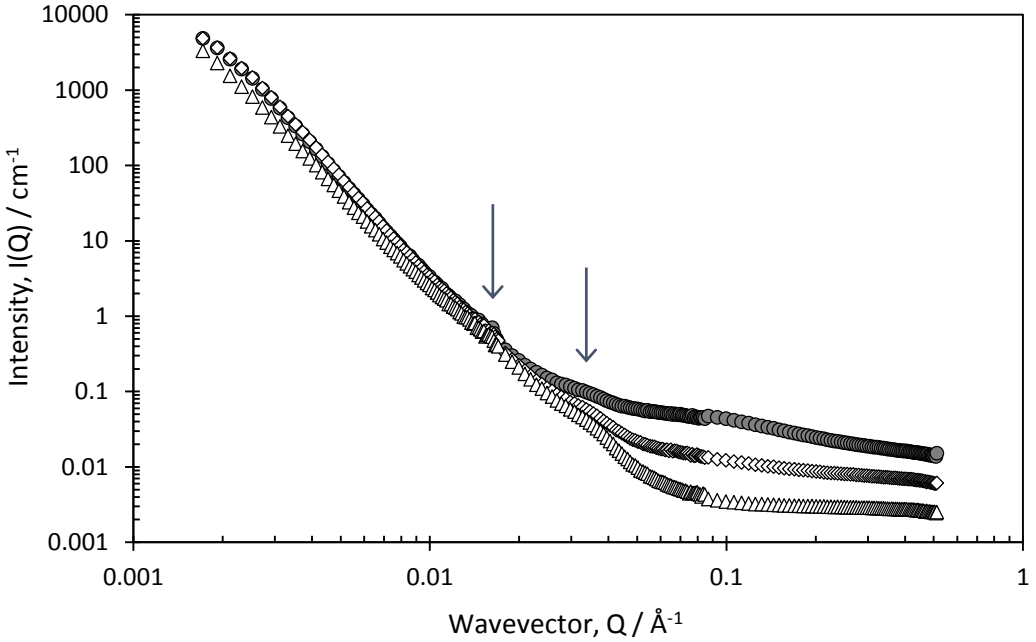

Figure 4.3; Small-angle neutron scattering from the air-in-water foams stabilised with polymeric surfactant PE6400 at various concentrations; 0.05% (w/v) (triangles), 0.5% (w/v) (diamonds) and 5% (w/v) (circles). Arrows indicate the points of inflexion.

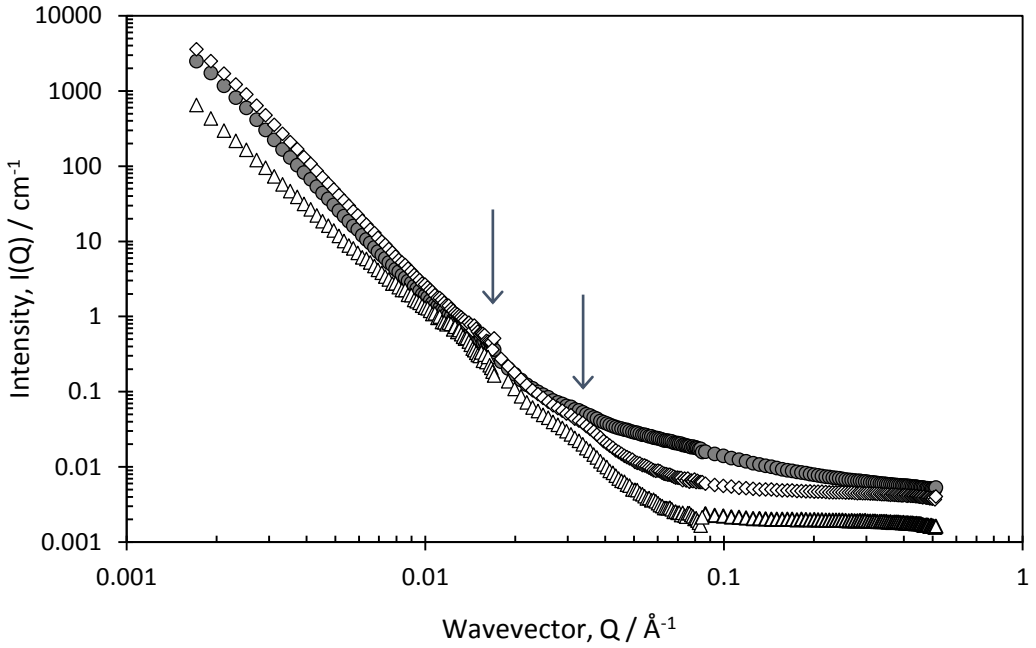

Figure 4.4; Small-angle neutron scattering from the air-in-water foams stabilised with polymeric surfactant F108 at various concentrations; 0.05% (w/v) (triangles), 0.5% (w/v) (diamonds) and 5% (w/v) (circles). Arrows indicate the points of inflexion,

4.3.3. Reproducibility

Data has been reproduced on various instruments (LOQ, D11 and SANS 2D) for multiple samples and the same scattering pattern is seen across the range of Pluronic foams studied (Figure 4.1, Figure 4.3 and Figure 4.14 respectively). The empty foam column was measured in the beam and no scattering was obtained indicating that the scattering we observe arises from the foam itself. This was confirmed in further experiments in which the foam height decayed to below the neutron beam throughout the timescale of the experiment (Figure 4.5). Scattering is substantially weakened due to the lower count of sample recorded ($I(Q) \sim 10cm^{-1}$ as Q tends towards zero compared to $\sim 10000cm^{-1}$ for the sample in which the regenerating foam is present). Furthermore this demonstrates that we are not observing residue of surfactant solution on the foil film windows of the column.

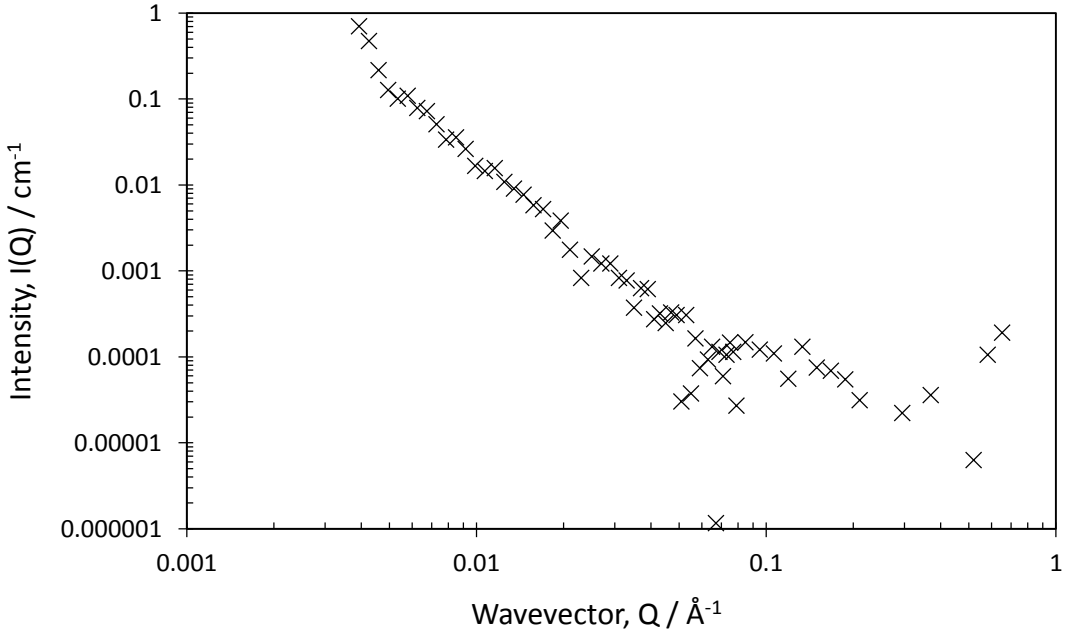

Figure 4.5; Small-angle neutron scattering from a representative PEO-PPO-PEO foam in which the foam has decayed to below the neutron beam throughout the timescale of the experiment.

In addition, the effect of air flow rate on the foam structure has been studied.[6] Figure 4.6 shows PE6800 stabilised foams generated at air flow rates of 0.2L/min and 0.4L/min and it can be seen that the scattering is identical. Typically the air flow rates used were below 1L/min and no effects on the scattering were observed. Therefore, it can be stated

that the relatively low air flows used in the research have no influence on the adsorbed layer structure. Furthermore, analysis of bubble size distribution (Chapter 3, Section 3.7) indicated that the bubble size does not appreciably vary across all of the Pluronic surfactants studied (at 0.08L/min) thus it can be assumed that the volume fraction of air within the bubble remains constant.

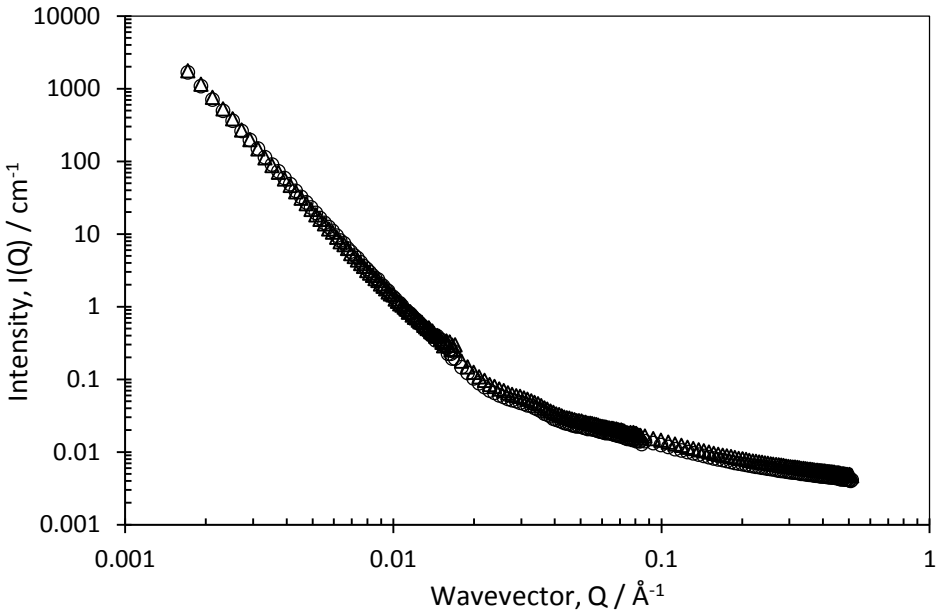

Figure 4.6; Small-angle neutron scattering from air-in-water foams stabilised with polymeric surfactant PE6800 at various air flow rates; 0.2L/min (triangles) and 0.4L/min (circles). Both scattering plots are identical and the 0.4L/min data overlays the 0.2L/min data.

To probe the effects of neutron path length a foam column with smaller diameter (2.5cm) was been implemented (Figure 4.7). The parameters in the SANS experiment were normalised to account for such differences in path length. The resulting scattering obtained from both columns indicates little difference and the intensities of the data are comparable regardless of the foam column size. This confirms the technique is probing the bulk foam and is sensitive to the amount of sample in the beam. Providing the data is normalised, the technique is insensitive to the column used.

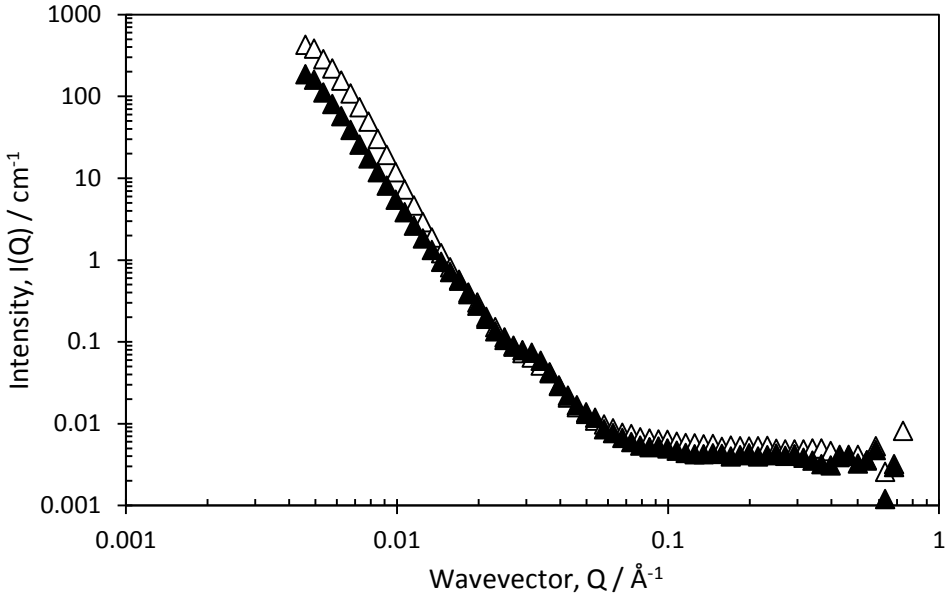

Figure 4.7; Small-angle neutron scattering from air-in-water foams stabilised with [SDS]=4mM recorded in narrow foam column (open triangles) and standard foam column (closed triangles).

4.3.4. Porod plot

The low Q^{-4} Porod region is valid when the size of the scattering objects is larger than than the range probed by the scattering radiation. At high Q the scattering intensity I(Q) can be approximated to;

$$I(Q) = \log(A) - n\log(Q)$$

and it is well known that a slope of n=4 characterises the smooth surfaces expected in foam systems. As all of the data follows an approximate Q^{-4} dependency, the inflexions in the scattering data as observed in Figure 4.1 can be highlighted by plotting the data on a Porod plot, $Q^4I(Q)$ *vs.* Q, as this effectively removes the Q^{-4} term. This approach is only valid providing the incoherent flat background is subtracted in order to magnify the additonal features in the data. This induces some uncertainty in absolute values as it is not known from the data if the incoherent background is completly flat and some estimation of how much background to subtract is necessary. Nevertheless, the Porod plots for scattering from representative surfactants recorded on SANS 2D are presented in Figure 4.8 (see Appendix 2 for remaining surfactants). Well defined peaks are now clearly evident at approximately Q ≈ 0.035Å^{-1} and 0.015Å^{-1}. From the standard equation, derived from Braggs Law, $d = 2\pi/Q_{peak}$, length scales (d) of approximately

200Å and 400Å can be obtained. It is interesting to note that the peak at Q ≈ 0.015Å is much weaker in intensity for some of the surfactants studied i.e. L62 and PE6400.

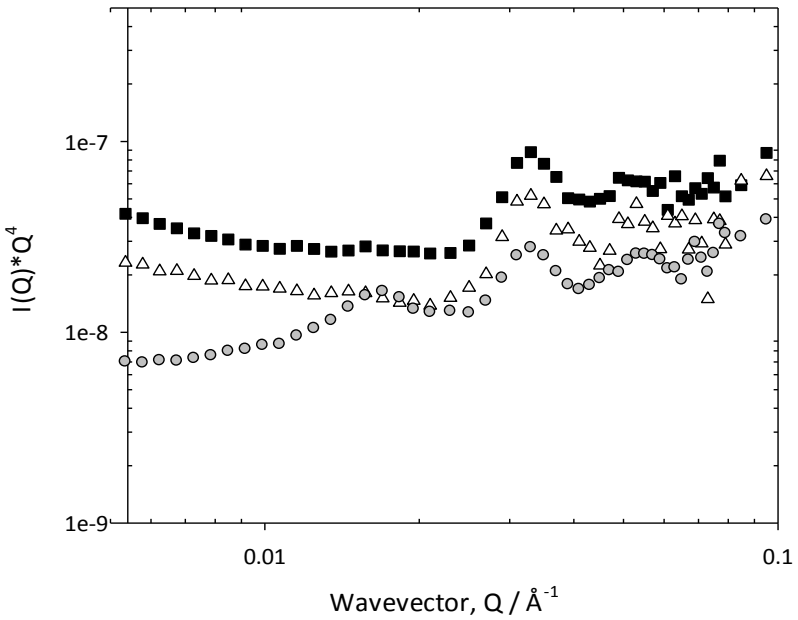

Figure 4.8; Porod plot of small-angle neutron scattering from the air-in-water foams stabilised by polymeric surfactants with constant PPO block size and increasing PEO block size; [Pluronic] = 0.05% (w/v), L62 (triangles), PE6400 (squares), PE6800 (circles).

Based on the intercept of the Porod plot for L62, the surface area of interface per unit volume is determined to be approximately 60cm^{-1}. This correlates well to the surface area per unit volume calculated based on a bubble radius of 0.05cm (~60cm^{-1}).

4.3.5. The origin of scattering peaks

It is shown in the literature that foams stabilised with the ionic surfactant sodium-dodecyl sulfate (SDS) have been investigated by SANS.[7] The authors saw a similar contribution to foam scattering from surfactant situated within the bubble walls and a Q^{-4} decay were observed however only in drained foams was the presence of an additional peak at Q ≈ 0.03Å^{-1} seen. (A peak at such Q position correlates with the data obtained in this work for SDS (Figure 4.7) however is observed in wet, dynamic foams). Further, when the contrast was suppressed between surfactant and solvent, by studying deuterated SDS foams in D_2O, the peak remained. Thus it was deduced by the authors that the peak must arise from parallel air-water interfaces and was attributed to the film thickness of the bubbles. An average film thickness of 160-180Å was calculated. In this

work however, wet foams are studied, with constant regeneration of bubbles. It is therefore seems unfeasible that the peaks observed here can originate from the total film thickness. Microscope analysis of dynamic foams generated in the laboratory foam column estimated bubble lamellae to be of micrometre size and are clearly visible to the naked eye. This suggests that a length scale of approximately 200Å cannot account for the film thickness and must instead be attributed to some other structure within the foam walls.

One origin of such features in the data could be the polymeric species present in solution, assuming sufficient liquid fraction in the foam (Figure 4.9).

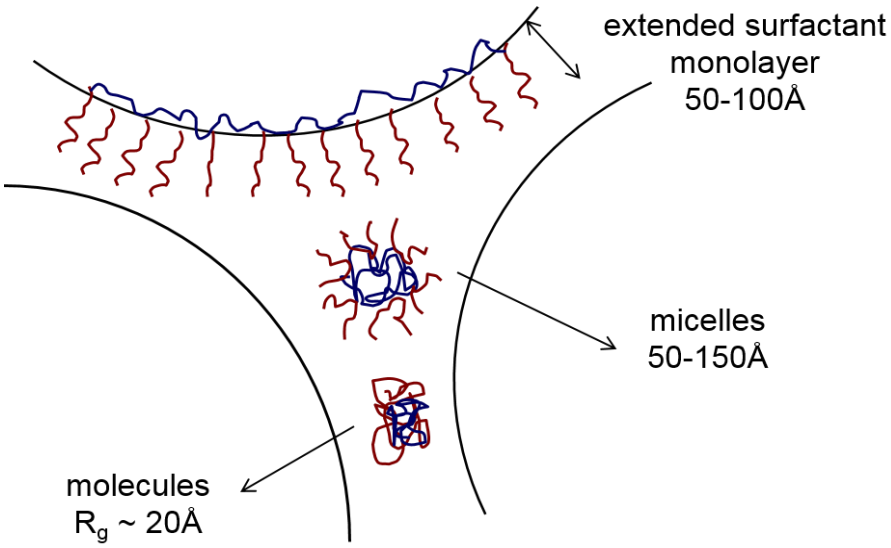

Figure 4.9; Cartoon to show possible contributions to the scattering from aqueous foams. Not to scale.

Analysis of solution scattering yields a radius of gyration of approximately 15-20Å, in agreement with literature values,[5] so that it is clear that the inflexions do not arise from molecular scattering within the bulk solution. Indeed, it has been identified in Figure 4.3, that scattering of this type is observed at higher Q values and can be removed by considerably reducing the bulk surfactant concentration. Pluronic micelles are typically 5-15nm in size with variations arising from structural differences and temperature[8] thus it could be reasonable to assume that such a peak at 200Å arises from the form factor of micellar structures in solution. However, this argument is weakened when explaining the peak observed at 400Å as such a length scale is considerably larger than Pluronic micelles typically observed in solution. As previously discussed, at bulk concentrations

above the CMC, scattering is dominated by micellar scattering as seen for the P123 system (Figure 4.2 (right)) so that fine features in the data originating from the foam are masked. However, at 0.05% (w/v) bulk surfactant concentration studied here, the systems are significantly below their bulk CMC suggesting that the polymer concentration within the lamellae walls is too dilute to contain micelles, unless however the interface induces novel structure.

The accepted mechanism of Pluronic surfactant adsorption at the air-water interface involves the hydrophobic PPO blocks anchoring the polymer to the interface whilst the hydrophilic PEO groups extend into the aqueous phase.[9] Neutron reflection has previously been employed throughout the literature to study the adsorption of Pluronic surfactant at the air-water interface.[10-12] Such studies showed the presence of a monolayer of adsorbed surfactant at the interface, typically of the order of 10nm in thickness. As these measurements were recorded on static systems, such adsorbed layer thicknesses appear too small to account for the 200Å length scale observed in our work (in dynamic foam systems it is unlikely that we are probing equilibrium layers).

One must also consider that the inflexions in the data may arise from structures in plane to the neutron beam, typically adsorbed molecules or micelles at the interface and any separation between such molecules (Figure 4.10). Previous neutron reflection studies of Pluronic surfactants adsorbed at the air-water interface show no evidence to support the observation of scattering from in plane structures.[10-12] Instead, data has been interpreted to arise from structures normal to the beam i.e. adsorbed polymer chains which protrude into solution. Therefore we postulate that we are most likely probing structures normal to the beam in aqueous foams studied here.

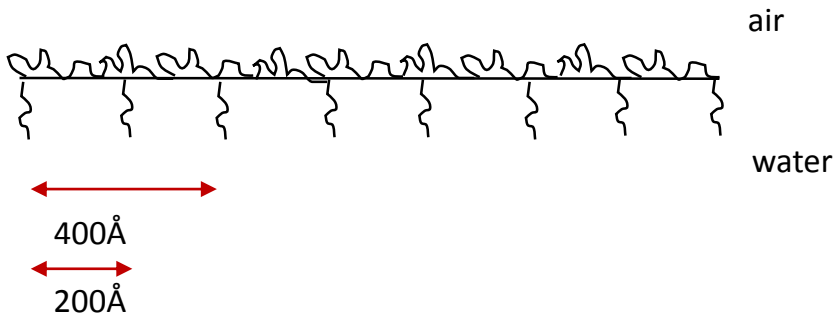

Figure 4.10; Cartoon demonstrating the in-plane structure within the neutron beam.

Referring again to neutron reflection studies,[10-12] the presence of multiple inflexions in the data has not been recorded and only monolayers of adsorbed surfactants have been detected for Pluronic systems. However, some caution should be taken when comparing the structure of an equilibrium adsorbed system to dynamic foam. Unlike neutron reflection studies in which the adsorbed amount is controllable, we do not know the local concentration of surfactant at the air-water interface in foam, particularly as concentration gradients are present throughout the foam as the films deplete. Thus making a direct comparison to neutron reflection data is non-trivial and it is inevitable that different structures at the interface will be probed depending on the technique used.

Previously lamellar ordering has been observed at the air-water interface for the cationic surfactant N,N-didodecyl-N,N-dimethylammonium bromide (DDAB) studied by neutron reflection across a concentration regime of 0.2-2%(w/v). A series of regularly spaced peaks consistent with a repeating structure at the interface was observed. The interface was described by two equally spaced layers separated by approximately 900Å.[13] Similar multilayered structures for Aerosol-OT have been observed at the air-water interface in which a d-spacing of approximately 370Å has been reported for 5wt% solutions. The authors postulate that the spacing is due to steric repulsion resulting from fluctuations in the bilayer as the spacing is too large to arise from electrical double layer repulsion.[14]

Perhaps the closest system to air-in-water foams stabilised with Pluronic surfactants are high internal phase emulsions (HIPEs) where the dispersed phase is comparable to that of foams, typically greater than 74% in volume fraction.[15] HIPEs have been studied extensively using neutron techniques by Reynolds and White.[15-21] Hexadecane and water emulsions stabilised with PIBSA surfactant (polyisobutylene oligomer tails and acid-amide headgroups) were shown to consist of a 90% internal phase of water in continuous hexadecane. Scattering consisted of a Q^{-4} decay in intensity and features characteristic of surfactant microstructure in the oil phase. Only approximately 6% of surfactant was shown to be present at the interface in a monolayer with tail lengths extending approximately 15-20Å into the aqueous phase. The remaining surfactant was present as micelles in the oil phase.[15, 16] Zank *et al.*[19] used SANS and USANS to study HIPEs stabilised by Pluronic L94 and unlike the PIBSA systems lamellar Bragg peaks in the scattering data were recorded across a Q range of approximately 0.05-0.1$Å^{-1}$ (Figure 4.11).

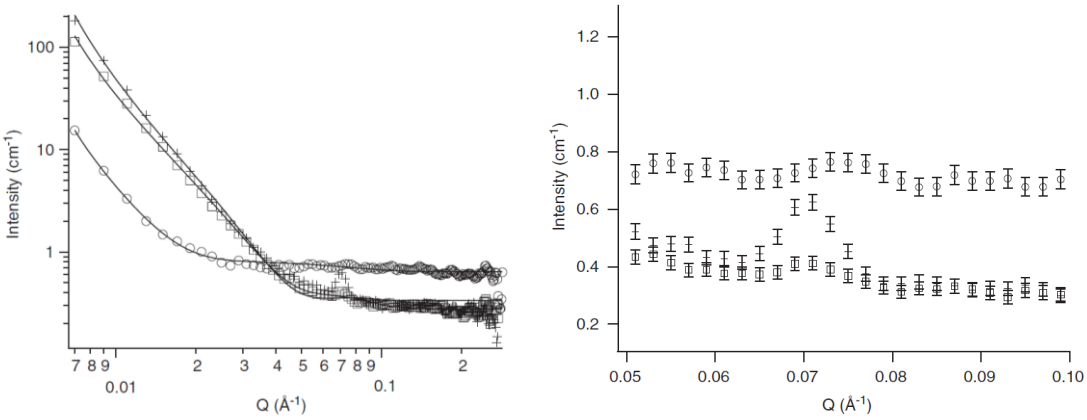

.

Figure 4.11; SANS data recorded by Zank et al.[19] for high internal phase emulsions (HIPEs) stabilised with Pluronic L92. Overall scattering plot (left) and magnified region (right) showing the presence of lamellar Bragg peaks.

Bragg scattering arises from scattering planes, which at certain wavelengths and angles produce intense beams of reflected radiation (Bragg peaks). The spacing of the planes can be determined from the position of the Bragg peaks. Thus, observations of lamellar Bragg peaks suggest the presence of a repeating structure within the sample. Based on the Bragg peak positions, it was determined that a 90Å period lamellar phase exists in L94 stabilised emulsions. This is composed of alternating ~15Å thick oil or aqueous layers sandwiched between ~30Å thick surfactant layers. The origin of such structures was not discussed. The thickness of the multilayers observed are smaller than those observed in the foams studied here. Further analysis by the same group of ordering between HIPEs and a solid silicon interface stabilised with sorbitan monooleate and a polymer diblock surfactant demonstrated that a transition from monolayer to multilayer structures is driven by increasing surfactant hydrophilicity.[18] This is not the case for the Pluronic surfactant stabilised foams in which scattering characteristic of multilayers are present across the whole series.

The presence of layered structures at the interface along with the Bragg peaks seen by Zank *et al.*[19] and the repeating nature of the peaks observed in our data suggest the presence of a multi-layer structure of adsorbed surfactant at the interface in our foam system.

4.3.6. The paracrystalline stack model

Features in the scattering data and previous literature findings provide compelling evidence to suggest that the PEO-PPO-PEO surfactants form multi-layers at the interface in dynamic foams. Based on these findings we have employed a model of the air-water interface that consists of a para-crystalline stack of *M* polymer / water layers of diffuseness *T* (the variation in interface structure perpendicular to the interface; an ideal interface will have zero diffuseness), thickness *L* and separation *D* (Figure 4.12).[22] To this a Q^{-n} term is added to account for the scattering from the smooth air-water interface and where necessary, a Debye term to account for the solution scattering. The para-crystalline stack model also incorporates the Lorentz factor, Rσ which defines the orientation of the interface. Rσ = 0 corresponds to a perfectly flat interface i.e the Q vector is always normal to the interface. In reality, the Rσ term is always significant. However, due to the complexity of the foam data fitting, Rσ is assumed to be zero and here this has to be considered a limitation of the model. However, providing there is a large contrast step between the air-surfactant-water interface then the data will tend to Q^{-4} over a long length scale regardless. The scattering length densities (contrast) of the various materials is such that scattering arises equally from the air/D_2O and polymer/D_2O interfaces, and any further de-convolution of the data is not feasible (using this model at least). Thus, the model consists of polymer rich and water rich layers and it is not possible to discern differences in scattering between the PEO and PPO blocks. To limit the functionality of the fit, the diffuseness T has been constrained to T=0.01. Typical starting values for the heterogeneity of L and D are $\sigma(L/L)$ and $\sigma(D/D)$ = 0.2, though these values had little impact on the overall fit.

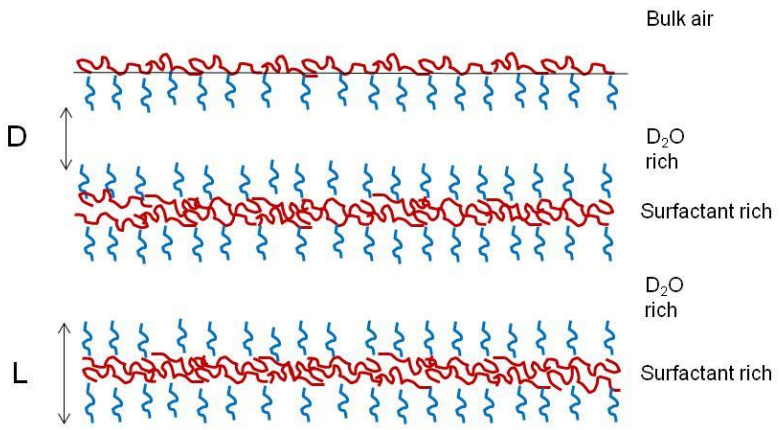

Figure 4.12; Cartoon of the paracrystalline stack model of adsorbed surfactant layers at the air water interface. D defines the layer separation and L the layer thickness.

4.3.7. Contrast plots

Whilst the contrast is incorporated into the scaling parameter of the model we can consider the contrast steps for both monolayer and multilayer structures at the interface in an attempt to discern the structure at the interface (Figure 4.13). Evidently, there is one primary contrast step in the data between polymer and D_2O. Smaller contrast steps exist if the head and tail groups of the polymer are considered separately. Whether these are sufficient to account for the peaks in the data will be discussed further in Section 4.4.

Monolayer

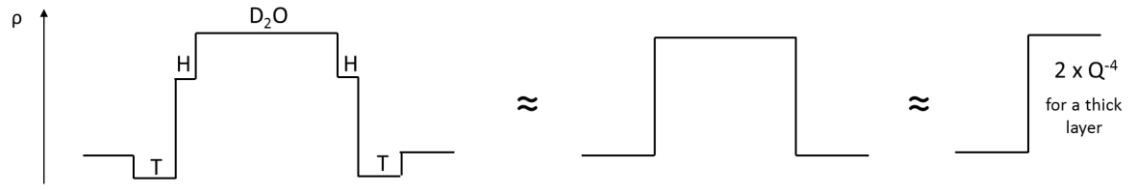

Single multilayer across air-water-air interface

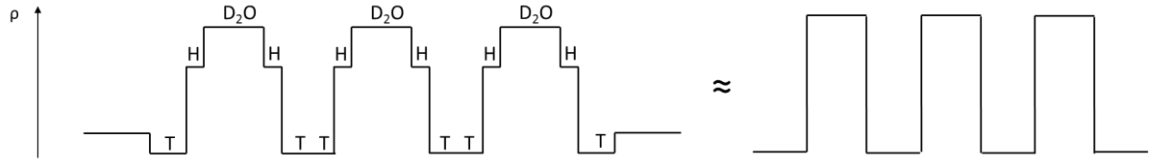

Multilayer sandwich across thick interface

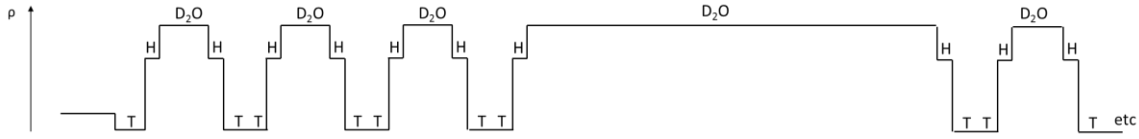

Figure 4.13; Contrast plots for possible surfactant structures at the air-water interface. Not to scale.

4.3.8. Fit to paracrystalline stack model

Figure 4.14 and Figure 4.15 show small-angle neutron scattering from two representative polymer foams and the model fit to the data. It can be seen that the model fits the data well in both cases. Remaining scattering and model fits are presented in Appendix 2. The Q^{-4} term dominates the scattering so the accuracy of the parameters are less than ideal, but the features are clearly reproduced in this approach. Important

parameters are presented in Figure 16. Due to variations in the heterogeneity of the surface structure only one peak is observed in the L62 and PE6400 scattering whereas P84, P103, PE6800, P104, P123 and F108 show two peaks. This means that across the various datasets the fitting routine is sensitive to which peak/inflexion is being fitted. For a perfectly crystalline stack, one would expect to see regularly spaced reflections at a common distance associated with n=1, n=2, n=3 *etc*. Here, the separation D is slightly different whether the fitting routine focuses on the n=1 (Q=0.015Å) or n=2 (Q=0.035Å) peak. This implies that the structure is not perfectly lamellar.

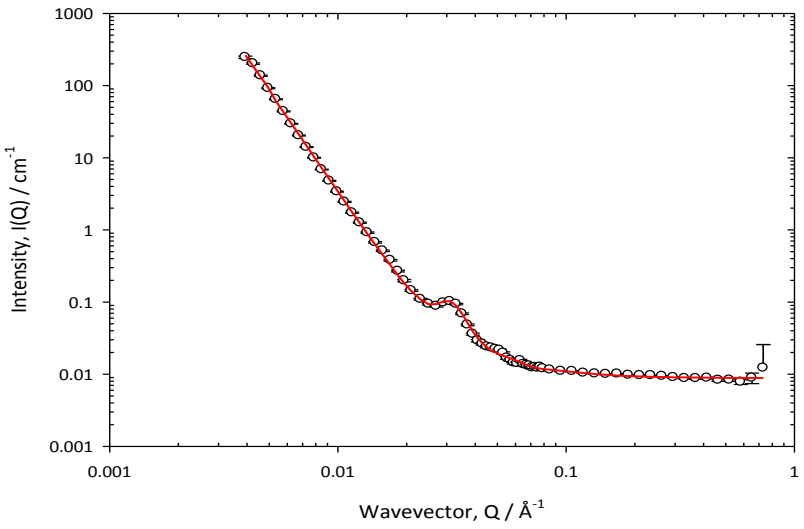

Figure 4.14; Small-angle neutron scattering from foam stabilised by 0.05% (w/v) L62 and the fit to the paracrystalline stack model described in the Experimental section.

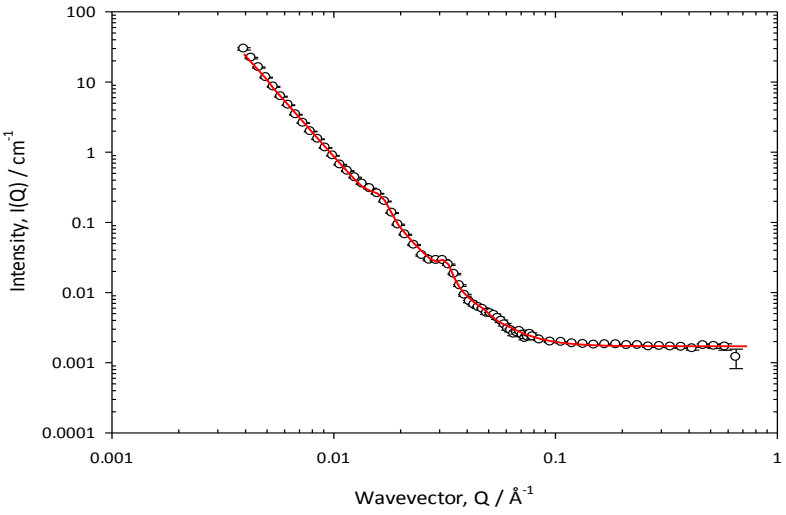

Figure 4.15; Small-angle neutron scattering from foam stabilised by 0.05% (w/v) PE6800 and the fit to the paracrystalline stack model described in the Experimental section.

Pluronic	L (±10) / Å	$\sigma_{L/L}$	M	D (±10) / Å	$\sigma_{D/D}$
PE6400	85	0.20	6	195	0.14
L62	90	0.22	6	195	0.15
P84	120	0.19	4	400	0.14
P103	155	0.28	4	400	0.11
PE6800	135	0.20	4	390	0.076
P104	140	0.23	4	395	0.11
P123	160	0.27	4	405	0.14
F108	220	0.25	4	430	0.14

Figure 16; Fit parameters to the scattering from Pluronic stabilised air-in-water foams, [Pluronic]=0.05% (w/v).

Regardless of Pluronic structure, a layer separation, D, of approximately 200Å is always observed. In terms of adsorbed surfactant layers, this is a considerable separation between layers and such a separation would imply the presence of long range interactions between the layers. In addition, empirically a value of M = 4-6 was found to be the smallest required to give a good fit to the data and increasing this value did not lead to appreciably better fits. The model is not sensitive to more than five layers and it is thought that for greater than five layers we are outside the limit of sensitivity of the data. The interference between layers as well as instrumental smearing and the high polydispersity of the layer thickness smears the resolution as the length scale increases thus it is not possible to distinguish between layers at such differences. Fitting the data to one stack alone i.e. M = 1 consistent with a monolayer structure at the interface yields a poor fit to the data thus providing evidence to suggest the presence of a higher order structure i.e. a multilayer. The layer thickness, L, varies substantially across the range of Pluronics studied indicating that the adsorbed layer thickness is influenced strongly by polymer structure. A discussion of the fitting parameters to surfactant structure and foaming behaviour is presented in Section 4.5.

From the surface area per unit volume determined from the Porod Plot (Figure 4.8) and the model scale factor, attempts were made to probe the contrast terms which could allow the volume fraction of surfactant in the foam and hence the area per molecule of surfactant to be determined. The results of such analysis proved inconclusive primarily due to the many unknown variables and assumptions involved;

- As described in Section 4.3.1, the exact bulk concentration of surfactant within the foam is unknown.

- The local surfactant concentration is unknown. The system is not at equilibrium and foam depletion mechanisms cause local surface tension gradients at the interface. Therefore it is not possible to determine the local surfactant density at the interface and any structures proposed are assumed to cover all of the air-water interface.
- The exact bubble size and volume fraction of interface is unknown.
- The interface is assumed to be perfectly flat i.e. $R\sigma = 0$. In reality some orientation is always observed.

4.4. Contrast experiments

To probe further the structure at the interface, contrast experiments were performed which allowed regions of the system to be selectively highlighted whilst making other regions "invisible" to the neutrons. This allows simplification of the data analysis.

Unfortunately, it was not possible to perform the contrast experiments for the Pluronics as time did not permit deuterated Pluronic samples to be synthesised. Instead, foams prepared from the ionic small molecule surfactants, sodium dodcyl sulfate (SDS) and cetyl trimethylammonium bromide (CTAB) (see Appendix 2) were investigated. The scattering length densities and contrast terms for the various components of the SDS foam are presented in Figure 4.17. A large value for $\Delta\rho^2$ signifies high contrast between molecule and solvent, for example h-SDS in D_2O whilst a small value indicates the neutron only "sees" a homogeneous medium, for example d-SDS in D_2O.

	ρ (10^{10} cm^{-2})
D_2O	6.345
H_2O	-0.561
h-SDS head	0.656
h-SDS tail	-0.488
d-SDS head	0.656
d-SDS tail	7.656
air	~0

	$\Delta\rho^2$ ($10^{10}cm^{-2}$)
h-SDS head / D_2O	32.36
h-SDS head / H_2O	1.481
h-SDS tail / h-SDS head	1.309
h-SDS tail / air	0.238
d-SDS head / D_2O	32.36
d-SDS head / H_2O	1.481
d-SDS tail / d-SDS head	49.0
d-SDS tail / air	58.61

Figure 4.17; Scattering length densities (ρ) and contrast term ($\Delta\rho^2$) for various foam components.

For greater insight into the structure of the adsorbed surfactant layer, both SDS head and tail groups have been treated separately such that contrast terms for each have been determined. The head groups will exhibit some degree of hydration, thus the scattering length density for the head groups has been calculated based on 30% hydration. Scattering from h-SDS in H_2O is presented in Figure 4.18 (top) and the contrast between air, water and surfactant depicted in the inset. The scattering length density of the components of the foam film is shown in Figure 4.18 (bottom). From the contrast calculations, it can be seen that there is no significant difference in scattering length densities for all components of the foam thus no scattering is expected as the neutron only "sees" a homogeneous medium. This correlates to the experimentally observed data in which no scattering is observed.

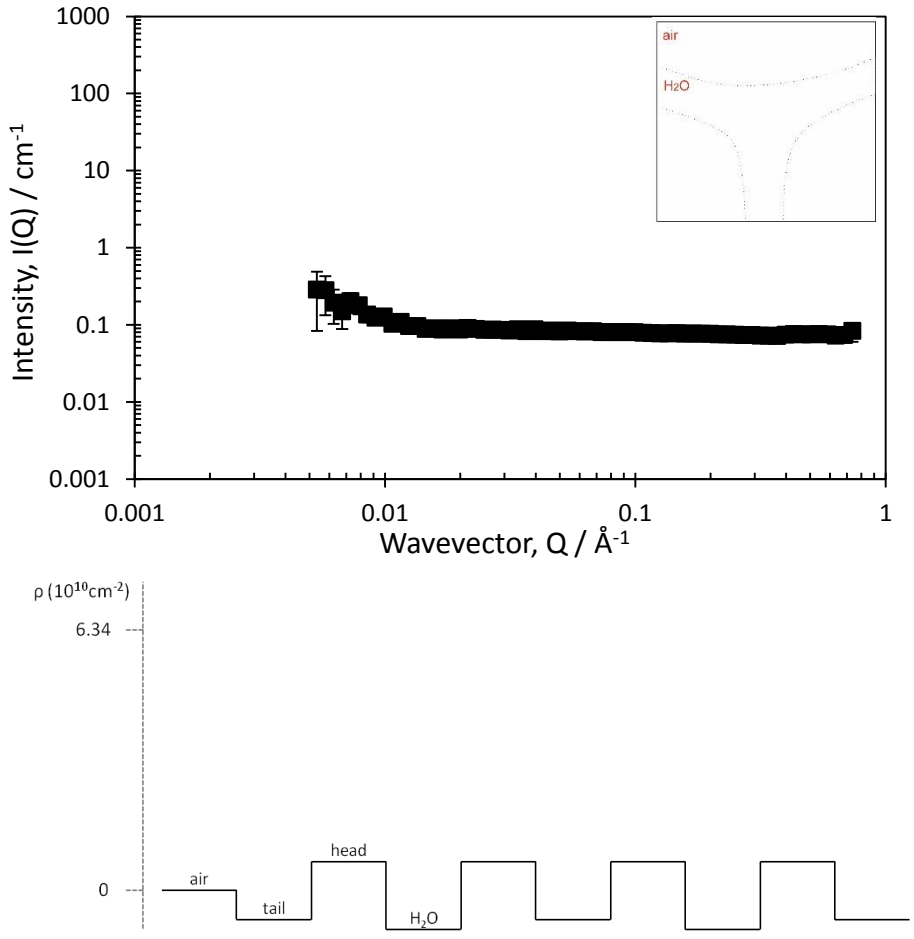

Figure 4.18;Small-angle neutron scattering from air-in-water foam stabilised with h-SDS in H_2O. [SDS]=4mM. Inset; cartoon of foam structure to show the contrast between molecules and solvent (top). Scattering length density profile of the foam components observed across the foam film (bottom). Not to scale.

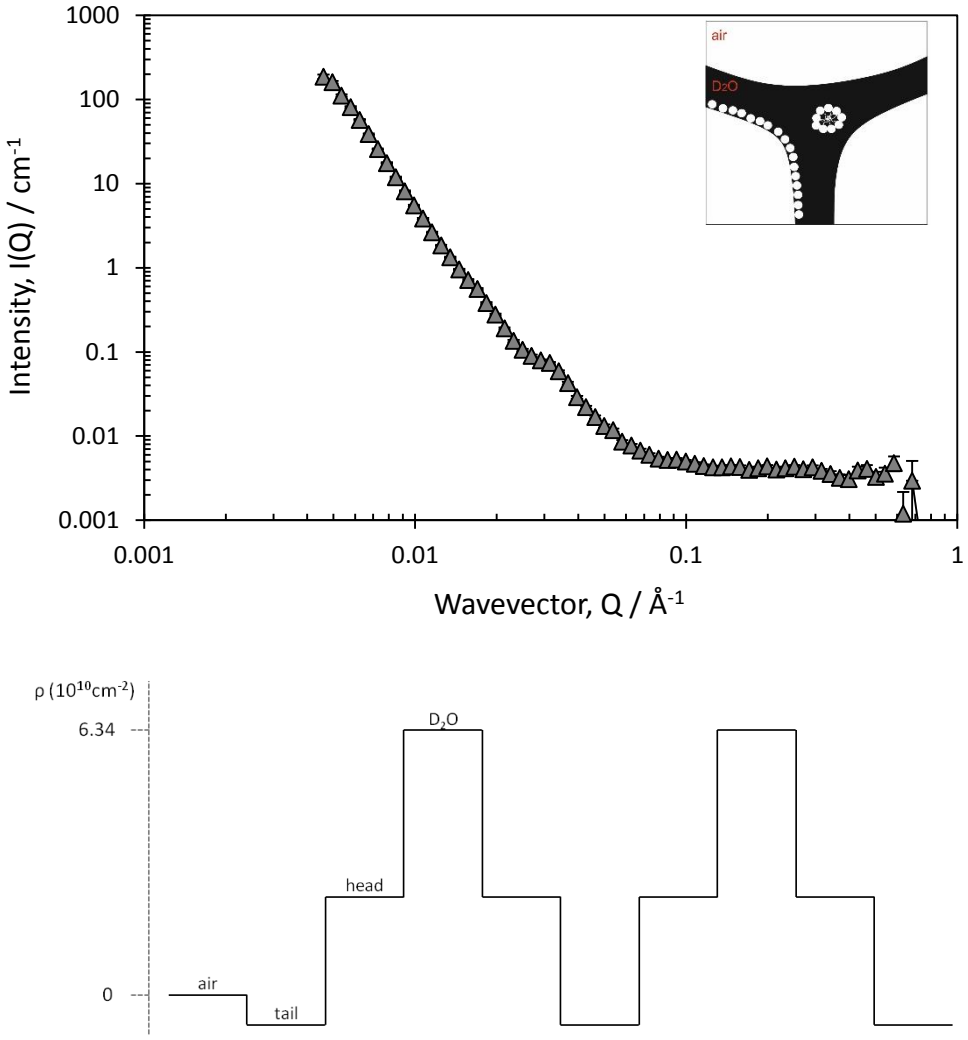

Figure 4.19; Small-angle neutron scattering from air-in-water foam stabilised with h-SDS in D_2O. [SDS]= 4mM. Inset; cartoon of foam structure to show the contrast between molecules and solvent (top). Scattering length density profile of the foam components observed across the foam film (bottom). Not to scale.

Therefore in order to observe scattering from foam systems selective regions of the foam need to be deuterated. If the solvent is substituted to D_2O then scattering from the foam can now be seen and there are some interesting features in the data. Scattering from h-SDS in D_2O is presented in Figure 4.19 (top) and the features in the data are analogous to foams prepared with the Pluronic block copolymers; a Q^{-4} dependence at low Q, an inflexion at 0.035$Å^{-1}$, which decays into an incoherent, flat background at high Q. Such similar scattering implies that both polymeric and small molecule surfactants induce common structure at the interface.

Analysis of the contrast terms for the main components of the foam (Figure 4.19 (inset)) and the scattering length density plots (Figure 4.19 (bottom)) indicate that scattering can arise from the air-water interface and the SDS-D_2O interface as seen by the high $\Delta\rho^2$ values of these components. In addition, assuming 30% hydration of the SDS head groups there are sufficient contrast steps between the head and tail groups and water. The paracrystalline stack model which showed a good fit to the data in Section 4.3.8 involves multiplying the scattering associated with the layered structure with the Q^4 term which magnifies the intensity of the peaks. Thus we propose that the inflexions in the data arise from the contrast between the surfactant and water whilst the strong Q^{-4} gradient is associated with the contrast between the air and water.

Interestingly, for the d-SDS in D_2O system (Figure 4.20 (top)) the inflexion present at 0.035Å still features in the scattering. This is somewhat unexpected if we consider the SDS molecule as a whole. The contrast between surfactant in solution and solvent is matched so that scattering can only arise from the air-water interface and surfactant-air interface. This was the conclusion drawn previously by Axelos *et al.*[7] Only in very thin, dry foams was a peak observed at ~0.025-0.03$Å^{-1}$ which remained on contrast matching the solvent and SDS. As mentioned in Section 4.3.5 the authors thus concluded that as no surfactant structure could be observed the peak must arise from parallel air-water interfaces i.e. the film thickness. This explanation cannot accurately describe the structure of the dynamic, wet foams observed here in which bubble walls are orders of magnitude thicker.

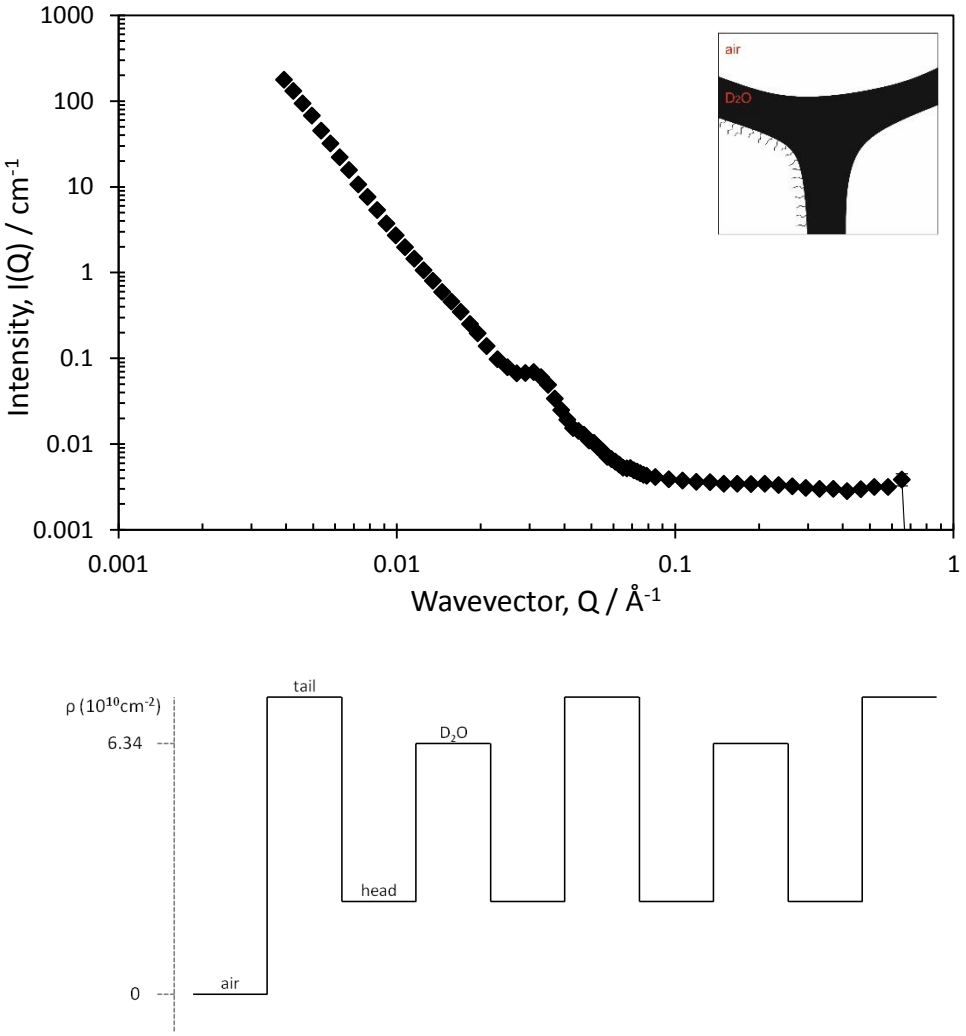

Figure 4.20; Small-angle neutron scattering from air-in-water foam stabilised with d-SDS in D_2O. [SDS] = 4mM. Inset; cartoon of foam structure to show the contrast between molecules and solvent (top). Scattering length density profile of the foam components observed across the foam film (bottom). Not to scale.

However, if we again consider both the hydrophilic and hydrophobic parts of the SDS molecule separately (Figure 4.20 (bottom)) it can be seen that there is a sufficiently large contrast step between the head group of the SDS molecule and water. This means that there is sufficient contrast between the surfactant and water to be observed via SANS. Thus based on the reasoning described above, this provides further evidence to suggest the peaks in the data arise from the surfactant layer.

The scattering from the d-SDS in H_2O system is presented in Figure 4.21 (top) and overall there is no scattering, however at low Q it appears that the data is beginning to follow a Q^{-4} dependency. The contrast plot depicted on the inset suggests that the peaks in the scattering have disappeared on suppression of the contrast between the air-water interface thus implying that the peaks in the data arise from the air-water interface. However, if we again focus on the differing contrast of surfactant head and tail groups (Figure 4.21 (bottom)) it can be seen that there is sufficient contrast between the tail groups and water, although, the contrast is indeed suppressed between both air and water.

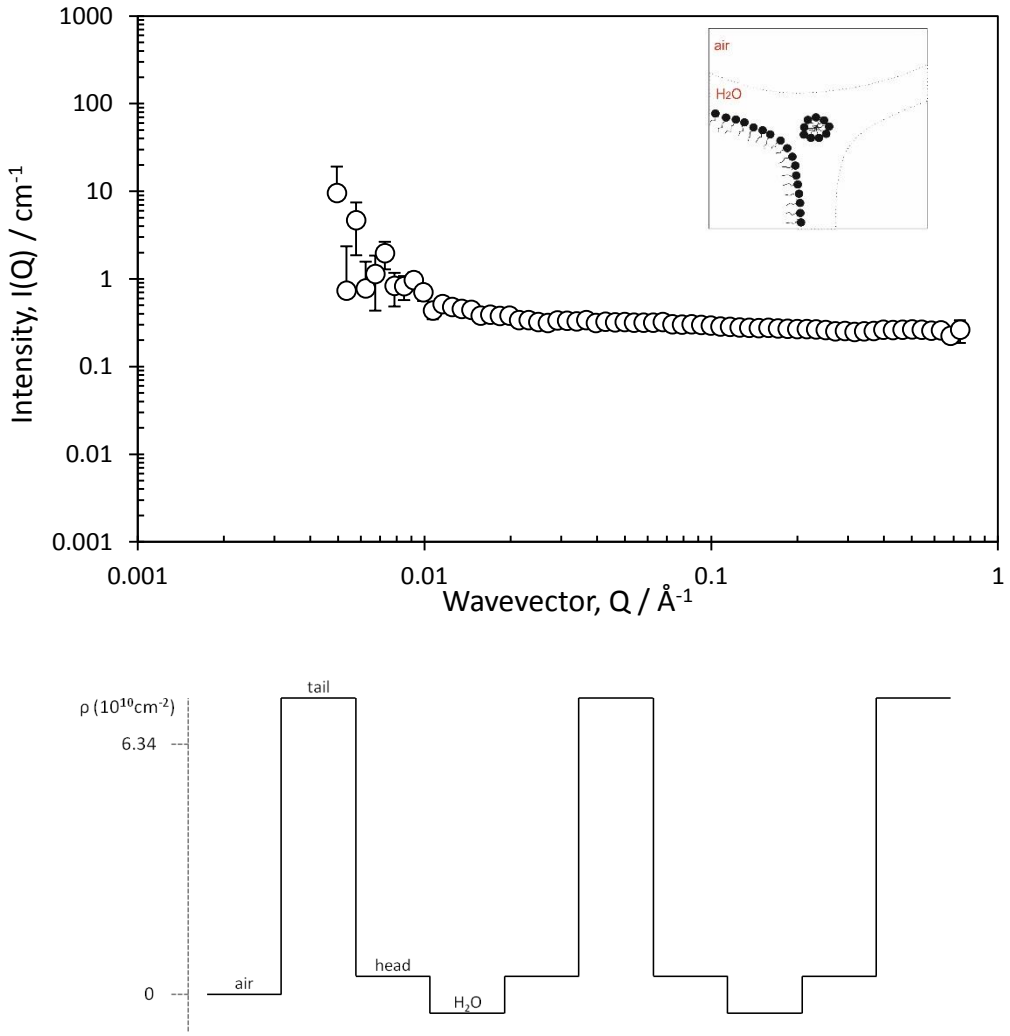

Figure 4.21;Small-angle neutron scattering from air-in-water foam stabilised with d-SDS in H_2O. [SDS]= 4mM. Inset; cartoon of foam structure to show the contrast between molecules and solvent (top). Scattering length density profile of the foam components observed across the foam film (bottom). Not to scale.

As previously described in discussion for the h-SDS in D_2O system, the paracrystalline stack model multiplies the scattering arising from the layered stacks with the Q^4 term. Hence, we postulate that when the contrast between air and water is suppressed, which defines the Q^{-4} decay in intensity and therefore the magnitude of the Q^{-4} term, the intensities of the peaks associated with the adsorbed layers are also reduced. Figure 4.22 shows the calculated scattering from the paracrystalline stack model in which the background intensity has been increased to higher values. In increasing the background intensity, the intensity of the peak at $0.035Å^{-1}$ decreases indicating that whilst the peak may indeed be present it is buried within the background. Given that the contrast between surfactant and solvent is large for the d-SDS in H_2O foam we propose that the peaks in the data are present however their intensity is much reduced due to the suppression of the contrast between air and water. This can be seen by rescaling the background intensity of calculated scattering to that of the h-SDS in D_2O foam (Figure 4.23). Overlaying the measured data of the d-SDS in H_2O foam to this calculated fit (Figure 4.23) shows the presence of a very weak inflexion at $Q \approx 0.035Å^{-1}$. This supports the conclusion that the inflexions in the data are obscured by the incoherent background in the d-SDS in H_2O foam which is higher ($\sim 0.3cm^{-1}$) than the background for h-SDS in D_2O ($0.003cm^{-1}$).

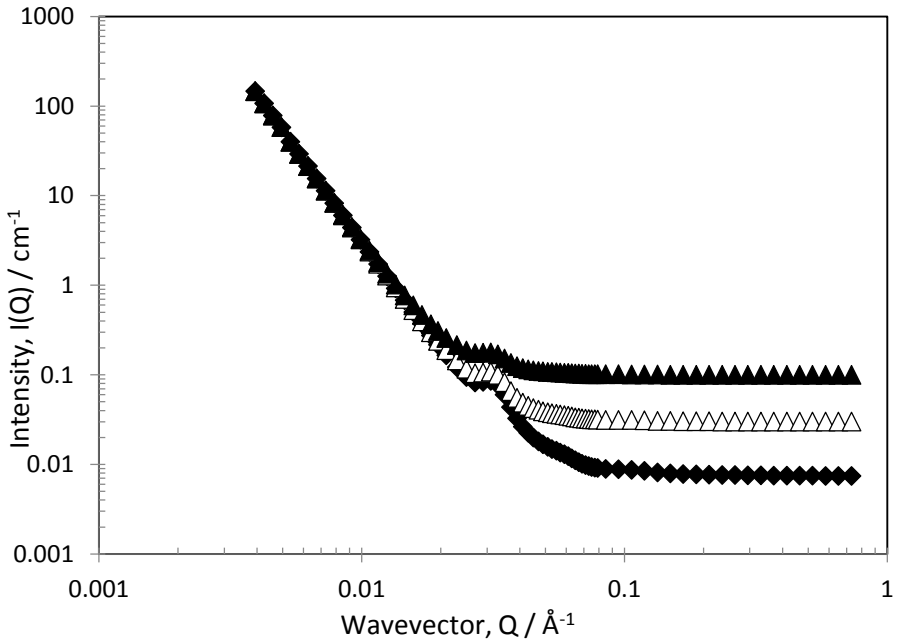

Figure 4.22; Calculated scattering to the paracrystalline stack model. Background intensities are varied to demonstrate the disappearance of the peaks at $Q \approx 0.035Å^{-1}$ upon increasing the background intensity.

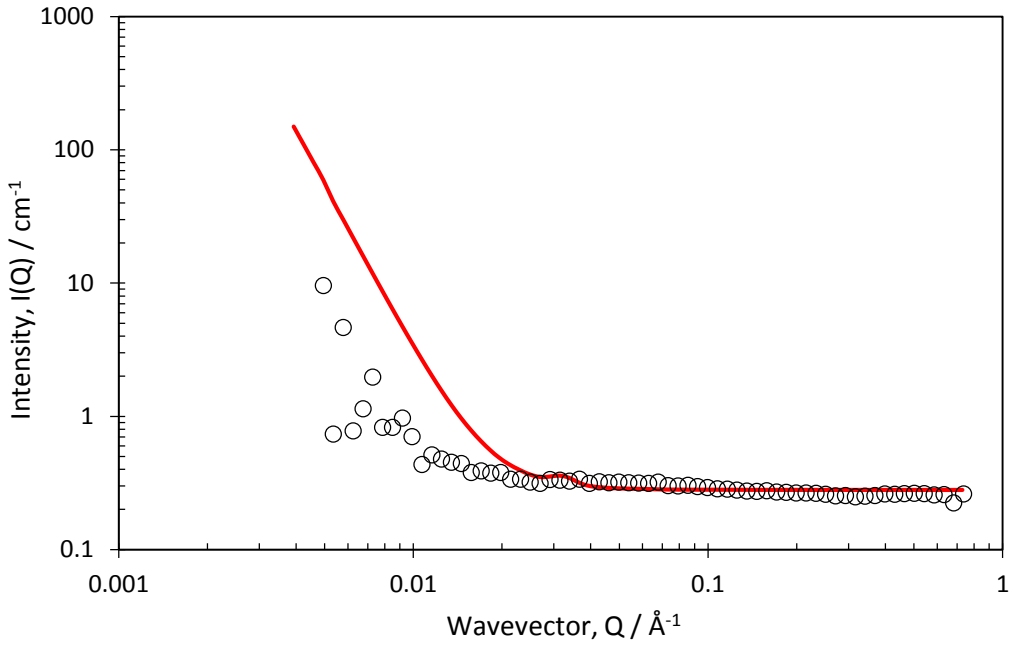

Figure 4.23; Calculated scattering to the paracrystalline stack model with background intensity increased to ~ 0.3cm^{-1}(line plot) showing the inflexion at Q ≈ 0.035Å^{-1} has virtually disappeared. The measured SANS data for d-SDS in H_2O foam is also shown (circles). Error bars have been removed for clarity.

Thus, to conclude this section we propose that the air-water interface in foams stabilised with PEO-PPO-PEO surfactants consists of paracrystalline stacks of surfactant layers separated by approximately 200Å of aqueous phase and typically ranging in thickness from 80-200Å. Contrast experiments support such arguments. In the absence of high contrast between air and water, inflexions in the data, which we attribute to the surfactant layers, may be obscured by the high incoherent background.

4.5. Comparison of model fitting parameters to PEO-PPO-PEO structure

The results of foaming studies for PEO-PPO-PEO surfactants presented in Chapter 3 have demonstrated that foaming is highly dependent on the structure of the stabiliser; whether this be overall molecular weight effects, or differences in PEO and PPO block size and ratio. Therefore, presumably these structural differences influence the nature of the adsorbed surfactant at the interface and this will be examined in the following section. In particular, comparisons of adsorbed layer thickness, L to foam stability will be made as it is likely that foam stability is most greatly affected by the nature of the adsorbed layer.

4.5.1. Effect of total molecular weight

Figure 4.24 shows layer thickness as a function of overall molecular weight for the Pluronic surfactants studied. Layer thickness typically increases with increasing molecular weight and based on the data obtained this could either follow a linear trend or begin to plateau at higher molecular weight. This suggests that overall molecular weight is a defining parameter in adsorbed layer thickness with larger molecular weight surfactants producing a thicker layer. Previous neutron reflection studies of the air-water interface stabilised with Pluronics at equilibrium have shown that layer thickness does in principle increase with increasing molecular weight.[12] This has also been found for Pluronic adsorption onto solid surfaces,[23] as well as at the emulsion droplet interface.[24] Baker *et al*.[25] determined the adsorbed layer thickness for various Pluronic surfactants onto latex particles using dynamic light scattering. A linear increase in layer thickness with molecular weight was shown suggesting the linear relationship shown here for adsorption at the air-water interface is realistic. It is difficult to quantify any changes in adsorbed layer thickness based purely on overall molecular weight as inevitably any increase in total molecular weight will also involve an increase in the size of the PEO and/or PPO blocks. This can also have a substantial influence on the nature of the adsorbed layer. Therefore, layer thickness will also be discussed in terms of the PEO and PPO block sizes.

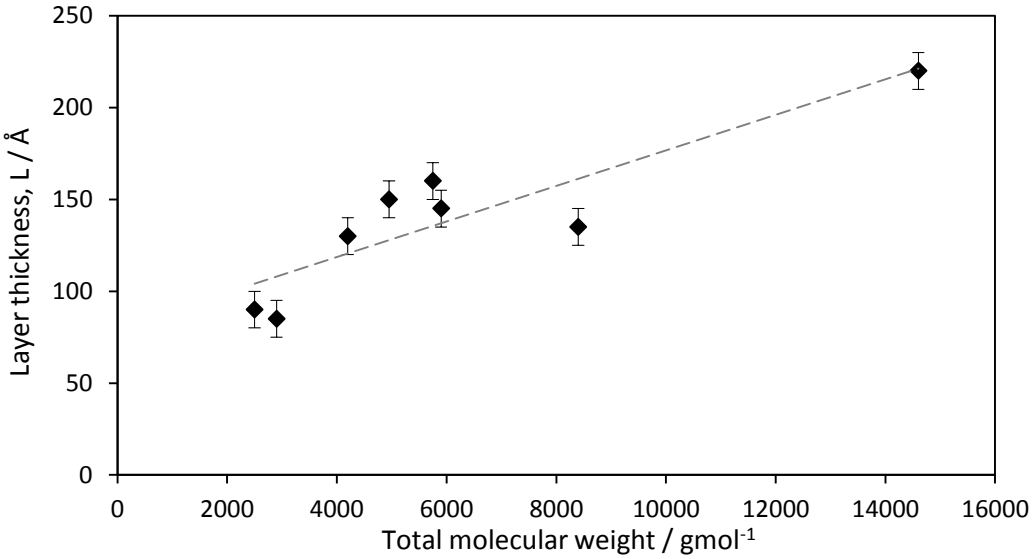

Figure 4.24; Adsorbed layer thickness of PEO-PPO-PEO stabilised foam determined by SANS as a function of total Pluronic molecular weight [Pluronic]=0.05%(w/v). The dotted lines act as a guide to the eye.

4.5.2. Effect of PEO block size

The effect of increasing PEO block size (at constant PPO) on layer thickness is presented in Figure 4.25 for two series of surfactants; L62, PE6400 and PE6800 (Mw PPO = 1750gmol^{-1}) and P103, P104 and F108 (Mw PPO = 3250gmol^{-1}). For both series, layer thickness increases with increasing PEO segments demonstrating that a thicker adsorbed layer is formed in the presence of more PEO.

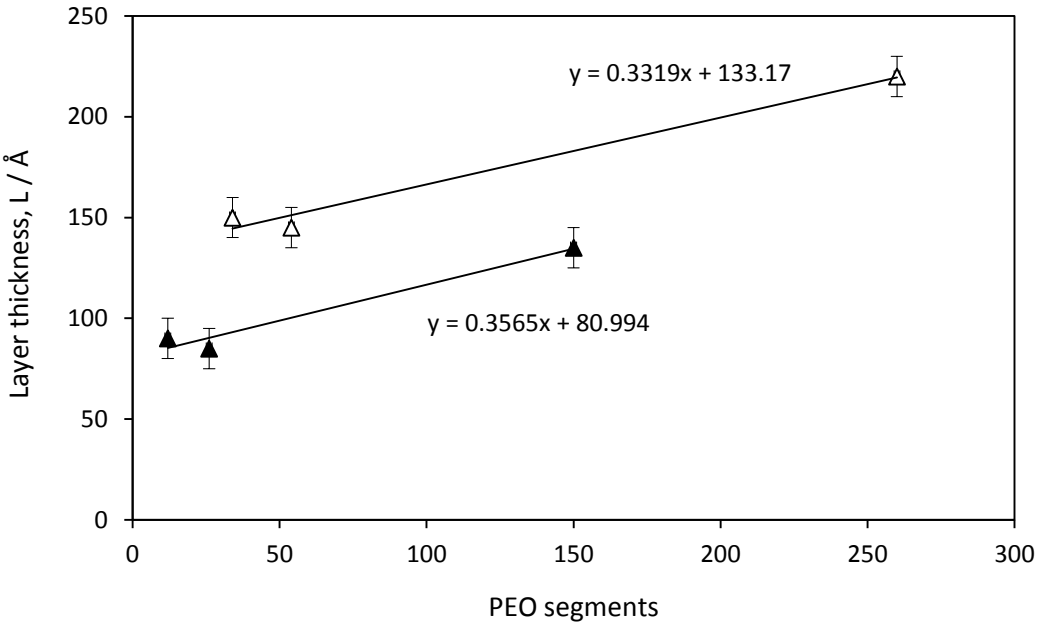

Figure 4.25; Adsorbed layer thickness determined by SANS as a function of number of PEO segments at constant PPO molecular weight for two surfactant series; L62, PE6400, PE6800 (PPO ≈ 30 segments, closed triangles); P103, P104, F108 (PPO ≈ 60 segments, open triangles). The gradients of the trend lines are shown for comparison.

Unfortunately, there are no commercially available Pluronics with number of PEO blocks that fit within the extremes of the data points. i.e. between approximately 50 and 125 segments for the L62, PE6400, PE6800 series. Time constraints also prevented these from being synthesised. Therefore it has not been possible to add further points to Figure 4.25 to confirm the trend in the data. However, previously a linear increase in layer thickness with increasing EO segments has been shown for equilibrium systems[12] and emulsions[24] thus this is the trend adopted here. Interestingly, the gradient in trend lines for both series is almost identical. This means that for PE6400 and P104, and PE6800 and F108 in which P104 and F108 are double the size of PE6400 and PE6800

respectively, the increase in L scales by a factor of 1.7, implying a predictive way to determine layer thickness.

The conformation of PEO-PPO-PEO surfactants at the interface in its most basic sense involves the anchoring of the polymer at the interface by the hydrophobic PPO block whilst the PEO blocks protrude into solution providing stabilisation. A study of Pluronic F127 at the hexane-water interface showed a stretched conformation at the interface, which extended beyond the micellar radius.[11] The area per molecule has also been shown to increase upon increasing PEO segments[26] suggesting a more extended conformation is adopted to minimise steric hindrance between the chains, subsequently increasing layer thickness.

4.5.3. Effect of PPO block size

Figure 4.26 shows the effect of increasing PPO block size, at constant PEO. There are no series available which have identical PEO segments however we can study P84, P103 and P123 which have approximately 38, 34 and 40 PEO segments respectively. Layer thickness shows a linear increase with PPO segments.

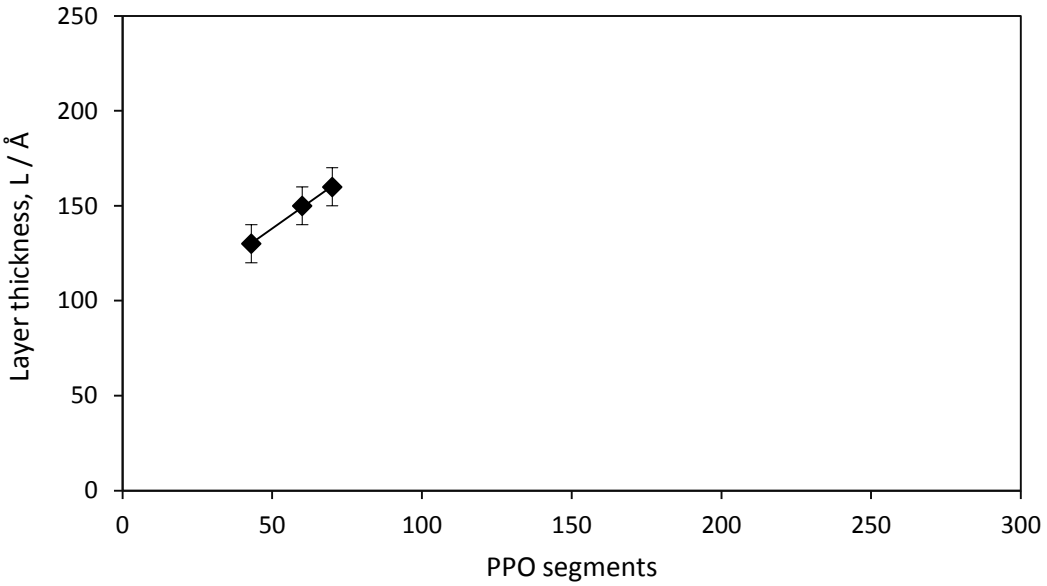

Figure 4.26; Adsorbed layer thickness determined by SANS as a function of number of PPO segments at approximately constant PEO molecular weight for the surfactant series P84, P103, P123. The axis is scaled for ease of comparison to Figure 4.25.

Such an increase in layer thickness with increasing hydrophobic block is perhaps surprising. Using the Gibbs adsorption isotherm, Alexandridis *et al.*[26] determined that

the area per molecule decreases with increasing number of PPO segments (at constant PEO). This suggests a more compact interfacial structure with greater dehydration of the larger PPO blocks so that when the area per molecule is large, the PEO blocks must adopt a more coiled conformation at the interface to reduce the contact of PPO with water (Figure 4.27). As the PPO block size increases, the area per molecule decreases and so the PEO segments can stretch into solution. The x axis in Figure 4.26 has been scaled for easier comparison to that in Figure 4.25 and the steeper slope of the variation in layer thickness with PPO segments therefore suggests that layer thickness is more strongly dependent on the number of PPO segments than PEO segments.

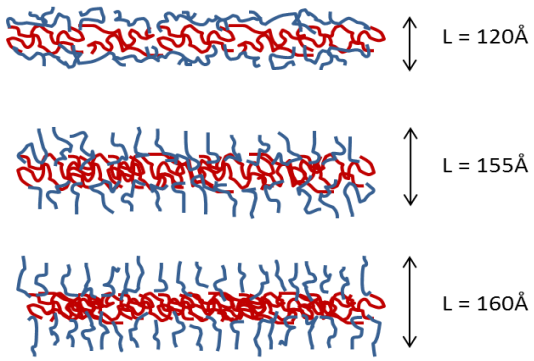

Figure 4.27; Cartoon showing the change in layer thickness for a series of surfactants with constant PEO block size and increasing PPO block size.

The behaviour is reminiscent of polymer adsorption theory developed by Marques and Joanny[27] from non-selective solvents. Following a multi-variant analysis a reasonable empirical correlation was found for L ~ $PO^{1}EO^{1/3}$ (Figure 4.28). Such a linear representation illustrates that the polymer forms a structure whose thickness is determined by the lateral associations of the PO groups. This implies that the PO blocks are the dominating factor in terms of layer structure.

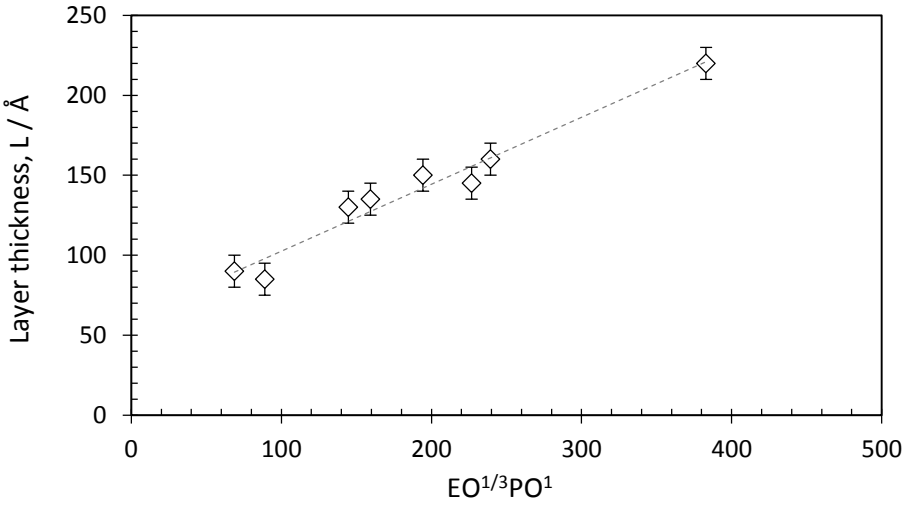

*Figure 4.28; Layer thickness as a function of $EO^{1/3}$*PO^{1}.*

4.6. Comparison of model fitting parameters to PEO-PPO-PEO foaming

The study of Pluronic foaming behaviour presented in Chapter 3 concluded that foaming ability and stability are closely intertwined with typically those surfactants producing greater volumes of foam also producing the most stable foams. Foam stability was more sensitive to structural changes within the molecule. This was characterised by greater differences in stability across the surfactants studied than that observed for foamability suggesting that stability is more strongly influenced by the nature of the adsorbed surfactant layer.

4.6.1. Effect of overall molecular weight

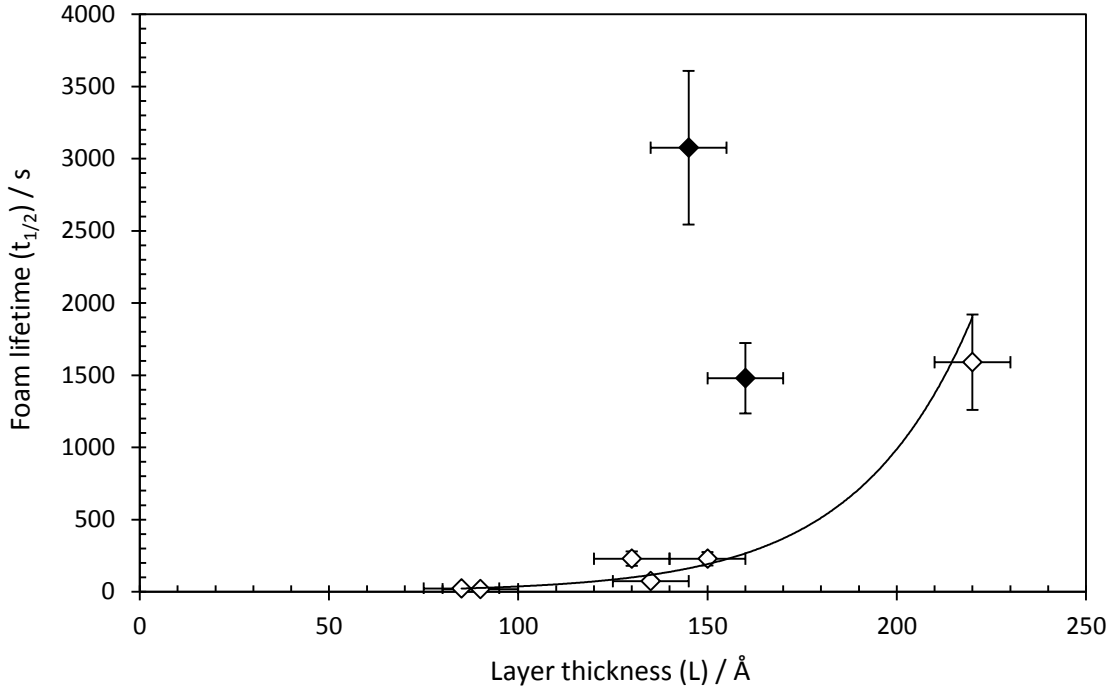

Figure 4.29; The relationship between adsorbed layer thickness and foam stability for various Pluronic surfactants. [Pluronic]=0.05%(w/v), 20°C. Foam stability is described by the foam half-life $t_{1/2}$ as defined in the Experimental chapter. [Surfactant]<CMT (empty diamonds), [Surfactant]>CMT (filled diamonds).

Layer thickness is compared to foam lifetime in Figure 4.29 for foams prepared with a bulk surfactant concentration of 0.05%(w/v). Those surfactants represented by the filled diamonds are above or very near to their CMT so that foam lifetime is higher due to the presence of micelles and therefore have not been included in any trends. Focussing on the surfactants highlighted by the empty diamonds, which are below the CMT and therefore all in the molecular phase, it can be seen that foam stability increases with layer thickness in an approximately exponential manner. To confirm this trend, further PEO-PPO-PEO surfactants with layer thicknesses ranging from 175-200Å need to be probed if they exist. As far as the author is aware, this is the first evidence in the literature that correlates the structure of three-dimensional Pluronic stabilised foams to its foam behaviour. A thicker adsorbed surfactant structure at the air-water interface correlates to a more stable foam structure. This is in agreement with previous studies of single thin films in which a thicker adsorbed layer led to more stable films.[28, 29] Thicker adsorbed layers promote steric stabilisation. In very thin films, when the total film

thickness is less than twice the adsorbed layer thickness a steric interaction between the hydrophilic PEO chains occurs preventing further contact. Long range repulsion is required to prevent drainage of the liquid from the film due to differences in capillary pressure and this effect will be greater for thicker adsorbed surfactant layers.[30] In addition, a thicker adsorbed layer will resist thinning and surface tension gradients more effectively[31] whilst closer packing of molecules at the interface minimises gas diffusion between bubbles.[32]

4.6.2. Effect of PEO block size

Both layer thickness and foam stability show a typically linear increase (Figure 4.30). Thus larger PEO blocks produce a thicker adsorbed layer which in turn produces more stable foam. This is as per the reasons described in Section 4.5.2 and 4.6.1. Increasing the PEO chain length suggests a more extended conformation in solution which promotes foam stabilisation. Therefore at constant PPO block, longer PEO chains are desirable for creating more stable films.

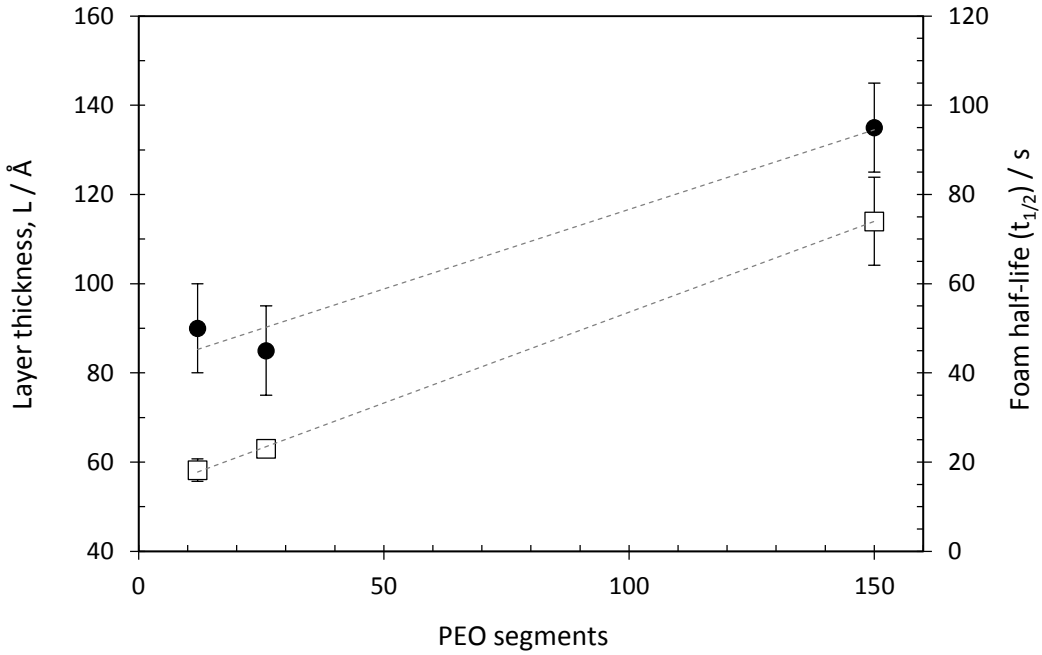

Figure 4.30; Adsorbed layer thickness (circles) and foam lifetime (squares) of aqueous foam stabilised with a series of PEO-PPO-PEO surfactants with constant PPO block size and increasing PEO block size (L62, PE6400, PE6800). [Pluronic]=0.05%(w/v).

4.6.3. Effect of PPO block size

Comparison of foam lifetime and layer thickness for varying number of PPO segments at constant PEO segments is shown in Figure 4.31. Whilst a definite linear trend in layer thickness and PPO segments is observed, the relationship between foam lifetime and PPO segments is less clear. A thicker adsorbed layer produces more stable foam for the Pluronic surfactant with the greatest number of PPO segments for this series. However, due to the limited number of data points available definitive conclusions cannot be drawn.

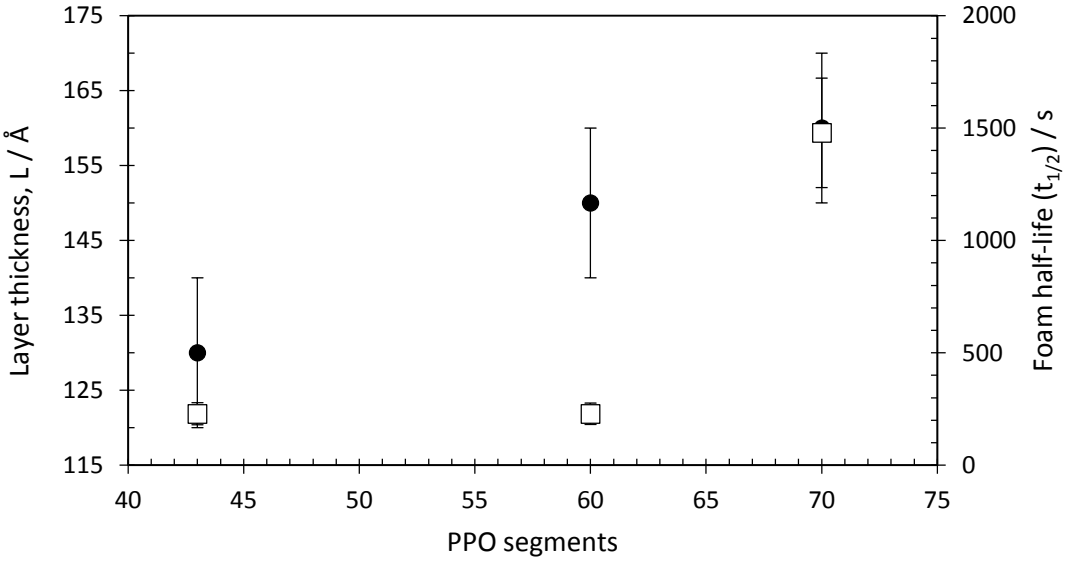

Figure 4.31; Adsorbed layer thickness (circles) and foam lifetime (squares) of aqueous foam stabilised with a series of PEO-PPO-PEO surfactants with constant PPO block size and increasing PEO block size (L62, PE6400, PE6800). [Pluronic]=0.05%(w/v).

4.7. Conclusion

To conclude, small-angle neutron scattering has been successfully implemented to probe the structure of PEO-PPO-PEO polymeric surfactant stabilised foams. We propose the structure at the interface comprises a multilayered structure of polymer rich and water rich layers. A model comprising a paracrystalline stack of roughly five polymer layers of thickness ranging from approximately 80-200Å was found to best fit the data. Such layers were separated by approximately 200Å of aqueous phase. Comparison of adsorbed layer thickness to surfactant structure indicated that layer thickness increased with increasing molecular weight postulated to be in linear manner. Similar linear increases were observed with increasing PEO and PPO block sizes. This

was attributed to the greater extension of the blocks into solution. Foam stability correlated well with adsorbed layer thickness, with foam exhibiting thicker layers producing more stable foam. Thus, the structure of the adsorbed layer is a key parameter in defining foam stability.

4.8. References

1. H. Fruhner, K. D. Wantke and K. Lunkenheimer, *Colloids and Surfaces A: Physicochemical and Engineering Aspects*, 2000, **162**, 193-202.

2. L. G. Wang and R. H. Yoon, *Minerals Engineering*, 2006, **19**, 539-547.

3. C. Stubenrauch, P. M. Claesson, M. Rutland, E. Manev, I. Johansson, J. S. Pedersen, D. Langevin, D. Blunk and C. D. Bain, *Advances in Colloid and Interface Science*, 2010, **155**, 5-18.

4. J. Higgins and C. Benoit, *Polymers and Neutron Scattering*, Clarendon Press, Oxford, UK, 1997.

5. K. Mortensen, *Journal of Physics-Condensed Matter*, 1996, **8**, A103-A124.

6. K. Malysa and K. Lunkenheimer, *Current Opinion in Colloid & Interface Science*, 2008, **13**, 150-162.

7. M. A. V. Axelos and F. Boue, *Langmuir*, 2003, **19**, 6598-6604.

8. P. Alexandridis and T. A. Hatton, *Colloids and Surfaces A: Physicochemical and Engineering Aspects*, 1995, **96**, 1-46.

9. A. F. Gallaugher and H. Hibbert, *Journal of the American Chemical Society*, 1937, **59**, 2514-2521.

10. J. B. Vieira, Z. X. Li, R. K. Thomas and J. Penfold, *Journal of Physical Chemistry B*, 2002, **106**, 10641-10648.

11. J. S. Phipps, R. M. Richardson, T. Cosgrove and A. Eaglesham, *Langmuir*, 1993, **9**, 3530-3537.

12. R. Sedev, R. Steitz and G. H. Findenegg, *Physica B-Condensed Matter*, 2002, **315**.

13. D. J. McGillivray, R. K. Thomas, A. R. Rennie, J. Penfold and D. S. Sivia, *Langmuir*, 2003, **19**, 7719-7726.

14. Z. X. Li, A. Weller, R. K. Thomas, A. R. Rennie, J. R. P. Webster, J. Penfold, R. K. Heenan and R. Cubitt, *Journal of Physical Chemistry B*, 1999, **103**, 10800-10806.

15. P. A. Reynolds, E. P. Gilbert and J. W. White, *Journal of Physical Chemistry B*, 2000, **104**, 7012-7022.

16. P. A. Reynolds, E. P. Gilbert and J. W. White, *Journal of Physical Chemistry B*, 2001, **105**, 6925-6932.

17. P. A. Reynolds, M. J. Henderson and J. W. White, *Colloids and Surfaces A: Physicochemical and Engineering Aspects*, 2004, **232**, 55-65.

18. P. A. Reynolds, M. J. Henderson, J. Zank and J. W. White, *Journal of Colloid and Interface Science*, 2011, **364**, 539-545.

19. J. Zank, P. A. Reynolds, A. J. Jackson, K. J. Baranyai, A. W. Perriman, J. G. Barker, M. H. Kim and J. W. White, *Physica B-Condensed Matter*, 2006, **385**, 776-779.

20. P. A. Reynolds, E. P. Gilbert, M. J. Henderson and J. W. White, *Journal of Physical Chemistry B*, 2009, **113**, 12231-12242.

21. P. A. Reynolds, E. P. Gilbert, M. J. Henderson and J. W. White, *Journal of Physical Chemistry B*, 2009, **113**, 12243-12256.

22. M. Kotlarchyk and S. M. Ritzau, *Journal of Applied Crystallography*, 1991, **24**, 753-758.

23. A. Nelson and T. Cosgrove, *Langmuir*, 2005, **21**, 9176-9182.

24. T. J. Barnes and C. A. Prestidge, *Langmuir*, 2000, **16**, 4116-4121.

25. J. A. Baker and J. C. Berg, *Langmuir*, 1988, **4**, 1055-1061.

26. P. Alexandridis, V. Athanassiou, S. Fukuda and T. A. Hatton, *Langmuir*, 1994, **10**, 2604-2612.

27. C. M. Marques and J. F. Joanny, *Macromolecules*, 1989, **22**, 1454-1458.

28. B. R. Blomqvist, S. Folke and P. M. Claesson, *Journal of Dispersion Science and Technology*, 2006, **27**, 469-479.

29. R. Sedev, B. Jachimska, K. Khristov, K. Malysa and D. Exerowa, *Journal of Dispersion Science and Technology*, 1999, **20**, 1759-1776.

30. R. Sedev and D. Exerowa, *Advances in Colloid and Interface Science*, 1999, **83**, 111-136.

31. R. J. Pugh, *Advances in Colloid and Interface Science*, 1996, **64**, 67-142.

32. M. Rosen, *Surfactants and interfacial phenomena*, 2nd edn., Wiley, New York, USA, 1989.

5. The effect of temperature on aqueous PEO-PPO-PEO surfactant stabilised foams

5.1. Abstract

Air-in-water foams stabilised with non-ionic poly(ethylene oxide)-poly(propylene oxide)-poly(ethylene oxide) (PEO-PPO-PEO) surfactants (2500-14500gmol^{-1}) were investigated as a function of temperature using foam column techniques, surface tension and small-angle neutron scattering (SANS). SANS was used to the probe the interfacial adsorbed layer of such foams from which the structure could be determined. Below the critical micelle temperature (CMT), adsorbed layer thickness was found to be independent of temperature across a range of 20-40°C. Foaming ability and foam stability were found to be highly affected by the phase of the surfactant with a sharp increase in foaming observed at the critical micelle temperature (CMT) indicating that at the CMT the presence of micelles promotes foaming. However, as temperature increases substantially above the CMT, both foam volume and lifetime decrease attributed to the slower kinetics associated with micellar break-down. The study suggests important implications for polyurethane foam formation in which temperature gradients typically in the region of the CMT are observed.

5.2. Introduction

The polyurethane (PU) foam forming process is highly temperature dependent; as well as the reaction being exothermic, induced temperature gradients throughout the curing process are essential to control the blow and gelation reaction rates. Polymeric surfactants of the PEO-PPO-PEO type are also highly temperature dependent due to the decreased hydrophilicity of the PEO blocks as temperature is increased. This results in significant differences in phase behaviour observed over relatively small temperature changes (tens of degrees Celsius). It is has previously been shown in the literature that the phase of the surfactant solution can dramatically influence its foaming properties.[1-4] Thus, the phase behaviour of the surfactant and phase transitions that occur throughout the PU foam forming process as a function of temperature may impact on the resulting structure and performance of the solid product.

In this chapter, both foaming ability and stability of various PEO-PPO-PEO surfactants are characterised as a function of temperature and correlated to the structure and phase behaviour of the surfactant. A model system of air-in-water foams is again adopted. Small-angle neutron scattering is employed to probe the influence of temperature on the structure of the adsorbed surfactant layer.

5.3. Foamability

5.3.1. *Effect of surfactant structure*

The effect of temperature on the foaming ability of the surfactant is likely to be more important in the initial stages of the polyurethane forming process as this is when the newly forming cells will begin to develop and it is necessary that there is a sufficient supply of surfactant to the interface.

Foamability as a function of temperature has been studied for the series of polymeric surfactants; L62, PE6400 and PE6800 which have constant molecular weight poly(propylene oxide) PPO block (1750 $gmol^{-1}$) but increasing proportion of poly(ethylene oxide) PEO (20, 40 to 80% respectively), Figure 5.1. There are three apparent regions of foaming; constant but relatively poor foaming at low temperatures; an increase in foamability over a temperature range specific to each surfactant culminating in a maximum, followed by an apparent levelling out of foam volume beyond this. The temperature at which the first break-point is observed varies depending on the surfactant.

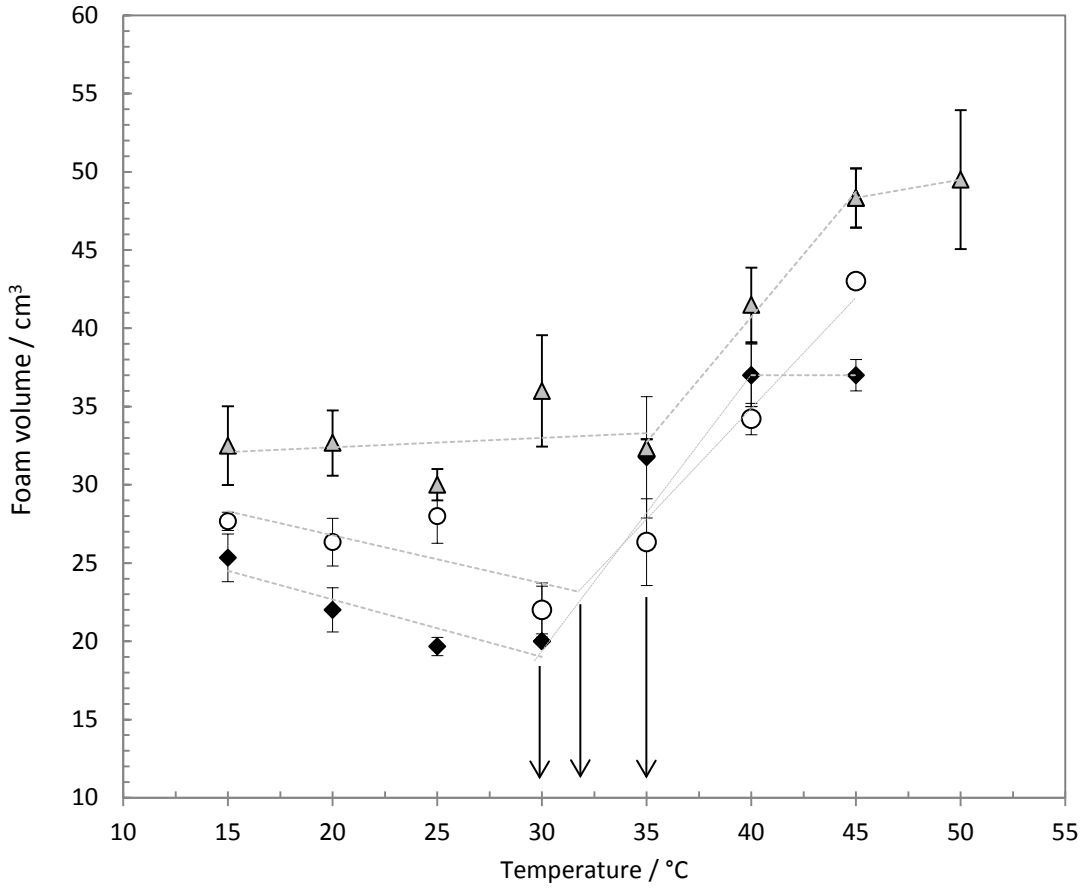

Figure 5.1; Foamability of the air-in-water foams as a function of temperature for three polymeric surfactants L62 (diamonds), PE6400 (circles) and PE6800 (triangles). [Pluronic] = 2% (w/v). Dotted lines act as a guide to the eye. The arrows indicate the breakpoint in the data which corresponds to the CMT.

Consultation of the literature phase diagrams for these systems and equilibrium surface tension plots measured (Appendix 1) indicates that the first break-point strongly correlates to the critical micelle temperature (CMT) for each surfactant. Typically, CMT's for polymeric type surfactants occur across a temperature range due to high polydispersity of the polymeric species, rather than at a well-defined value as is the case for small molecule surfactants. Therefore, the increase in foamability observed is not defined by a sharp break point. Thus, as the CMT is passed (CMT; L62 28°C, PE6400 31°C, PE6800 38°C) a steady increase in foamability is observed until at a temperature individual to each surfactant a maximum in foamability is reached. It is known that the transition from unimers to micelles typically occurs across a temperature range of 10-15°C above the CMT[5] suggesting that the maximum in foamability observed corresponds to the formation of well-defined micelles in solution. This is supported by

small-angle neutron scattering (SANS) from bulk PE6400 surfactant solution (Appendix 1) indicating that across the temperature range studied here a transition from Debye polymer coils in solution to well defined micelles occurs. Therefore, the sharp increase in foam volume has been attributed to the formation of micelles and the maximum in foam lifetime observed is the point at which well-defined micelles are present.

As temperature is increased, PEO-PPO-PEO surfactants become more insoluble in water.[6] Numerous theories are present in the literature[7-9] attempting to describe such temperature dependent micellisation however most importantly it must be recognised that as PEO-PPO-PEO surfactants are more hydrophobic at elevated temperatures it is therefore expected that they exhibit a stronger driving force for adsorption at the interface, thus promoting foaming. This is confirmed by the dynamic surface tension as a function of temperature for L62 (Appendix 1). Surface tension decreases rapidly upon increasing the temperature from 20 to 30°C corresponding to the breakpoint in the foaming data. At the CMT, the interface is generally at (or very near to) maximum surface coverage and so molecules will begin to aggregate in the bulk phase in order to reduce the free energy of the system.

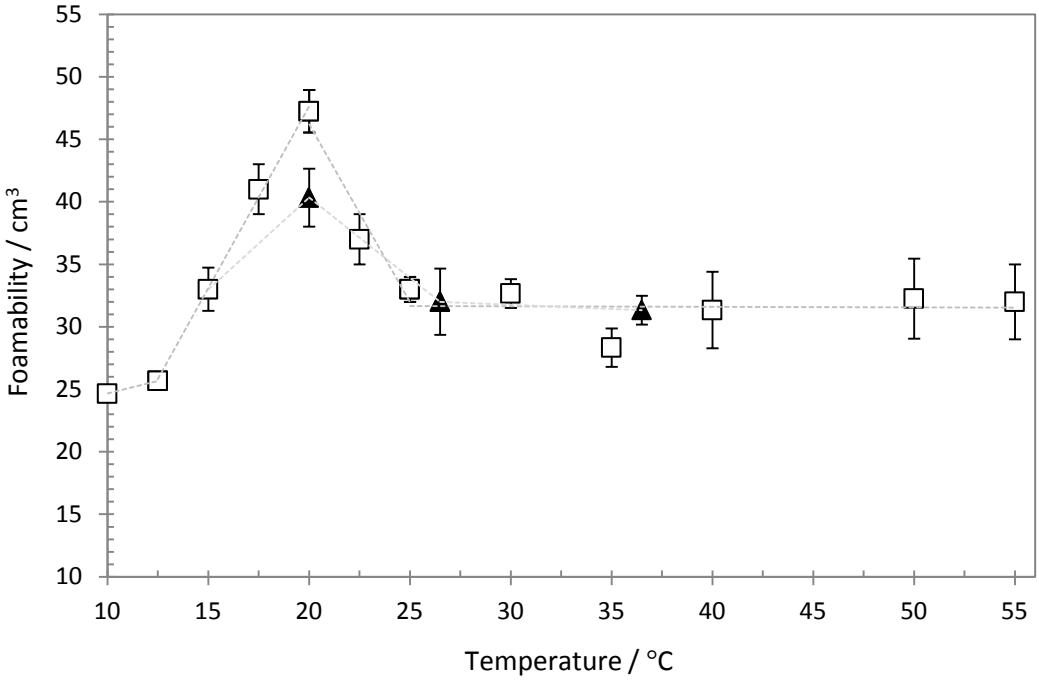

Figure 5.2; Foamabillity of the air-in-water foams as a function of temperature for two representative polymeric surfactants P123 (squares) and P104 (triangles); [Pluronic] = 2% (w/v). Dotted lines act as a guide to the eye.

Figure 5.2 shows foamability data for surfactants P123 and P104 in which the CMT's for these surfactants are much lower, occurring at 16°C and 18.5°C respectively (Appendix 1). This allows further study into the effect micelles have on foamability by probing temperatures well above the CMT. Here, it can be seen that again foam volume increases rapidly in the region of the CMT (i.e. before 20°C). Interestingly, whilst a maximum in foamability is observed at a defined temperature, beyond this a sharp decrease in foamability is seen. Whilst the presence of micelles appears to promote foaming to a degree, with regards to foamability their presence in Pluronic stabilised foams appear to induce an antagonist effect beyond a defined temperature. One such reason for this could be that in order to provide surfactant to the rapidly forming interface, the micelles must breakdown before providing the reservoir of surfactant needed. If this breakdown process is slow then the reservoir of surfactant that supplies the newly forming interface will not be available. Micelle breakdown kinetics are therefore likely to be highly important here. As the temperature is increased beyond the CMT, the micellar radius of Pluronic micelles has been shown to remain constant however the aggregation number increases, consistent with micelle dehydration[10, 11] suggesting that the micelles become more stable. Micellar breakdown kinetic studies have shown that the relaxation time τ_2 associated with micelle formation and dissolution increases upon increasing temperature[5] i.e. the breakdown process is slower. Such result is as expected given that micelle formation is favoured at higher temperatures. Therefore since the kinetics of micelle breakdown is much slower at higher temperature, the supply of surfactant unimers to the interface is reduced across the timescale of bubble formation and foamability decreases. In addition, dynamic surface tension data for P123 (Appendix 1) shows that at 20°C, corresponding to the maximum in foaming, surface tension is at its lowest. As the temperature is increased and the CMT is crossed, dynamic surface tension increases suggesting that the surfactant is less surface active as per the micelle breakdown kinetics reasoning. Eventually, a plateau in foamability is reached, presumably due to the breakdown kinetics becoming the rate limiting step.

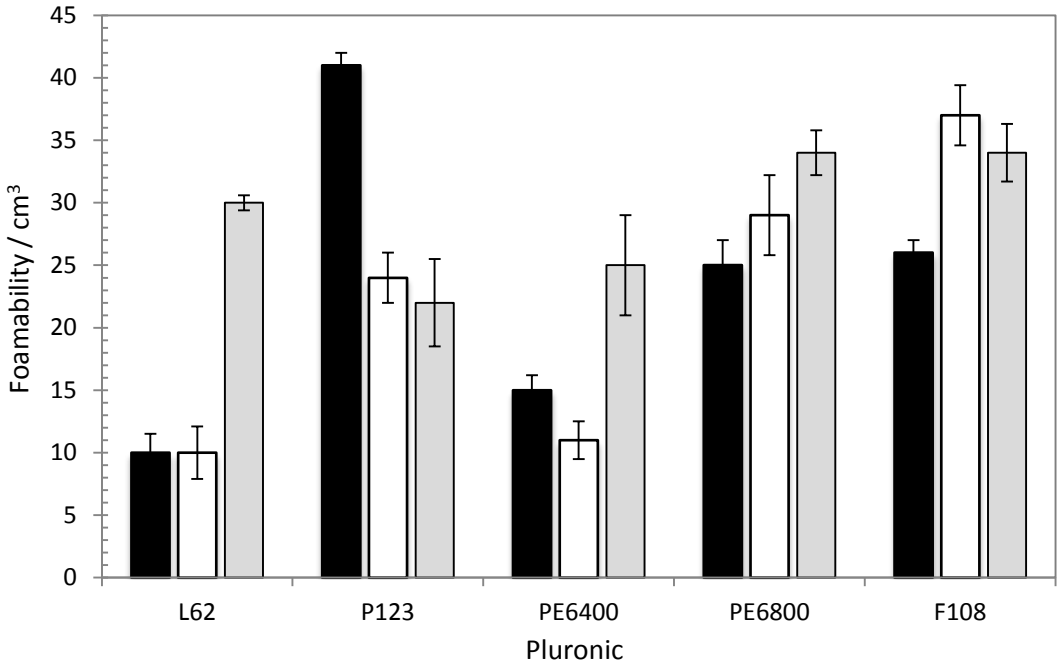

Figure 5.3; Foamability of the air-in-water foams for various Pluonics as a function of temperature; 20°C (black bars), 30°C (white bars), 40°C (grey bars). [Pluronic] = 2% (w/v).

Foamability for a variety of surfactants at 20, 30 and 40°C is presented in Figure 5.3 and it can be seen how reasonably small temperature changes can induce large differences in foamability across individual surfactants and the whole series of surfactants. This highlights the importance of defining the phase behaviour of the surfactant when discussing foamability. As described previously it is known that foaming increases in the region of micellisation due to the fact that these polymeric surfactants become more hydrophobic in water as temperature is increased and thus there is a stronger driving force for adsorption at the interface. Therefore the CMT is a good indicator for surfactant foamability.

5.3.2. *Effect of PEO block size*

Focussing on the L62, PE6400, PE6800 series (increasing PEO at constant PPO) it can be seen that at 20°C when all surfactants are in their molecular phase, foamability follows the order L62<PE6400<PE6800 (Figure 5.3). Reasons for this trend are discussed in Chapter 3, Section 3.3.2.1. As the temperature is increased to 40°C foamability now follows the order PE6400≈L62<PE6800. Referring to the equilibrium surface tension plots as a function of temperature indicates that at 40°C L62 is further

beyond its CMT than PE6400 or PE6800 (Appendix 1). In addition, L62 shows the greatest reduction in dynamic surface tension at a bubble lifetime of 0.05s, i.e. it is more surface active and this is reflected in its low hydrophobic-lipophilic balance (HLB) value. Thus, in theory, based on phase behaviour effects alone L62 is expected to exhibit a greater foam volume. However, whilst phase behaviour is important the structure of the surfactant and the nature of the adsorbed layer must also be considered. SANS data presented in Chapter 4 demonstrated that PE6800 displays a thicker layer at the air-water interface than L62 (135 and 90Å respectively). The larger PEO block (and larger structure) of PE6800 has a greater influence on foamability than phase behaviour changes (across the concentration and temperature regime studied).

5.3.3. *Effect of surfactant concentration*

Foamability at various concentrations and temperatures for two representative surfactants L62 and PE6800 are presented in Figure 5.4. Focussing first on PE6800 it can be seen that regardless of temperature foamability increases rapidly at low concentrations before attaining a plateau value at higher concentrations. The trend in the data shows similar characteristics to that of an adsorption isotherm (rapid change with concentration at low surfactant concentration followed by a plateau at a defined concentration). This suggests that at a concentration corresponding to the maximum foamability no further surfactant in solution will improve foaming (for a more in-depth discussion see Chapter 3 Section 3.4.4). This is an important consideration in the design of formulations for use in polyurethane foam systems. As temperature is increased the foam volume increases at all concentrations. In order to explain this, one needs to consider the relative position of the surfactant from its CMT at a defined concentration and temperature. At a constant concentration, a higher temperature (i.e. 40°C studied here) will mean that the surfactant is closer to or beyond its CMT. In fact the CMT for PE6800 at 2%(w/v) concentration is approximately 38°C. Therefore the surface coverage will be closer to or at a maximum, there will be a stronger driving force for adsorption and greater foamability is observed.

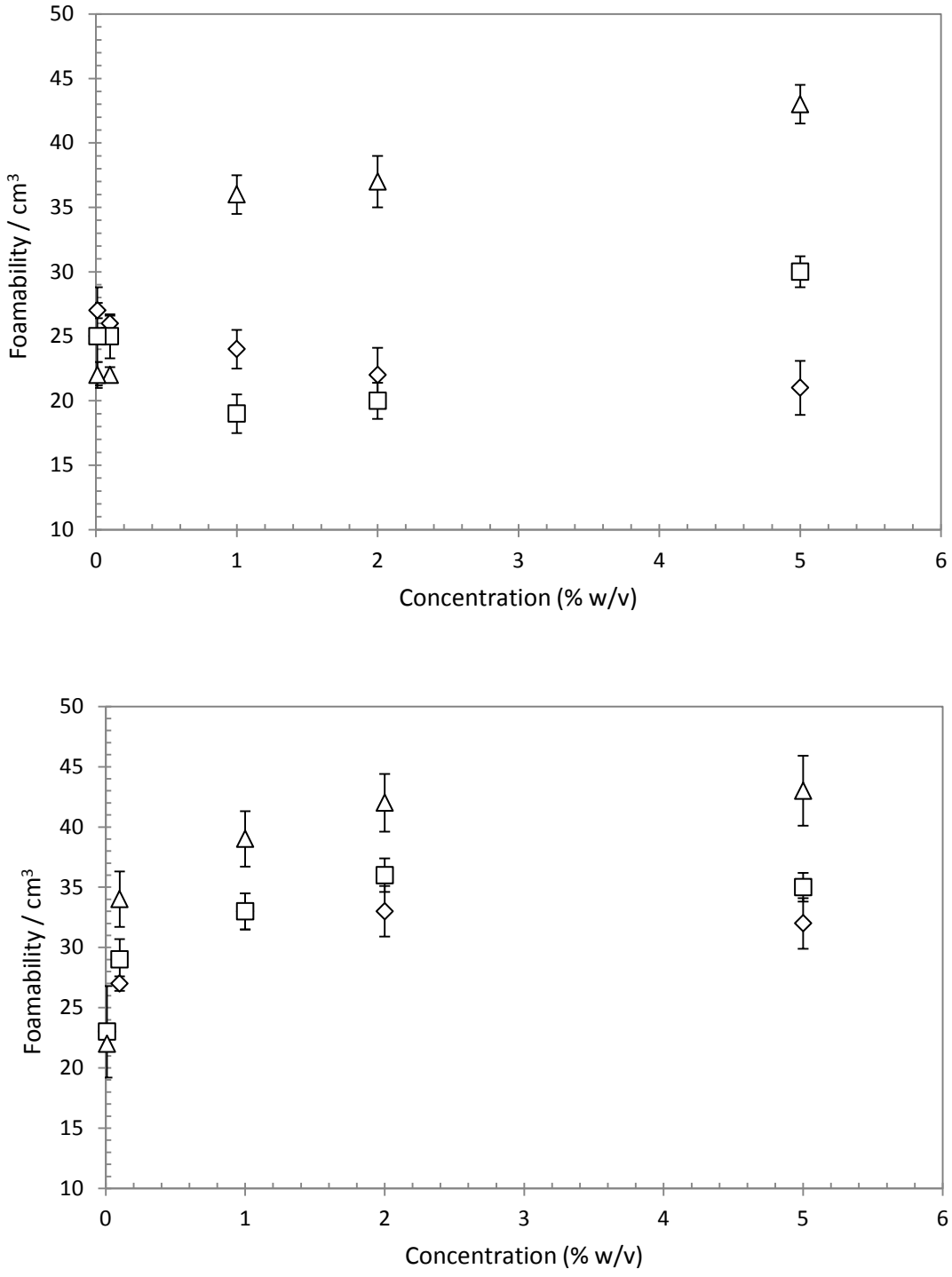

Figure 5.4; Foamability of the air-in-water foams stabilised by Pluronic L62 (top) and PE6800 (bottom) as a function of concentration at various temperatures; 20°C (diamonds), 30°C (squares) and 40°C (triangles).

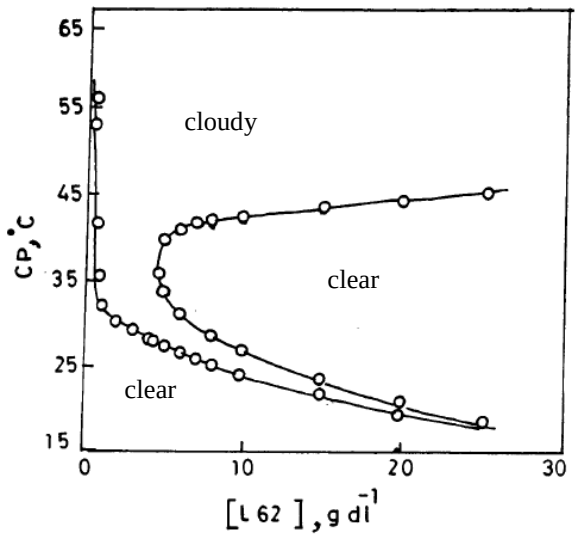

Figure 5.5; Partial phase diagram for L62 in water showing the cloud point temperatures.[12]

For L62, the situation is the same at a temperature of 40°C, with foamability increasing with increasing concentration until a plateau is attained. However at 20°C, foamability decreases with increasing concentration. Whilst at 30°C the situation is further complicated by an apparent decrease in foamability with concentration followed by an increase as temperature is further increased. L62 displays complicated phase behaviour with the phase diagram measured by Desai *et al*. showing the presence of two cloud points under certain conditions (Figure 5.5).[12] From Figure 5.5 it can be seen that at 5wt% one cloud point is observed at approximately 25°C suggesting that for the foamability data as the concentration is increased at 20°C, foamability decreases due to the onset of phase separation in the form of a cloud point. The foamability of non-ionic ethoxylated surfactants ($C_{10}E_4$) has been shown to decrease significantly above the cloud point and it has been postulated that this is due to the surfactant rich phase acting as an anti-foam.[3] Again from Figure 5.5, at bulk solution temperature of 30°C two cloud points are observed at approximately 1wt% and 8wt%. Comparing this to the foaming data suggests that foamability decreases as the first cloud point is crossed and then increases again as normal phase behaviour is returned. At 40°C only one cloud point is observed at low concentration, less than 1wt% suggesting that an increase in foamability will be observed across the concentration regime studied here and the trend will be similar to that of PE6800 which does not exhibit a cloud point.

5.4. Foam stability

5.4.1. *Effect of temperature*

Foam stability for PE6400 surfactant as a function of temperature is depicted in Figure 5.6 at 5% (w/v) bulk surfactant concentration.

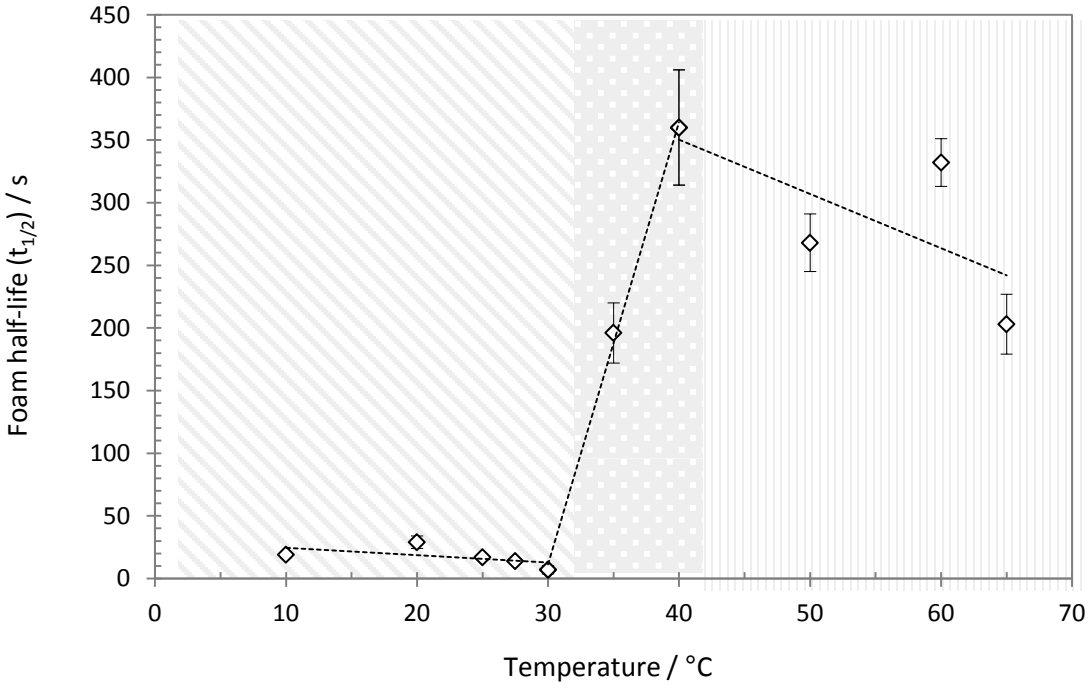

Figure 5.6; Stability of the air-in-water foam stabilised by Pluronic PE6400 as a function of temperature; [Pluronic] = 5% (w/v), flow rate 0.08L/min, 0.8bar. The stability of the foam is quantified in terms of the foam half-life, $t_{1/2}$ as described in the experimental section.

Stability displays strong temperature dependence over the temperature range studied. The same trend as that of foamability is visible and much more clearly defined. Again, there are three main regions of interest; poor foam stability at low temperature which decreases slightly with increasing temperature until foam stability is essentially non-existent, a sharp increase in stability over a fairly broad temperature range which culminates in a maximum in foam lifetime and beyond this a reduction in foam stability upon further increasing the temperature. For PE6400 at 5% (w/v) the significant increase in foam stability occurs at approximately 30-40°C. Again this can be attributed to the onset of micelle formation in solution. Consultation of the literature phase diagram for PE6400[13] shows that a transition from molecules to micelles in solution occurs at approximately 25-30°C for 5wt% surfactant in water (indicated by the CMC-

CMT line), corresponding to the region in which increased foam stability is observed. Small-angle neutron scattering has also been employed to confirm that the phase behaviour of the surfactant used here correlates to literature findings. Small-angle neutron scattering of 5% (w/v) PE6400 in solution with temperature is presented in Appendix 1. Scattering at 20°C is indicative of molecules in solution and fits to a Gaussian coil model with radius of gyration (R_g) of 20Å. As the temperature is increased to 30°C an upturn in the data is visible at low Q characteristic of the inter-particle structure factor S(Q) and representing attractive interactions between molecules in solution. Upon further increasing the temperature the form factor, P(Q) for micelles in solution becomes visible until at 40°C strong micellar scattering is observed corresponding to the maximum in foam lifetime as seen in the foam stability plots. Hence, the transition from unimers to micelles in solution promotes foam stability.

It has previously been shown that the presence of organised molecular structures, in the form of micelles, situated within thin film walls contribute to thin film stability by providing a step wise thinning mechanism known as stratification.[2, 14] The formation of ordered micellar structures provides an additional contribution to the disjoining pressure. Throughout the drainage process, micelle layers corresponding to a specific concentration drain from the cell walls into the Plateau borders so that drainage and reduction in film thickness occurs in a step-wise fashion resulting in more stable foam.[2] In addition, as mentioned in Section 5.3.1 on approach to the CMT, the driving force for adsorption is at a maximum, therefore the decrease in surface tension is greatest and a thick adsorbed layer is formed, promoting stability. Both foaming ability and stability are intrinsically linked thus it is almost impossible to discuss the trends in foam stability without considering foamability effects also. It is worth noting that there is a much lesser notable difference between absolute values of foamability compared to foam stability suggesting that temperature has a more profound effect on the stability of Pluronic stabilised foams rather than their foaming ability.

The absolute reasons as to why a decrease in foam stability is observed as temperature is increased beyond the maximum has not been confirmed experimentally however possible factors are discussed here. The stratification mechanism is highly dependent on both temperature and micellar volume fraction. As temperature is increased, the size of

Pluronic micelles remains the same however a larger aggregation number is observed due to dehydration of the PEO groups and so the volume fraction decreases.[10] Thus, the formation of ordered layers within the film walls is depressed i.e. the stratification mechanism is less evident. Foam viscosity is also an important parameter with higher bulk or surface viscosity linked to slower drainage rates.[15-18] For PEO-PPO-PEO surfactants it has been shown that a decrease in viscosity is observed with increasing temperature again due to the micelles becoming more compact as a result of dehydration of the PEO chains.[19] Therefore this decrease in viscosity, along with absent or reduced stratification effects may account for the decline in foam stability observed at higher temperature.

5.4.2. *Effect of concentration*

The temperature at which the increase in foam stability occurs, corresponding to the transition from molecules to micelles, is shifted to lower temperatures with increasing surfactant concentration (Figure 5.7). In other words, the CMT decreases with increasing concentration. This is not unexpected and is as a result of the hydrophobic effect.[20] The tendency to form micelles is greatest when there are more hydrophobic moieties present in solution disrupting the hydrogen bonding within the water. This disruption results in a reduction in entropy and thus an unfavourable contribution to the free energy of the system. Micelles will form spontaneously in solution to reduce the interactions between the polar water molecules and nonpolar surfactant.

For PE6400 there appears to be little difference in absolute foam stability at and above the maximum value attained upon increasing the concentration from 1% (w/v) to 5% (w/v) suggesting that excess surfactant in solution does not appreciably improve stability. This is an important consideration in PU systems implying that for those stages of the reaction in which foam stability is important, having higher concentrations of surfactant in solution will not improve stability, thus potentially reducing raw material costs.

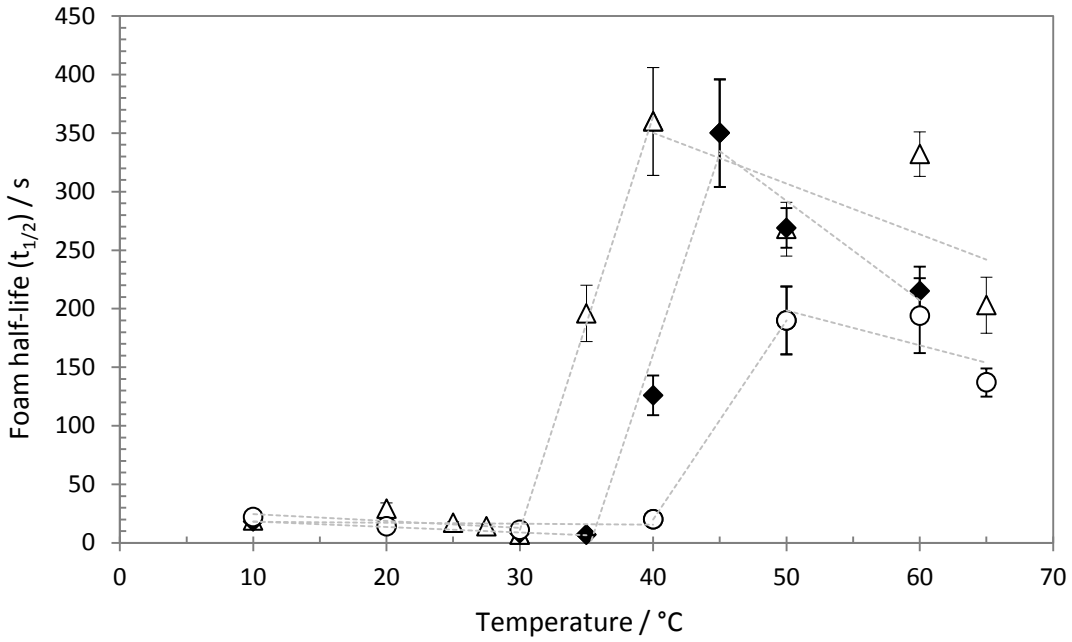

Figure 5.7; Stability of the air-in-water foam stabilised by Pluronic PE6400 as a function of temperature at various surfactant concentrations; 0.1% (w/v) (circles), 1% (w/v) (diamonds), 5% (w/v) (triangles), flow rate 0.08L/min, 0.8bar. The stability of the foam is quantified in terms of the foam half-life, $t_{1/2}$ as described in the experimental section. Dotted lines act as a guide to the eye.

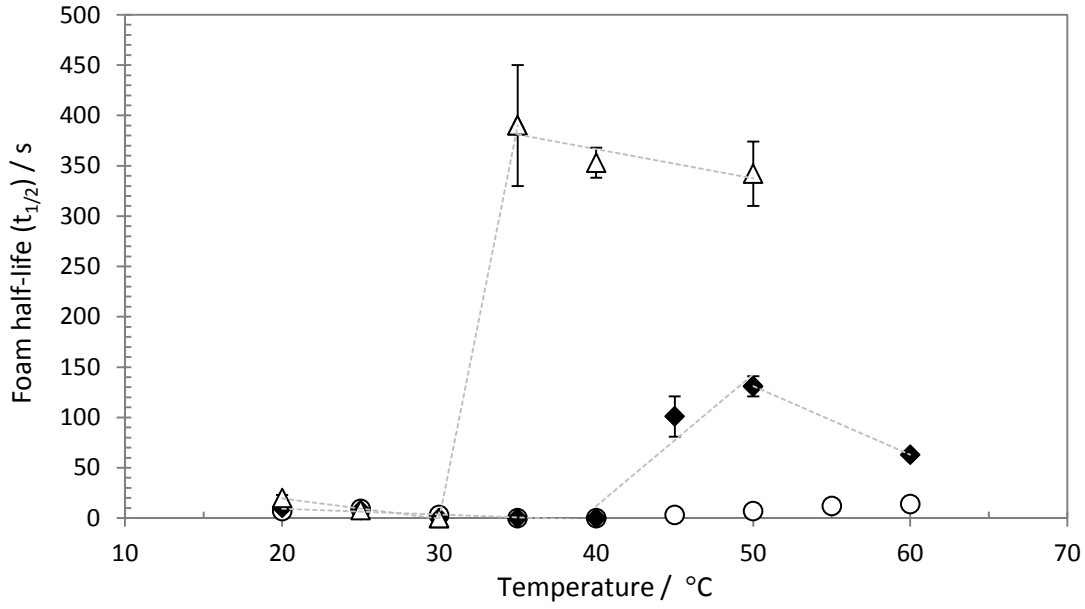

Figure 5.8; Stability of the air-in-water foam stabilised by Pluronic L62 as a function of temperature at various surfactant concentrations; 0.1% (w/v) (circles), 1% (w/v) (diamonds), 5% (w/v) (triangles), flow rate 0.08L/min, 0.8bar. The stability of the foam is quantified in terms of the foam half-life, $t_{1/2}$ as described in the experimental section. Dotted lines act as a guide to the eye.

Similar trends in foam lifetime as a function of concentration and temperature are observed for L62 (Figure 5.8) and PE6800 (Figure 5.9). In comparison to PE6400, the breakpoint and increase in foam lifetime for 5%(w/v) concentration L62 occurs across a narrower temperature range of approximately 30-35°C. Consultation of the HLB values[6] for both surfactants indicates that L62 (HLB=1-7) is more hydrophobic than PE6400 (HLB=12-18) due to the fact that it has a smaller PEO block size. Therefore L62 is expected to exhibit a stronger driving force for micellisation at a lower temperature and the formation of micelles occurs across a smaller temperature range as seen in the foam stability plots. Again, study of the temperature versus equilibrium surface tension plot indicates the CMT occurs at 30°C for L62 (at 5% (w/v)) as indicated by the break-point in surface tension (Appendix 1). As the concentration decreases, the temperature at which the breakpoint occurs increases corresponding to the sharp increase in foam increase. This confirms the conclusion that the onset of a sharp increase in foam stability corresponds to the formation of micelles within the bubble walls. Interestingly, for PE6800 (Figure 5.9) the increase in stability occurs across a much wider temperature range compared to the lower molecular weight surfactants L62 and PE6400. PE6800 is the largest, most hydrophilic surfactant of this series and the foaming behaviour perhaps suggests that the polydispersity of this surfactant is greater.

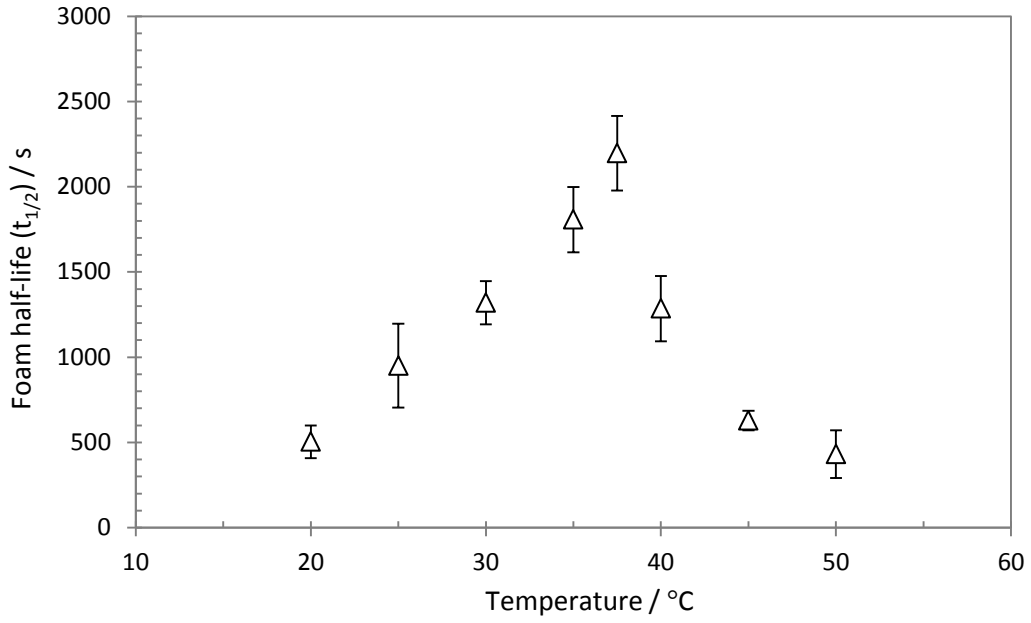

Figure 5.9; Stability of the air-in-water foam stabilised by Pluronic PE6800 as a function of temperature at 5% (w/v) surfactant concentration, flow rate 0.08L/min, 0.8bar. The stability of the foam is quantified in terms of the foam half-life, $t_{1/2}$ as described in the experimental section.

5.5. Small-angle neutron scattering

The findings from small-angle neutron scattering experiments used to investigate the nature of the adsorbed surfactant layer in aqueous PEO-PPO-PEO stabilised foams are presented in Chapter 4 and include analysis of surfactant structure and concentration. It was shown that scattering from an air-in-water foam stabilised with Pluronic surfactants is characterised by various features in the data; a Q^{-4} dependency at lower Q, characteristic of a smooth sharp interface, high Q scattering consistent with the polymer in solution situated within the lamellae walls and regular repeating inflexions characteristic of a layered structure at the interface. A model based on surfactant rich layers at the interface was found to best fit the data, and the layer thickness, L showed pronounced variation with surfactant structure. Here, small-angle neutron scattering experiments have been extended to study the effects of temperature on the interfacial structure of such foams.

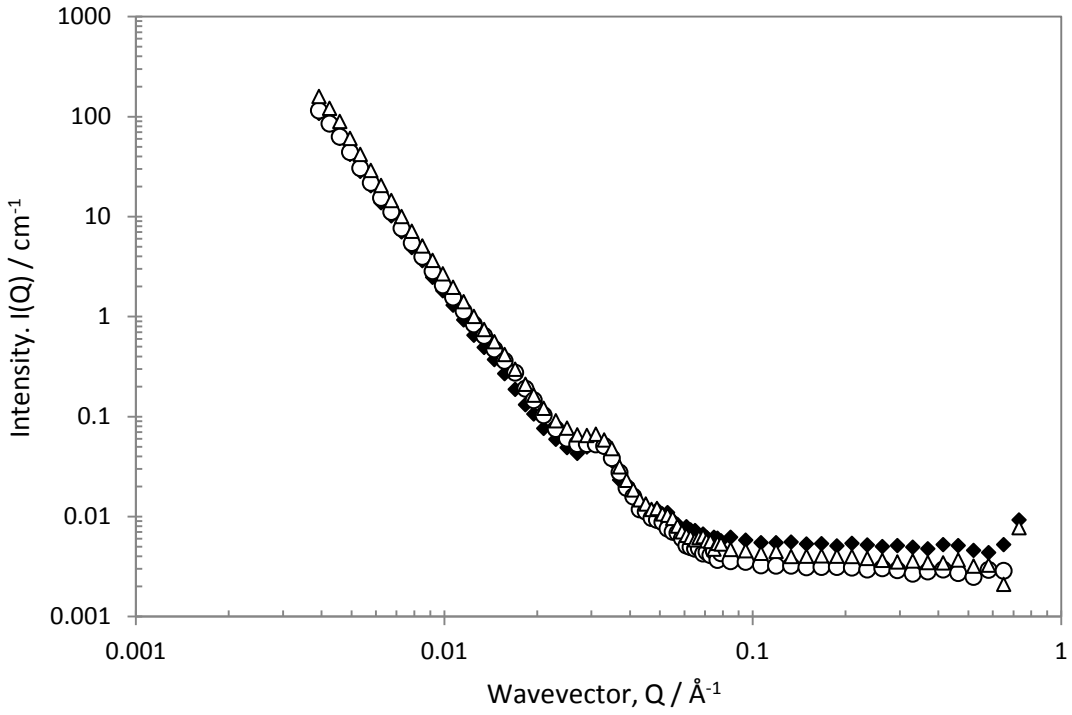

Figure 5.10; Small-angle neutron scattering from the air-in-water foams stabilised with polymeric surfactant PE6400 at various temperatures; 20°C (diamonds), 30°C (circles), 40°C (triangles). [Pluronic] = 0.05% (w/v)

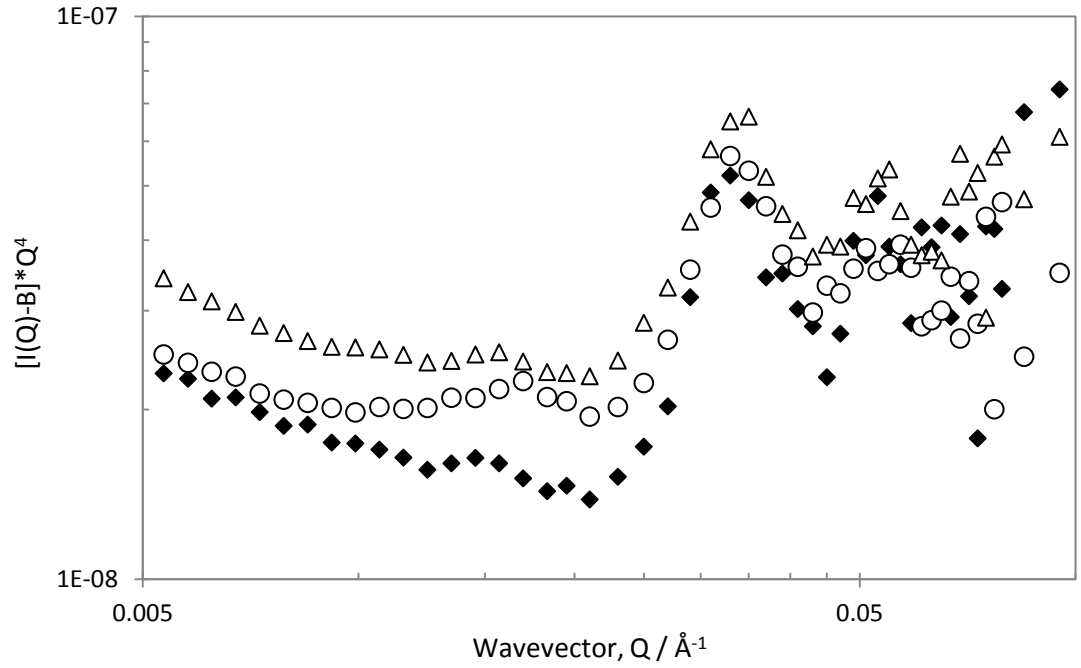

Figure 5.11; Porod plot of small-angle neutron scattering from the air-in-water foams stabilised by polymeric surfactant PE6400 at various temperatures; 20°C (diamonds), 30°C (circles), 40°C (diamonds). [Pluronic] = 0.05% (w/v).

Figure 5.10 shows the scattering from air-in-water foams stabilised with polymeric surfactant PE6400 at 0.05% (w/v) and various temperatures. As temperature is increased, the appearance of the scattering remains remarkably the same with the Porod plot in Figure 5.11 highlighting that the Q position of the inflexions do not change with temperature. Fits of the polycrystalline stack model to the data at 20 and 40°C are presented in Figure 5.12 and important parameters described in Figure 5.13. It can be seen that the fitting parameters do not vary at all within the error of the data indicating that at this concentration and temperature regime at least, the adsorbed layer structure is not affected by temperature.

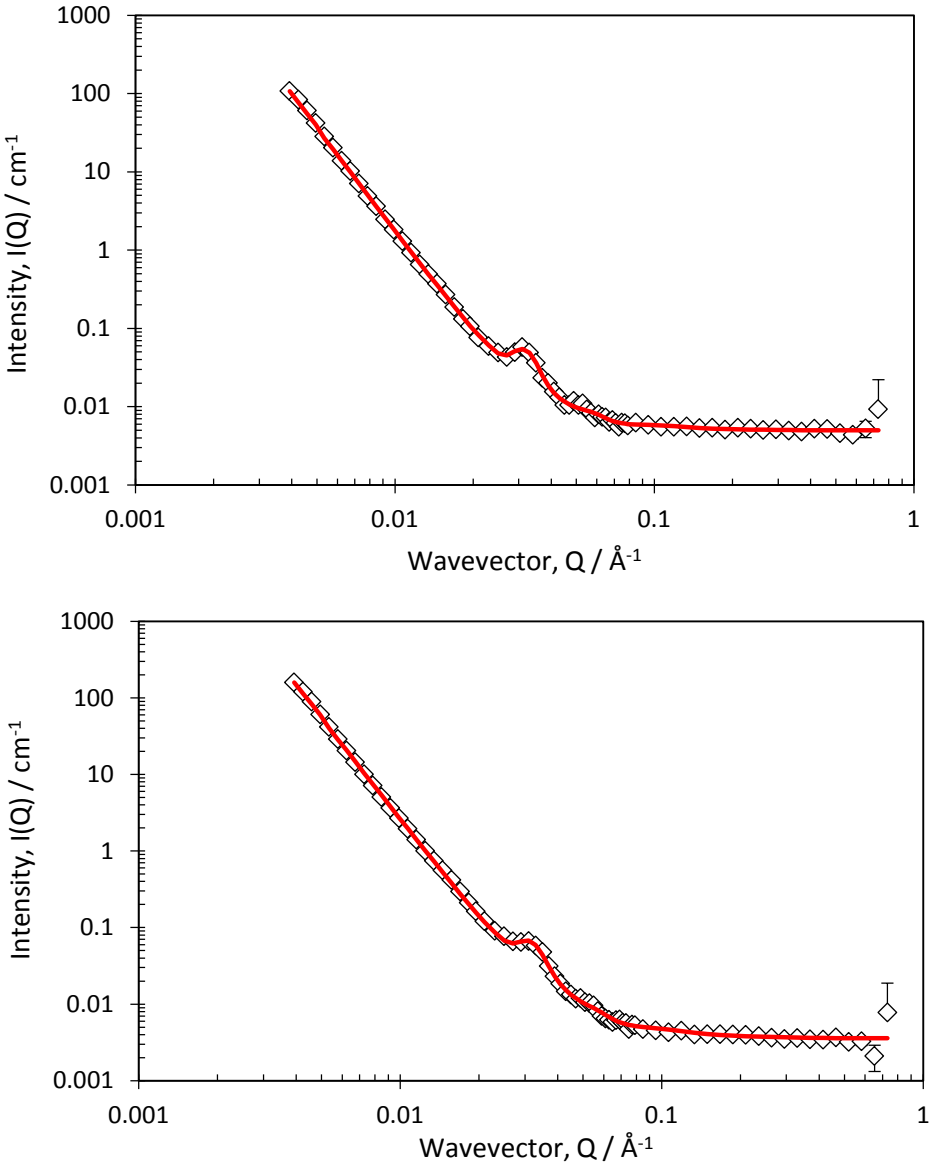

Figure 5.12; Small-angle neutron scattering from foam stabilised by 0.05% (w/v) PE6400 at 20°C (top) and 40°C (bottom) and the fit to the paracrystalline stack model described in the Experimental section.

	Temp / °C	L / Å (±10)	M	D / Å (±10)
L62	20	90	5	195
L62	40	100	5	195
PE6400	20	90	5	195
PE6400	30	90	5	190
PE6400	40	95	5	195

Figure 5.13; Fit parameters to the scattering from Pluronic stabilised air-in-water foams at varying temperature, [Pluronic]=0.05% (w/v).

The critical micellisation temperature for PE6400 at 0.05% (w/v) is 42°C [21] and thus the phase boundary from molecules to micelles in solution is not crossed over the temperature range studied here. In a neutron reflectivity study of Pluronic block copolymers at the air-water interface it was shown that below the CMC whilst the surface coverage of surfactant at the interface increases with increasing temperature the adsorbed layer thickness hardly changes.[22] Therefore it can be concluded that when the surfactant is far from a phase change no effect on the structure of surfactant at the interface is observed.

Figure 5.14 shows foam stabilised with PE6400 at 5% (w/v) and it can now be seen that temperature clearly has an effect on the foam scattering. At 20°C the characteristic inflexion at Q~0.035Å^{-1} is present however when the temperature is increased to 40°C this inflexion broadens over a much wider Q range (approximately 0.01-0.1Å^{-1}). As already noted, aqueous solution scattering of PE6400 in water (Appendix 1) shows a transition from molecules to micelles in solution at approximately 30-35°C, with scattering from well-defined micelles visible at 40°C. Therefore, this smearing effect has been attributed to the formation of micelles in solution. By arbitrarily scaling the scattering intensity to match the incoherent background of both PE6400 foam scattering and solution scattering at 40°C (Figure 5.15), it is evident that micelles within the bubble lamellae contribute significantly to the scattering and it is this which dominates the more subtle scattering of the layered surfactant structure within the foam at the interface.

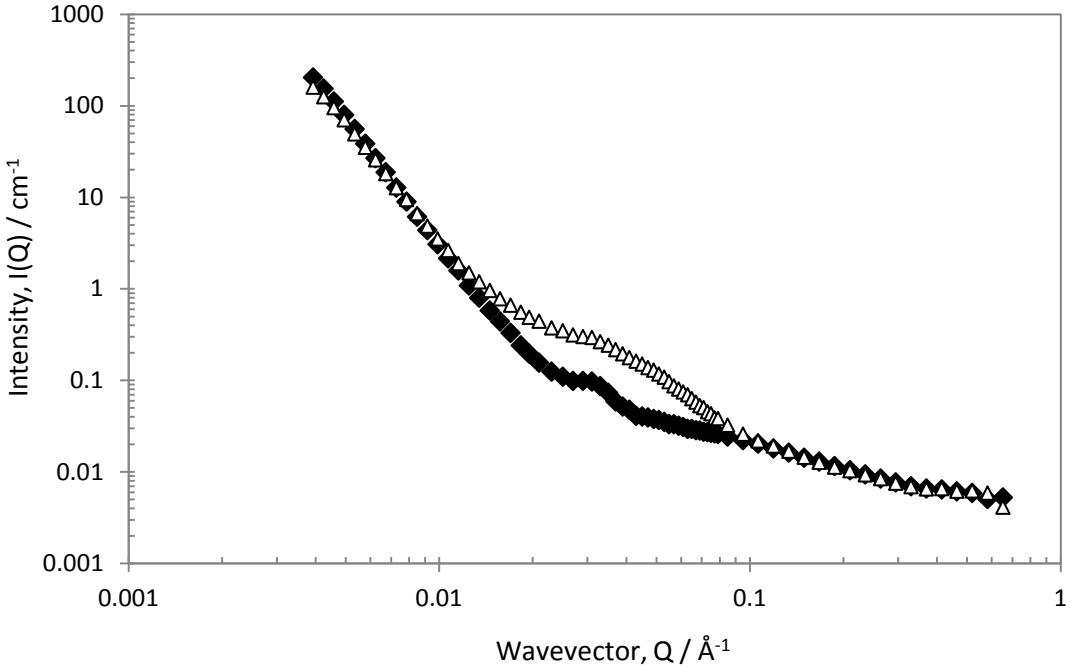

Figure 5.14; Small-angle neutron scattering from the air-in-water foams stabilised with polymeric surfactant PE6400 at various temperatures; 20°C (diamonds), 40°C (triangles). [Pluronic] = 5% (w/v). Intensity arbitrarily scaled for comparison.

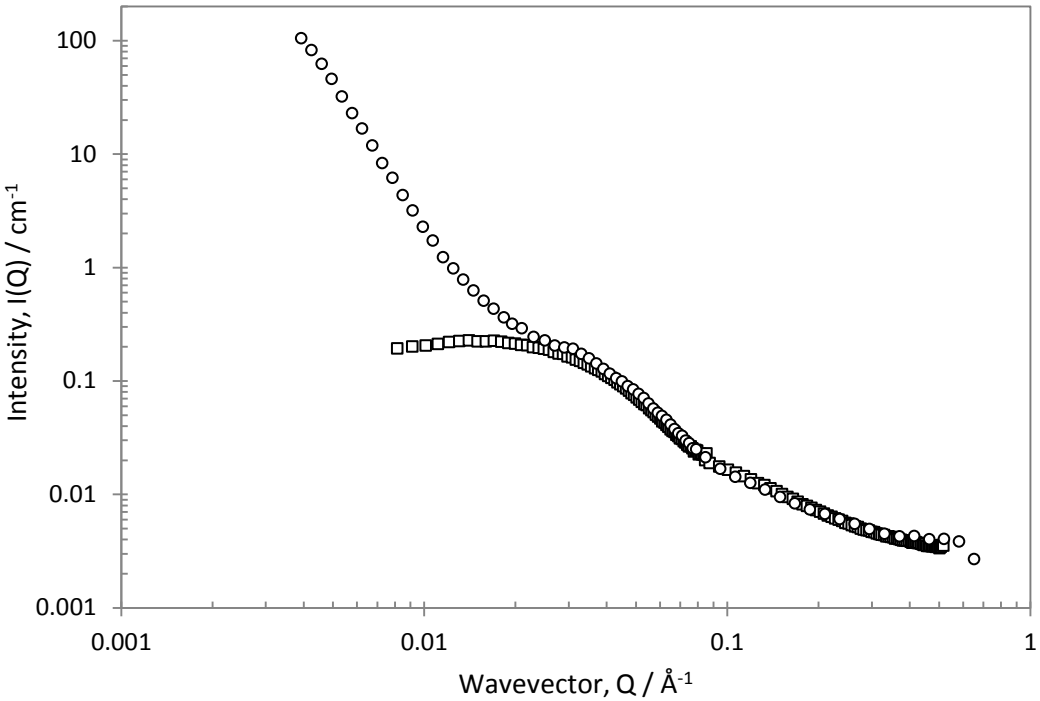

Figure 5.15; Small-angle neutron scattering from the air-in-water stabilised foam (circles) and a simple aqueous solution (squares) for polymeric surfactant PE6400 at 40°C. [Pluronic] = 5% (w/v). Intensity arbitrarily scaled for comparison.

A similar reasoning is applied to L62 stabilised air-in-water foam (Figure 5.16, Figure 5.17) with important parameters described in Figure 5.13. The phase transition from molecules to micelles is beautifully defined with a gradual broadening of the inflexion at 0.03Å until at 32°C scattering reminiscent of micelles in solution is seen. This is also the same for PE6800, in which the CMT is higher (40°C)[21] and the smearing of the inflexion at 0.035Å is just visible.

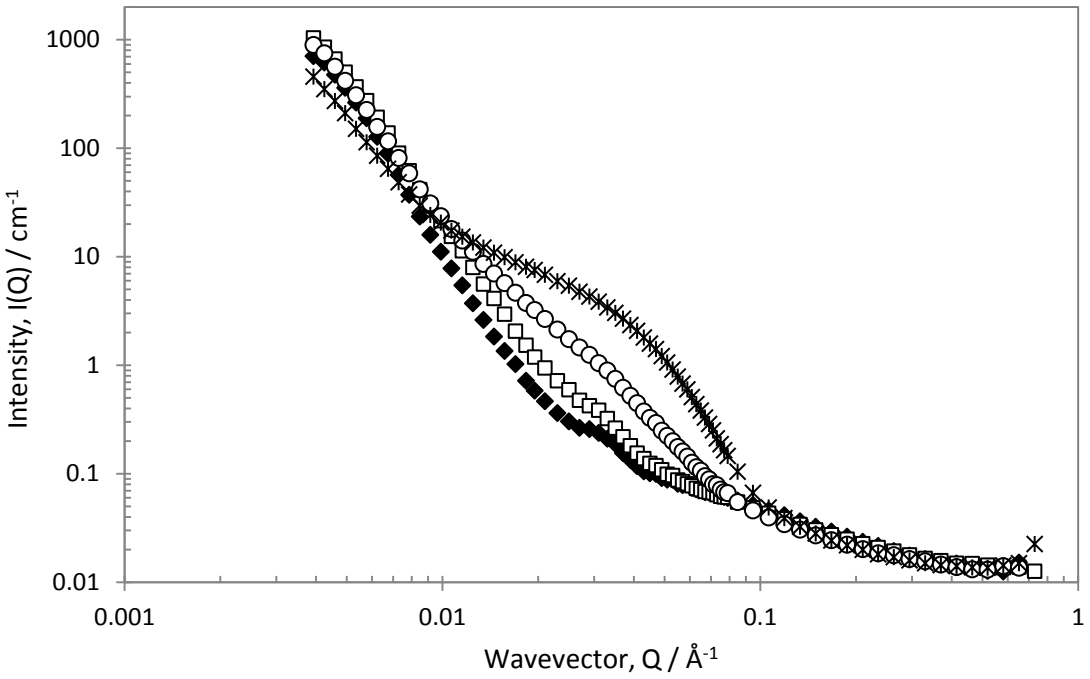

Figure 5.16; Small-angle neutron scattering from the air-in-water foams stabilised with polymeric surfactant L62 at various temperatures; 20°C (diamonds), 25°C (squares), 30°C (circles), 32°C (crosses). [Pluronic] = 5% (w/v). Intensity arbitrarily scaled for comparison.

Thus, using small-angle neutron scattering to study the structure of aqueous foams is most valuable when the surfactant is below its CMT or critical micelle concentration (CMC). When micelles are present in solution, scattering is dominated by micellar features, in particular the micelle structure factor (Q≈0.03Å) and this masks the fine features in the scattering attributed to the foam structure (the inflexion at Q≈0.035Å). Therefore it is not possible to elucidate the adsorbed layer structure or define parameters such as layer thickness. However, scattering clearly demonstrates the phase changes that occur within the system and indicate that micelles are indeed present within the bulk solution of the bubble lamellae walls.

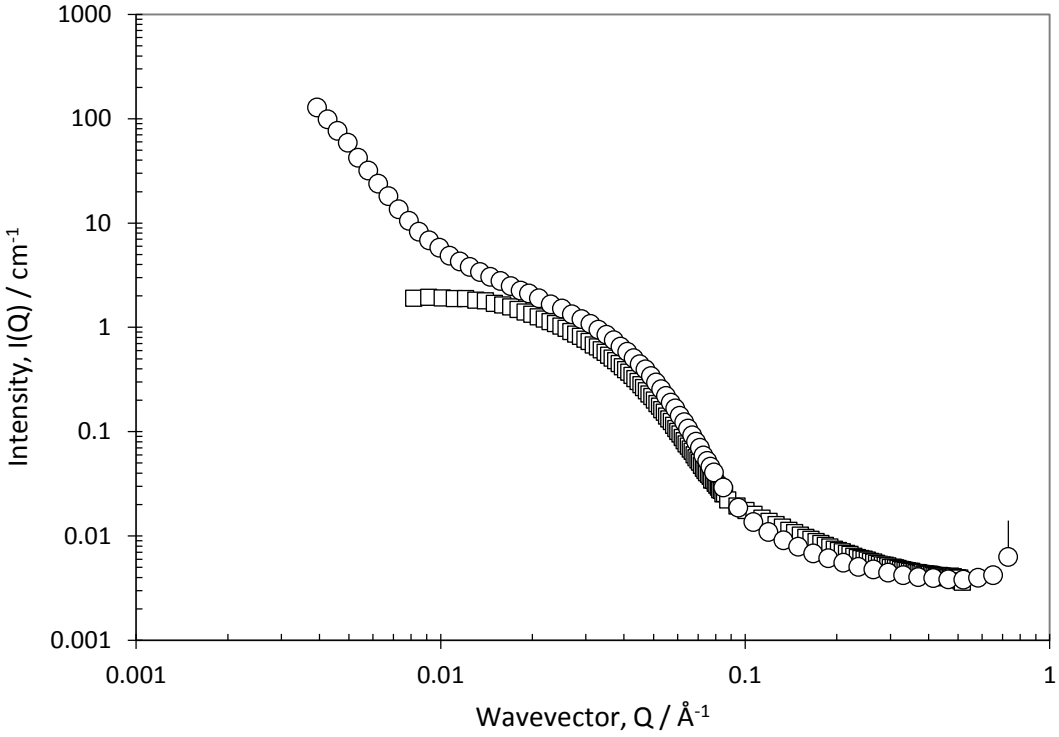

Figure 5.17; Small-angle neutron scattering from the air-in-water stabilised foam (circles) and a simple aqueous solution (squares) for polymeric surfactant L62 at 35°C. [Pluronic] = 5% (w/v). Intensity arbitrarily scaled for comparison.

5.6. Conclusion

The foaming behaviour of a variety of PEO-PPO-PEO surfactants has been characterised as a function of temperature and both foaming ability and stability were found to be highly influenced by the phase of the surfactant. A sharp increase in maximum foam volume and foam lifetime is observed upon crossing the CMT for each surfactant with maximum foaming behaviour assigned to the formation of well-defined micelles in solution. This corresponded to the point at which maximum reduction in surface tension was observed. The study has demonstrated how important it is to quote the exact position from the CMT when defining foaming behaviour as foaming properties were shown to substantially worsen as the micelles became more stable (i.e. upon further increasing temperature). SANS studies of foams below the CMT, indicated that adsorbed layer thickness was not affected by an increase in temperature across the range of 20-40°C studied. For those foams in which the phase boundary was crossed, SANS was dominated by micellar scattering which obscured the fine features relating to the adsorbed layer. Thus the technique is most suitable for probing foams in which the bulk surfactant solution is below its CMT/CMT. The findings here will be discussed in relation to PU foaming in Chapter 6 with particular emphasis on whether the phase of the surfactant throughout the curing process influences foam structure and properties.

5.7. References

1. C. Morrison, L. L. Schramm and E. N. Stasiuk, *Journal of Petroleum Science and Engineering*, 1996, **15**, 91-100.

2. D. T. Wasan, A. D. Nikolov, P. A. Kralchevsky and I. B. Ivanov, *Colloids and Surfaces*, 1992, **67**, 139-145.

3. A. BonfillonColin and D. Langevin, *Langmuir*, 1997, **13**, 599-601.

4. K. Oetjen, C. Bilke-Krause, M. Madani and T. Willers, *Colloids and Surfaces A: Physicochemical and Engineering Aspects*.

5. I. Goldmints, J. F. Holzwarth, K. A. Smith and T. A. Hatton, *Langmuir*, 1997, **13**, 6130-6134.

6. P. Alexandridis and T. A. Hatton, *Colloids and Surfaces A: Physicochemical and Engineering Aspects*, 1995, **96**, 1-46.

7. R. Kjellander and E. Florin, *Journal of the Chemical Society-Faraday Transactions I*, 1981, **77**, 2053-2077.

8. G. Karlstrom, *Journal of Physical Chemistry*, 1985, **89**, 4962-4964.

9. P. Linse, *Journal of Physical Chemistry*, 1993, **97**, 13896-13902.

10. K. Mortensen, *Journal of Physics-Condensed Matter*, 1996, **8**, A103-A124.

11. D. Attwood, J. H. Collett and C. J. Tait, *International Journal of Pharmaceutics*, 1985, **26**, 25-33.

12. P. R. Desai, N. J. Jain and P. Bahadur, *Colloids and Surfaces a-Physicochemical and Engineering Aspects*, 2002, **197**, 19-26.

13. X. Zhou, X. Wu, H. Wang, C. Liu and Z. Zhu, *Physical Review E*, 2011, **83**, 041801.

14. V. Bergeron and C. J. Radke, *Colloid and Polymer Science*, 1995, **273**, 165-174.

15. Z.-L. Chen, Y.-L. Yan and X.-B. Huang, *Colloids and Surfaces A: Physicochemical and Engineering Aspects*, 2008, **331**, 239-244.

16. R. J. Pugh, *Advances in Colloid and Interface Science*, 1996, **64**, 67-142.

17. D. O. Shah, N. F. Djabbarah and D. T. Wasan, *Colloid and Polymer Science*, 1978, **256**, 1002-1008.

18. H. Fruhner, K. D. Wantke and K. Lunkenheimer, *Colloids and Surfaces A: Physicochemical and Engineering Aspects*, 2000, **162**, 193-202.

19. P. Bahadur and K. Pandya, *Langmuir*, 1992, **8**, 2666-2670.

20. J. v. Duijneveldt, *Colloid Science; principles, methods and applications.* , Wiley, Sussex, UK, 2010.

21. P. Alexandridis, J. F. Holzwarth and T. A. Hatton, *Macromolecules*, 1994, **27**, 2414-2425.

22. J. B. Vieira, Z. X. Li, R. K. Thomas and J. Penfold, *Journal of Physical Chemistry B*, 2002, **106**, 10641-10648.

6. The role of PEO-PPO-PEO surfactant in the formation of hydrophilic polyurethane foam

6.1. Abstract

The study of polyurethane foams is experimentally challenging due to the complex nature of the reaction scheme and processing conditions. Polyurethane (PU) foam has been manufactured on an industrial manufacturing line and the effect of different poly(ethylene oxide)-poly(propylene oxide)-poly(ethylene oxide) surfactant additions studied. Correlations were made to foaming behaviour and surface tensions in aqueous solution. Good PU foam fluid absorption was associated with smaller cell size and it was typically the smaller molecular weight, most hydrophobic surfactants which showed the greatest reduction in surface tension that produced these foams. There was no obvious correlation between surfactant foamability and foam stability in aqueous solution. Concentration studies allowed the molecular-micellar phase boundary to be crossed for a series of surfactants and the phase of the surfactant had no apparent effect on the structure of the foam. Results suggest that it is the absolute reduction in surface tension that the surfactant can obtain that is the most important parameter in defining foam structure.

6.2. Introduction

The physical properties of flexible hydrophilic polyurethane (PU) foams such as cell size and degree of cell opening strongly affect their performance as wound dressings. For example, high fluid absorption, low wicking times (i.e. how quickly the liquid wets the surface of the foam) and high fluid retention are desirable for PU foams in the treatment of chronic wounds. Such properties are believed to be influenced in part by the surfactant adsorption at the interface throughout the foam forming process.

PU foams, stabilised with PEO-PPO-PEO surfactants, have been manufactured on an industrial manufacturing line and. The surfactant structure and concentration has been varied to probe such effects on foam structure. Foaming behaviour (Chapter 3), the effect of temperature (Chapter 5) and the structure of the adsorbed surfactant layer (Chapter 4) in model air-in-water foams have been characterised for a variety of PEO-PPO-PEO surfactants. The physical properties of the PU foam are correlated to aqueous

foam behaviour in an attempt to understand the surfactant properties which produce desirable PU foam structure and properties.

6.3. PU foam structure

Illustrative microscope images of representative PU foams are presented in Figure 6.1. Foams were prepared with 2wt% surfactant concentration allowing the effects of surfactant structure and phase behaviour to be clearly observed.[1] It can clearly be seen that altering the surfactant has a significant effect on the structure of the foam. Those foams which exhibit smaller cell sizes typically appear more uniform in nature and, with regards to texture feel "softer" and are more conformable (Figure 6.1c and d). Such properties are highly desirable for foams used in contact with the skin. Those foams with larger cell structures are highly non-uniform in structure with large distorted cell structures (Figure 6.1a) which from a commercial perspective is not aesthetically pleasing.

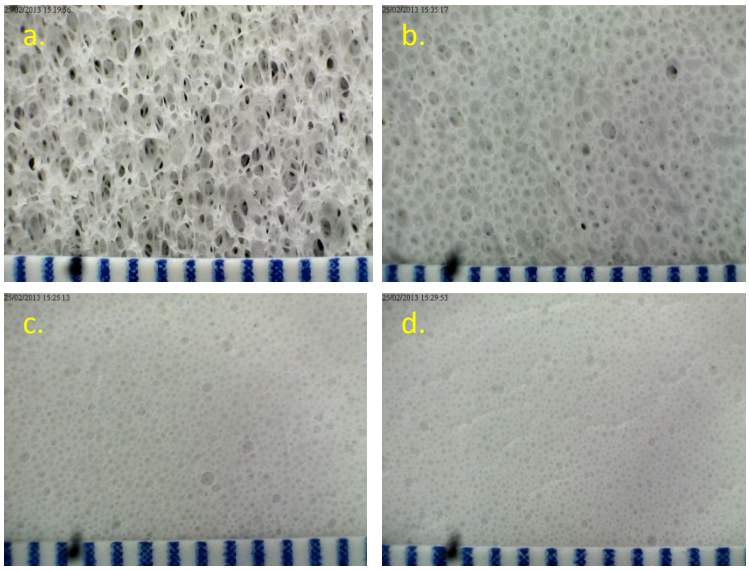

Figure 6.1; Microscope images of PU foam prepared with; a. PE6800, b.F108, c.L62, d.PE6400. [Pluronic = 2wt%].Each blue increment on the scale bar defines 1mm.

The structure of polyurethane foams prepared with various Pluronic surfactants have been probed in a more quantitative manner using optical microscopy to elucidate cell size and cell count within a given area of foam (8x8mm) allowing thee volume fraction of air in the foam to be estimated (Figure 6.2).

Surfactant	Average cell size / mm	Bubble count (± 20%)	Volume fraction of air (± 20%)
L62	0.6	770	25
PE6400	0.4	1040	12
P84	0.4	840	30
P103	1	340	28
P123	0.6	510	17
P104	1.8	150	44
PE6800	2.1	100	36
F108	1.4	250	40

Figure 6.2; Average cell size and bubble count within 1cm^2 of polyurethane foam prepared with various PEO-PPO-PEO surfactants.

Figure 6.3 compares the average cell size to cell count within a given area for the various Pluronic stabilised PU foams produced. Smaller cell size is inevitably linked to more cells per unit area of foam which follows a typical exponential decay. Some caution should be employed with regards to the PE6800 foam (denoted by *) as the cell structure was highly irregular and broken which made it difficult to accurately record cell size and bubble count, however the cells that could be observed were typically larger and fewer in number.

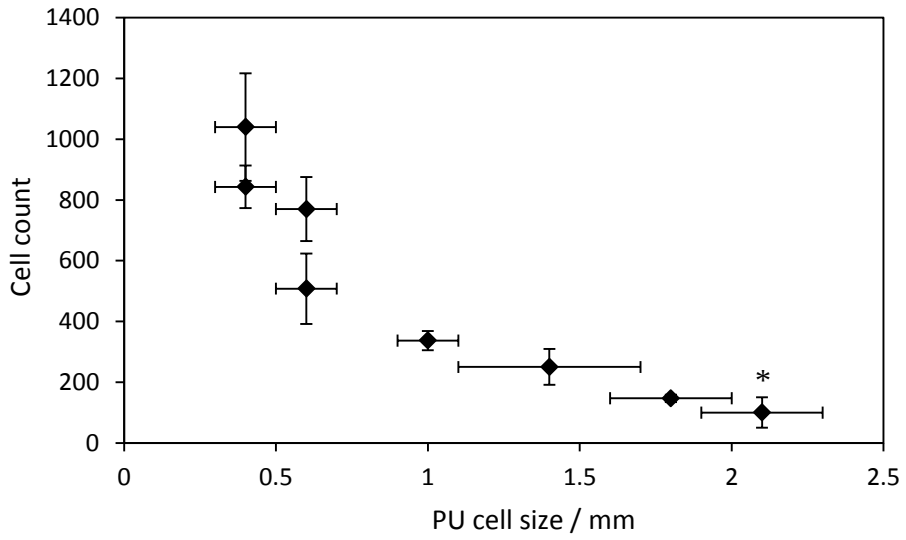

Figure 6.3; Cell count as a function of polyurethane foam cell size for foams stabilised with different PEO-PPO-PEO surfactants.

Based on the average cell size and cell count within a given area, the volume fraction of air in the PU foam can be estimated (Figure 6.4). The calculation is based on a number of assumptions and therefore should only be used for indicative purposes;

i. all the cells are treated as spherical when in reality a range of distorted oval shapes are typically observed,
ii. it is assumed that the cell distribution is uniform throughout the foam based on what is observed at the surface,
iii. all spherical cells are evenly packed.

Nonetheless, such a calculation should give insight into how the foam structure varies with surfactant structure.

Average cell size versus volume fraction of air is presented in Figure 6.4 and it can be seen that with the exception of the data point at 2.1mm cell size (corresponding to PE6800), a fairly linear relationship is observed. The anomalous data point for PE6800 arises from the reasons mentioned above (irregular and broken cell structure). Smaller cell size is associated with a smaller volume fraction of air in the foam.

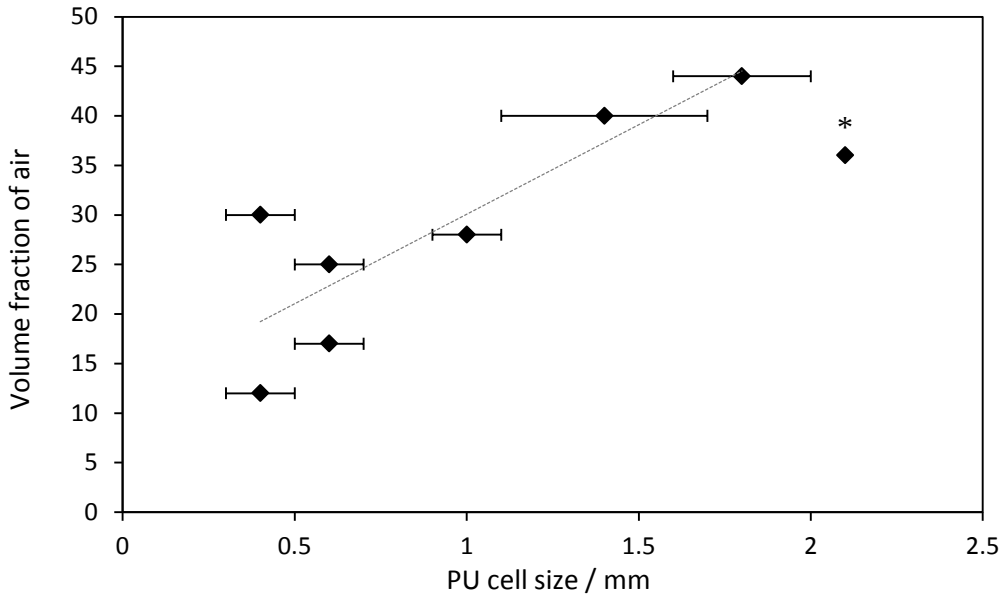

Figure 6.4; The relationship between PU foam cell size and volume fraction of air within the foam. Dotted line is a guide to the eye.

Surfactant	Density (kg/m^3)	Absorption (g/g)	Wicking (s)
L62	116	25.4	3
PE6400	119	25.7	8
P84	114	16.3	3
P103	103	16.9	2
P123	120	18.4	11
P104	104	8.6	5
PE6800	131	8.7	11
F108	132	10.2	9

Figure 6.5; Physical properties of polyurethane foam prepared with various Pluronic surfactants. [Pluronic]=2%(w/v).

6.4. PU foam properties

Figure 6.5 shows the fluid handling properties of PU foams prepared with various Pluronic surfactants at a concentration of 2%(w/v). Such properties are measured immediately after foam formation. Perhaps one of the most important properties of PU foam utilised for wound care materials is its ability to absorb fluid, thus maintaining a moist wound environment to promote healing. The relationship between fluid absorption and average cell size is presented in Figure 6.6.

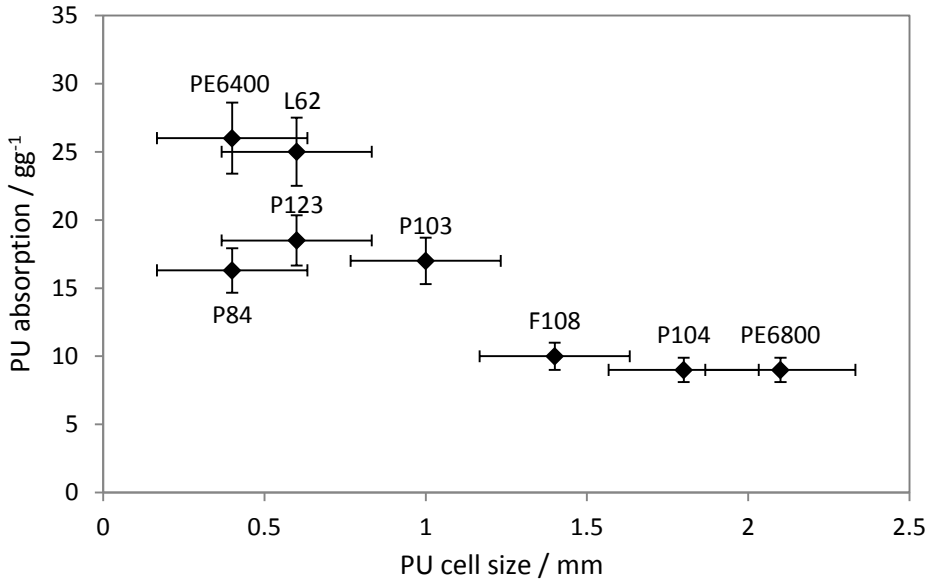

Figure 6.6; PU foam cell size as a function of water absorption for foams prepared with various Pluronic surfactants. [Pluronic]=2%(w/v).

PU foam absorption decays with increasing cell size indicating that the absorption properties of such foams are highly dependent on the structure of the foam itself. Based on the error bars of the data it is not possible to determine the absolute trend in the data (exponential / plateau) however absorption is at a maximum for the smallest cell sizes signifying that those surfactants which produce small cells are necessary to produce PU foams with absorption properties desirable for wound care materials. Referring to Figure 6.4, smaller cell size was associated with lower volume fraction of air in the foam. Typically a minimum absorption specification of $12gg^{-1}$ is specified for PU foams used as wound dressings. Thus, based on the data in Figure 6.4 and Figure 6.6 the average cell size within such systems stabilised with Pluronic surfactants cannot be larger than approximately 1mm diameter and the maximum volume fraction of air should be approximately 30%, otherwise absorption properties will be unsatisfactory.

The absorption measurement recorded here represents in reality a net balance of the ability of the foam to absorb fluid as well as retain it. The fact that greater absorption is observed for smaller cell sizes suggests that smaller cells are better at retaining the fluid they absorb (i.e. it doesn't immediately drain from the foam after removal from the liquid). As all of the foams absorb fluid to some degree, this indicates that the cells are not just isolated entities within the structure but create an interconnecting network through which liquid can pass.

There are a number of forces which influence the retention and drainage of liquid from a porous structure; gravity, surface tension and adhesion.[2] Gravity is the main driving force for drainage of water from foam whilst surface tension and adhesion resist such movement of liquid. However, this is highly dependent on the size of the cells within the foam. When the cells are small, the adhesion interaction between water and polyurethane will be greater as a larger proportion of water molecules are in contact with the solid surface (Figure 6.7). Thus, the retention of fluid within the foam will be higher. In addition, surface tension effects are important in the form of capillarity; the action in which a fluid is drawn up in small pore spaces. Capillary action occurs when the adhesive interactions between the solid foam and water are stronger than the cohesive interactions between the water molecules themselves. This is only possible if the water can wet the solid foam. Smaller pores within the foam exhibit greater capillary action. Furthermore, at the interface between water and air, due to surface tension a meniscus forms. Smaller interfacial area leads to more curved menisci. As gravity pulls

liquid from the foam cell, the menisci is stretched and bent creating further curvature which subsequently strengthens the menisci. More force is then required to further remove water from the cell. Thus both adhesion and surface tension effects are greater for smaller cell sizes explaining the better water absorption properties observed for those foams with smaller cell sizes.

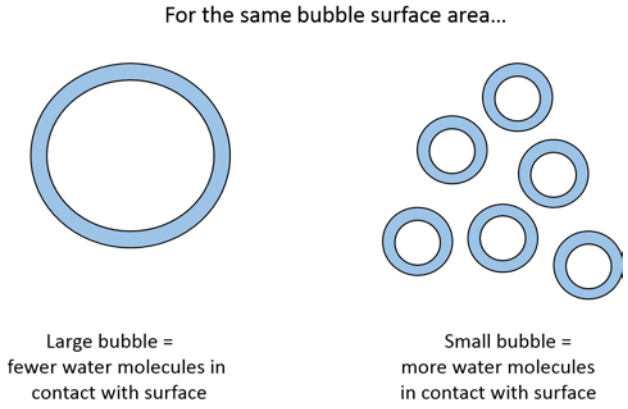

Figure 6.7; Cartoon to demonstrate how the number of water molecules in contact with the bubble interface varies depending on bubble size.

Plotting cell size as a function of cell size divided by absorption yields a linear relationship as shown in Figure 6.8. It is worth noting that PU foam prepared in the absence of surfactant displays satisfactory fluid absorption properties indicating that components within the commercial pre-polymer mix must also have some degree of surface activity.

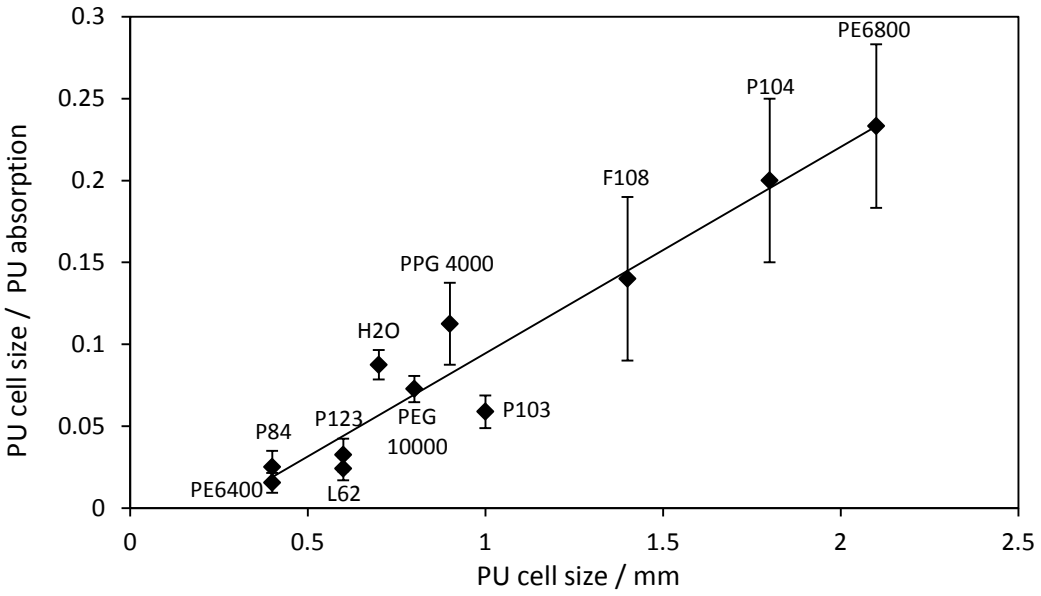

Figure 6.8;PU cell size as a function of cell size divided by absorption. [Surfactant]=2%(w/v).

6.5. Comparison to surfactant structure

Figure 6.9 shows the water absorption of polyurethane foam as function of Pluronic molecular weight. Characteristically, a decrease in absorption with increasing molecular weight of surfactant is observed.

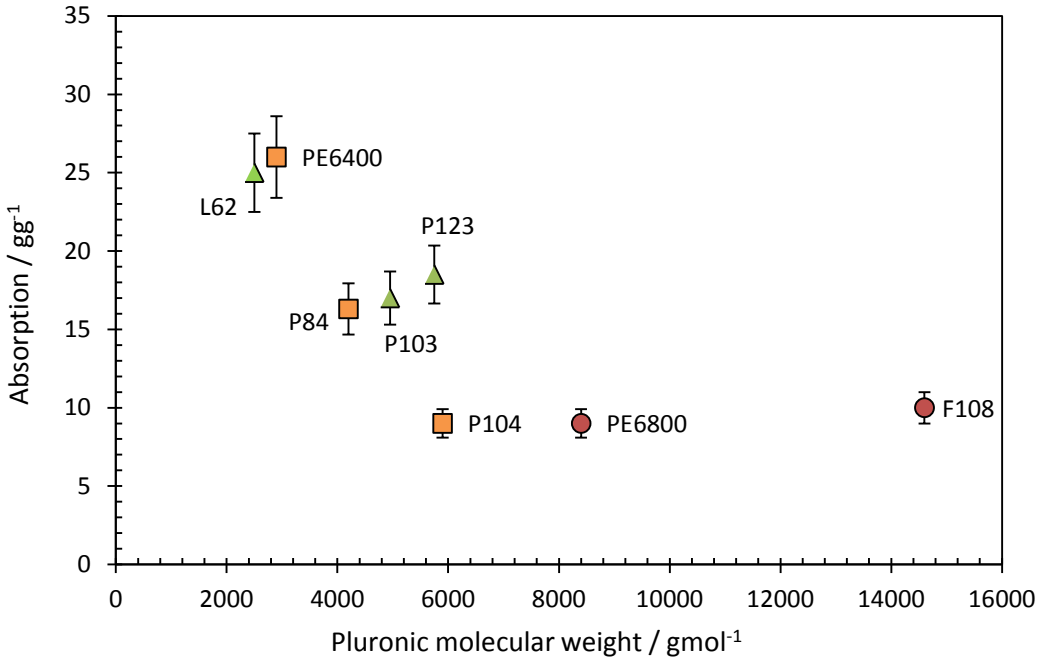

Figure 6.9; Polyurethane foam absorption for various molecular weight Pluronic surfactants. [Pluronic]=2%(w/v). HLB=1-12 (triangles), 12-18 (squares), >24 (circles).

It has already been shown in Section 6.4 that greater fluid absorption is associated with smaller cell size; from Figure 6.9 it can therefore be concluded that lower molecular weight surfactants produce smaller cells. One would expect that smaller surfactants diffuse to the interface more quickly[3] however the relative hydrophobicity of the surfactant also needs to be considered in order to understand the driving force for adsorption to the interface. The hydrophilic-lipophilic balance (HLB) categories that each surfactant occupy are also shown in Figure 6.9 indicated by the different shaped data points. Due to the high polydispersity observed for polymer surfactants of this type, HLB values are defined by a range rather than a specific value and so it is not possible to compare the data more fully. However based on the HLB groups it can be seen that typically PU fluid absorption increases with increasing hydrophobicity of the surfactant. The most hydrophilic surfactants (PE6800 and F108), which are also the highest molecular weight surfactants of those studied produce PU foam with the poorest fluid absorption properties. Hence, a combination of fast diffusion to the interface and a strong driving force for adsorption appear to be requirements of Pluronic surfactants used in PU foam manufacture. Based on the HLB ranges for each surfactant studied it is postulated that a HLB value of less than 12 is required for block copolymer of this series to produce PU foam with absorption properties within specification.

To probe further the effect of surfactant surface activity on the fluid handling properties of PU foam the phase of the surfactant during the reaction process needs to be considered. This requires an understanding of the temperature during the key part of the reaction in which the foam is formed, however this is highly non-trivial. Temperature gradients exist throughout the curing process; the cure tables are externally heated to various temperatures and the reaction itself is exothermic. Therefore it is impossible to define a specific temperature which is the most important during the foam forming process. However, previous literature suggests that the cream and rise times, in which the role of the surfactant is most important, take place within approximately 30 seconds of mixing.[4, 5] Temperature studies performed on the manufacturing line suggest that the phase boundary for all of the surfactants is crossed early on in the curing process. Therefore we estimate that all surfactants are very near to or above their CMT's when the foam structure begins to form.

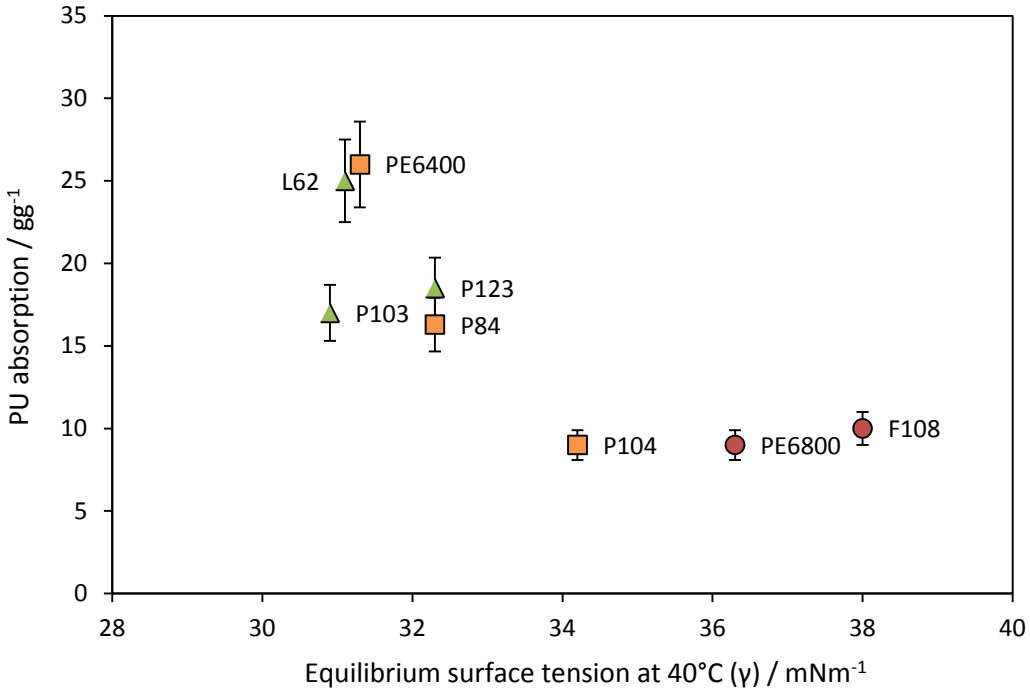

Figure 6.10; Polyurethane foam absorption for various molecular weight Pluronic surfactants [Pluronic]=2%(w/v) as a function of the equilibrium surface tension of the corresponding aqueous solution at 40°C. HLB=1-12 (triangles), 12-18 (squares), >24 (circles).

Equilibrium surface tension at 40°C as a function of PU absorption is presented in Figure 6.10. At 40°C all of the surfactants are above their critical micelle temperatures so the lowest surface tension values attainable are observed. In general, higher absorption values, and consequently smaller cell sizes, are associated with lower equilibrium surface tension. It has previously been shown by Zhang *et al*.[6] that those surfactants which exhibit the lowest surface tension values produce smaller cells as they are more efficient at reducing the bubble generation energy. Thus, from the data presented in Figure 6.10 for Pluronic surfactants it is estimated that equilibrium surface tension values should be approximately less than 32mNm^{-1} in order to produce foams with sufficient absorption properties. The reduction in surface tension must be significant to reduce the surface tension of the prepolymer mixture. Larger cells are produced for those surfactants with surface tension greater than 32mNm^{-1} suggesting that these surfactants cannot adequately stabilise the reaction process. Dynamic surface tension data presented in Chapter 3 indicated that across the bubble lifetime range measured (0.05-20s) PE6800 and F108 surfactants showed the greatest reduction in surface tension with time (dy/dt). However based on the properties of the PU foam it appears that the absolute reduction in surface tension from that of pure solvent is most

important for surfactants employed in PU systems rather than the rate at which the surface tension is decreased. The dynamic surface tension data is limited in that timescales lower than 0.05s cannot be probed with the instrument available so the significance of $d\gamma/dt$ at shorter timescales could not be determined.

6.6. Comparison to aqueous foaming behaviour

PU foam absorption is compared to foamability of the aqueous surfactant solutions in Figure 6.11. It was discussed in Section 6.5 that based on temperature investigations on the manufacturing line, all surfactants are above their CMT's early on in the reaction process. Thus, comparison to foamability values at approximately CMT+10°C is presented, as this compares the micellar phase of the surfactants whilst ensuring the surfactants are at a similar position on their phase diagram. Inevitably, an exact comparison of all the surfactants at a specified temperature is impossible as the surfactant passes across a substantial temperature range. Under these conditions, similar foam volumes are produced by the majority of the surfactants in the series so it is impossible to draw any quantitative conclusions. This may be a consequence of the insensitivity of the technique. Nonetheless, some qualitative conclusions can be drawn.

If we compare L62 and PE6800 (the extremes of hydrophobicity and hydrophilicity) it is L62, the most hydrophobic surfactant which exhibits the smaller foam volume and produces foam with better fluid handling properties. As already discussed, L62 and similar (e.g. PE6400), the most hydrophobic surfactants, show some of the greatest reductions in surface tension from that of pure water (Section 6.5) thus suggesting that it is the ability of the surfactant to reduce the surface tension rather than its overall foaming power which is most important in PU foam systems.

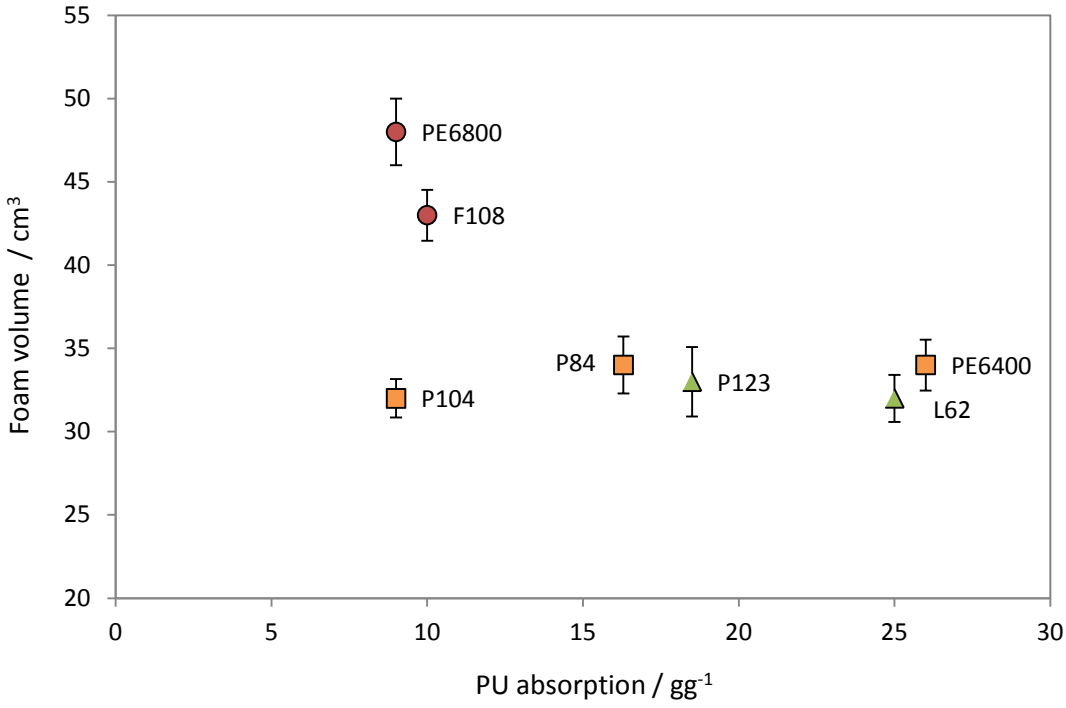

Figure 6.11; Polyurethane foam absorption for various molecular weight Pluronic surfactants [Pluronic]=2%(w/v) as a function of the foaming ability of the corresponding aqueous solution at CMT+10°C. HLB=1-12 (triangles), 12-18 (squares), >24 (circles).

In this study, foamability at a constant bulk solution concentration has been investigated. Due to the substantially different molecular weights of the surfactants this means the number of molecules present in solution will be different i.e. there will be more L62 molecules in solution that PE6800. Smaller molecular weight Pluronics adopt a smaller area per molecule at the interface so that more molecules will be required to stabilise a given area of interface for L62 than PE6800. Thus whilst the L62 molecules are the most hydrophobic and show the greatest reduction in surface tension, the overall amount of interface they can stabilise may be smaller than that of PE6800. In theory, at a comparable number of molecules in solution and comparable surfactant size the more hydrophobic surfactants would be expected to exhibit a larger foam volume due to their stronger driving force for adsorption. Furthermore, it is impossible to decouple foam stability effects which will be enhanced for higher bulk solution viscosity. As described in Chapter 3 the increased viscosity of PE6800 solution will promote foam stability which will inevitably result in a greater foam volume formed.

If we further consider the PU reaction in comparison to foaming in aqueous solution, the presence of the prepolymer dramatically increases the viscosity of the overall system

and the formation of the polyurethane network will likely create obstruction effects reducing the diffusion rate of the surfactant i.e. the surfactant will have to diffuse around the polyurethane network thus increasing the diffusion path length. For example, in a study of the diffusion of non-ionic linear poly(ethylene glycol) polymers at various molecular weights in mucin the diffusion coefficient decreased in the presence of mucin attributed to such obstruction effects.[7] The generally observed phenomenon of the diffusion coefficient decreasing with increasing molecular weight was also observed suggesting that here the smaller molecular weight Pluronic surfactants will exhibit faster diffusion to the interface in the polyurethane system.

Analysis of foam properties to aqueous foam stability showed no relationship across the whole series suggesting that the stability of the bubble itself is not a defining parameter in the structure of polyurethane foam. For example at 1%(w/v) concentration, L62 ($t_{1/2}$ = 14s) and P123 ($t_{1/2}$ = 5000s) show similar PU foam cell size and properties but very different aqueous foam stabilities.

6.7. Concentration studies

Three surfactants were down selected to study the effect of surfactant concentration on the structure and properties of the polyurethane foam (P123, L62 and PE6800). These surfactants were selected as they have low, intermediate and high CMC values. Concentration has been studied across a range from 0.001% to 2% inevitably meaning that phase boundaries will be crossed. As discussed in Section 6.5 it is difficult to identify a single temperature which is most important in the foam forming reaction. Furthermore, it is inevitable that the surfactant crosses a temperature range throughout the reaction process.

Figure 6.12 shows PU cell size as a function of PU fluid absorption for each of the surfactants at various concentrations. Focussing first on L62 it can be seen that smaller cell sizes are associated with increased fluid absorption (as per the discussion in Section 6.4) and that cell size decreases with increasing surfactant concentration. Increased surfactant concentration will result in a greater reduction in surface tension thus reducing the bubble generation energy and promoting interface formation.

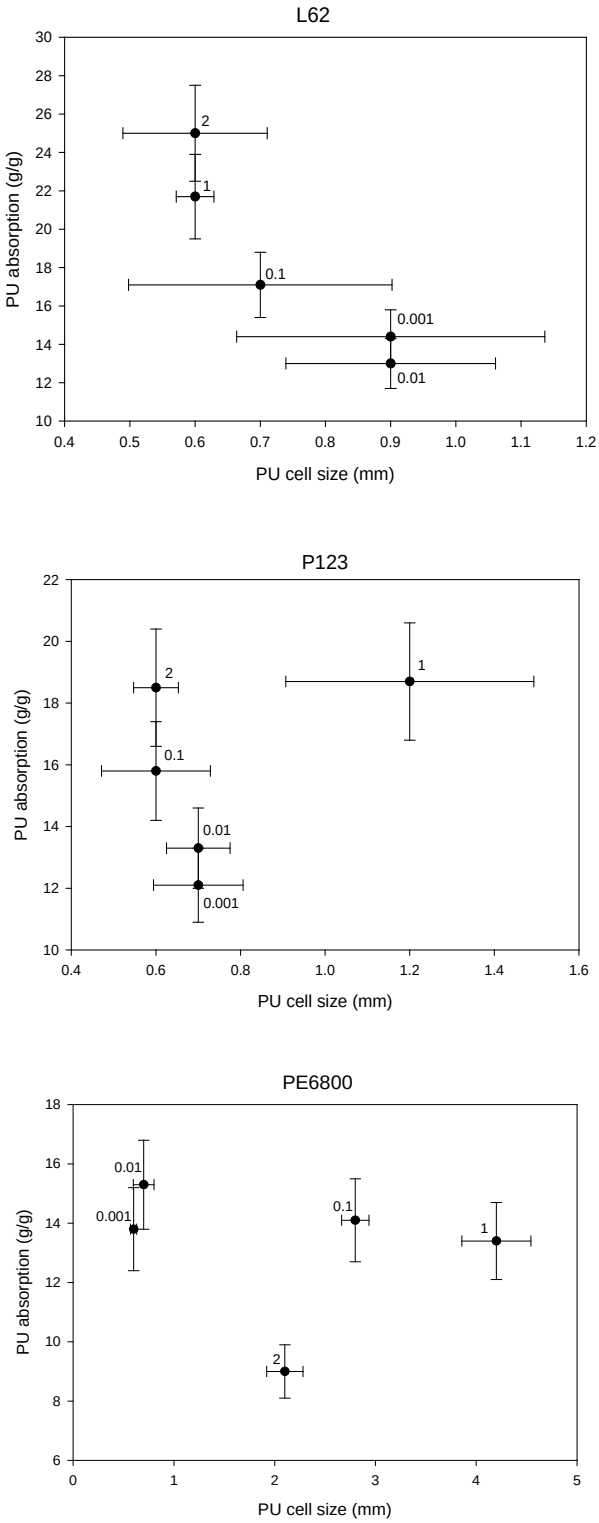

Figure 6.12; Cell size versus fluid absorption for polyurethane foams prepared with Pluronic surfactants L62 (top), P123 (middle) and PE6800 (bottom) at various surfactant concentrations (specified in the labels adjacent to each data point in %(w/v)).

Across the concentration regime studied, the bulk of phase of the surfactant will transition from molecules to micelles as the CMC is crossed. However, this doesn't affect the bubble structure i.e. the overall reduction in surface tension is apparently more important than the phase of surfactant. The process involves the rapid formation of large areas of newly forming interface so it is unclear whether the surfactants will actually aggregate to form micelles or perhaps an increase in driving force for adsorption is more likely. Similar behaviour is observed for P123 with the exception of the 1wt% concentration foam. This may be an anomalous result as the error bars on the data are significant.

Interestingly for PE6800, an increase in cell size with increasing concentration is observed and the structure appears more open. As previously discussed, at 2wt% concentration, the structure was highly broken and open therefore it was difficult to measure an exact cell size. This surfactant is the most hydrophilic of those studied therefore will typically display a greater tendency to remain in solution, slower diffusion to the interface and an inability to reduce the surface tension of prepolymer sufficiently to stabilise the interface. It is known that the prepolymer itself has some surface activity as demonstrated by the experiment in which polyurethane foam was manufactured in the absence of surfactant. Therefore, the PE6800 may show competition at the interface with these surface active species. Furthermore, the surfactant has a role in the initial emulsification of the prepolymer and aqueous phases. Thus, the lower surfactant activity of PE6800 may result in the formation of an inhomogeneous mix which produces a non-uniform cell structure.

6.8. Conclusion

Hydrophilic polyurethane foams prepared with a homologous series of PEO-PPO-PEO surfactants have been prepared on an industrial manufacturing line in order to better understand how the nature of the surfactant influences foam structure and properties. Polyurethane foams for wound care applications are characterised by fine cell structure and good fluid handling properties. This was achieved for those PEO-PPO-PEO surfactants which are typically the most hydrophobic, smallest molecular weight of those studied. It is apparently the ability of the surfactant to lower the surface tension which is most important in defining PU cell structure. Surfactant concentration studies suggested that the phase of the surfactant was not significant in defining structure. It is worth noting that the processing conditions on the manufacturing line used in this work have been optimised for the commercial product. Thus a more in-depth analysis, particularly of the temperature parameters, may allow further conclusions to be drawn.

6.9. References

1. M. J. Owen, T. C. Kendrick, B. M. Kingston and N. C. Lloyd, *Journal of Colloid and Interface Science*, 1967, **24**, 141-150.

2. D. Aldous, *International Turf Management*, Routledge, Oxon, UK, 2011.

3. R. J. Stokes and D. Fennell Evans, *Fundamentals of Interfacial Engineering*, Wiley, Canada, 1997.

4. R. Herrington and K. Hock, *Flexible Polyurethane Foams*, 2nd edn., Dow Chemical Company, USA, 1998.

5. M. Szycher, ed., *Szycher's Handbook of Polyurethanes*, 2nd edn., CRC Press, Florida, 2013.

6. X. D. Zhang, C. W. Macosko, H. T. Davis, A. D. Nikolov and D. T. Wasan, *Journal of Colloid and Interface Science*, 1999, **215**, 270-279.

7. P. C. Griffiths, P. Occhipinti, C. Morris, R. K. Heenan, S. M. King and M. Gumbleton, *Biomacromolecules*, 2010, **11**, 120-125.

7. Conclusion

Fully understanding the role of surfactants in the formation of flexible hydrophilic polyurethane foam is a complex task. It was discussed in the Introduction that there is limited theory that can be translated from one commercial system to another due to differing raw materials and numerous processing parameters. Furthermore, isolating the behaviour of the surfactant in the reaction process is difficult due to the occurrence of simultaneous reactions and temperature gradients. Therefore based on this rationale, the methodology selected for this research involved studying the behaviour and structure of aqueous polymeric surfactant stabilised foams using fundamental surface science techniques (foaming methods, surface tension, small-angle neutron scattering). The key challenge was to relate such behaviour to the properties of polyurethane foam manufactured with various surfactants on an industrial manufacturing line.

Our most significant contribution to the understanding of aqueous foams has been the successful implementation of small-angle neutron scattering (SANS) to probe the structure of non-ionic poly(ethylene oxide)-poly(propylene oxide)-poly(ethylene oxide) (PEO-PPO-PEO) (Pluronic) surfactant stabilised foams. A novel sample environment that allows foam to be generated in-situ in the neutron beam has been designed, tested and validated allowing the real-time structure of dynamic foams to be probed. Previous understanding of the adsorbed surfactant layer has typically relied on probing thin films at equilibrium; a less accurate representation of foam systems.

Scattering data obtained for the homologous series of PEO-PPO-PEO stabilised foams showed characteristic features in the data; a Q^{-4} decay, representative of the air-water interface and multiple inflexions in the data characteristic of Bragg scattering from multiple adsorbed layers. Based on our understanding of Pluronic stabilised foams and contrast experiments performed using deuterated and hydrogenated forms of the ionic surfactants sodium dodcyl sulfate (SDS) and cetyl trimethyl ammonium bromide (CTAB) we propose that the interface comprises a multi-layered structure of polymer rich and water rich layers. Interestingly, similar scattering was obtained for the Pluronics, SDS and CTAB suggesting that such structures are common for both polymeric and small molecule surfactants and such studies could be extended to additional surfactant families to identify further trends.

The paracrystalline stack model developed by Kotlarchyk *et al*, to which a Q^{-4} term was added fitted well to the data. Typically layer thicknesses ranging from 80-200Å was observed depending on polymer structure. Such variation allowed us to correlate adsorbed layer structure to foaming behaviour providing the first study of its kind for dynamic Pluronic stabilised foams.

A key aim of this research was to characterise the aqueous foaming behaviour of Pluronic stabilised foams based on surfactant structure, concentration and phase behaviour. For those surfactants below their CMT (i.e. in their molecular state) foaming ability and foam stability typically increased with increasing overall molecular weight due to increased bulk solution viscosity and a thicker adsorbed layer, as determined by SANS. Such behaviour was further investigated by studying the molecular weights of the PEO and PPO blocks separately. Foaming increased with increasing PEO block size attributed to the formation of a thicker adsorbed layer. Similar behaviour was noted for increasing PPO block size. Interestingly, those foams which displayed the greatest foam volumes and stabilities were typically the most hydrophilic of those studied and exhibited the smallest reduction in surface tension from that of pure water. Slower diffusion to the interface and a smaller reduction in bubble generation energy is expected for these surfactants. However, SANS experiments indicated that the layer thickness was greater for these foams demonstrating that surface activity alone is not the only defining parameter in foam behaviour, and the nature of the adsorbed surfactant layer is also highly important.

Foaming behaviour was compared at a standard concentration and temperature and it was identified that the phase of the surfactant can significantly alter such behaviour over a very narrow temperature regime. A sharp increase in foam volume and lifetime was observed at the CMT associated with the formation of micelles. Thus, for highly temperature sensitive polymer surfactants it is essential to consider the surfactant phase diagram when making comparisons.

Polyurethane foams were prepared on a commercial manufacturing line and the structure and physical properties were highly sensitive to the surfactant raw material used. A key aim of this study was to identify the characteristics of the surfactant that produce ‘ideal’ foam wound dressings whether this be good foaming behaviour, thick adsorbed layer for example. Fine, uniform cell structure was necessary to produce foam

with good absorption properties (a key requirement for wound care materials). Typically this was achieved by the smallest molecular weight, most hydrophobic surfactants which display fast diffusion to the interface and a strong driving force for adsorption at the interface. Whilst a thicker adsorbed layer structure is most important for interface stability it appears here that stability is not a critical factor in defining the structure of the foam. Rather it is the ability of the surfactant to reduce the surface tension of the mixture which thus reduces bubble generation energy, controlling cell size. Therefore when designing surfactant formulations for polyurethane foam reactions, the surface tension lowering ability of the surfactant must be considered. For the commercial blend used in this work we estimate the equilibrium surface tension of the surfactant in water must be less than $32mNm^{-1}$ to produce PU foam with satisfactory properties. Unfortunately, it is unlikely that such results could be translated to another polyurethane foam manufacturing system as the processing parameters and formulation are will be very different. Nevertheless, we have shown that the surface activity of the surfactant is highly important in PU foam manufacture and the results obtained for Pluronic systems may give a guideline for studying other polymeric surfactant families.

A1. Appendix 1

A1.1. Critical micelle temperature determination

A1.1.1. Equilibrium surface tension

(Gareth Jones is acknowledged for obtaining equilibrium surface tension data)

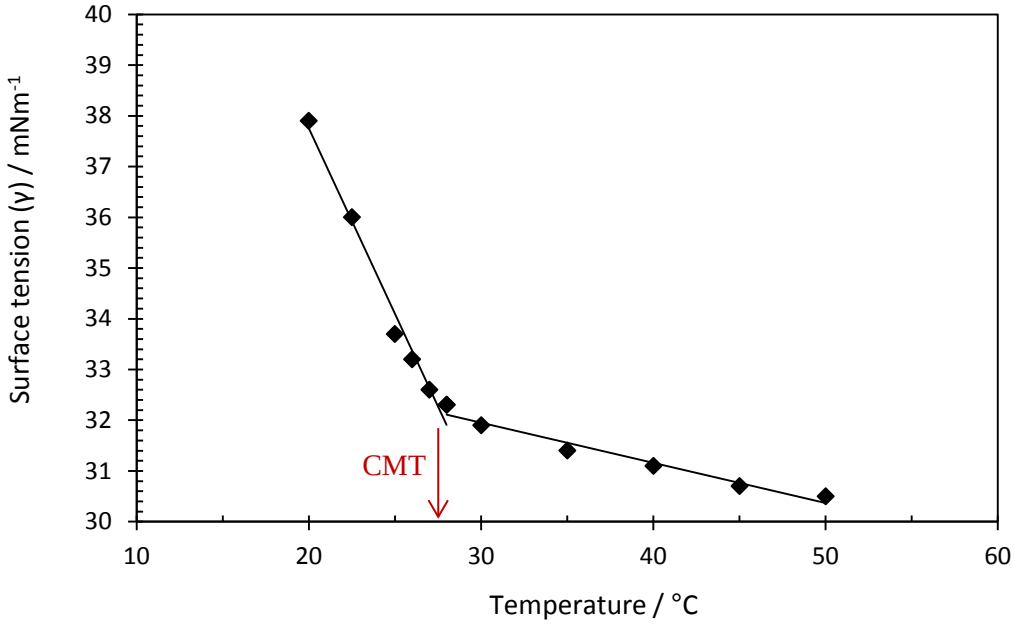

Figure A1.1; Equilibrium surface tension as a function of temperature for [L62]=2%(w/v).

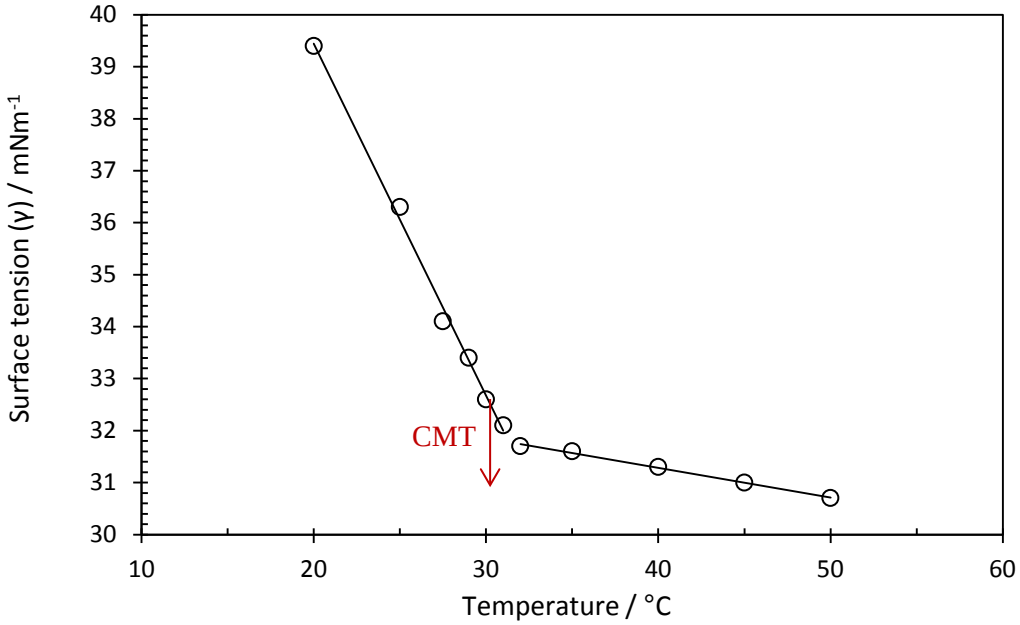

Figure A1.2; Equilibrium surface tension as a function of temperature for [PE6400]=2%(w/v).

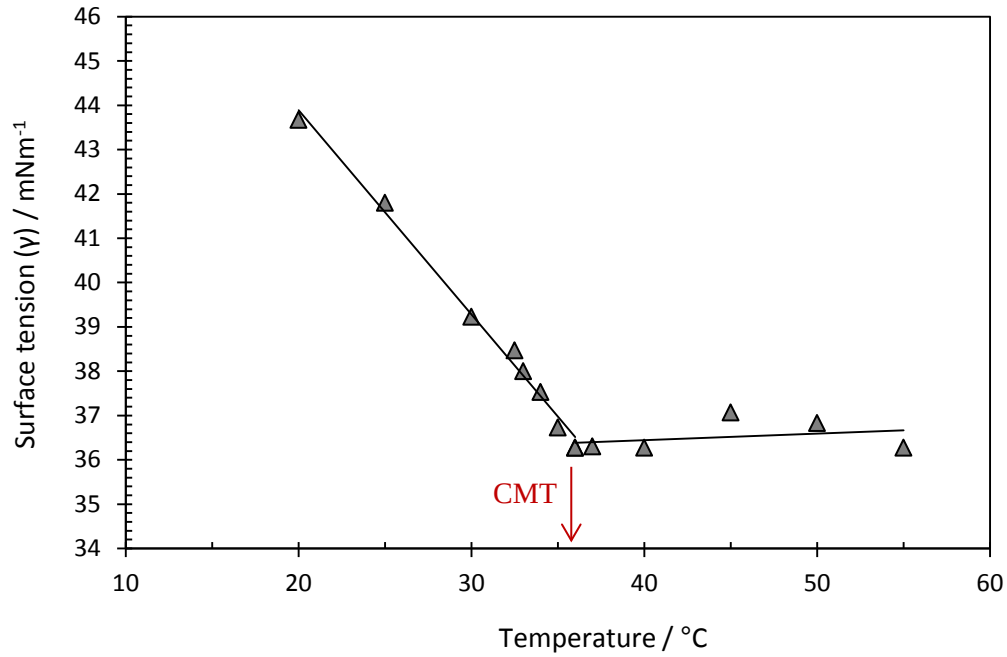

Figure A1.3; Equilibrium surface tension as a function of temperature for [PE6800]=2%(w/v).

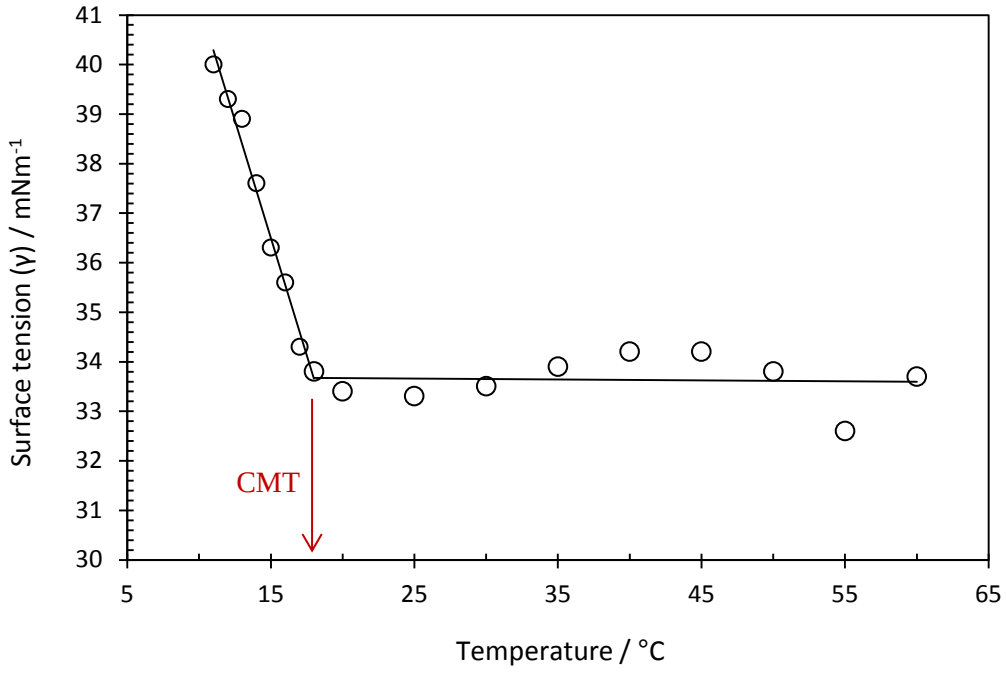

Figure A1.4; Equilibrium surface tension as a function of temperature for [P104]=2%(w/v).

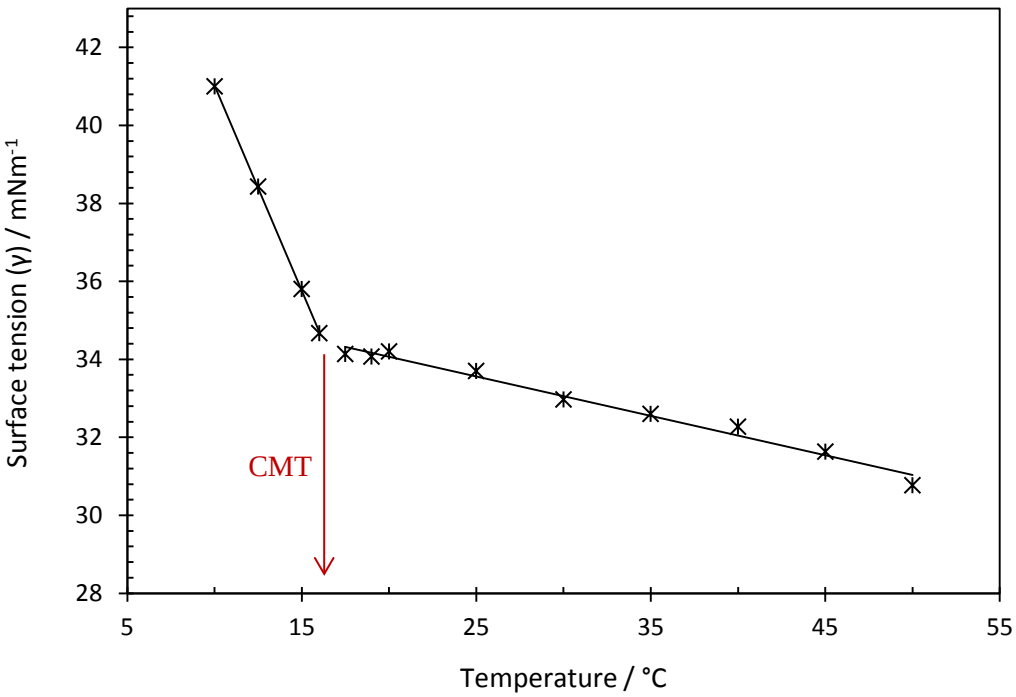

Figure A1.5; Equilibrium surface tension as a function of temperature for [P123]=0.05%(w/v).

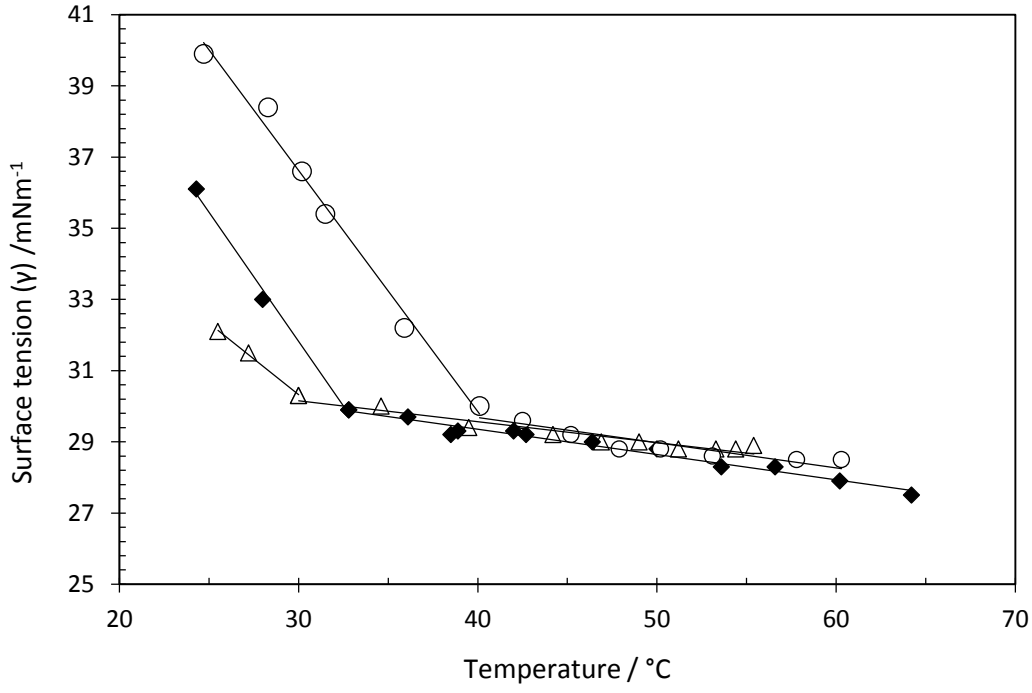

Figure A1.6; Equilibrium surface tension as a function of temperature for various concentrations of L62; 0.1wt% (circles), 1wt% (diamonds), 5wt% (triangles).

A1.1.2. Small-angle neutron scattering

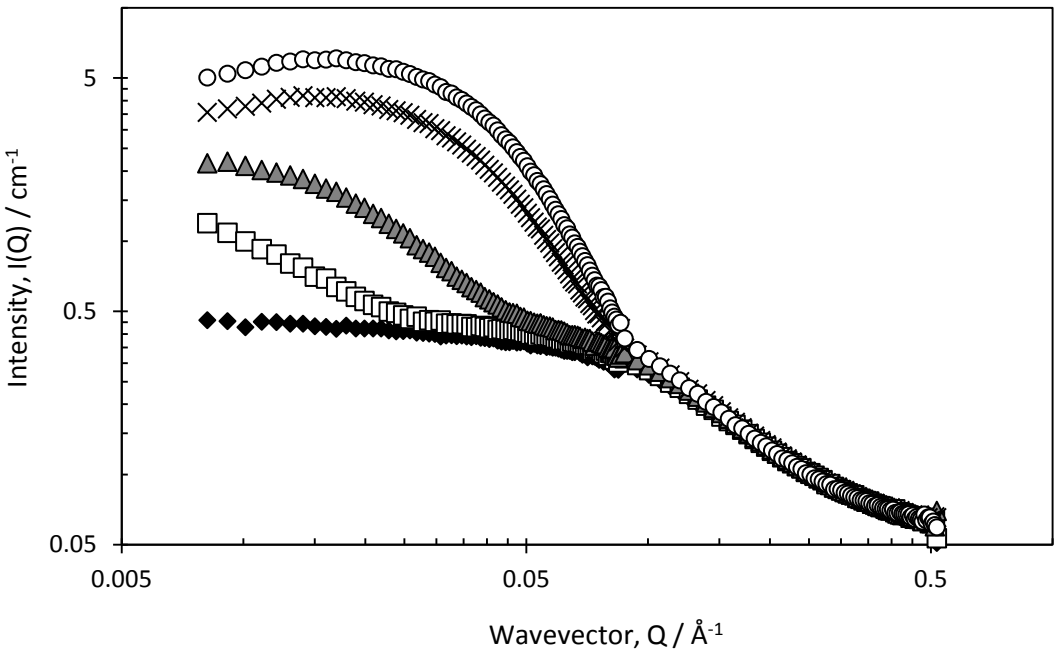

Figure A1.7; Small-angle neutron scattering of an aqueous solution of PE6400, 5% (w/v) as a function of temperature; 20°C (diamonds), 30°C (squares), 35°C (triangles), 40°C (crosses) and 45°C (circles).

A1.2. Dynamic surface tension

(Oliver Hayes is acknowledged for obtaining equilibrium surface tension data)

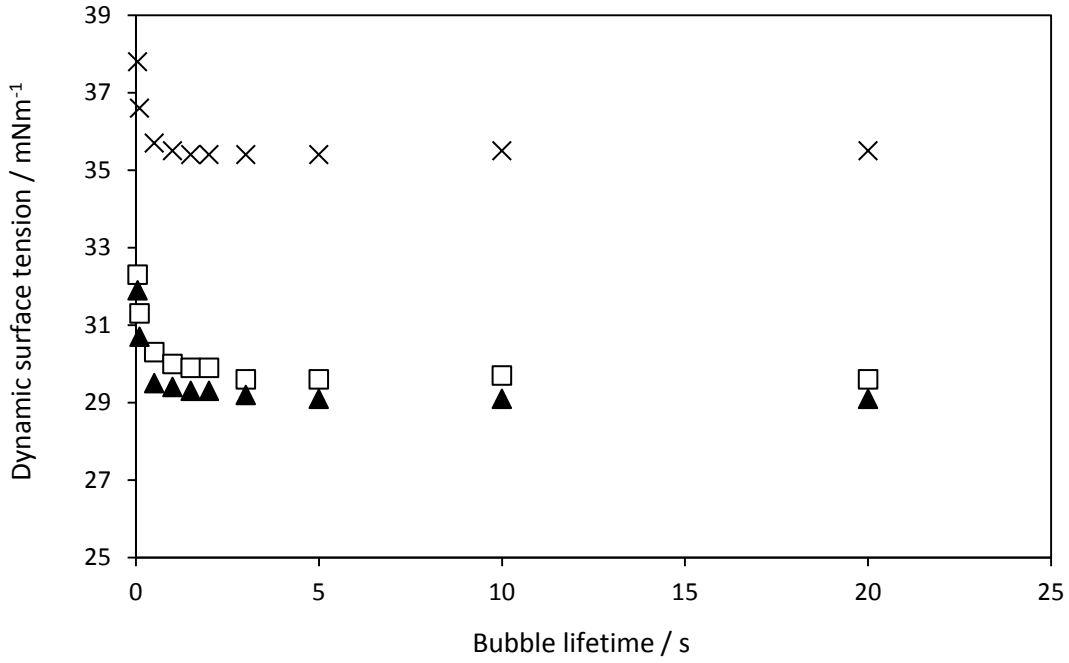

Figure A1.8; Dynamic surface tension for [L62]=2wt% at various temperatures; 20°C (crosses), 30°C (squares) and 40°C (triangles).

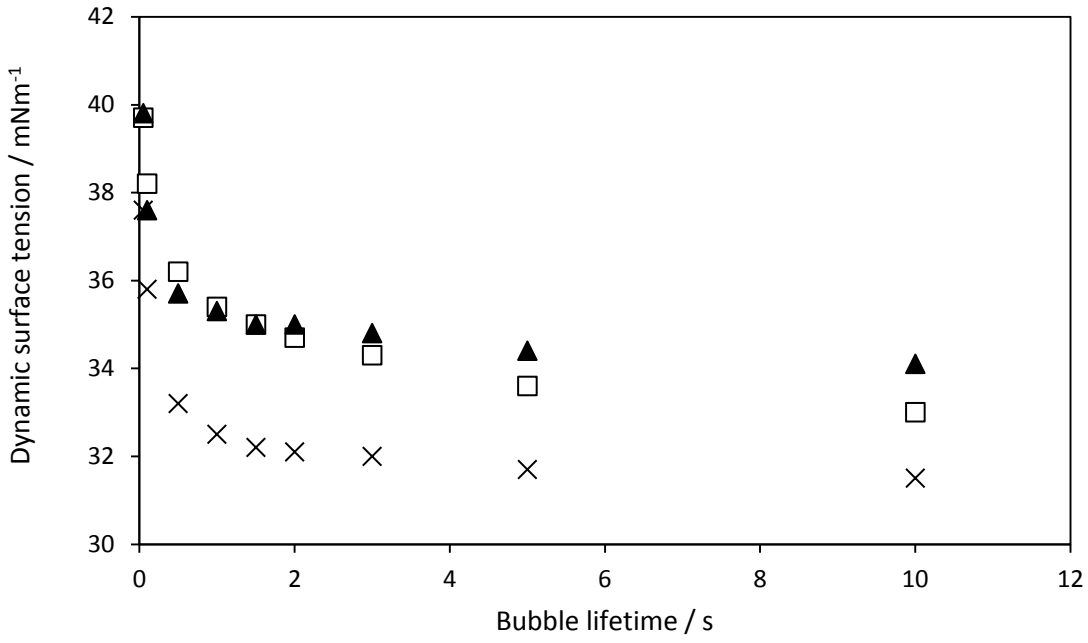

Figure A1.9; Dynamic surface tension for [P123]=2wt% at various temperatures; 20°C (crosses), 30°C (squares) and 40°C (triangles).

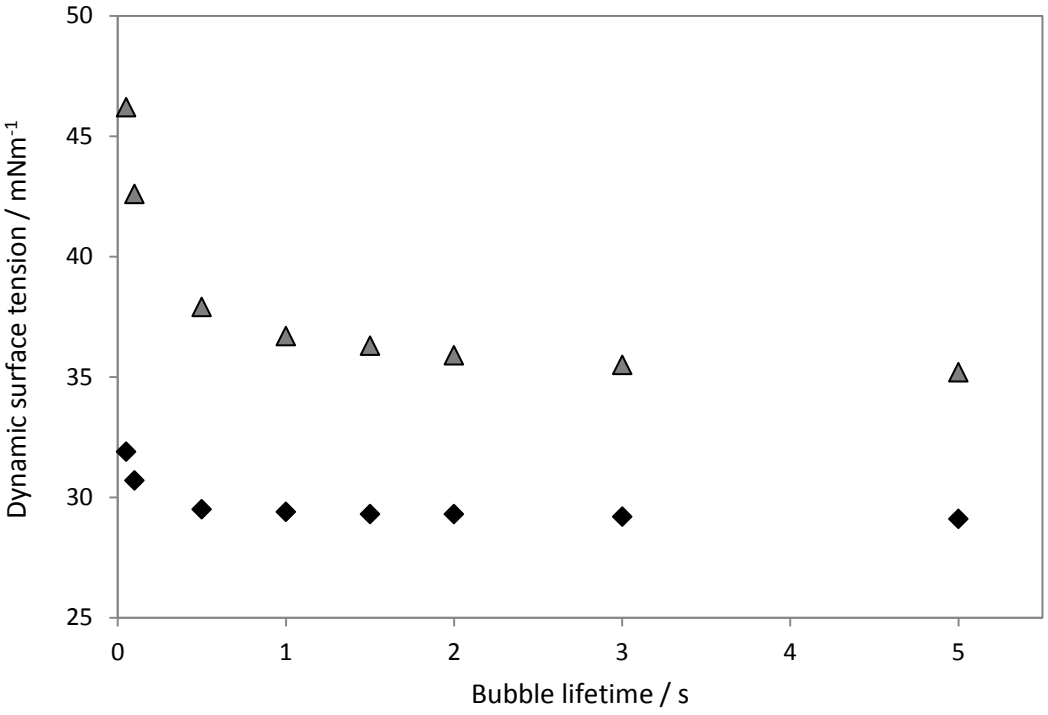

Figure A1.10; Dynamic surface tension for L62 (diamonds) and PE6800 (triangles) at [Pluronic]=2wt% and 40°C.

A2. Appendix 2

A2.1. Porod Plots

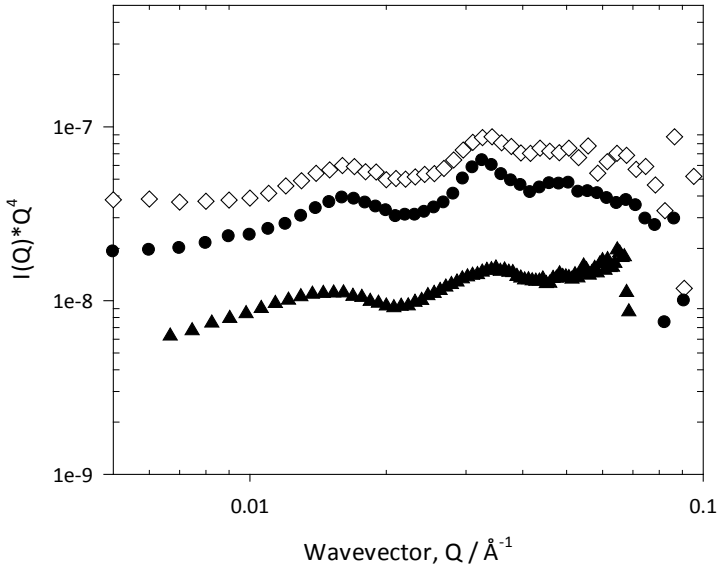

Figure A2.1; Porod plot of small-angle neutron scattering from the air-in-water foams stabilised by polymeric surfactants with constant PPO block size and increasing PEO block size; [Pluronic] = 0.05% (w/v), P103 (diamonds), P104 (circles), F108 (triangles).

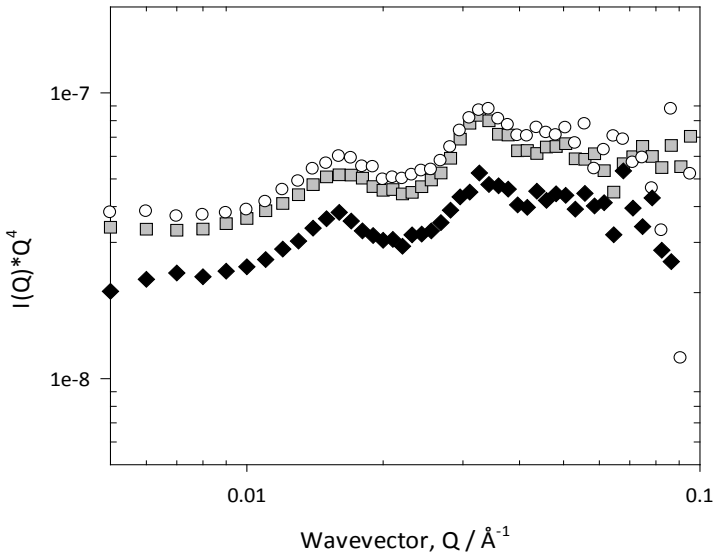

Figure A2.2; Porod plot of small-angle neutron scattering from the air-in-water foams stabilised by polymeric surfactants with 40% PEO content and increasing PPO block size; [Pluronic] = 0.05% (w/v), P84 (squares), P103 (circles), P123 (diamonds).

A2.2. Small-angle neutron scattering from PEO-PPO-PEO foams

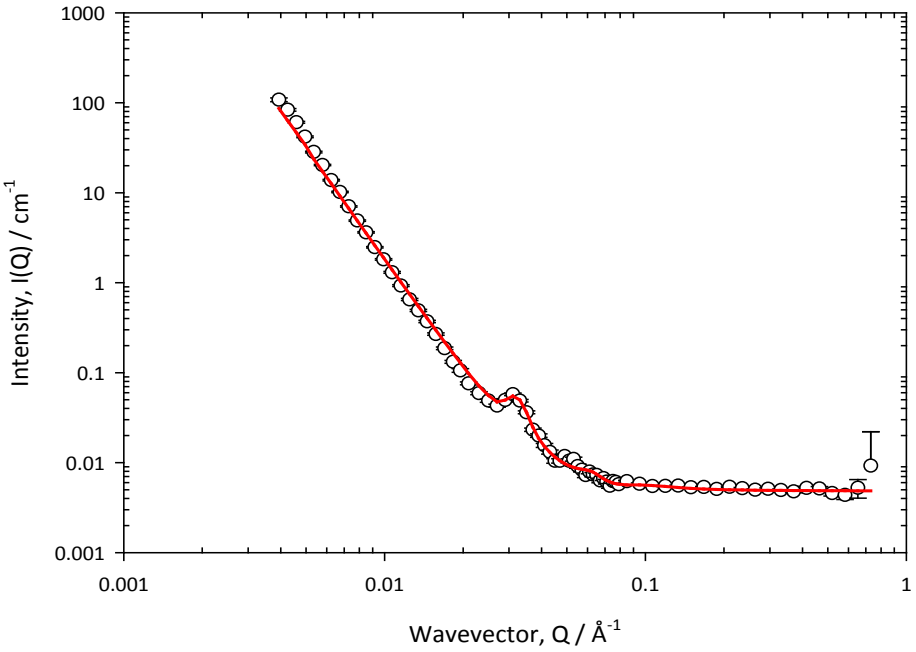

Figure A2.3; Small-angle neutron scattering from foam stabilised by 0.05% (w/v) PE6400 and the fit to the paracrystalline stack model described in the Experimental section.

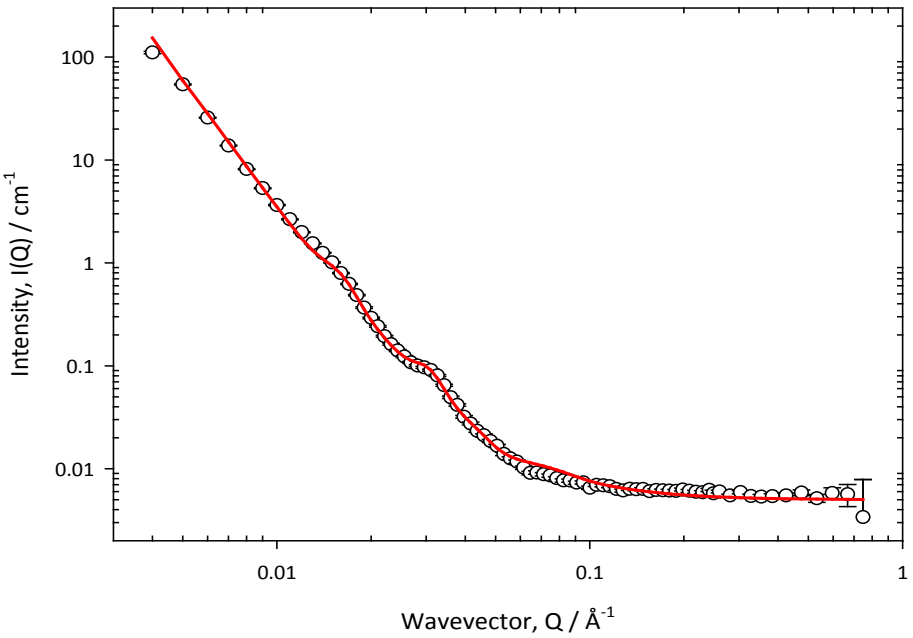

Figure A2.4; Small-angle neutron scattering from foam stabilised by 0.05% (w/v) P84 and the fit to the paracrystalline stack model described in the Experimental section.

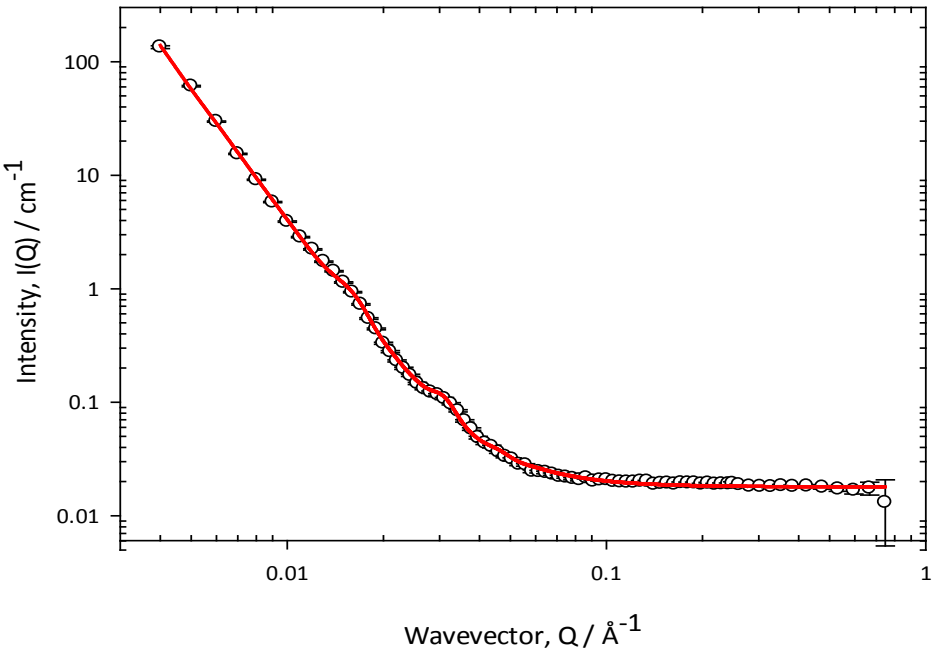

Figure A2.5; Small-angle neutron scattering from foam stabilised by 0.05% (w/v) P103 and the fit to the paracrystalline stack model described in the Experimental section.

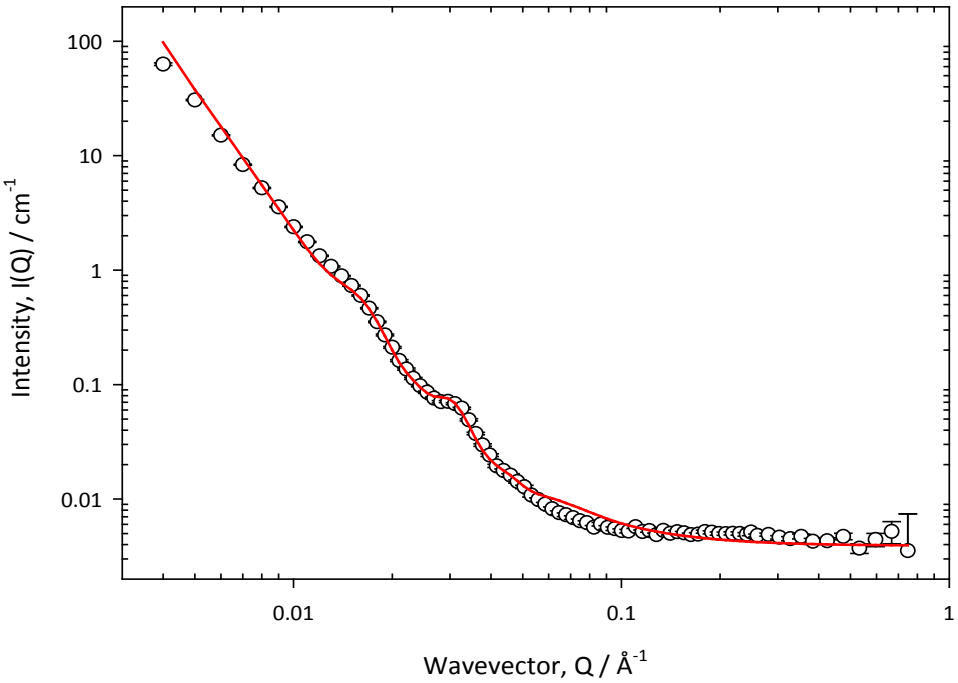

Figure A2.6; Small-angle neutron scattering from foam stabilised by 0.05% (w/v) P104 and the fit to the paracrystalline stack model described in the Experimental section.

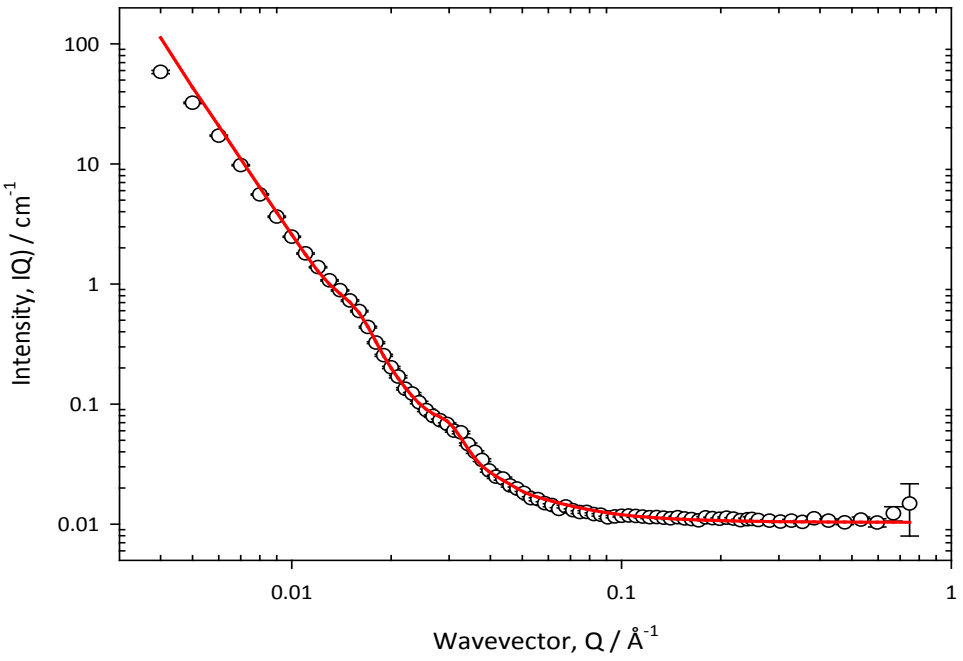

Figure A2.7; Small-angle neutron scattering from foam stabilised by 0.05% (w/v) P123 and the fit to the paracrystalline stack model described in the Experimental section.

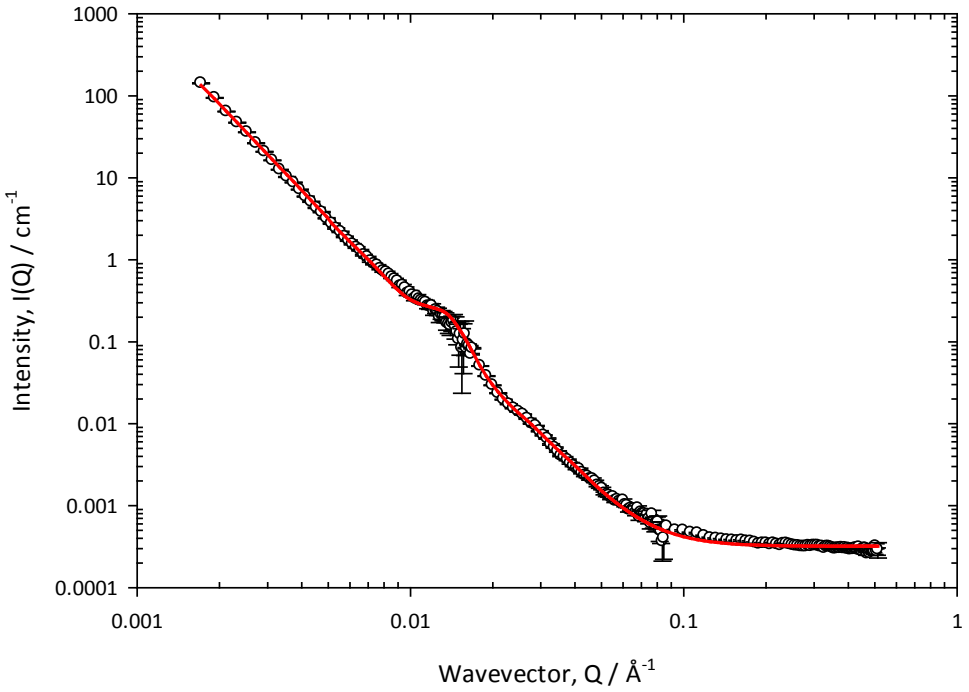

Figure A2.8 Small-angle neutron scattering from foam stabilised by 0.05% (w/v) F108 and the fit to the paracrystalline stack model described in the Experimental section.

A2.3. CTAB contrast experiments

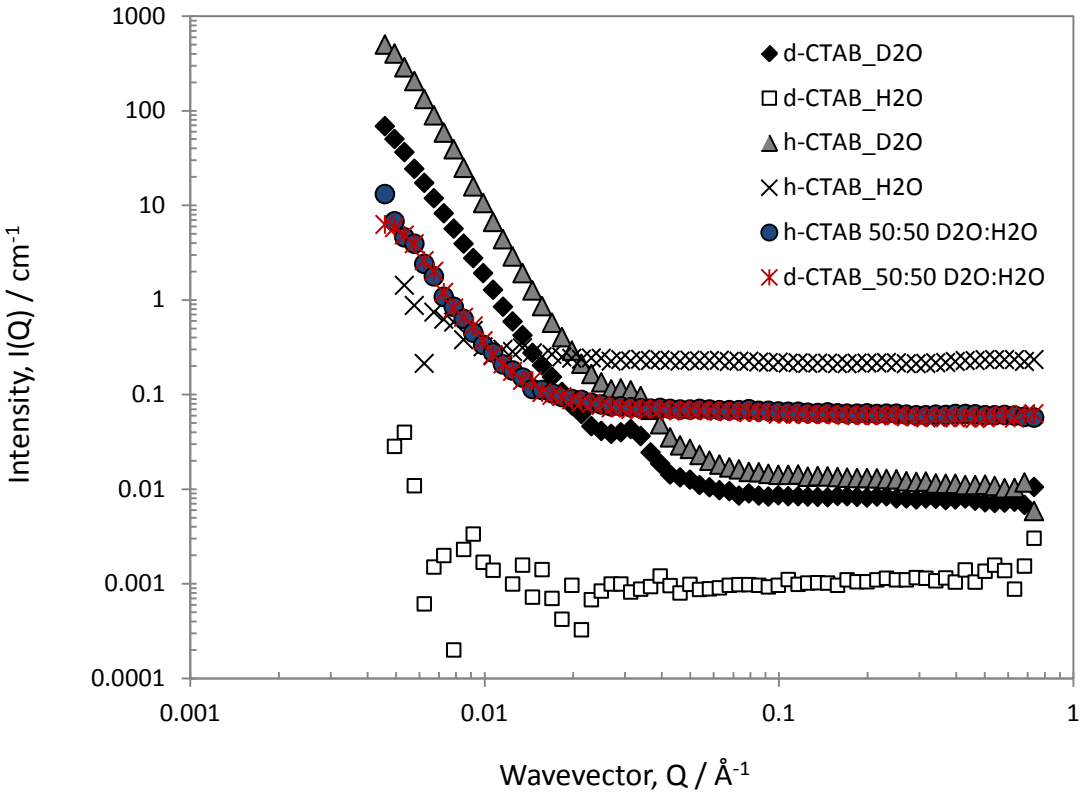

Figure A2.9; Small-angle neutron scattering from air-in-water foams stabilised with CTAB. d-CTAB in D_2O (diamonds), d-CTAB in H_2O (squares), h-CTAB in D_2O (triangles), h-CTAB in H_2O (crosses), h-CTAB in 1:1 H_2O: D_2O (circles), d-CTAB in 1:1 H_2O:D_2O.

Soft Matter

PAPER

View Article Online
View Journal | View Issue

Cite this: *Soft Matter*, 2014, **10**, 3003

The interfacial structure of polymeric surfactant stabilised air-in-water foams†

Jamie Hurcom,[a] Alison Paul,[a] Richard K. Heenan,[b] Alun Davies,[a] Nicholas Woodman,[c] Ralf Schweins[d] and Peter C. Griffiths*[e]

Received 14th November 2013
Accepted 17th February 2014

DOI: 10.1039/c3sm52877d

www.rsc.org/softmatter

Small-angle neutron scattering was used to probe the interfacial structure of nitrogen-in-water foams created using a series of tri-block polymeric surfactants of the poly(ethylene oxide)–poly(propylene oxide)–poly(ethylene oxide) (EO_x–PO_y–EO_x) range, from which the nature of the polymeric interface could be characterised. The data follow a pronounced Q^{-4} decay, along with a number of inflexions and weak but well-defined peaks. These characteristics were well-described by a model embodying paracrystalline stacks of adsorbed polymer layers, whose formation is induced by the presence of the air–water interface, adsorbed at the flat air–water (film lamellae) interface. A minimum of approximately five paracrystalline polymer layers of thickness of the order of 85–160 Å, interspersed with somewhat thicker (400 Å) films of continuous aqueous phase were found to best fit the data. The thickness of the layer (L) was shown to follow a relationship predicted by anchor block dominated polymer adsorption theories from non-selective solvents, $L \sim EO^{1}PO^{1/3}$. The insight gained from these studies should permit a more rational design of polymeric stabilisers for hydrophilic polyurethane foams.

Introduction

Foams are dispersions of gas in an aqueous continuous phase and are formed in the presence of surfactant. Solid polymeric foams such as polyurethanes (PU) find use in a variety of applications including biomedical materials, insulation and soft furnishings.[1] The chemistry of these foams is well-documented involving step-growth polymerisation of di-isocyanate and polyalcohol monomers.[2] The structure and performance of PU foams is highly dependent on the surfactant behaviour at the air–liquid interface with the polymer chemistry locking in an otherwise transient structure.

It has long been known that small molecule and polymeric surfactants can be used to produce a stable foam, and more recently, colloidal silica nanoparticles have also been shown to adsorb at the air–water interface stabilising these interfaces[3,4] Foam destruction occurs *via* a number of processes:[5] drainage due to gravity or surface tension gradients; Ostwald ripening or coarsening driven by the diffusion of gas across thin films from smaller to larger bubbles; and bubble coalescence leading to the thinning and eventual rupture of thin films. By adsorbing at the air–liquid interface, surfactants lower the surface tension providing a surface elasticity mechanism, the Gibbs–Marangoni effect, that opposes localised film thinning.[6] However the ability to form persistent or long-lived foams is not solely dependent on this effect. The adsorbed surfactant layer must also have the ability to resist these depletion processes which is highly dependent on the structure of the adsorbed layer.

In the manufacture of solid polymeric foam, the stability of the wet foam has important consequences for cell window opening and porosity of the final cured polymeric foam. Thus, understanding the structure of surfactant at the air–water interface should allow greater insight into the role of polymeric stabilisers in polymeric foam systems.

Many attempts have been made to relate the structural and interfacial properties of non-ionic surfactants to aqueous single thin film and foam behaviour.[7–16] Conclusions have generally been qualitative, largely due to the inherent complexity of such foam systems, and a lack of detailed understanding of the assembly of stabilisers at the air–water interface. Against this context, the current study was conceived.

Small-angle neutron scattering (SANS) has been used previously to probe the structure of stabilisers at foam interfaces. The most elegant studies were presented by Axelos and Boue and co-workers[17] where they studied a series of dry and wet foams formed from aqueous solutions of the anionic surfactant sodium dodecylsulphate (SDS) at concentrations above and

[a]*School of Chemistry, Cardiff University, Main Building, Park Place, Cardiff CF10 3TB, UK*

[b]*Science and Technology Facilities Council, Rutherford Appleton Laboratory, Harwell Oxford, Didcot, OX11 0QX, UK*

[c]*Polymer Health Technology, Festival Drive, Ebbw Vale, NP23 8XE, UK*

[d]*Institut Laue Langevin, Grenoble, Cedex 9, France*

[e]*Faculty of Engineering and Science, University of Greenwich, Central Avenue, Chatham Maritime, Kent ME4 4TB, UK. E-mail: p.griffiths@gre.ac.uk*

† Electronic supplementary information (ESI) available: Foam stability behaviour for 5 surfactants (L62, P123, PE6400, PE6800, F108) at 5% w/v and 20 °C. See DOI: 10.1039/c3sm52877d

below the critical micelle concentration (CMC). Both X-ray and neutron scattering were deployed. Under steady-state foaming conditions, wet films yielded a characteristic scattering pattern comprising a pronounced Q^{-4} dependence, with a number of superimposed peaks or "bumps". Through comparison with the solution scattering, these authors defined the foam interface as comprising two fully extended dodecyl chains (18.6 Å) separated by a water film of ~260 Å, with some additional features in the scattering arising from the micellar structures present within the aqueous regions of the wet foam (film lamellae). For the dry foams, the number of peaks was fewer, associated with the loss of the surfactant-like scattering from the aqueous regions.

In this work, we explore the nitrogen/water foams formed from ABA triblock copolymers of the poly(ethylene oxide)–poly(propylene oxide)–poly(ethylene oxide) type (EO_x–PO_y–EO_x), known commercially as Pluronics. Of principle interest is the analysis of small-angle neutron scattering data to probe the interfacial structure of surfactant in the foam from which the definition of the relationship between the molecular structure of the stabiliser and its foaming characteristics (ESI†) has been inferred.

Experimental

Materials

A series of structurally analogous poly(ethylene oxide)–poly(propylene oxide)–poly(ethylene oxide) tri-block polymeric surfactants known commercially as Pluronics were used as received, as listed in Table 1.

Solutions were prepared by dissolving various concentrations of the block copolymer in deuterated water (99.9%, Sigma Aldrich).

Small-angle neutron scattering

Foam generation. In all experiments, the foam sample was contained in a purpose built Perspex column of height 25 cm into which a 2 cm wide groove has been removed, and covered with aluminium foil to act as the neutron transparent windows for beam access, Scheme 1. Approximately 50 cm^3 of surfactant solution was added to the sample holder at the base of the column. The foam is generated by bubbling gas through the frit at A. The neutron beam impinges on the aluminium foil between B and C behind which the Perspex has been partially removed. For stable foams, the reservoir D collects the foam sample and returns it to the base *via* the plastic tube at E. The heating jackets at F and G have been removed in this picture.

Scheme 1 SANS sample environment for studying foams.

Steady state wet foams were studied in which a continuous air flow produces constantly regenerated foam. As such, the bubbles appear spherical and are separated by thick lamella walls. Experiments were conducted at room temperature. Experimental measuring times were approximately 5 minutes.

Instrument configuration. Small-angle neutron scattering experiments were performed on either (i) the time-of flight LOQ or SANS2d diffractometers at the ISIS pulsed Spallation Neutron Source, Rutherford Appleton Laboratory, Didcot, UK. Typically, a range defined by $Q = (4\pi/\lambda)\sin(\theta/2)$ between 0.005 and ≥0.3 $Å^{-1}$ is obtained by using neutron wavelengths (λ) spanning 2.2 to 10 Å (LOQ) or 1.75 to 16.5 Å (SANS2d) with a fixed sample–detector distance of ~4 m, or (ii) the steady-state reactor source, D11 diffractometer at the ILL, Grenoble where a Q range between 0.005 and 0.5 $Å^{-1}$ was obtained by choosing three instrument settings at a constant neutron wavelength (λ) of 8 Å and sample–detector distances of 1.2, 8 and 39 m.

All scattering data were (a) normalized for the sample transmission, (b) background corrected using the empty foam cell, and (c) corrected for the linearity and efficiency of the detector response using the instrument specific software package and the scattering from a polystyrene standard taped to the front of the foam cell.

Table 1 Molecular weight and approximate composition characteristics of the Pluronic copolymers used in this work. The stated PEO composition is for both blocks

	PPO block		PEO block				
Name	g mol^{-1}	Segments	g mol^{-1}	Segments	%	Total MW/ g mol^{-1}	HLB
L62	1750	30	500	12	20	2500	1–7
PE6400	1750	30	1160	26	40	2900	7–12
P84	2250	43	1680	38	40	4200	12–18
P103	3250	60	1485	34	30	4950	7–12
P123	4000	70	1725	40	30	5750	12–18
P104	3250	60	2360	54	40	5900	12–18
PE6800	1750	30	6720	150	80	8400	>24
F108	3250	60	11 680	260	80	14 600	>24

Results and discussion

Small-angle neutron scattering was used to characterise the distribution of the polymer within the foam system whether that be dissolved in the aqueous regions or adsorbed at the interface. Accordingly, there may be several contributions to the measured scattering;

(1) any structure normal to the air–water interfaces, which would follow an approximate Q^{-4} dependence given that these interfaces would not be perfectly flat,

(2) any in plane structure normal to the air–water interface,

(3) fluctuations in composition of the interfaces parallel to the beam,

(4) structures that would be present in the liquid junctions between bubbles, that may resemble "bulk solutions" at appropriate concentration, and,

(5) in aged, polyhedral foams, the long almost cylindrical regions at the junctions of bubbles associated with the plateau borders.

Representative data are presented in Fig. 1, and it is evident as suggested, that there are a number of features in the data. At low Q, the decay of the intensity with wavevector Q shows the pronounced Q^{-4} dependence, characteristic of the Porod scattering from a smooth interface of large radius. At high Q, there is a much slower decay, reminiscent of the solution scattering of these polymeric surfactants, into an incoherent background that varies for the four cases reflecting the fact that there is a different amount of sample in the beam in each case (the background is dominated by the incoherent scattering from the residual hydrogen content in the solvent as well as the polymer). Over the intermediate Q range, for three cases, there are noticeable points of inflexions, around $Q = 0.025$ and 0.04 Å^{-1}, associated with an oscillatory signature. For the P123 case, the scattering is far more intense, a point discussed in more detail later.

Focusing first on the high Q scattering, it is possible to identify this as the scattering from the polymeric surfactant in solutions comprising the plateau borders. Indeed, scattering from the appropriate solutions recorded in a conventional sample cell *e.g.* as in Fig. 2 (top), [PE6800] = 5% (w/v), can be overlaid onto the foam scattering, arbitrarily scaling the intensities after subtracting a flat incoherent background (a simplistic attempt to match the relative amounts of sample in the beam). Such an analysis was appropriate for the three cases, PE6400, PE6800 and L62, and to some extent P123. The high Q region of the data may therefore be associated with solution

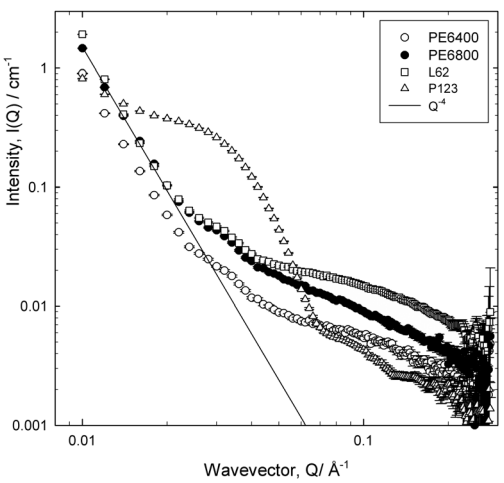

Fig. 1 Small-angle neutron scattering from foams stabilised by four polymeric surfactants with [Pluronic] = 5% (w/v). Gas flow varied slightly through this series in order to generate foam of sufficient height. Also shown is the low Q limiting value of Q^{-4}.

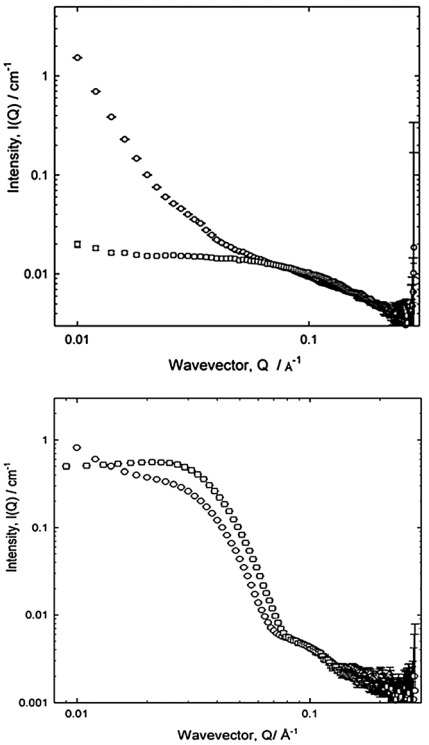

Fig. 2 Small-angle neutron scattering from an air-in-water stabilised foam (circles) and a simple aqueous solution (squares) for polymeric surfactants PE6800 (top) and P123 (bottom). [Polymer] = 5% (w/v), arbitrarily scaled for comparison.

scattering, and indeed when fitted to the Debye model for a random coil polymer in solution, yielded radii of gyration typical of the appropriate molecular species *e.g.* $R_g = 14$ Å, 16.5 Å or 20 Å for PE6400, L62 and PE6800 respectively, in good agreement with dimensions obtained from an analysis of the solutions cell scattering for the monomeric species. Thus, it is concluded that for these systems there is a quantifiable contribution to the overall scattering from the polymer dissolved in the aqueous film forming the lamellae of the bubble.

The same conclusion may in fact be drawn from the P123 case, Fig. 2 (bottom), noting that the solution in this case is above its CMC and thus, the form of the scattering over both the intermediate and high Q regions is reminiscent of micellar rather than monomeric scattering, with an initial steeper decay at low Q.

Interestingly in this case, it is not possible to simultaneously overlay the (intensity of the) peaks associated with the intermicellar structure factor ($Q = 0.03$ Å) and those associated with the core–shell morphology of the micelle ($Q = 0.1$ Å) implying that the structure of the micelle may be perturbed in the foam relative to the solution. Nonetheless, this initial data recorded on LOQ indicate that in order to isolate the foam scattering, the polymer concentration requires substantial dilution.

Fig. 3a and b present data recorded on D11 for two polymeric surfactants, over an extended Q range (compared to Fig. 1), as a function of dilution. The pronounced Q^{-4} is even more evident now due to the lower Q range accessed on this instrument

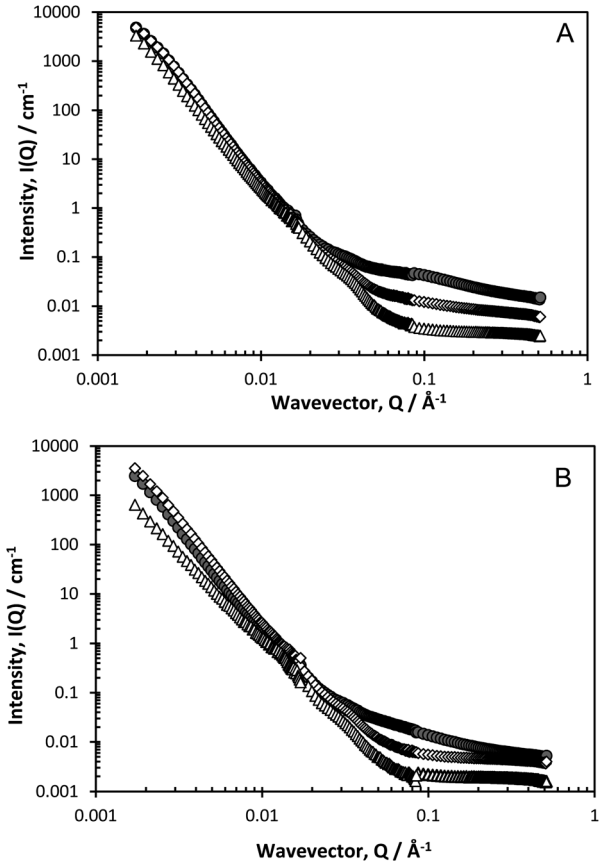

Fig. 3 (a) Small-angle neutron scattering for foams stabilised with polymeric surfactant PE6400 at various concentrations; 0.05% (w/v) (triangles), 0.5% (w/v) (diamonds) and 5% (w/v) (circles). (b) Small-angle neutron scattering for foams stabilised with polymeric surfactant F108 at various concentrations; 0.05% (w/v) (triangles), 0.5% (w/v) (diamonds) and 5% (w/v) (circles).

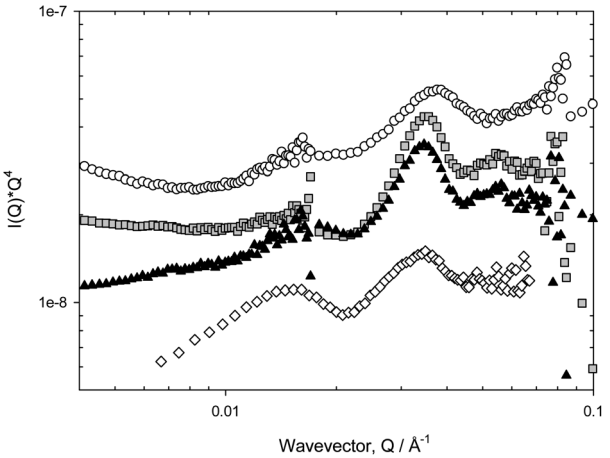

Fig. 4 Porod plot of small-angle neutron scattering from foams stabilised by four polymeric surfactants with [Pluronic] = 0.05% (w/v); PE6400 (circles), L62 (squares), PE6800 (triangles), F108 (diamonds).

(which could potentially introduce issues of multiple scattering), but the inflexion at $Q \approx 0.03$–0.04 Å^{-1} and the flat incoherent background at low polymer concentrations become more evident, as does a second inflexion at $Q \approx 0.01$–0.015 Å^{-1}.

The Porod region is valid when the size of the scattering object is larger than the range probed by the scattering radiation, and it is well-known that Q^{-4} behaviour characterises the smooth surfaces expected in foam systems. The points of inflexions in the scattering, as observed in Fig. 3a and b, can be highlighted by plotting the data on a Porod plot, $Q^4I(Q)$ *vs.* Q, Fig. 4, as this effectively removes the Q^{-4} term. Well-defined peaks are now clearly evident at approximately $Q = 0.018$ Å^{-1} and $Q = 0.035$ Å^{-1}, though the positions of these peaks change slightly depending on surfactant type. The peak at $Q = 0.018$ Å^{-1} unfortunately overlapped with the edge of the detector used in one particular experimental geometry, but subsequent experiments confirmed this second peak to be real.

The observation of such correlation peaks of this nature clearly indicates the presence of regular structures, and since $r = 2\pi/Q_{peak}$, we may estimate $r = 180$ Å (± 10 Å) These cannot be attributed, as suggested by Axelos *et al.*,[17] to the total film thickness as the dimensions are inconsistent with this; bubble lamella are estimated to be of micrometre size in the wet foams observed here. In addition, at 0.05% (w/v) the systems studied here are at concentrations significantly below their CMC, so the polymer concentration within the film lamellae are too dilute to contain micelles, thus we conclude also that the peaks cannot arise due to the presence (form factor) of aqueous micellar structures. Further, since the analysis of the solution scattering from these surfactants yields a radius of gyration of approximately 15–20 Å, in agreement with literature values,[18] it is also clear that this feature does not arise from molecular scattering. Therefore, we conclude that the foam introduces additional structure to the polymeric species near the interfaces.

Observations of such features in SANS data has previously been noted but not discussed; Zank *et al.*[19] reported lamellar Bragg peaks from high internal phase emulsions (HIPE) stabilised by Pluronic L92. Therefore, here, we have employed a model of the air–water interface that is assumed to consist of a para-crystalline stack of M thin polymer/water layers, of diffuseness T, thickness L and separation D,[20] to which is added if necessary, a Debye term to account for the solution scattering. The scattering length densities (contrast) of the various materials is such that in D_2O, the scattering arises equally from the air–D_2O and polymer–D_2O interfaces, and any further deconvolution of the data is not feasible (in this system at least). To limit the functionality of the fit, the diffuseness T has been constrained to $T = 0.01$. Typical starting values for the heterogeneity of L and D are $\sigma(L)/L$ and $\sigma(D)/D = 0.2$, though these values had little impact on the overall fit. Similarly, it was found empirically that a value of $M = 4$–6 was found to be the smallest necessary to produce suitable fits, and that larger values did not lead to appreciably better fits.

As may be seen from Fig. 5a and b, this model fits the experimental data rather well. The Q^{-4} term dominates the scattering so the accuracy of the parameters defining the inflexions are less than ideal, but the features are clearly reproduced in his approach. Pertinent parameters are given in Table 2. The heterogeneity in the surface structure varies with

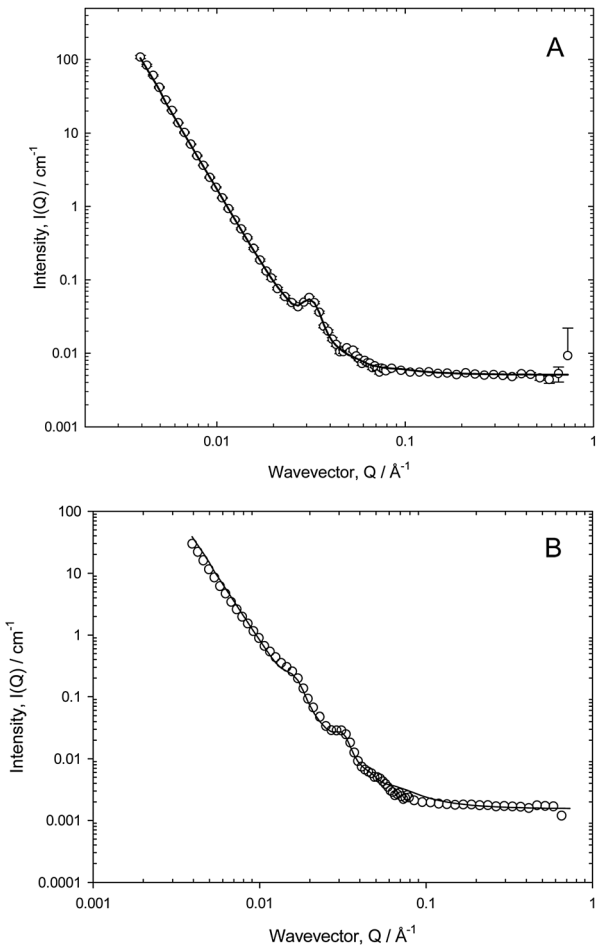

Fig. 5 (a) Small-angle neutron scattering from foams stabilised by 0.05% (w/v) L62 and the fit to the paracrystalline model described in the text. (b) Small-angle neutron scattering from foams stabilised by 0.05% (w/v) PE6800 and the fit to the paracrystalline model described in the text.

Table 2 Fit parameters to the scattering from Pluronic stabilised nitrogen-in-water foams (0.05% (w/v))

Name	L	$\sigma L/L$	M	D	$\sigma D/D$
PE6400	85	0.2	6	195	0.14
L62	90	0.22	6	195	0.15
P84	130	0.22	4	400	0.14
P103	150	0.27	4	400	0.15
PE6800	135	0.23	4	390	0.12
P104	145	0.24	3	400	0.13
P123	160	0.27	4	405	0.14
F108	220	0.25	4	430	0.14

surfactant in that PE6400 and L62 show only one peak in the scattering whereas P84, P103, PE6800, P104, F108 and P123 show two peaks.

In the various datasets, measured across the various instruments, the fitting routine is sensitive to which peak/inflexion is being fitted. For a perfectly crystalline stack, one would expect

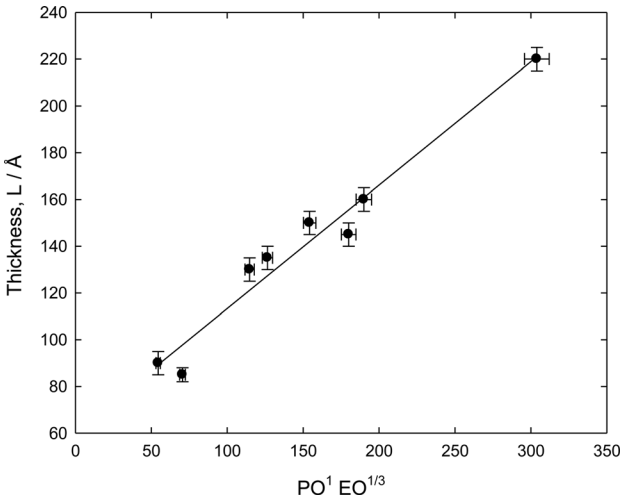

Fig. 6 Thickness of Pluronic [0.05% (w/v)] layers stabilising air-in-water foams, derived from the paracrystalline model described in the text recast in terms of a non-selective solvent polymer adsorption theory.

to see regularly spaced reflections at a common distance associated with $n = 1$, $n = 2$, $n = 3$ *etc.* Here, the separation D is slightly different whether the fitting routine focuses on the $n = 1$ ($Q = 0.015$ Å), or $n = 2$ ($Q = 0.035$ Å) peak. This implies that the structure is not a perfect lamellar one.

There is no obvious relationship between the thickness L and the molecular structure of the various Pluronic samples though L does seem to correlate more strongly with the PO content rather than the EO content, but also varies with the overall molecular weight. This behaviour is reminiscent of polymer adsorption from non-selective solvents.[21] Following a multivariant analysis, a reasonable empirical correlation was found for the thickness data, $L \sim PO^1EO^{1/3}$, Fig. 6. This rather linear representation illustrates that the copolymer is forming a structure whose thickness is determined by the lateral association of the PO groups. The PO groups would therefore seem to be the dominating factor in terms of the structure, whereas the stability was found to correlate more strongly with the EO group characteristics, *viz.* PE6400 ≈ L62 < PE6800 < F108.

Conclusions

Small-angle neutron scattering has been deployed in an attempt to understand better the relative stabilities of air-in-water foams stabilised by a series of Pluronic block copolymers. A novel interfacial templated surfactant structure is observed, which may be interpreted as a paracrystalline stack of lamellae at the air–water interface. The thickness of these layers was shown to be dependent on both EO and PO block size characteristics, whereas the foam stability seems to correlate better with the EO block size, PE6400 ≈ L62 < PE6800 < F108, demonstrating a link between the nature of the adsorbed polymer layer and the overall composition and molecular weight of these poly(ethylene oxide)–poly(propylene oxide)–poly(ethylene oxide) (EO_x–PO_y–EO_x) copolymers.

Notes and references

1 D. Randall and S. Lee, *The Polyurethanes Book*, Wiley, New York, 2002.
2 C. S. Sipaut, N. Ahmad, R. Adnan, I. A. Rahman and M. N. M. Ibrahim, *Cell. Polym.*, 2010, **29**, 1–25.
3 A. Stocco, E. Rio, B. P. Binks and D. Langevin, *Soft Matter*, 2011, **7**, 1260–1267.
4 B. P. Binks and T. S. Horozov, *Angew. Chem., Int. Ed.*, 2005, **44**, 3722–3725.
5 D. K. Exerowa and P. M. Kruglyakov, *Foam and Foam Films; Theory, Experiment, Application* Elsevier, Amsterdam, NL, 1998.
6 R. J. Pugh, *Adv. Colloid Interface Sci.*, 1996, **64**, 67–142.
7 D. Exerowa and D. Platikanov, *Adv. Colloid Interface Sci.*, 2009, **147–148**, 74–87.
8 N. Kristen, A. Vullings, A. Laschewsky, R. Miller and R. von Klitzing, *Langmuir*, 2010, **26**, 9321–9327.
9 R. Petkova, S. Tcholakova and N. D. Denkov, *Langmuir*, 2012, **28**, 4996–5009.
10 E. Carey and C. Stubenrauch, *Colloids Surf., A*, 2013, **419**, 7–14.
11 R. Petkova, S. Tcholakova and N. D. Denkov, *Colloids Surf., A*, 2013, **438**, 174–185.
12 S. Samanta and P. Ghosh, *Chem. Eng. Res. Des.*, 2011, **89**, 2344–2355.
13 S. Samanta and P. Ghosh, *Ind. Eng. Chem. Res.*, 2011, **50**, 4484–4493.
14 T. Tamura, Y. Kaneko and M. Ohyama, *J. Colloid Interface Sci.*, 1995, **173**, 493–499.
15 T. Tamura, Y. Takeuchi and Y. Kaneko, *J. Colloid Interface Sci.*, 1998, **206**, 112–121.
16 Z.-L. Chen, Y.-L. Yan and X.-B. Huang, *Colloids Surf., A*, 2008, **331**, 239–244.
17 M. A. V. Axelos and F. Boue, *Langmuir*, 2003, **19**, 6598–6604.
18 K. Mortensen, *J. Phys.: Condens. Matter*, 1996, **8**, A103–A124.
19 J. Zank, P. A. Reynolds, A. J. Jackson, K. J. Baranyai, A. W. Perriman, J. G. Barker, M. H. Kim and J. W. White, *Phys. B*, 2006, **385**, 776–779.
20 M. Kotlarchyk and S. M. Ritzau, *J. Appl. Crystallogr.*, 1991, **24**, 753–758.
21 C. M. Marques and J. F. Joanny, *Macromolecules*, 1989, **22**, 1454.